

NEW GEOCHRONOLOGIC AND STRATIGRAPHIC EVIDENCE CONFIRMS THE PALEOCENE AGE OF THE DINOSAUR-BEARING OJO ALAMO SANDSTONE AND ANIMAS FORMATION IN THE SAN JUAN BASIN, NEW MEXICO AND COLORADO

James E. Fassett

ABSTRACT

Dinosaur fossils are present in the Paleocene Ojo Alamo Sandstone and Animas Formation in the San Juan Basin, New Mexico, and Colorado. Evidence for the Paleocene age of the Ojo Alamo Sandstone includes palynologic and paleomagnetic data. Palynologic data indicate that the entire Ojo Alamo Sandstone, including the lower dinosaur-bearing part, is Paleocene in age. All of the palynomorph-productive rock samples collected from the Ojo Alamo Sandstone at multiple localities lacked Cretaceous index palynomorphs (except for rare, reworked specimens) and produced Paleocene index palynomorphs. Paleocene palynomorphs have been identified stratigraphically below dinosaur fossils at two separate localities in the Ojo Alamo Sandstone in the central and southern parts of the basin. The Animas Formation in the Colorado part of the basin also contains dinosaur fossils, and its Paleocene age has been established based on fossil leaves and palynology.

Magnetostratigraphy provides independent evidence for the Paleocene age of the Ojo Alamo Sandstone and its dinosaur-bearing beds. Normal-polarity magnetochron C29n (early Paleocene) has been identified in the Ojo Alamo Sandstone at six localities in the southern part of the San Juan Basin.

An assemblage of 34 skeletal elements from a single hadrosaur, found in the Ojo Alamo Sandstone in the southern San Juan Basin, provided conclusive evidence that this assemblage could not have been reworked from underlying Cretaceous strata. In addition, geochemical studies of 15 vertebrate bones from the Paleocene Ojo Alamo Sandstone and 15 bone samples from the underlying Kirtland Formation of Late Cretaceous (Campanian) age show that each sample suite contained distinctly different abundances of uranium and rare-earth elements, indicating that the bones were mineralized in place soon after burial, and that none of the Paleocene dinosaur bones analyzed had been reworked.

James E. Fassett. U. S. Geological Survey, Emeritus, 552 Los Nidos Drive, Santa Fe, New Mexico 87501
jimgeology@qwest.net

KEY WORDS: Paleocene dinosaurs; K-T interface, geochronology, palynology, paleomagnetism, vertebrate paleontology

INTRODUCTION

This paper reports new paleomagnetic, palynologic, radiometric, and geochemical data related to the Paleocene age of the dinosaur-bearing Ojo Alamo Sandstone and Animas Formation in the San Juan Basin of New Mexico and Colorado. These data provide the primary evidence for the ages of rock strata adjacent to the K-T interface in the San Juan Basin.

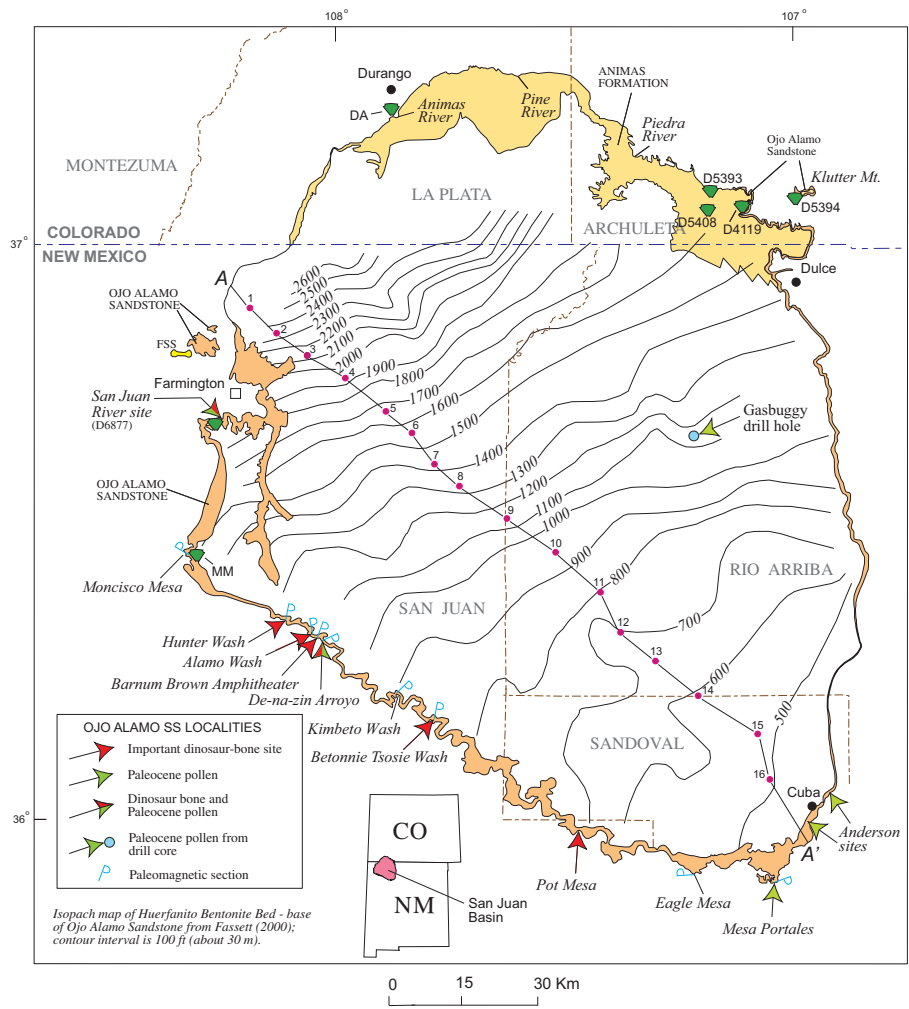
Because the Ojo Alamo Sandstone contains in situ dinosaur fossils, its Paleocene age has been questioned over the years. Multiple workers, beginning with Reeside (1924), suggested (or implied) that the dinosaur fossils of the Animas Formation and the Ojo Alamo Sandstone were Paleocene in age, however until recently, the evidence for the Paleocene age of the Ojo Alamo has been suggestive, but not entirely conclusive (Fassett 1982, 1987). Fassett and Lucas (2000) and Fassett et al. (2002), however, presented new data supporting the Paleocene age of the Ojo Alamo Sandstone. Fassett et al. (2002) presented geochemical data showing that all dinosaur fossils from the Ojo Alamo Sandstone that were analyzed, had been mineralized in place during Paleocene time and thus could not have been reworked from underlying Cretaceous strata. These new data, plus the expanded paleontologic, paleomagnetic, and geochemical analyses presented in this report, fully support earlier conclusions of Fassett and Lucas (2000) and Fassett et al. (2002) that some dinosaurs lived on into earliest Paleocene time in the San Juan Basin area. This study shows that these Lazarus dinosaurs lived for as long as 0.5 m.y. into Paleocene time. The presence of dinosaur fossils in the Paleocene Animas Formation of the northern San Juan Basin, first noted by Reeside (1924), seems to have been forgotten or ignored since that time; a discussion of Reeside's data plus new information related to Animas Formation dinosaur fossils are presented herein.

PHYSICAL STRATIGRAPHY OF K-T BOUNDARY STRATA

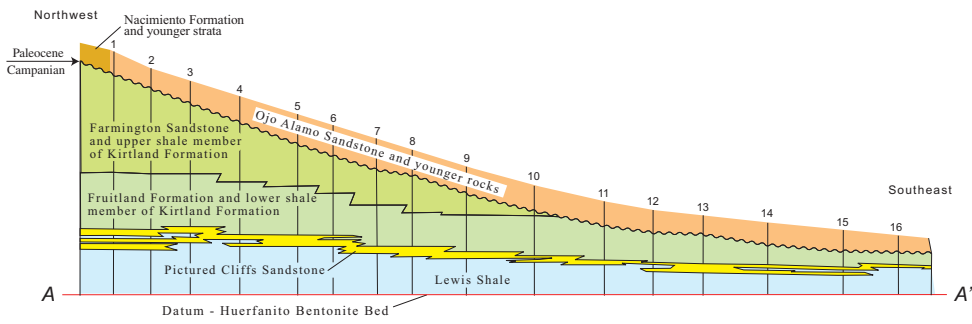
Lithology and Mode of Deposition of Ojo Alamo Sandstone

The Paleocene Ojo Alamo Sandstone is a prominent stratigraphic unit throughout the New Mexico part of the San Juan Basin. This formation forms the striking, massive, 100 m high vertical cliffs along the south side of the San Juan River on the south side of the city of Farmington in the west-central part of the basin (Figure 1). The Ojo Alamo is a coarse-grained, conglomeratic sandstone that crops out around the periphery of most of the New Mexico part of the San Juan Basin but is absent in the northern part (mostly in Colorado, Figure 1). The Ojo Alamo was deposited on a basin-wide erosion surface in early, but not quite earliest, Paleocene time by south-to-southeasterly flowing, high energy, braided streams (Fassett 2000, Fassett et al. 2002). A hiatus of nearly 8 m.y., at (or in a few places, slightly below) the base of the Ojo Alamo, separates Cretaceous and Tertiary rocks in the southern part of the basin (Fassett 1982, 1987, 2000, Fassett and Steiner 1997, Fassett and Lucas 2000, Fassett et al. 2002).

The Ojo Alamo is a multi-storied conglomeratic sandstone with highly varied internal architecture and thicknesses throughout the basin (Fassett et al. 2002, figures 4 and 5). Conglomerate clasts range from near-boulder size in the northwest part of the basin to small pebbles and grit in the southeast part. The rock-stratigraphic definition and age of the formation have been characterized differently by various workers over the years as discussed in numerous papers; those discussions are summarized and referenced in Fassett et al. (2002). Figure 2 shows the principal differences in the ways the Ojo Alamo has been characterized in its type area and the way the name is used in this report. The so-called middle, "shaly" part of the Ojo Alamo in the type area of the Ojo Alamo Sandstone is a mischaracterization of this interval because it contains multiple sandstone beds, and these sandstones represent a significant part of the interval. In the type area, the sandstones of the middle part of the Ojo Alamo are white and rela-



1.1



1.2

Figure 1. Index map and cross section of San Juan Basin. Outcrops of Ojo Alamo Sandstone and Animas Formation modified from Fassett and Hinds (1971, plate 1). 1.1 Important fossil localities and paleomagnetic-section localities through parts of Ojo Alamo Sandstone and adjacent strata. Isopach map shows thickness of interval between Huerfanito Bentonite Bed and base of Ojo Alamo Sandstone. Area between Hunter Wash and De-na-zin Arroyo is type area for Ojo Alamo Sandstone. D4119, D5393, D5394, D5408, D6877, and MM are USGS paleobotany localities. DA (Durango area) palynologic site from Newman (1997). Bone symbol labeled FSS shows locality of dinosaur-bone sample collected for chemical analysis. 1.2 Stratigraphic cross section A-A' showing interval from Huerfanito Bentonite Bed to base of Ojo Alamo Sandstone. Wells shown on cross section listed in Fassett and Hinds (1971). Modified from Fassett et al. (2002).

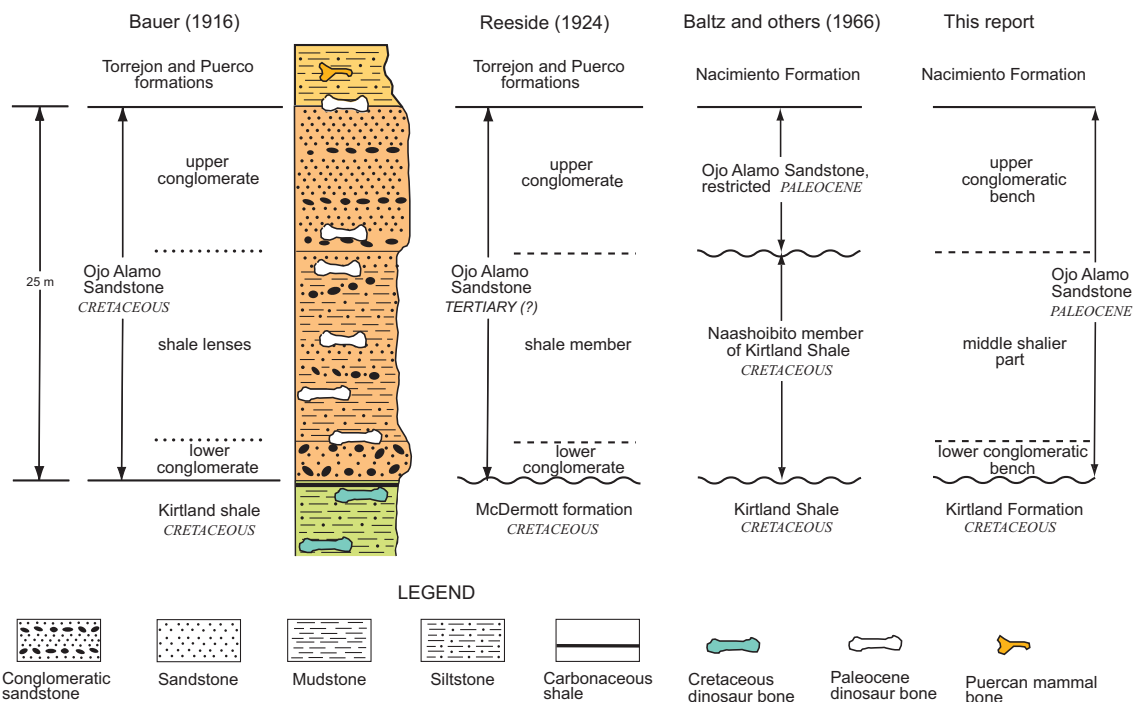


Figure 2. Generalized stratigraphic column showing lithology of Ojo Alamo Sandstone and adjacent strata in Ojo Alamo type area (Figure 1), original rock-stratigraphic definition of Ojo Alamo of Bauer (1916), two subsequent principal redefinitions, and definition used in this report.

tively friable rather than having the rusty-brown color of the harder lower and upper benches, thus these beds do not typically form cliffs or ledges. Photographs of the Ojo Alamo Sandstone at several outcrop localities are included in this report and show the nature and variability of the lithology of this formation.

The uppermost sandstone bench of the Ojo Alamo Sandstone at most exposures, is rusty brown in color, tightly cemented, and forms a vertical cliff face. In some exposures, such as south of Farmington (Figure 1), where the Ojo Alamo consists of as many as four, stepped-back benches, the uppermost sandstone bed capping each bench is also rusty brown, tightly cemented, and forms a vertical cliff. At many localities, sandstone beds of the Ojo Alamo lying below the upper, cliff-forming, rusty-brown bed, are less well cemented, are whiter in color, and weather into gentler slopes.

This phenomenon is probably the result of downward-moving ground water, containing more iron in solution, moving laterally and selectively through the relatively more permeable, uppermost Ojo Alamo sandstone beds, thus cementing them more tightly and giving them their distinctive rusty-

brown color. In the southern part of the San Juan Basin, this relationship has misled some workers into thinking that there is a continuous uppermost sandstone bed of the Ojo Alamo that is widespread throughout large parts of the basin, whereas in reality, these upper beds are separate lenses of the Ojo Alamo that happen to be rusty brown and more tightly cemented. This misconception has been exacerbated by the presence of numerous sand-filled arroyos that cut through the Ojo Alamo outcrop preventing the continuous tracing of this rock unit.

Relation of Ojo Alamo Sandstone to Underlying Strata

The stratigraphy of the rocks adjacent to the Cretaceous-Tertiary interface in the San Juan Basin has been discussed in numerous papers since about the beginning of the 20th century. The first publication to describe the geometry of these strata over a large part of the basin was Reeside (1924). Reeside presented a series of 20 measured sections around the north, west, and south edges of the basin; these sections showed thinning of the Fruitland-Kirtland interval from 561 m north-

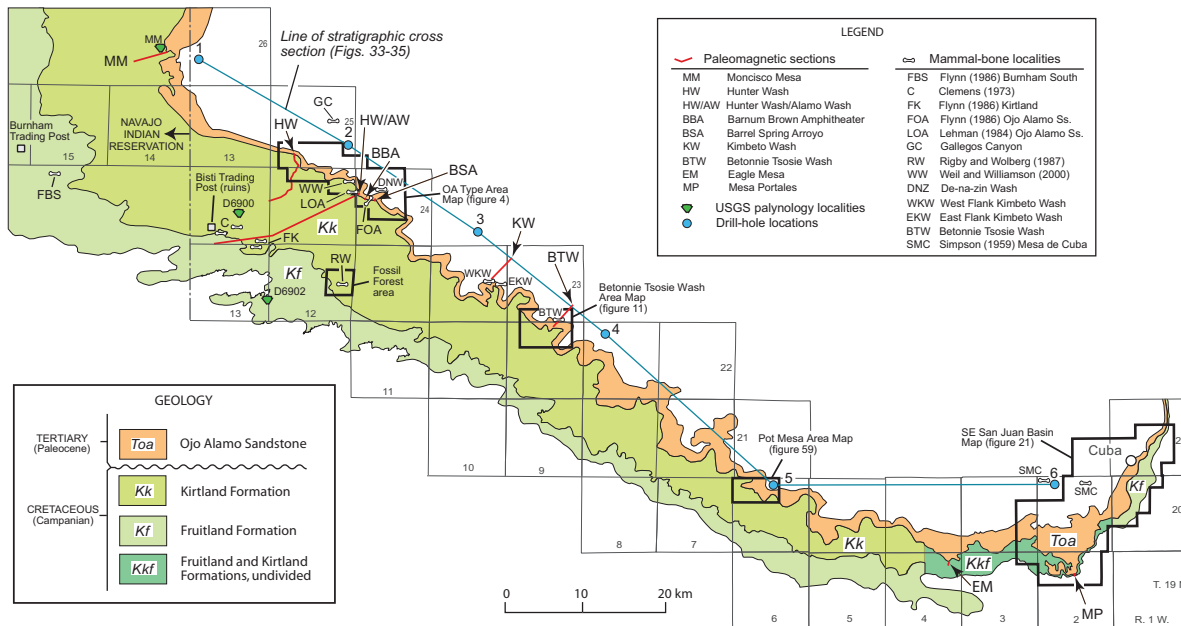


Figure 3. Geologic map of southern San Juan Basin showing locations of paleomagnetic sections through Cretaceous and (or) Paleocene strata plus selected fossil-mammal bone and palynologic localities; mammal-bone localities are approximate. Geology modified from Fassett and Hinds (1971). Areas of large-scale map figures are shown.

west of Farmington (Figure 1) to 0 m northeast of Cuba, New Mexico. Reeside (1924, p. 52, 53, figure 3) suggested that the thinning of Kirtland-Fruitland strata, from northwest to southeast across the basin, was the result of uplift and erosion of Cretaceous strata that was much greater in the southeast part of the basin. Reeside acknowledged that at some outcrops, the base of the Ojo Alamo Sandstone appeared to be concordant with underlying Cretaceous strata, but in spite of that, he was convinced that there was a significant erosional hiatus at or below the base of the Ojo Alamo.

Dane (1936), however, on the basis of surface mapping of Cretaceous and Tertiary rocks in the southeastern part of the basin, concluded that there was no erosional unconformity at the base of the Ojo Alamo. He reached this conclusion because he found places where a sandstone bed at the base of the Ojo Alamo thinned laterally and pinched out. At those localities, the shale above thickened and appeared to merge with the underlying Kirtland Shale. Dane indicated that at such places, the base of the Ojo Alamo should be shifted upward to the base of the next-highest sandstone bed. Dane thus concluded that there was continuous deposition across the Kirtland-Ojo Alamo contact, and thus there was no significant hiatus at this contact.

The geometry of the Ojo Alamo Sandstone at Mesa Portales (Figures 1, 3) illustrates the exact situation described by Dane. There, a lower bench of the Ojo Alamo Sandstone pinches out into mudstones to the east, and its basal contact is then apparently at the base of the higher sandstone bed (Fassett 1966, Fassett and Hinds 1971, figure 12). At this locality, however, the actual erosion surface at the K-T interface is about 22 m below the base of the rock stratigraphic Ojo Alamo at the base of a sandy interval (Fassett and Hinds 1971). Farther east on Mesa Portales, where the lower sandy interval marking the unconformity pinches out, the Cretaceous-Tertiary interface becomes difficult to discern, although it usually can be found with diligent searching.

Following Dane's 1936 paper, dozens of local studies of the rocks adjacent to the Cretaceous-Tertiary interface were published, with authors taking varying positions regarding the presence or absence of an unconformity at (or near) the base of the Ojo Alamo. These different interpretations were reviewed in Fassett and Hinds (1971); Fassett (1973, 1987, 2000); and Fassett et al. (2002). Fassett and Hinds (1971) presented a synthesis of all previously published data and included an analysis of hundreds of geophysical logs of drill holes throughout the basin to precisely map the subsurface relations of uppermost Cretaceous and lower-

most Paleocene strata and to assess the coal resources of the Fruitland Formation throughout the basin. This study confirmed Reeside's interpretation of the thinning of the Fruitland-Kirtland interval from northwest to southeast (Figure 1).

Fassett and Hinds (1971) concluded that Fruitland and Kirtland rocks were deposited by streams flowing northeastward toward the retreating shoreline of the Western Interior Seaway, and that this shoreline trended generally northwest throughout the time it was retreating northeastward across the San Juan Basin area. Moreover, they challenged an earlier contention by Silver (1950) that a basin of deposition had existed in the northwestern part of the San Juan Basin in Kirtland Formation time (named by Silver the "Kirtland basin"). Silver had inferred the presence of this basin solely on the basis of an isopach map of the Fruitland-Kirtland interval that showed much greater thicknesses of these rocks in the northwestern part of the basin. Fassett and Hinds (1971, figure 11) produced a more detailed Fruitland-Kirtland isopach map that showed in much greater detail how these rocks thinned southeastward across the basin. They also concluded that Silver's concept of a Kirtland basin was incorrect because the strata beneath the Ojo Alamo had been truncated from northwest to southeast across the basin during a pre-Ojo Alamo erosion cycle.

The only published study of paleo-current directions for the Fruitland-Kirtland interval was by Dilworth (1960) who measured cross-bedding in the Farmington Sandstone Member of the Kirtland Formation at five localities west of Farmington (Figure 1). Dilworth observed that streams depositing the Farmington Sandstone flowed from southwest to northeast. Dilworth's paleo-current study supports the findings of Fassett and Hinds (1971) that Fruitland and Kirtland strata were deposited by northeast-flowing streams.

Two comprehensive studies of paleo-current directions of the Ojo Alamo Sandstone (Powell 1973, Sikkink 1987) showed that the Ojo Alamo Sandstone was deposited by high-energy streams flowing from the north or northwest. Those conclusions are supported by the fact that the conglomerate clasts of the Ojo Alamo Sandstone become smaller from north to south and from west to east across the basin. Sandstone beds in Fruitland-Kirtland strata are fine to very-fine grained, whereas Ojo Alamo Sandstone beds are coarse-grained sandstone and conglomerates containing near-boulder-size clasts in the northwest part of the basin. These contrasting lithologies have made the

mapping of the basal contact of the Ojo Alamo Sandstone on the outcrop and in well logs straightforward and uncontroversial.

Butler and Lindsay (1985) resurrected Silver's (1950) "Kirtland basin" model and argued for a northwest sediment source for the Kirtland Formation and the Ojo Alamo Sandstone. They named this the "clastic-wedge" model for Fruitland-Kirtland deposition. This "clastic-wedge" model was based primarily on the assumption that there had been continuous deposition across the Kirtland-Ojo Alamo contact. These authors, however, stated that their model would effectively be disproved if precise dating of Kirtland strata proved that a substantial hiatus was present at the base of the Ojo Alamo Sandstone. Subsequent radiometric dating of altered volcanic ash beds in the Kirtland Formation, to within 5 m of its upper contact with the Ojo Alamo Sandstone by Fassett and Steiner (1997), demonstrated that nearly 8 m.y. are missing from the rock record at the Kirtland-Ojo Alamo contact in the southern San Juan Basin. Thus, the "clastic wedge" model of Butler and Lindsay (1985) has been refuted by their own suggested test of their model.

In summation, present data show that the Fruitland and Kirtland Formations were deposited by streams flowing northeastward toward the retreating Pictured Cliffs Sandstone paleo-shoreline. A single-crystal $^{40}\text{Ar}/^{39}\text{Ar}$ age of 73.04 ± 0.25 Ma for sanidine crystals from an altered volcanic ash bed in uppermost Kirtland Formation strata (Fassett and Steiner 1997) indicates that a nearly 8 m.y. hiatus exists between the top of the Kirtland Formation and the base of the Ojo Alamo Sandstone.

Animas and McDermott Formations

The Animas Formation was defined by Reeside (1924), and that definition was revised by Barnes et al. (1954). Those authors extended the base of the Animas Formation downward to incorporate the upper part of the underlying McDermott Formation of Reeside (1924) renaming these strata the McDermott Member of the Animas Formation. Barnes et al. (1954) reassigned the lower part of Reeside's McDermott Formation to the upper part of the Kirtland Formation (then named "Kirtland Shale"). The Animas Formation of Reeside (1924) thus became the "upper member of the Animas" as part of this redefinition. The southern extent of the McDermott Member was later restricted by Baltz et al. (1966) to the west side of the La Plata River, northwest of Farmington, New Mexico.

It is here recommended that the original definitions of the Animas Formation and McDermott Formation, as defined by Reeside (1924), be reinstated. Reeside's original McDermott Formation is an easily mappable unit of Late Cretaceous age (upper Campanian to lower Maastrichtian, as demonstrated by Newman 1987). The Animas Formation of Reeside (1924) is also an easily mappable unit of Paleocene age (Knowlton 1924, Newman 1987). An unconformity of several million years, representing the upper part of the Maastrichtian Stage separates these rock units. In retrospect, no useful purpose was served by the Barnes et al. (1954) redefinition of the Animas Formation, thus it is recommended that that redefinition be vacated in its entirety. The southern limit of the McDermott Formation suggested by Baltz et al. is still considered valid and should thus still stand.

The Animas Formation is present mostly in the Colorado part of the San Juan Basin (Figure 1) where it unconformably overlies, from west to east, the Cretaceous McDermott, Kirtland, and Fruitland Formations and is overlain by the Eocene San Jose Formation. The most detailed description of the lithology and stratigraphy of the Animas Formation is discussed in Reeside (1924). The Animas is a volcanoclastic rock unit that consists of coarse-grained to conglomeratic, reddish sandstone beds interbedded with olive-green, finer grained, over-bank deposits. Knowlton (1924) presented a detailed study of the fossil leaves in the Animas and concluded that this flora indicated that the Animas was Paleocene.

The lower part of the Animas Formation is equivalent in age to the Ojo Alamo Sandstone. The Ojo Alamo has been mapped separate from the Animas in the northeastern part of the basin north and south of the Colorado-New Mexico State line (Figure 1). The upper part of the Animas is time-equivalent to the Nacimiento Formation in the southern (New Mexico) part of the San Juan Basin. The volcanoclastic content of the Animas is most prominent in the northern part of the basin and the formation grades southward into volcanoclastic-free fluvial and lacustrine sandstones and mudstones of the Nacimiento Formation near the Colorado-New Mexico State line (Figure 1); mudstones dominate the Nacimiento throughout most of the San Juan Basin.

Cretaceous-Tertiary Interface

The striking contrast between the fine- to medium-grained rocks of the uppermost Cretaceous Kirtland and Fruitland Formations and the

coarse-grained to conglomeratic strata of the Paleocene Ojo Alamo Sandstone and the Animas Formation has made the mapping of the contact between these formations a relatively easy process in the San Juan Basin. This distinct physical contrast alone is clearly suggestive of a significant hiatus at the K-T interface. When the totally different current directions for rocks above and below the interface are added to the equation, northeast-flowing streams for Cretaceous strata and south- to southeast-flowing streams for Paleocene strata, the case for a substantial hiatus at the K-T interface is strengthened even more. Clearly, significant tectonic events (representing millions of years) must have occurred between the time of deposition of Cretaceous strata and Paleocene strata in the San Juan Basin. The geochronologic data obtained over the past few decades have now allowed us to precisely quantify this hiatus, as discussed below.

GEOCHRONOLOGY

The presence of abundant dinosaur bone in the Ojo Alamo Sandstone in the San Juan Basin has bedeviled researchers for more than 80 years because all other paleontological data, and the physical stratigraphic relations discussed above, indicated that the Ojo Alamo was Paleocene in age. Indeed, had it not been for the presence of abundant dinosaur remains in the Ojo Alamo Sandstone, its Paleocene age would probably never have been questioned. Because the last occurrence of dinosaur bone has always been considered by vertebrate paleontologists to mark the end of the Cretaceous Period, various explanations were suggested to explain away the presence of these dinosaur remains in what otherwise appeared to be Paleocene rocks. (For a complete discussion of those explanations, see Fassett et al. 2002.)

The relative age of sedimentary rock formations was originally based on the fossils found in those rocks (Winchester 2001). This criterion worked extremely well for marine rocks containing abundant fossils of small, steadily evolving, mostly invertebrate life forms, but was much less useful for continental strata containing far fewer diagnostic fossils, such as those of vertebrates. Where present, the last occurrence of dinosaur fossils was traditionally used to mark the top of the Cretaceous and Paleocene mammal fossils helped to locate the base of the Tertiary. These vertebrate fossil are normally not abundant in continental strata, thus in most areas they did not allow for a precise placement of the K-T interface. Exacerbating the prob-

lem, the endemic nature of vertebrate faunas in the northern and southern parts of the Western Interior of North America made correlations of these fossils difficult. Plant fossils, being much more abundant in most continental strata, have proven to be a much more valuable biochronologic tool. In particular, fossil pollen and spores have proven to be a precise tool for locating the K-T interface in the Western Interior of North America.

Relatively recently, geophysical tools have been developed to precisely date sedimentary rock strata, including radiometric dating and paleomagnetism. In the San Juan Basin, $^{40}\text{Ar}/^{39}\text{Ar}$ dating of sanidine crystals from altered volcanic ash beds has provided a series of eight precise ages for Late Cretaceous strata ranging from 75.76 Ma to 73.04 Ma (Fassett and Steiner 1997, Fassett 2000). Thus far, in spite of much searching, only one dateable ash bed has been found in Paleocene strata (in the Nacimiento Formation) in the southeast part of the San Juan Basin. Several paleomagnetic traverses, however, have been conducted across the K-T interface in the basin, and the magnetochron reversal boundaries from those studies provide excellent geochronologic tie points for the ages of K-T interface strata.

This report focuses on the radiometric dating of ash beds, the determination of remanent paleomagnetism of rocks adjacent to the K-T interface, and palynologic dating of rock strata to precisely locate the K-T interface in the San Juan Basin. It will be shown that these independent geochronologic tools are mutually supportive in locating this interface at or below the base of the Ojo Alamo Sandstone. Vertebrate paleontology, on the other hand, has not proven to be a very precise tool for biochronology in the San Juan Basin. Rather, the radiometric, paleomagnetic, and palynologic data for rock samples from strata adjacent to the K-T interface have established a precise geochronologic framework that can now be used to more precisely assign ages to the vertebrate faunal assemblages in these strata.

PALEOMAGNETISM

Remanent magnetism of rock strata adjacent to the K-T interface in the San Juan Basin provides an objective geochronologic tool for placement of the K-T interface and for estimating a more precise age for the base of the Ojo Alamo Sandstone. Paleomagnetic studies of these rocks have been conducted by different workers in the southern San Juan Basin at nine localities (Figures 1, 3). This report presents published paleomagnetic data from

eight localities and one previously unpublished paleomagnetic data set from the Mesa Portales study area (Figures 1, 3) in an integrated format. Eight of the published paleomagnetic studies were in: Butler et al. (1977); Lindsay et al. (1978, 1981, 1982); Butler and Lindsay (1985); and Fassett and Steiner (1997). The paleomagnetic data presented herein demonstrate that the dinosaur-bearing part of the Ojo Alamo Sandstone in the southern San Juan Basin is within the lower part of normal-polarity chron C29n and is thus Paleocene in age.

Four of the paleomagnetic sections through the Ojo Alamo Sandstone were discussed in Lindsay et al. (1981): South Mesa, Barnum Brown Amphitheater, Barrel Spring, and Betonnie Tsosie Wash (Figures 3 and 4). The South Mesa, Barnum Brown Amphitheater, and Barrel Spring sections are 1.3 km and 1.8 km apart, respectively, (Figure 4) and are in the heart of what is known as the Ojo Alamo Sandstone type area (Bauer 1916, Baltz et al. 1966, Fassett 1973, Fassett 2000, Fassett et al. 2002). These three sections are also within the Bisti - De-na-zin Wilderness Area on the south edge of a topographic feature named "South Mesa" by Clemens (1973b, figure 3); South Mesa is capped by the Ojo Alamo Sandstone. Clemens defined South Mesa as being outlined by the 6,400ft contour line on the USGS 1:24,000 Alamo Mesa East Topographic Quadrangle (the name "South Mesa" does not appear on that map). The Betonnie Tsosie Wash section is about 27 km southeast of the Ojo Alamo type area (Figure 3).

The South Mesa paleomagnetic section through the Ojo Alamo Sandstone is the upper part of a longer section labeled the Hunter Wash-Alamo Wash section in Lindsay et al. (1981). In a later report by Butler and Lindsay (1985), the part of this paleomagnetic section through the Ojo Alamo Sandstone was named the South Mesa section. The Betonnie Tsosie Wash section (Figure 3) was named the "Tsosie Wash" section in Lindsay et al. (1981), however, the wash this section is named for is Betonnie Tsosie Wash (USGS 1:24,000 Kimbeto Topographic Quadrangle). The Moncisco Mesa and Eagle Mesa sections do not include the Ojo Alamo Sandstone and were published in Butler and Lindsay (1985). The Hunter Wash section (Fassett and Steiner 1997) includes all of the Kirtland Formation and the lower part of the Ojo Alamo Sandstone in the western part of the type area (Figure 4).

Rock samples for the Mesa Portales paleomagnetic section were collected in 1983 by E.M. Shoemaker (USGS, deceased), M.B. Steiner (U. of

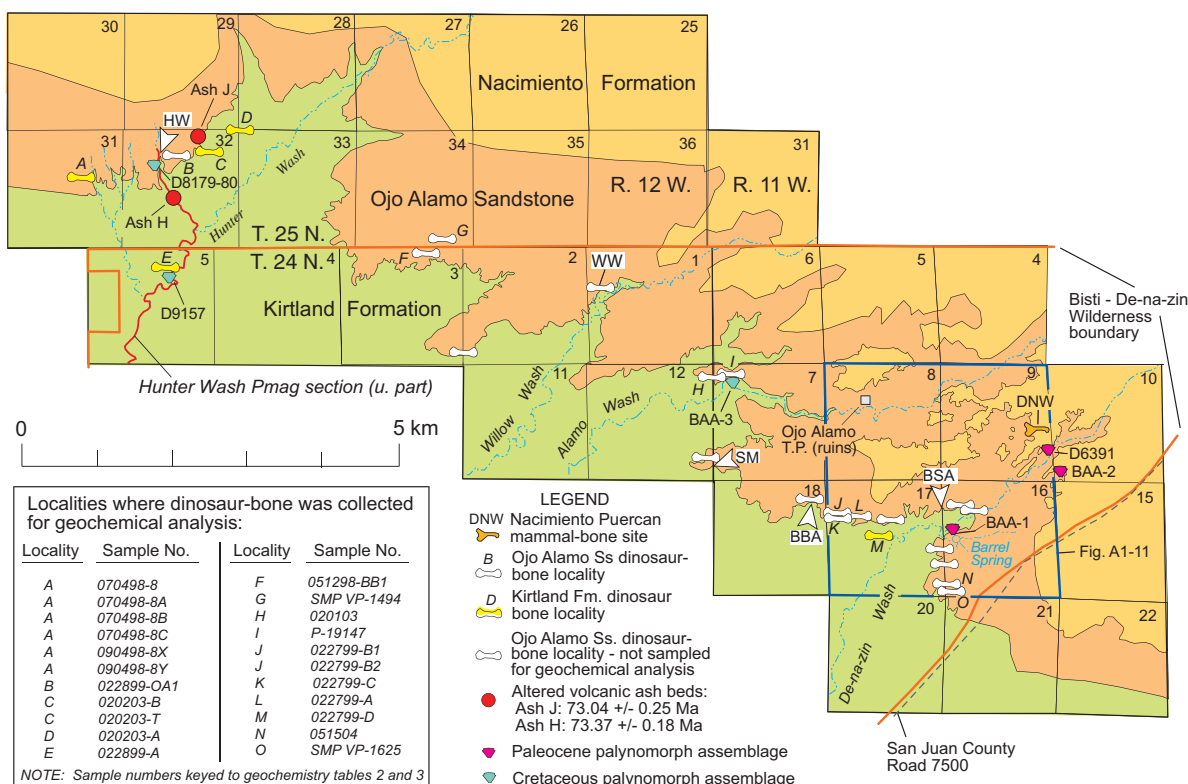


Figure 4. Geologic map of the Ojo Alamo Sandstone type area. White arrowheads point to areas where paleomagnetic data were obtained from the Ojo Alamo Sandstone; HW = Hunter Wash, SM = South Mesa, BBA = Barnum Brown Amphitheater, and BSA = Barrel Spring Arroyo; WW marks the Williamson-Weil mammal quarry. Dinosaur-bone locality I, in the NW 1/4 Sec. 7, T. 24 N., R. 11 W., is locality where 34 bones from a single *Hadrosaur* were discovered and collected from Ojo Alamo Sandstone. Geology modified from Brown (1982) and Scott et al. (1979); base of Ojo Alamo Sandstone was remapped for this study. Numbers with D prefixes are USGS paleobotany locality numbers. Published palynomorph lists from this area and other areas are in tables in the Appendix. BAA-1 through BAA-3 are palynologic sample localities of Baltz et al. (1966). Radiometric ages for sanidine crystals from altered volcanic ash beds H and J from Fassett and Steiner (1997) and Fassett (2000).

Wyoming), and the author and in 1989 by Steiner and the author. Paleomagnetic analyses of these samples were performed by Steiner at the University of Wyoming and by J.L. Kirschvink (for Shoemaker) at the California Institute of Technology. The Mesa Portales section is especially important because it is supplemented by detailed palynologic data from multiple stratigraphic levels through the Upper Cretaceous Fruitland-Kirtland Formation (undivided), across the Cretaceous-Tertiary interface, and upward through most of the Paleocene Ojo Alamo Sandstone. Some of the Mesa Portales palynologic data were published in Fassett and Hinds (1971); additional palynologic data from that locality are presented herein for the first time. An earlier palynologic study of the Ojo Alamo Sandstone about 15 km northeast of Mesa Portales (Figure 3) was published by Anderson (1960) and

the significance of Anderson's data, as related to the Paleocene age of the Ojo Alamo Sandstone, is discussed in the "Palynology" section of this report.

Because magnetochrons contain no inherent geochronologic information, it is essential that paleomagnetic data be supported by other geochronologic data to uniquely identify them. For Cretaceous rocks underlying the Ojo Alamo Sandstone, a robust sequence of eight precise $^{40}\text{Ar}/^{39}\text{Ar}$ radiometric ages exists (Fassett and Steiner 1997, Fassett 2000, Fassett et al. 2002), thus the two magnetochrons identified in the southern San Juan Basin in these strata are unquestionably chrons C33n and C32r. Moreover, the stratigraphically highest radiometric date: 73.04 ± 0.25 Ma, for an altered volcanic ash bed (ash J, Figure 4) less than 5 m below the base of the Ojo Alamo Sandstone near Hunter Wash, confirmed

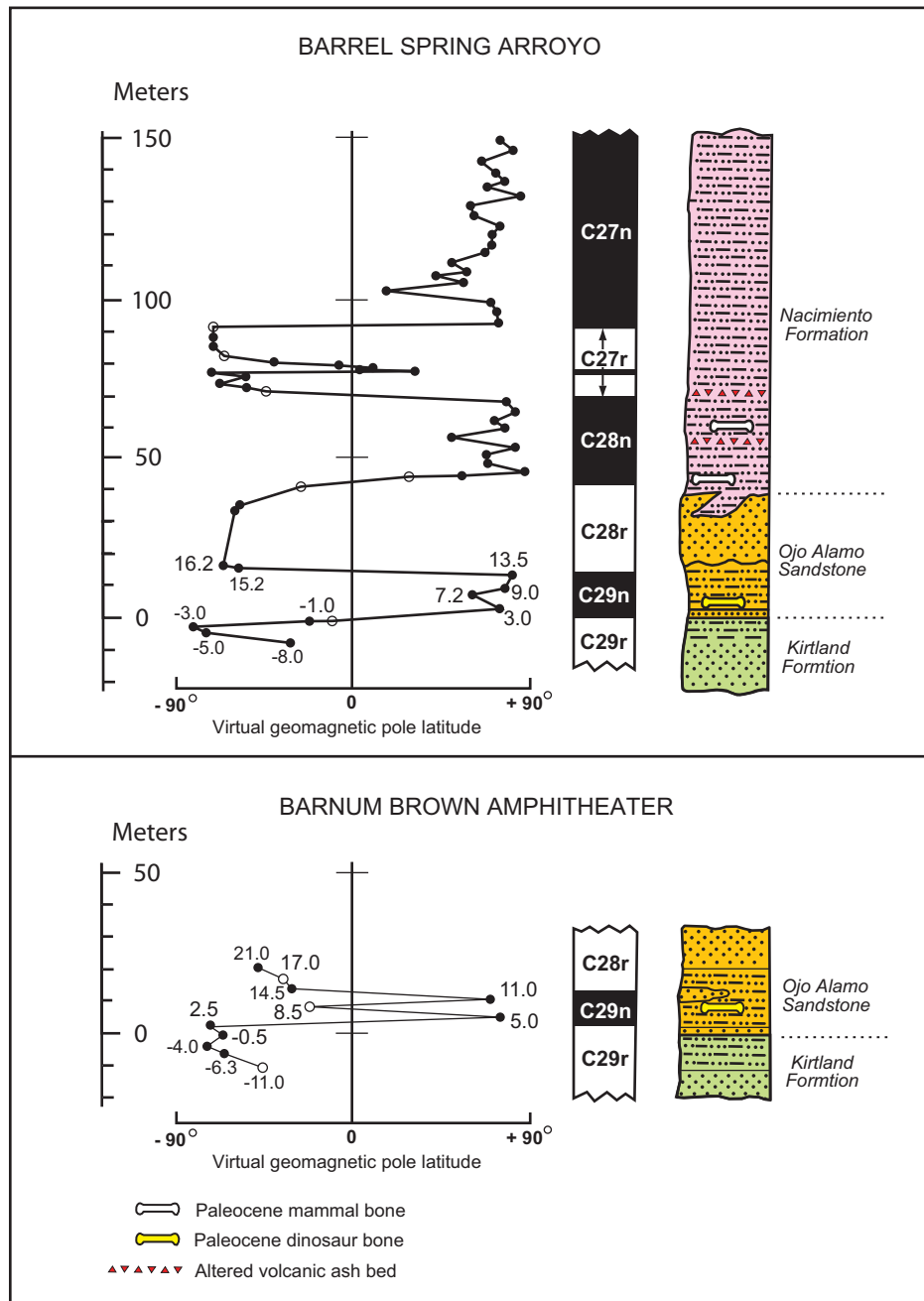


Figure 5. Paleomagnetic and stratigraphic sections at Barrel Spring Arroyo and Barnum Brown Amphitheater, modified from Lindsay et al. (1981): "Solid data points indicate sites with grouping of directions significant from random at the 95% confidence level. Open circles indicate data points from sites with poorer clustering." (Lindsay et al. 1981). The same symbology applies for all subsequent figures of these authors reproduced herein. These localities are labeled BSA and BBA, respectively, on Figures 3 and 4. (Barrel Spring Arroyo of the Lindsay et al. report is now named De-na-zin Wash (Alamo Mesa East, 1:24,000 USGS quadrangle map.) Labels of magnetochrons (as applied by Lindsay et al. 1981, elsewhere in their paper) have been added to this illustration, for ease of discussion. (Note: some magnetochron labels shown are now known to be incorrect as discussed in the section of this paper labeled "Identification of Kirtland Formation-Ojo Alamo Sandstone Magnetochrons.") Distances of selected paleomagnetic-samples sites, above and below the base of Ojo Alamo Sandstone (in meters), are added. Dinosaur-bone symbol on Barnum Brown Amphitheater column was added by author.

the presence of a 7.8-m.y. hiatus separating the Kirtland Formation of Cretaceous (Campanian) age from the overlying Ojo Alamo Sandstone of Paleocene age. Palynomorphs identified from these strata also help to date them, although somewhat less precisely. Tschudy (1973) and Newman (1987) published palynologic data from the stratigraphically highest Cretaceous rocks in the San Juan Basin. Both of these studies indicated that a significant hiatus existed at the K-T interface representing all or most of Maastrichtian time; the radiometric dates published by Fassett and Steiner (1997) and Fassett (2000) confirmed the biochronologic findings of Tschudy and Newman.

All attempts to radiometrically date the Ojo Alamo Sandstone have thus far been unsuccessful; however, all paleobotanical evidence suggests a Paleocene age (Reeside 1924, Knowlton 1924, Anderson 1960, Fassett and Hinds 1971, Tschudy 1973, Fassett 1982, Fassett 1987, Fassett and Steiner 1997, Fassett 2000, Fassett and Lucas 2000, and Fassett et al. 2002). New, robust palynologic data from the Mesa Portales locality confirm these earlier studies that showed that the age of the entire formation is Paleocene; a summary of this palynologic data is contained in the "Palynology" section of this report.

Puercan-age (lowermost Paleocene) vertebrate fossils have been identified in the lowermost part of the Nacimiento Formation. The Nacimiento directly overlies and intertongues with the Ojo Alamo Sandstone at five localities in the southern San Juan Basin. These data provide additional, if inferential, evidence that at least the upper part of the Ojo Alamo is Paleocene (Williamson and Lucas 1992, 1993; Williamson 1996). Vertebrate paleontologists have disagreed about the biochronologic age of the lower, dinosaur-bearing part of the Ojo Alamo Sandstone. For example, Sullivan et al. (2005) contended that the Ojo Alamo contains a dinosaur fauna that is latest Campanian or early Maastrichtian whereas Weil and Williamson (2000) and Farke and Williamson (2006) state that the vertebrate fauna of the lower Ojo Alamo is clearly Lancian (latest Maastrichtian) in age. These different vertebrate-fossil ages for the Ojo Alamo are evaluated in the "Vertebrate Paleontology" section of this paper.

The following sections discuss the several published paleomagnetic studies that include the Ojo Alamo Sandstone. These publications are presented in chronologic order to best show the evolution of thinking about the numbering of the magnetic-polarity intervals identified in the rock

strata adjacent to the K-T interface in the southern San Juan Basin. In this historical discussion, the relatively thin, normal-magnetic-polarity interval within the Ojo Alamo Sandstone is labeled C29n, after Lindsay et al. (1981), Fassett and Steiner (1997), and Fassett (2000). This thin Ojo Alamo-normal interval is now known to be only the lowermost part of chron C29n and is therefore designated C29n.2n as discussed in the "Identification of Magnetochrons" section of this paper.

Localities of Lindsay et al. (1981)

Barrel Spring Arroyo. The Barrel Spring Arroyo paleomagnetic section (BSA, Figure 4) is on the north side of De-na-zin arroyo, about 0.4 km north of Barrel Spring. The paleomagnetic data plot for this section of Lindsay et al. (1981, figure 7) is shown on Figure 5. This plot contains five data points of reversed polarity in the Kirtland Formation, four data points with normal polarity in the lower part of the Ojo Alamo Sandstone, and five data points with reversed polarity in the upper part of the Ojo Alamo. Additional alternating zones of normal and reversed polarity are shown in the overlying Nacimiento Formation. The entire section is about 160 m in length, and critical data points below, within, and above the Ojo Alamo Sandstone are numbered in meters, below or above the base of the Ojo Alamo Sandstone. The magnetochrons in the lower part of the section were labeled B-, C+, D-, E+, F-, and G+ by Lindsay et al. (1981) on their figure 7, but in a subsequent section of their paper were relabeled C29r, C29n, C28r, C28n, C27r, and C27n, respectively, as shown on Figure 5.

Figure 6 is an annotated photograph of the Barrel-Spring-Arroyo locality showing that the Ojo Alamo Sandstone consists of a lower conglomeratic sandstone, a middle "shaly" part, and an upper, massive, conglomeratic-sandstone bench. The stratigraphic positions of the paleomagnetic data points from Lindsay et al. (1981) were placed on this photograph based on the locations of these points shown on Figure 5. Figures 5 and 6 show that the Ojo Alamo at this locality contains in its lower part a normal magnetochron (labeled C29n by Lindsay et al. 1981). This normal interval is shown to be about 14 m thick, based on the assumption that a thin, reversed-polarity interval, the uppermost part of chron C29r, is present here in the lowermost part of the Ojo Alamo Sandstone. This assumption is based on the fact that all other paleomagnetic sections through the Ojo Alamo Sandstone in the southern San Juan Basin show the presence of a thin reversed paleomagnetic

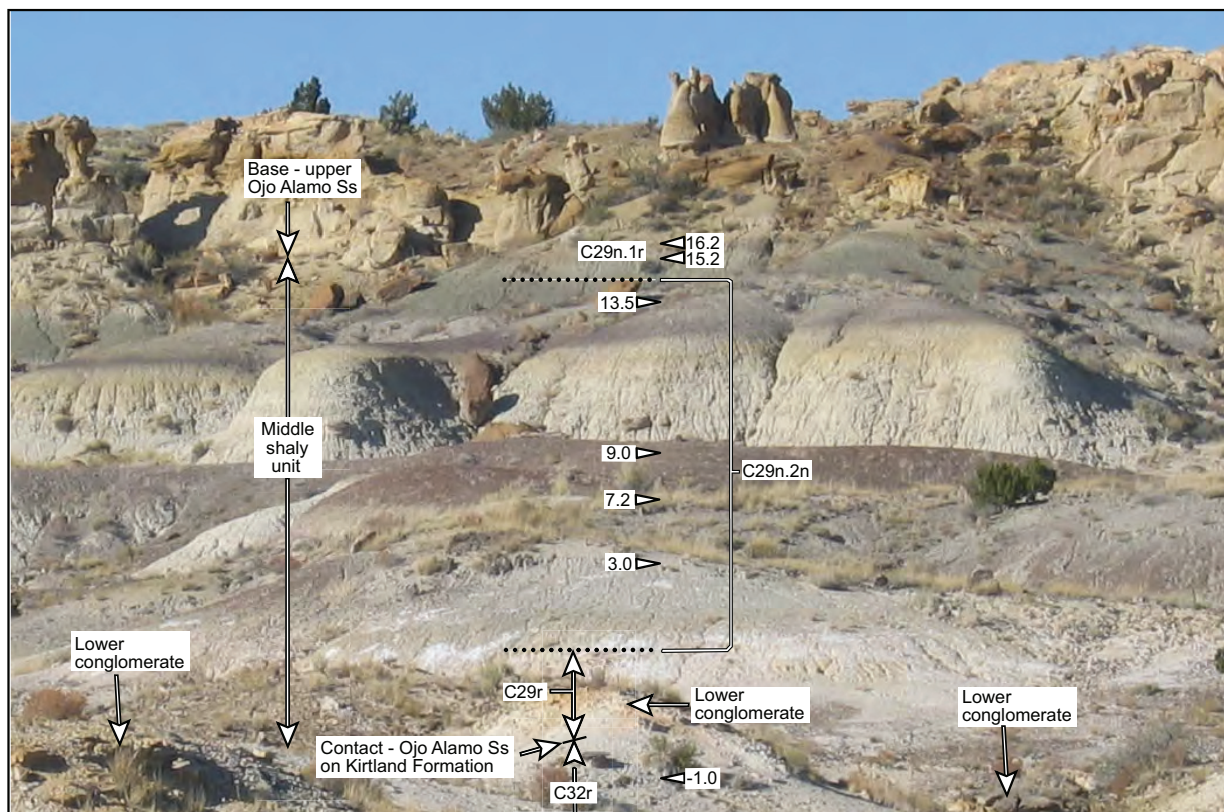


Figure 6. Photograph of Barrel Spring locality (looking north) of Lindsay et al. (1981); location is shown on Figures 3 and 4. Magnetochron labels for Ojo Alamo Sandstone are corrected as discussed in the “Identification of Kirtland Formation-Ojo Alamo Sandstone Magnetochrons” section of this report. Lindsay et al.’s (1981) paleomagnetic data plot at this locality is on Figure 5. Numbered arrow heads are distances above base of Ojo Alamo Sandstone in meters; sample levels are approximate. Arrow heads pointing left indicate reversed polarity, arrow heads pointing right indicate normal polarity. Sample levels are estimated from Figure 5, but exact original sample localities are not known.

interval in the lowermost part of this formation. All but one of the samples collected for paleomagnetic analyses were from gray mudstones; the sample at 9.0 m above the base of the Ojo Alamo (Figure 6) is from a slightly reddish-brown mudstone. The lower samples are from a gently sloping topographic bench, whereas samples 13.5, 15.2, and 16.2 are from more steeply dipping terrain. Note on Figure 6 that all samples were collected from mudstone layers avoiding the prominent white sandstone beds present in the middle “shaly” part of the Ojo Alamo. The lensing nature of all of the strata in the middle part of the Ojo Alamo is apparent at this locality.

Barnum Brown Amphitheater. The Barnum Brown Amphitheater paleomagnetic section (BBA, Figure 4) is on the south edge of South Mesa; this locality is about 1.8 km west of the Barrel Spring Arroyo (BSA) section. (The name “Barnum Brown Amphitheater” was apparently coined by Lindsay et

al. (1981) for this locality and should not be confused with the amphitheater referred to by Barnum Brown (1910) that is several kilometers northeast of this locality in Alamo Wash stratigraphically above the Ojo Alamo Sandstone in the Nacimiento Formation.) The paleomagnetic section at the BBA locality is short (~32 m), consisting of only 11 sample levels; samples were collected from the uppermost Kirtland Formation and the lower part of the Ojo Alamo Sandstone (Figure 5). The five Kirtland samples exhibit reversed polarity; the lowest Ojo Alamo sample also exhibits reversed polarity, the next three samples in the lower Ojo Alamo exhibit normal-reversed-normal polarity, and the uppermost three samples show reversed polarity. Lindsay et al. (1981, p. 411) stated that the reversed site in the middle of the Ojo Alamo Sandstone normal interval at the Barnum Brown locality was weakly magnetized and that “. . . the site mean VGP moved toward positive values during AF demagnetization. Thus we do not interpret the data

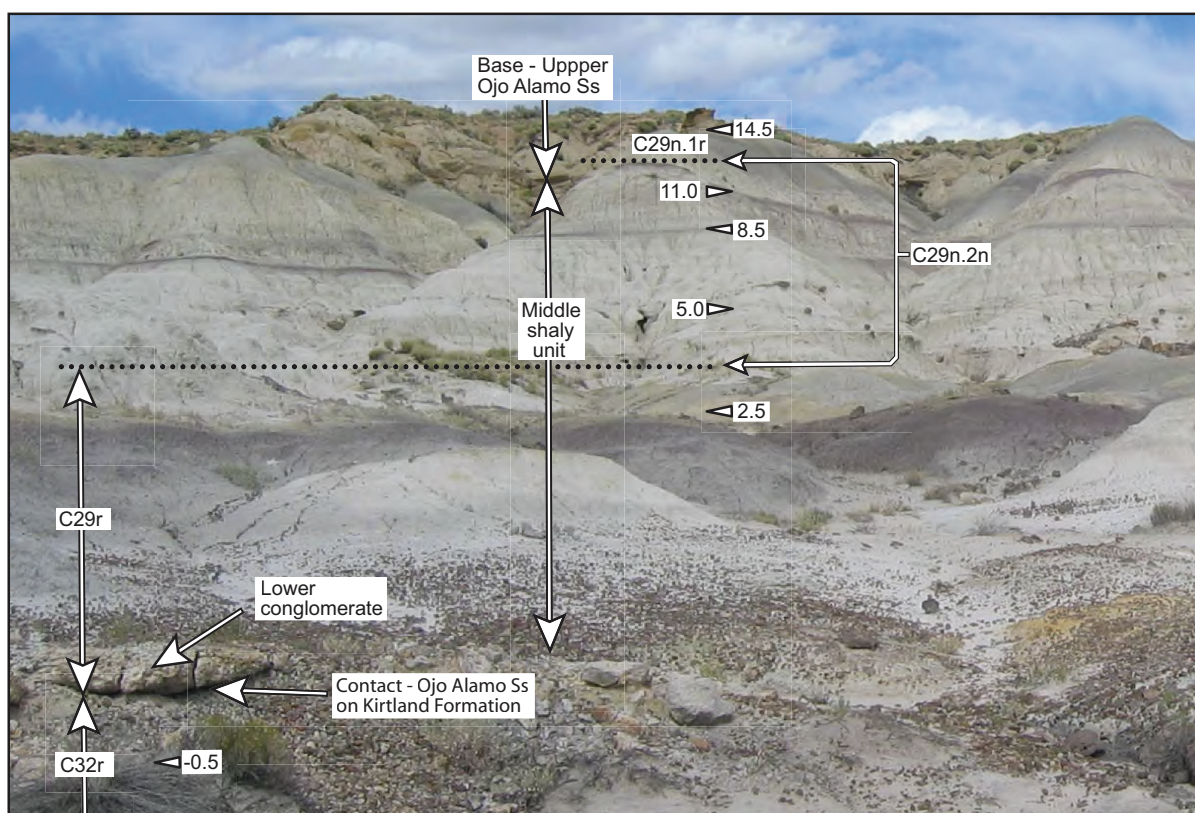


Figure 7. Photograph of Barnum Brown Amphitheater locality (looking north) of Lindsay et al. (1981); location is on Figures 3 and 4. The paleomagnetic data plot at this locality is on Figure 5. Magnetochron labels in Ojo Alamo Sandstone are corrected as discussed in section of this paper labeled “Identification of Kirtland Formation–Ojo Alamo Sandstone Magnetochrons.” Numbers at arrow heads are distances above base of Ojo Alamo Sandstone in meters; sample levels are approximate. Arrow heads pointing left indicate reversed polarity, arrow heads pointing right indicate normal polarity. Sample levels are estimated from Figure 5, but exact original sample localities are not known.

from this site to be a reliable indication of a reversed subzone within normal C+ [C29n].”

Figure 7 is an annotated photograph showing that the Ojo Alamo Sandstone at the BBA locality consists of a lower conglomerate, a middle “shaly” unit, and an upper more massive sandstone bench. The lithologies of the Ojo Alamo Sandstone at the BBA and BSA localities are similar, except there is more sandstone present at the BBA locality in the middle part of the Ojo Alamo. The stratigraphic locations of the paleomagnetic data points from the Lindsay et al. (1981) report are placed on this photograph based on the positions of these points shown on Figure 5. The normal-polarity interval labeled C29n by these authors is 11 m thick at the BBA locality; the underlying interval of reversed polarity in the lowermost Ojo Alamo—labeled C29r—is 2.6 m thick. All of the samples collected at this locality were from gray mudstones. The lowermost, reversed-polarity sam-

ple (2.5) was from a gently sloping hill, whereas the higher Ojo Alamo samples were from a much steeper cliff face. This steeper cliff face reflects the topographic expression of the white sandstone beds in the upper part of the middle interval of the Ojo Alamo Sandstone. Figure 7 shows that the samples collected for paleomagnetic analyses at this locality were from relatively thin interbeds of mudstone.

South Mesa. The South Mesa (SM) paleomagnetic section is at the west end of South Mesa near a westward-projecting spur capped by the cliff-forming Ojo Alamo Sandstone (Figure 4). This section is the uppermost part of a much longer paleomagnetic section through the underlying Fruitland and Kirtland Formations. Lindsay et al. (1981) named this the Hunter Wash/Alamo Wash section (Figure 8). Figure 9, a large-scale paleomagnetic plot through the uppermost Kirtland Formation and lower part of the Ojo Alamo Sandstone, contains

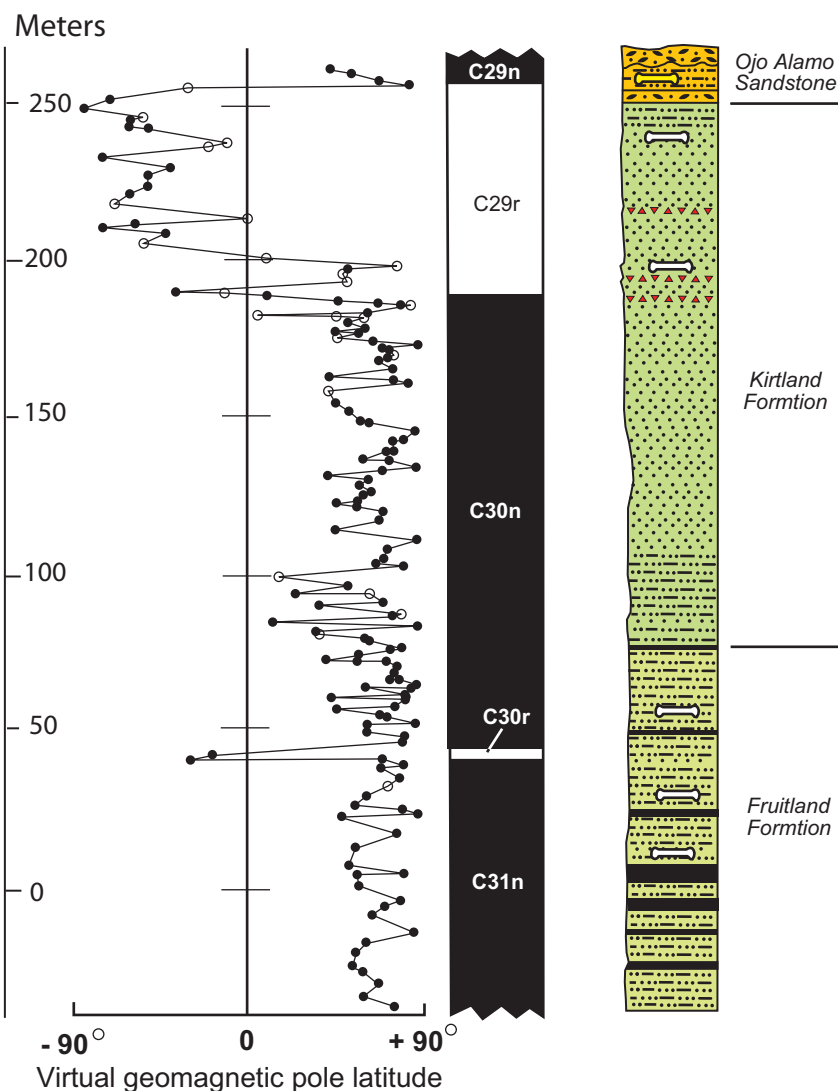


Figure 8. Paleomagnetic data plot at “Hunter Wash/Alamo Wash” locality. (Figure is modification of figure 6 of Lindsay et al. 1981 and is reproduced herein with permission of the American Journal of Science.) Upper part of section through upper Kirtland Formation and lower Ojo Alamo Sandstone is labeled SM on Figures 3 and 4. Cretaceous-Tertiary boundary plus magnetochron labels as identified by Lindsay et al. (1981) are added for ease of discussion. Bone symbols represent important vertebrate-fossil levels. (Note: some magnetochron labels shown are now known to be incorrect as discussed in the section of this paper labeled “Identification of Kirtland Formation-Ojo Alamo Sandstone Magnetochrons.”)

three reversed-polarity and four normal-polarity data points. The numbers shown for each data point are distances in meters above or below the base of the Ojo Alamo Sandstone. This paleomagnetic section ended just beneath the base of the upper massive sandstone bed of the Ojo Alamo, thus the top of magnetochron C29n was not located at this locality. Magnetochrons C29n and C29r are shown on Figure 9 as identified by Lindsay et al. (1981).

Figure 10 is an annotated photograph of the South Mesa paleomagnetic locality, and here, as at the Barrel Spring and Barnum Brown Amphitheater localities, the Ojo Alamo Sandstone consists of a lower conglomerate bed, a middle “shaly” unit, and an upper, massive, conglomeratic sandstone bench. The stratigraphic locations of the paleomagnetic data points from Lindsay et al. (1981) are placed on this photograph based on the positions of these points shown on Figures 8 and 9. Magnetic normal interval C29n is 5.9 m thick here (top

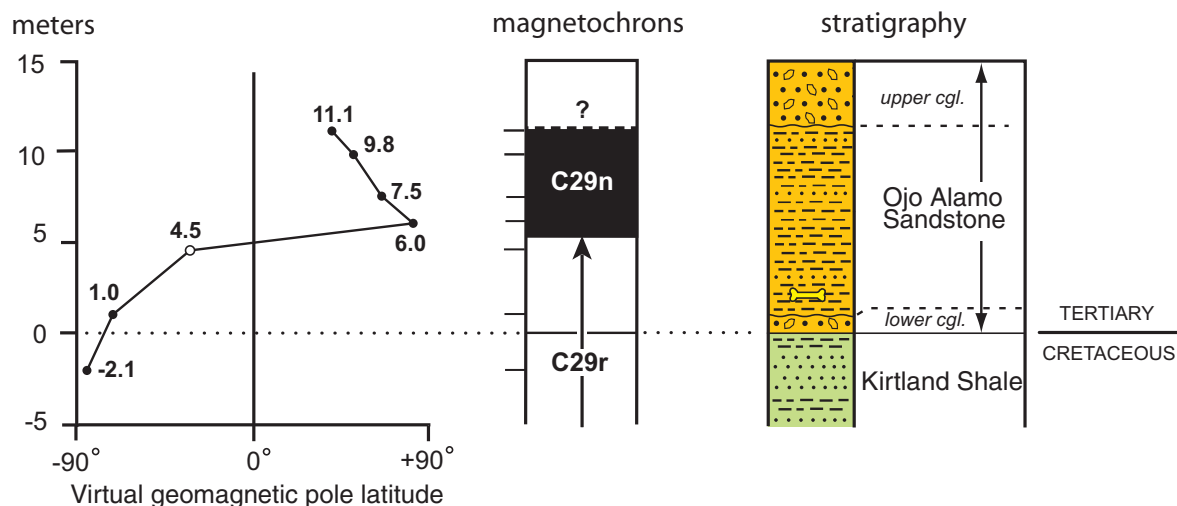


Figure 9. Large-scale view of South Mesa paleomagnetic section (labeled SM on Figures 3, 4). Stratigraphic levels of samples collected for paleomagnetic analyses are shown in meters above or below base of Ojo Alamo Sandstone. Plot is expanded-scale rendition of upper part of Hunter Wash/Alamo Wash section of Lindsay et al. (1981) of Figure 8; top of chron C29n was not determined. (Magnetochron labels are now known to be incorrect as discussed in section of this paper labeled “Identification of Kirtland Formation-Ojo Alamo Sandstone Magnetochrons.”)

not determined), and the underlying reversed-polarity chron C29r (in the lowermost part of the Ojo Alamo) is 5 m thick. All samples collected for paleomagnetic analysis at this locality appear to have come from gray mudstones. The reversed-polarity sample 1 m above the base of the Ojo Alamo in the basal part of the middle “shaly” unit is from a gently sloping topographic bench. Reversed polarity sample 4.5 and the four overlying samples of normal polarity, were from a much steeper cliff face. The middle “shaly” interval of the Ojo Alamo Sandstone contains multiple sandstone beds at this locality.

Betonnie Tsosie Wash. The Betonnie Tsosie Wash (BTW) paleomagnetic section (“Tsosie Wash” section of Lindsay et al. 1981) is about 28 km southeast of the Ojo Alamo Sandstone type area (Figure 3). This locality is on an outlier of middle and upper Ojo Alamo Sandstone strata on the east side of a north-trending tributary of Betonnie Tsosie Wash (Figure 11). The paleomagnetic data plot for samples collected from this locality (Figure 12) contains five normal-polarity sites at the base overlain by two reversed-polarity sites in the middle Ojo Alamo Sandstone; one normal-polarity sample is in the upper part of the Ojo Alamo. The overlying Nacimiento Formation contains a large number of data points with normal polarity (and one sample with reversed polarity). The middle and upper parts of the Ojo Alamo Sandstone at this

locality are about 27 m thick. The base of the Ojo Alamo is about 5 m stratigraphically below the 26.6 sample locality (Figure 12). This paleomagnetic section is particularly important because it includes a Puercan mammal quarry only 12 m above the top of the Ojo Alamo (Figures 11 and 12). (The bio-chronology of the paleomagnetic sections included in this report is discussed in detail in subsequent sections of this paper.) The magnetochron labeled C29n (Figure 12) is 7.1 m thick, however, its base was not determined because of alluvial cover immediately below sample 26.6. Chron C29n is overlain by chrons labeled C28r, C28n, C27r, and C27n by Lindsay et al. (1981). (These labels are revised in a subsequent section of this paper.)

Figure 13 is a photograph of the small butte where samples from the Ojo Alamo Sandstone part of the Betonnie Tsosie Wash paleomagnetic section were collected (Figure 12). This butte is capped by a 4 m thick, hard, iron-cemented, cliff-forming, conglomeratic sandstone layer that is the uppermost part of the upper bench of the Ojo Alamo. The underlying shaly interval is about 11 m thick here with its base masked by alluvium. (A lower sandstone bench of the Ojo Alamo Sandstone is exposed farther south in this tributary of Betonnie Tsosie Wash (Figure 11) and its base is about 5 m below the exposed part of the Ojo Alamo seen on Figure 13.) The upper part of magnetochron C29n is in the lower part of the middle shaly unit of the Ojo Alamo Sandstone (Figure 13). Most

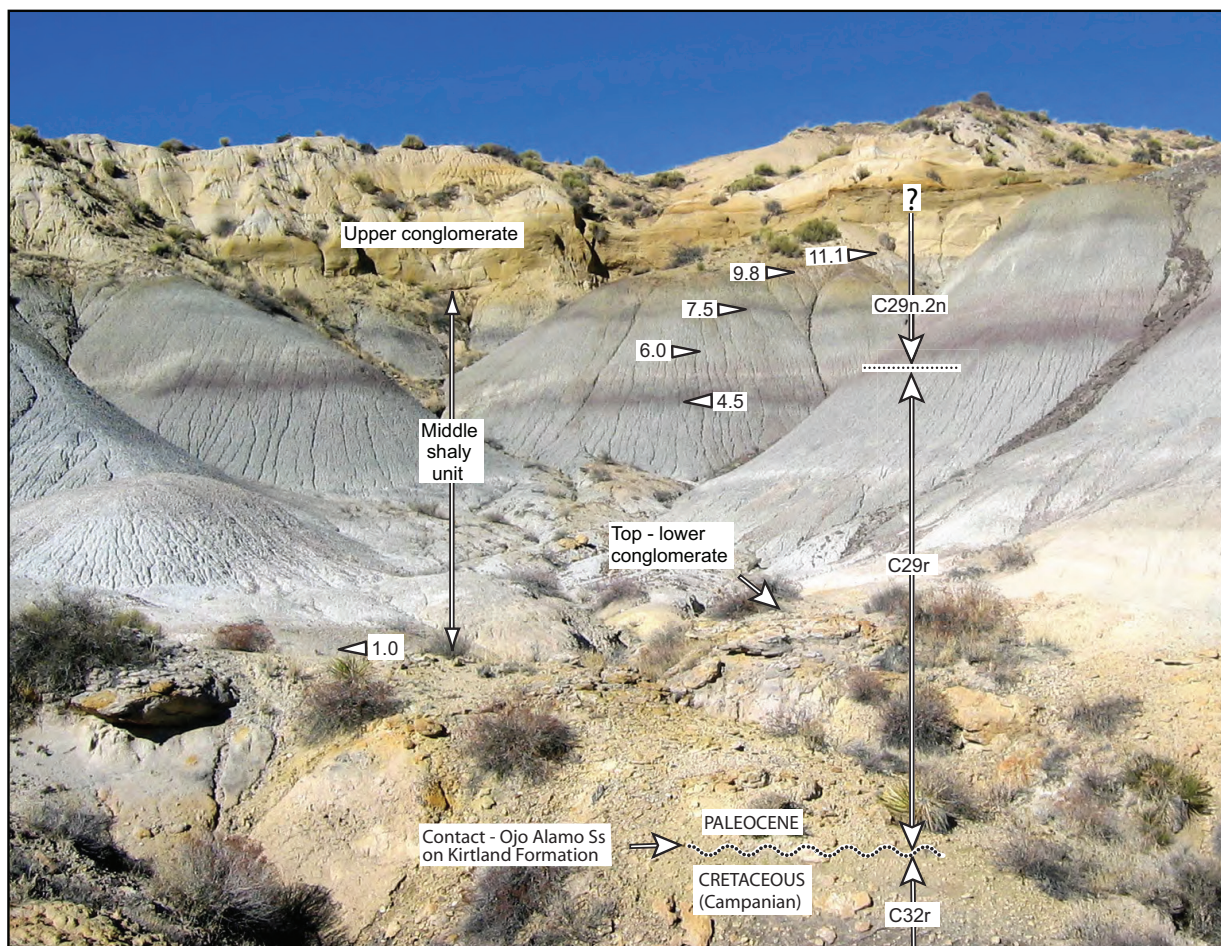


Figure 10. Photograph of South Mesa locality (looking north) of Lindsay et al. (1981); location is on Figures 3 and 4. The paleomagnetic data plot at this locality is on Figures 8, 9. (Paleocene magnetochron labels shown are corrected as discussed in the section of this paper labeled “Identification of Kirtland Formation-Ojo Alamo Sandstone Magnetochrons.”) Numbers at arrow heads are distances above base of Ojo Alamo Sandstone in meters; sample levels are approximate. Arrow heads pointing left indicate reversed polarity, arrow heads pointing right indicate normal polarity. Sample levels estimated from Figure 9, but exact original sample localities are not known.

of the paleomagnetic samples were collected from gray mudstone beds; sample 23.6, however, was from maroon-colored strata. All of the sample sites are on a relatively steep topographic slope (Figure 13).

Summary. As a result of their paleomagnetic and biochronologic studies of the rock strata adjacent to the Cretaceous-Tertiary (K-T) interface in the southern San Juan Basin, Lindsay et al. (1981) concluded that there was continuous deposition across it. They identified magnetochrons C31n, C30r, C30n, and the lower part of C29r in the Cretaceous Kirtland Formation beneath the K-T interface and found the upper part of C29r, C29n, C28r, and the lower part of C28n to be within the Ojo Alamo Sandstone, above the K-T interface. In addition, they identified chrons C27n, and C27r

higher in the Nacimiento Formation. Lindsay et al. (1981) thus determined that chron C29n was present in the lower part of the Ojo Alamo Sandstone at all four localities where they had conducted paleomagnetic traverses through that formation.

Lindsay et al. (1982)

Lindsay et al. (1982) reexamined their identification of magnetochron C29n in the Ojo Alamo Sandstone because they were apparently troubled by the fact that their data indicated (p. 449) “that the extinction of dinosaurs was not coincident with the extinction of marine organisms at the end of the Cretaceous Period, as recorded in several marine sequences.” They were also responding to numerous challenges to their earlier findings by Alvarez and Vann (1979), Fassett (1979), and Lucas and

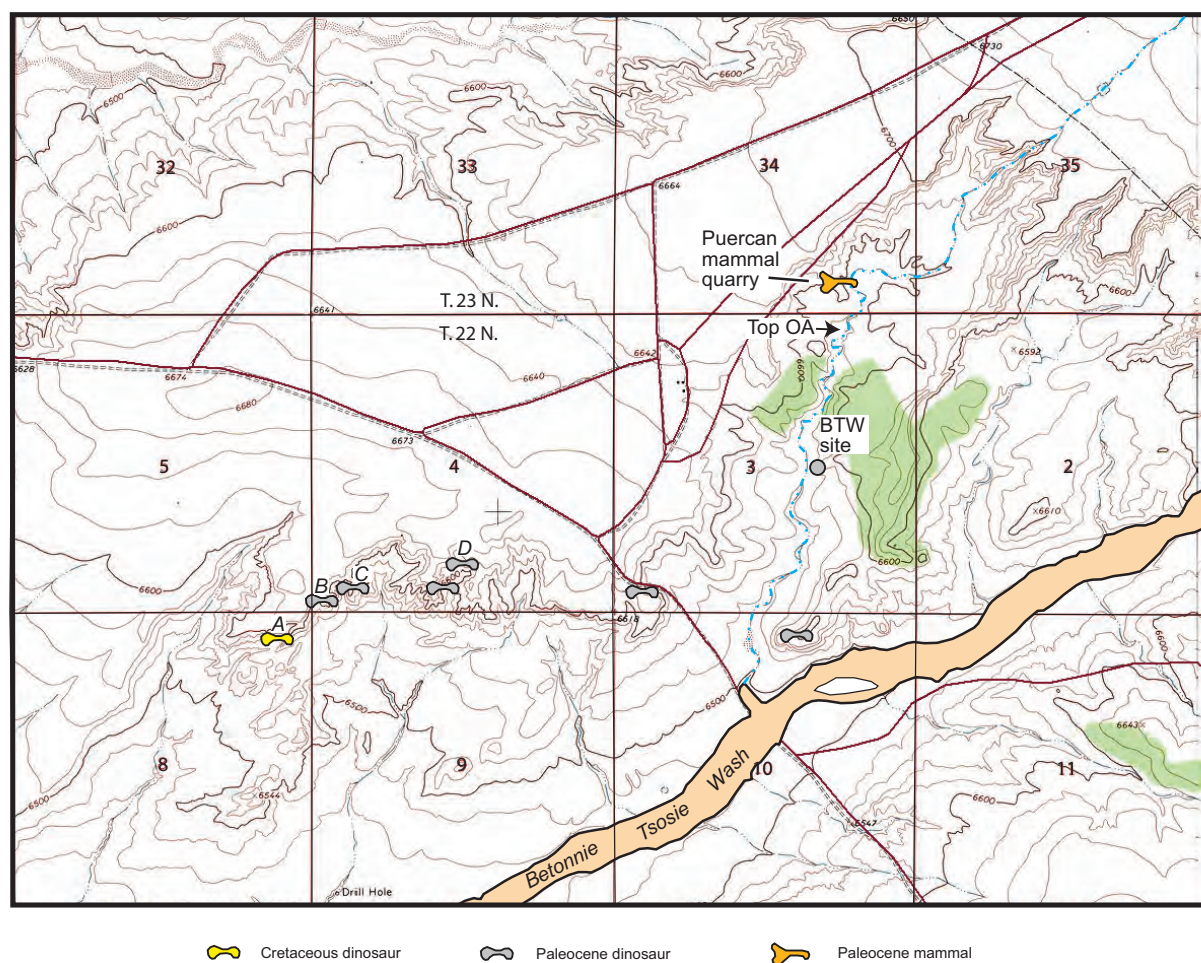


Figure 11. Map showing location of Bettonie Tsosie Wash (BTW) paleomagnetic section (“Tsosie Wash” locality of Lindsay et al. 1981). Also shown are places where mammal- and dinosaur-fossils have been found. Dinosaur-bone sample letters keyed to tables showing chemistry of bone samples collected from Cretaceous Kirtland Formation and Paleocene Ojo Alamo Sandstone; unlettered dinosaur-bone localities from Lucas and Sullivan (2000). Mammal-bone site is Bettonie Tsosie Wash locality of Williamson and Lucas (1992). Map from USGS 1:24,000-scale Kimbeto Topographic Quadrangle map.

Rigby (1979). Those criticisms primarily related to their conclusion that there had been continuous deposition across the K-T interface in contravention to numerous previous publications indicating that a substantial hiatus existed at this boundary. (Several papers in Fassett and Rigby 1987 subsequently presented evidence for a substantial hiatus at the K-T interface in the San Juan Basin.) Lindsay et al. (1981) were also criticized for stating that the K-T boundary in the San Juan Basin was not synchronous with the K-T boundary in the marine sequence near Gubbio, Italy. In their 1982 paper these authors reaffirmed their correlation of the normal-polarity interval in the lower part of the Ojo Alamo Sandstone with magnetochron C29n and

concluded (p. 451): “We believe that correlation is accurate, which implies *Paleocene dinosaurs lived in the San Juan Basin* [my emphasis].” They also reaffirmed their earlier contention that there was no significant hiatus at the K-T interface in the San Juan Basin.

In addition, Lindsay et al. (1982) stated: “We doubt that magnetochron + [C29n] is caused by a normal overprint . . .” and discussed tests of the reliability of their identification of the lower Ojo Alamo Sandstone normal chron, C29n. They stated that each of their sites that yielded normal remanent magnetic polarity in the Ojo Alamo Sandstone was represented by multiple samples, and that a statistical “test for nonrandom distribution” of

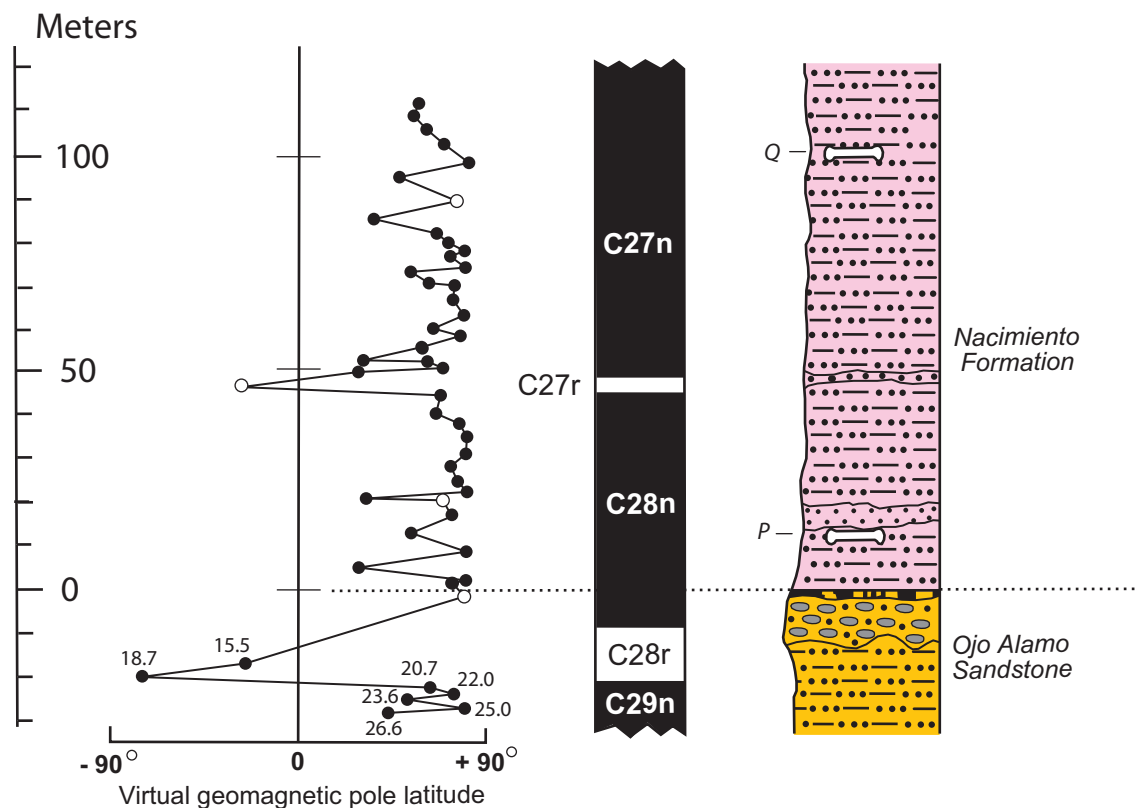


Figure 12. Paleomagnetic data plot and stratigraphic section at Bettonie Tsosie Wash locality, modified from Lindsay et al. 1981. Bettonie Tsosie Wash labeled “Tsosie Wash” in Lindsay et al. report. Q = fossiliferous interval containing *Periptychus*, Torrejonian age; P = fossiliferous interval containing Puercan mammals (listed in Lindsay et al. 1981). Distances of P and Q fossil levels above top of Ojo Alamo Sandstone and thickness of upper bed of Ojo Alamo Sandstone, are shown. Labeling of magnetochrons C29n, C28r, C28n, C27r, and C27n are also added as are distances, in meters, below top of Ojo Alamo Sandstone of selected paleomagnetic sample-collection sites. (Magnetochron labels shown are now known to be incorrect as discussed in section of this paper labeled “Identification of Kirtland Formation-Ojo Alamo Sandstone Magnetochrons.”)

their data showed that 87% passed this “rigorous test.” In a discussion of the minerals carrying the remanent magnetism in the Kirtland Formation and Ojo Alamo Sandstone in their study localities, they concluded that “the dominant ferromagnetic mineral in sediments of the San Juan Basin is detrital stoichiometric titanomagnetite in the 0.51 x 0.54 proportionality range.” They further determined that the Ojo Alamo Sandstone samples did contain a relatively high hematite content but that this higher hematite content existed in both normal and reversed polarity intervals in the Ojo Alamo and stated that “The available data do not favor an overprint origin for magnetozone + [C29n].” They concluded: “Thus, the available data suggest that magnetozone + [C29n] in the San Juan Basin is reliable, and we continue to correlate it with magnetic anomaly 29.”

Butler and Lindsay (1985)

Butler and Lindsay (1985) published the results of further tests of possible overprinting of the normal-polarity interval in the lower part of the Ojo Alamo Sandstone. However, they stated (in some parts of this paper) that the normal interval C29n (labeled + in their report) was in the Kirtland Formation rather than in the Ojo Alamo Sandstone, contrary to the placement of this magnetochron in the Ojo Alamo Sandstone in all of their previous publications. Normal chron C29n (also designated “C+”) is clearly shown to be within the Ojo Alamo in their 1981 paper.

Butler and Lindsay (1985) offered no explanation as to why they considered chron C29n to be in the Kirtland Formation in this report. Adding to the confusion, they show this normal to be in the Ojo Alamo in figure 7 of their 1985 paper, even though

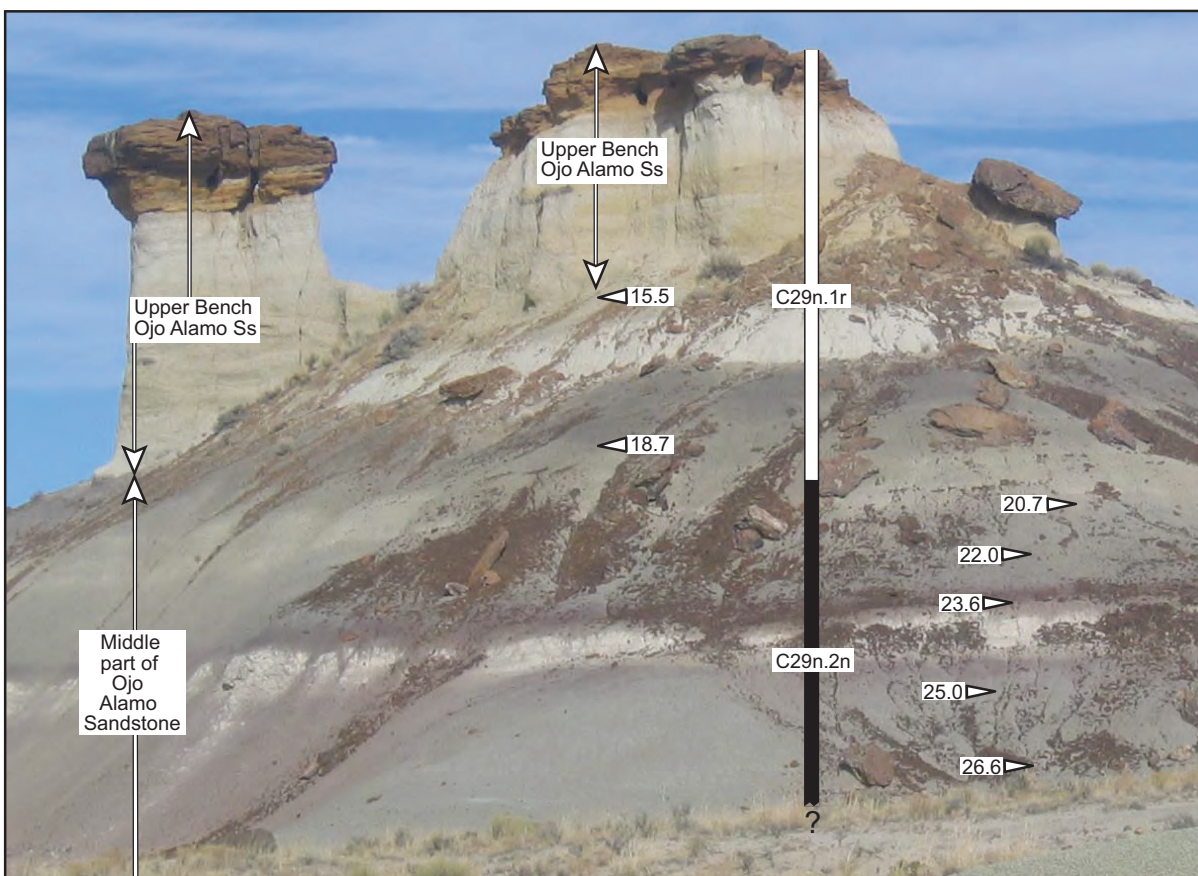


Figure 13. Photograph of Betonnie Tsosie Wash paleomagnetic locality, looking north (“Tsosie Wash” of Lindsay et al. 1981.) Locality is just east of north-trending tributary of Betonnie Tsosie Wash (Figure 11), about 28 km southeast of Barrel Spring locality (Figure 4). Magnetochron labels shown are corrected as discussed in section of this paper labeled “Identification of Kirtland Formation-Ojo Alamo Sandstone Magnetochrons.” Numbers at arrowheads are distances in meters below base of iron-cemented cap rock of upper bench of Ojo Alamo Sandstone. Arrow heads pointing left indicate reversed polarity; arrowheads pointing right indicate normal polarity. Paleomagnetic data plot at this locality shown on Figure 12. Sample levels estimated from Figure 12, but exact original sample sites not known. Lindsay et al. (1981) placed base of upper Ojo Alamo Sandstone at base of hard, iron-cemented-sandstone cap rock at this locality, however, as figure shows, this cap rock is just a harder layer at top of upper bench of Ojo Alamo Sandstone.

they state in their figure 7 caption that this figure shows: “Paleomagnetic data from re-recollections of the three sections *below* [my emphasis] Ojo Alamo Sandstone on South Mesa originally used by Lindsay et al. (1981) to define Magnetozone + [C29n].” Because of these conflicting statements, it is not possible to assess with certainty where in the measured sections the “re-recollections” discussed by these authors were made.

The 1985 paper by Butler and Lindsay contains a comprehensive discussion of the magnetic minerals that carry the normal-polarity signal in the Ojo Alamo Sandstone at the South Mesa, Barnum Brown Amphitheater, and Barrel Spring Arroyo sections (Figure 4). (Curiously, there is no mention

in this paper of the normal-polarity interval identified in 1981 as C29n in the Ojo Alamo at their “Tsosie Wash” locality.) These authors concluded that their previous publications showing the presence of the normal-polarity interval C29n in the lower Ojo Alamo were in error, and stated that this normal interval was in reality a Bruhnes (present-day-normal) overprint, and thus should be removed from their San Juan Basin paleomagnetic section. As a consequence of the elimination of C29n, these authors were forced to re-number the several other magnetochrons they had previously identified overlying it, by changing the next-highest normal from C28n to C29n, changing C27n to C28n, etc. Butler and Lindsay (1985) concluded

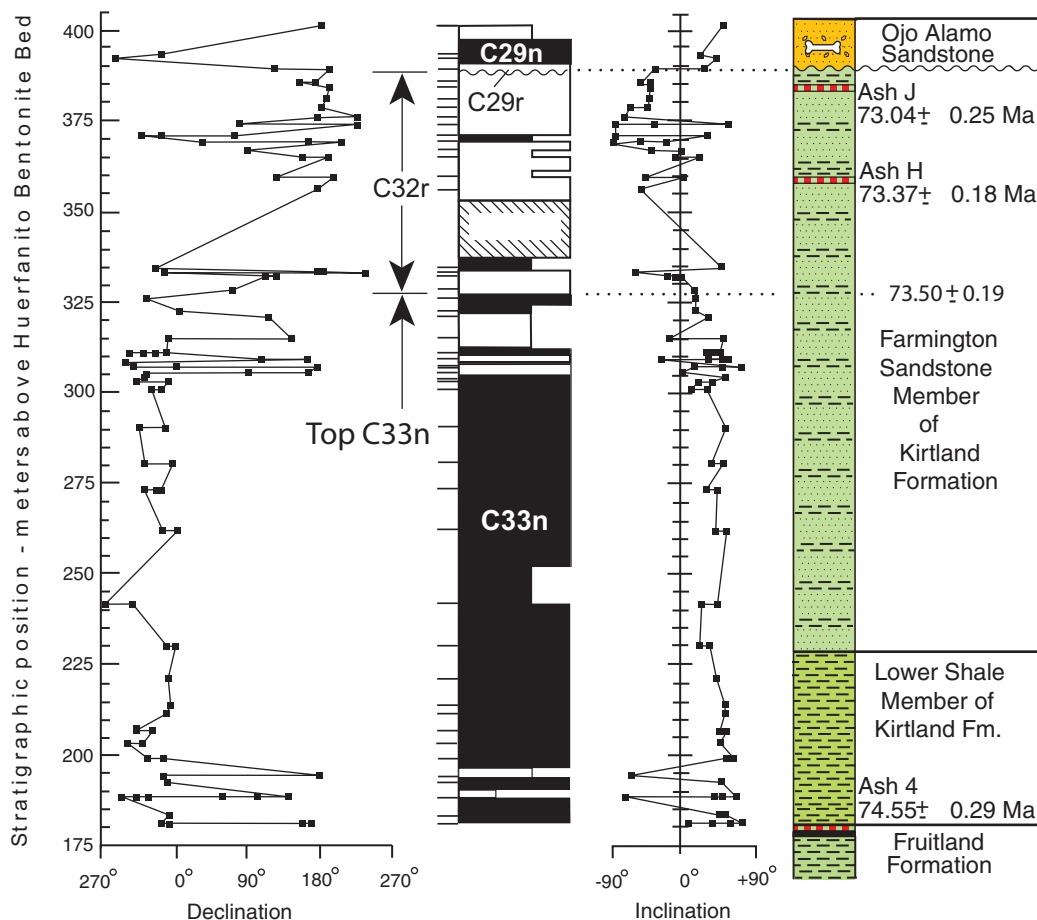


Figure 14. Paleomagnetic data plot of Fassett and Steiner (1997, figure 2), and Fassett (2000, figure 11) at Hunter Wash locality (Figures 3, 4). Magnetic-polarity chron labels are added. (Label for chron C29n revised as discussed in section of this paper labeled “Identification of Kirtland Formation-Ojo Alamo Sandstone Magnetochrons.”) Full column width indicates Cretaceous or Paleocene magnetization, two-thirds column width indicates probable Cretaceous or Paleocene magnetization, one-third column width means there is some indication of Cretaceous or Paleocene magnetization.

that the dinosaur fossils in the Ojo Alamo Sandstone were Cretaceous in age, and they continued to maintain that there was no significant hiatus at the Cretaceous-Tertiary boundary in the San Juan Basin. The question of the validity of the remanent paleomagnetism of the normal interval in the lower Ojo Alamo Sandstone is further addressed in a subsequent section of this paper.

Fassett and Steiner (1997) - Hunter Wash Paleomagnetic Section

The Hunter Wash paleomagnetic section of Fassett and Steiner (1997) is in the southwestern part of the San Juan Basin in Hunter Wash and in the headwaters of a northwest-trending tributary of Hunter Wash (Figures 2, 4). The paleomagnetic data plot for the Hunter Wash section is on Figure 14. The upper part of this section through the

uppermost Kirtland Formation and lower part of the Ojo Alamo Sandstone is shown at an expanded scale on Figure 15. This figure shows reversed remanent magnetism 4 m below the base of the Ojo Alamo in the Upper Cretaceous Kirtland Formation, a reversed polarity site 0.8 m above the base of the Paleocene Ojo Alamo Sandstone, two normal-polarity sites higher in the Ojo Alamo, and a reversed site 14.2 m above the base of the Ojo Alamo. Thus, the normal-polarity interval (lower part of C29n) is 7.1 m thick here and is bracketed by reversed-polarity intervals within the Ojo Alamo. The Ojo Alamo Sandstone is mostly sandstone at this locality without the distinct lower conglomerate and middle “shaly” parts found at the South Mesa, Barnum Brown Amphitheater, and Barrel Spring Arroyo localities.

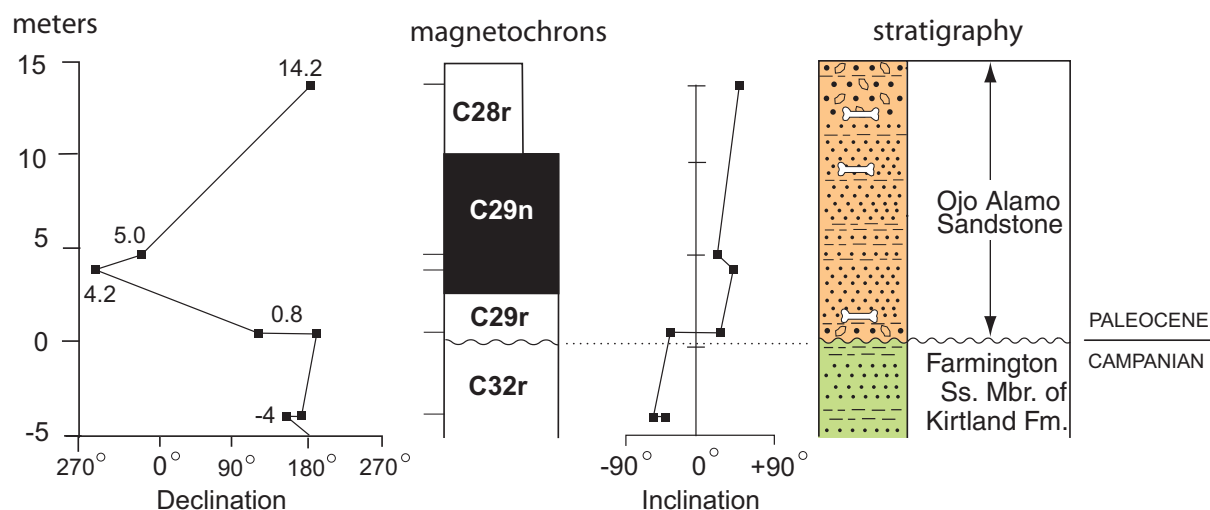


Figure 15. Large-scale view of Hunter Wash paleomagnetic section (HW on Figures 3, 4). Stratigraphic levels of sample-collection sites for paleomagnetic analysis are shown in meters above or below the base of the Ojo Alamo Sandstone. Plot is expanded-scale rendition of upper part of Hunter Wash section of Fassett (2000) of Figure 14. (Magnetochron labels for intervals shown as C29n and C28r are revised as discussed in section of this paper labeled "Identification of Kirtland Formation-Ojo Alamo Sandstone Magnetochrons.")

Figure 16 is a photograph of the Ojo Alamo Sandstone outcrop at the Hunter Wash locality. The sandier nature of the lower part of the Ojo Alamo is readily apparent in this photograph. Relatively few rock samples suitable for paleomagnetic analysis could be obtained in the Ojo Alamo at this locality because of the paucity of fine-grained mudstone layers here. The stratigraphic levels of paleomagnetic sample sites on Figure 15 are shown on this photograph. All of the samples collected here were from thin, gray, mudstone beds on relatively gentle slopes. One of the Ojo Alamo Sandstone dinosaur bones collected for chemical analysis (specimen 022899-OA1, discussed in a subsequent section of this report) was found about 30 m east of the area shown on Figure 4 and 7.3 m above the base of the Ojo Alamo Sandstone. This bone is within magnetochron C29n.

Identification of Kirtland Formation-Ojo Alamo Sandstone Magnetochrons

Figure 17 is a nearly 40 km long stratigraphic cross section from Hunter Wash to Betonnie Tsosie Wash through the Upper Cretaceous Kirtland Formation and Paleocene Ojo Alamo Sandstone in the southwestern part of the San Juan Basin. This cross section illustrates the relations of the five paleomagnetic sections discussed above. Reversal boundaries are placed at the midpoint between the nearest-to-the-reversal-boundary data points.

The remarkable thing about this cross section is that it shows that every published paleomagnetic section through the Ojo Alamo Sandstone in the southern San Juan Basin reveals the presence of a normal-polarity interval in the lower part of the Ojo Alamo. At two of the localities: HW and BBA, this normal interval is bracketed within the Ojo Alamo by reversed-polarity intervals. At two other localities: SM and BTW, either the top or base of the normal interval was not determined. And at one locality: BSA, the base of this normal is not bracketed within the Ojo Alamo.

The number of paleomagnetic sample sites defining this normal interval varies from two to five. The average thickness of the normal interval, as shown, is 9.1 m; the average thickness at the localities where the normal's top and bottom were determined is 9.6 m; normal-polarity-interval thicknesses range from at least 5.9 m at the South Mesa locality (top not determined) to 12.8 m at the Barrel Spring locality. Thicknesses for the reversed-polarity interval C29r (between the base of C29n and the base of the Ojo Alamo) range from 1 m at Barrel Spring to 5.3 m at the South Mesa locality, and average 3.3m. (Labels of magnetochrons on Figure 17 are shown as indicated by Lindsay et al. 1981 and Fassett and Steiner 1997; a revised labeling scheme for these magnetochrons is recommended in the "Revision of Paleo-

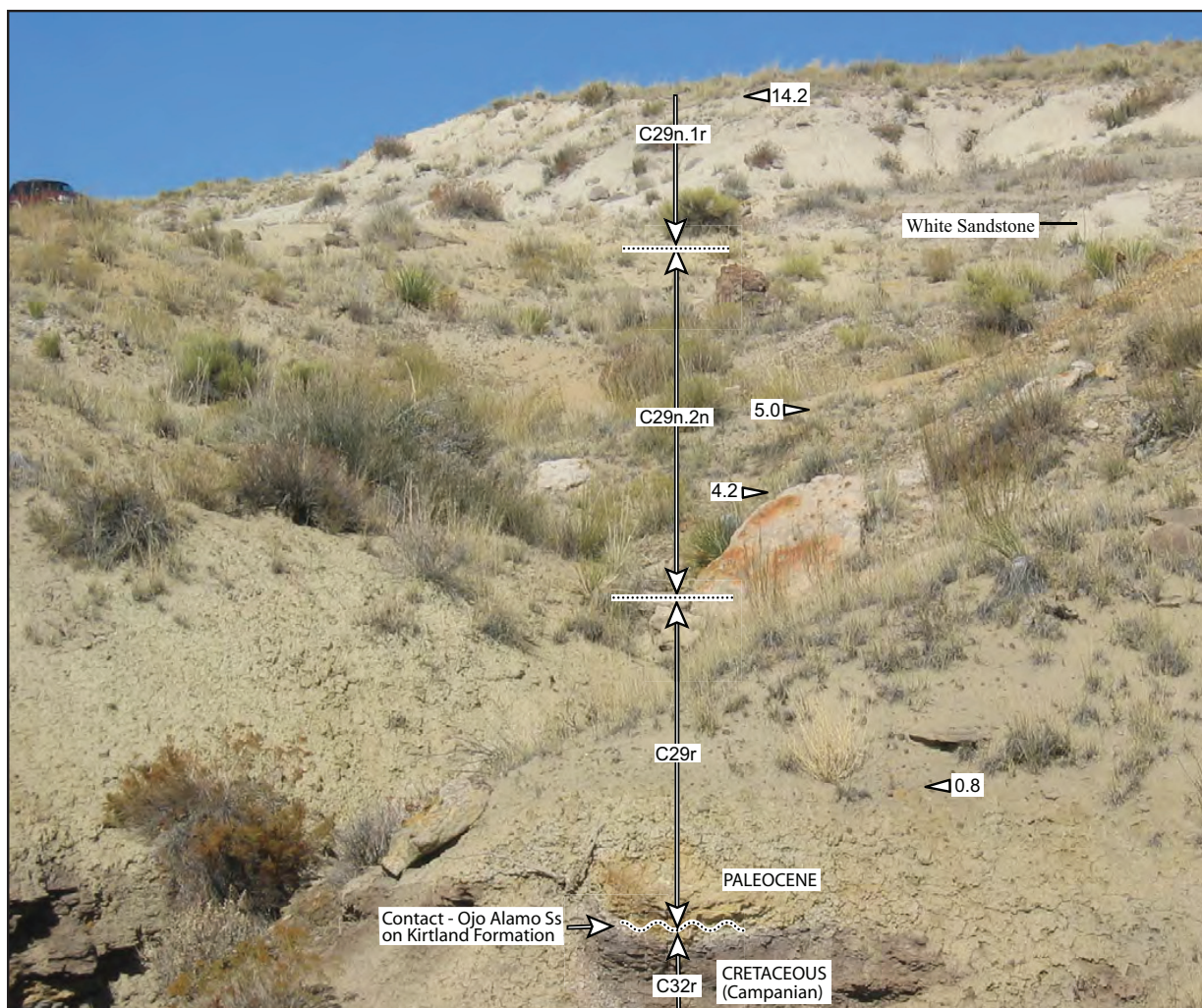


Figure 16. Photograph of Ojo Alamo Sandstone near head of tributary of Hunter Wash (looking north); location is shown on Figures 3 and 4. Dinosaur-bone locality 022899-OA1 (Figure 4) is near base of white sandstone bed shown in upper right of photograph and is about 30 m to southeast. This dinosaur-bone collection site is 7.3 m above base of Ojo Alamo Sandstone. Sample levels of paleomagnetic data points are shown in meters above base of Ojo Alamo Sandstone; arrowheads pointing left indicate reversed polarity, arrowheads pointing right indicate normal polarity. Stratigraphic levels of samples are relatively accurate, as shown, but locations are not exact. Magnetochron labels are corrected as discussed in section of this paper labeled “Identification of Kirtland Formation-Ojo Alamo Sandstone Magnetochrons.” Note vehicle in upper left on skyline for scale. See Figures 14 and 15 for paleomagnetic data plots for this area.

cene-Magnetochron Designations” section of this report.)

The sample-collection methodology of Fassett and Steiner (1997) at Hunter Wash was different from that of Lindsay et al. (1981) at the South Mesa, Barnum Brown Arroyo, Barrel Spring Arroyo, and Betonnie Tsosie Wash localities. The Fassett and Steiner samples consisted of oriented drill cores of the rock, whereas Lindsay et al. (1981) carved out oriented blocks of rock for their samples. In addition, samples were processed dif-

ferently in different labs on different instruments at different times. The samples for the Fassett and Steiner (1997) Hunter Wash study were obtained at a locality 9 km west of the closest part of the Lindsay et al. (1981) section (Figures 3, 4). In spite of these differences, the patterns of remanent magnetic polarity resulting from these independent studies are virtually identical. Figure 18 shows a comparison of paleomagnetic data plots from Fassett and Steiner (1997) and Lindsay et al. (1981).

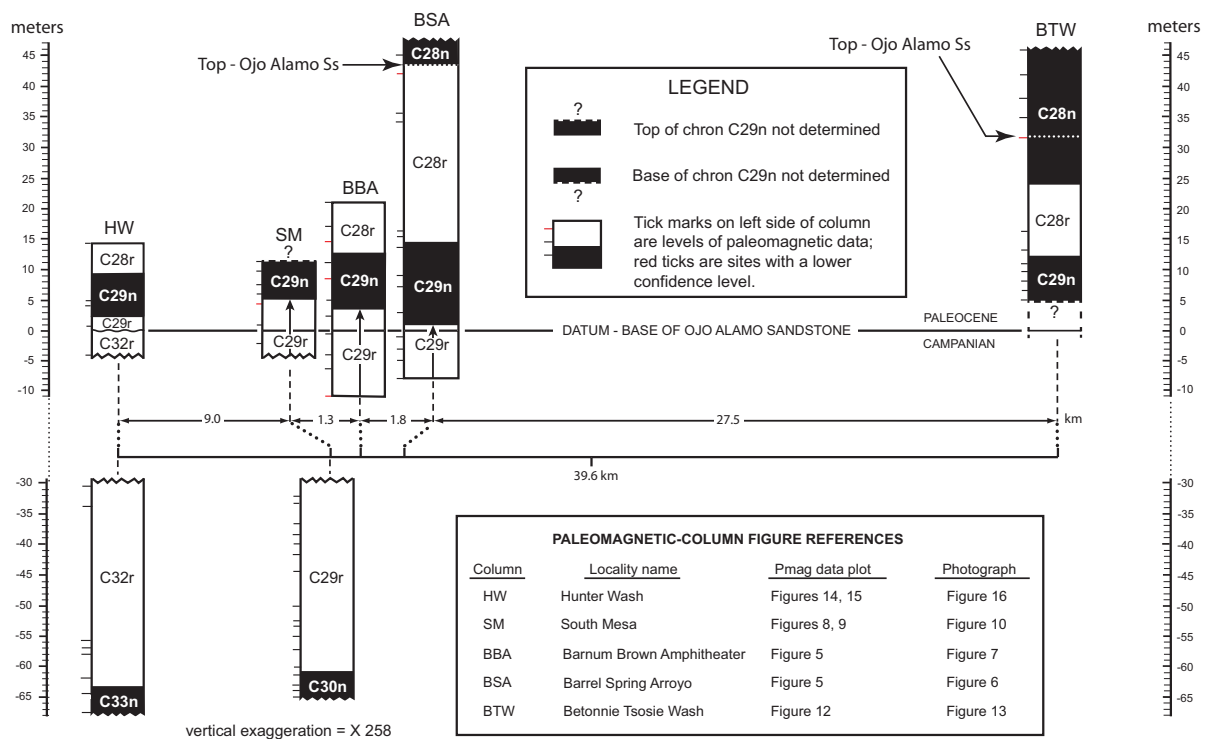


Figure 17. Cross section through five published paleomagnetic sections in southwestern San Juan Basin. (Section localities are shown on Figures 3 and 4; full data plots for all sections are on the figures indicated.) Section HW from Fassett and Steiner (1997), four other sections from Lindsay et al. (1981); labels of magnetochrons and top of Ojo Alamo Sandstone are as shown by those authors. (Some magnetochron labels shown are now known to be incorrect as discussed in section of this paper labeled "Identification of Kirtland Formation-Ojo Alamo Sandstone Magnetochrons.") Columns are broken by a gap of 25 m to show position of top of chron C33n (C30n of Lindsay et al. 1981) at Hunter Wash and South Mesa localities at a reasonable scale. Alignment of column BTW is based on field measurements of distance from lowermost C29n data point to base of Ojo Alamo Sandstone at BTW locality.

(For ease of discussion, these sections are referred to as HW and HW/AW, respectively.)

Just above the top of C33n in the HW plot at 335 m (Figure 18), there is a thin normal interval and on the HW/AW plot a similar thin normal is present. Just below the top of the HW C33n normal chron, there is a thin reversed interval, and on the HW/AW plot at about the same level, there is a single-site polarity excursion that almost reaches reversed polarity. At the 370 m level there is the suggestion of a thin normal interval on the HW data plot; at exactly the same level on the HW/AW data plot, two data points represent an excursion toward normal polarity. Gradstein et al. (2004) showed a thin normal interval above C33n labeled C32r.1n with a duration of 0.087 m.y.; this chron is separated from the top of C33n by a reversed-polarity interval (C32r.2r) of 0.239 m.y. duration. It is possible, therefore, that the thin normal interval at 370 m on the HW plot is chron C32r.1N. On both the HW and HW/AW paleomagnetic plots, thin reversed

polarity intervals are present within chron C33n at the 188-195 m interval on the HW plot. Within this interval there are two thin reversals on the HW plot and only one on the HW/AW plot; this difference could be an artifact of the more closely spaced samples collected at the HW locality. Gradstein et al. (2004) did not show this reversed interval in magnetochron C33n, probably because the much slower rates of crustal formation at the mid-Atlantic ridge did not allow this thin reversal to be recognized.

There has been reluctance on the part of some paleomagnetists to fully embrace the potential of paleomagnetic studies of sedimentary rocks because of the possibility of overprinting of hematitic minerals incorporated within those strata, but the close agreement in the results of the two independent paleomagnetic studies discussed above demonstrates that such strata did accurately record and preserve the remanent magnetic polar-

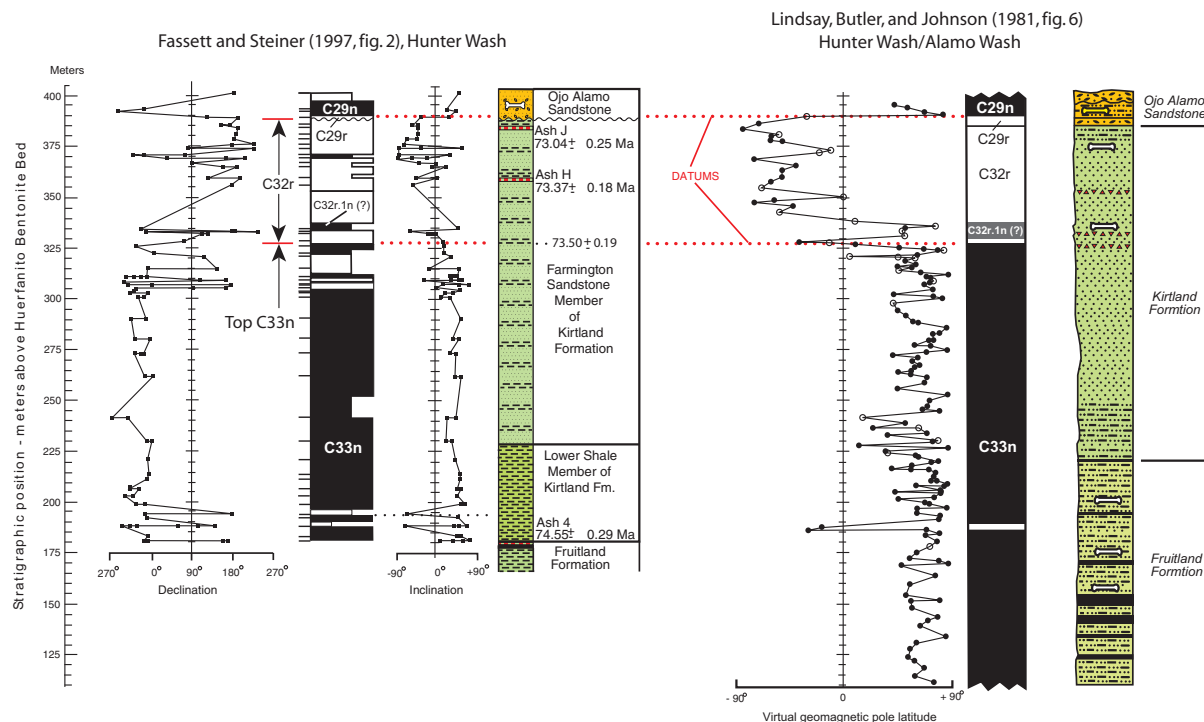


Figure 18. Comparison of independent paleomagnetic studies at two nearby sections in type area of Ojo Alamo Sandstone in southwestern San Juan Basin (see Figure 4 for locations); the two localities are 9 km apart; modified from Lindsay et al. 1981. The two sections are aligned on top of chron C33n and base of chron C29n. Chron labels on Lindsay et al. figure are corrected from their original designations as discussed in section of this paper headed “Identification of Kirtland Formation-Ojo Alamo Sandstone Magnetostratigraphy.”

ity of the earth’s magnetic field at the time those rocks were deposited.

Because the Ojo Alamo Sandstone was deposited on an erosion surface, using the base of the Ojo Alamo as a horizontal datum (Figure 17) is misleading for comparing thicknesses of the Ojo Alamo normal intervals at the five localities. Figure 19 reconfigures the upper part of this cross section using the base of the Ojo Alamo normal interval—a time horizon—as a datum. The boundaries of the Ojo Alamo normal interval are adjusted on Figure 19, to the extent reasonably possible, to make these intervals as close as possible to the same thickness at each locality, while still honoring the sample-polarity data. In addition, the SM and BTW normal intervals are extended to match the tops and bases of the adjacent normal intervals. The results of this interpretation show that the Ojo Alamo Sandstone normal-polarity interval is about 11 m thick at all localities, and the maximum relief on the pre-Ojo Alamo erosion surface is about 4 m. These thicknesses are reasonable because the rates of sediment accumulation across this relatively small area were probably uniform, thus the thickness of the Ojo Alamo normal at these localities should be nearly the same.

Figure 20 is a modification of figure 7 of Butler and Lindsay (1985). These authors stated that: “Data from sites where evidence indicates normal polarity VRM [viscous remanent magnetism] overprinting are indicated with lines through the data points.” but they are unclear as to why these particular sites were considered to be overprinted. Note that the Barrel Spring and South Mesa localities are shown (Figure 20) to contain two “overprinted” normal sites, and the Barnum Brown section has one “overprinted” normal site. Butler and Lindsay (p. 543) stated that one of the features “crucial” to their interpretation was that “these reversed polarity sites occur throughout the stratigraphic interval from which + [C29n] was originally defined..

This statement is puzzling because there is only one reversed-polarity site shown within their original C29n chron, and that site is at the Barnum Brown locality (Figure 20, site 7). The reversed-polarity site shown on this figure is at exactly the same level as a reversed-polarity site shown to be present at Barnum Brown by Lindsay et al. (1981) on their figure 7 (Figure 5 of this report), and the significance of this reversed site at that locality was discounted in the Lindsay et al. (1981) report. Therefore the “crucial” evidence purporting to dis-

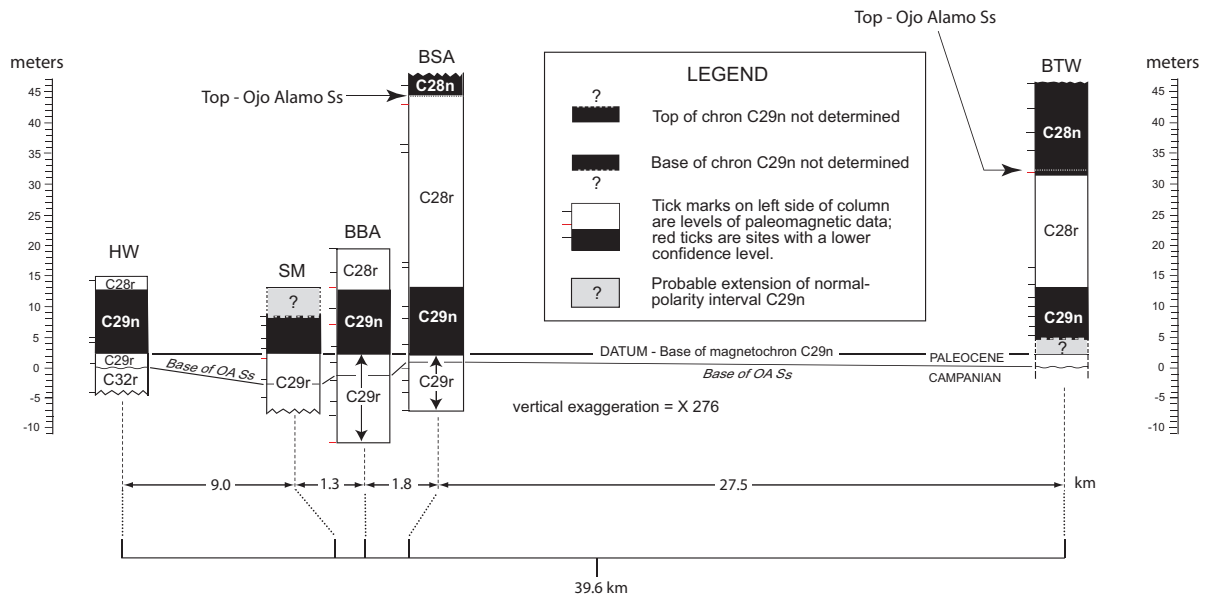


Figure 19. Stratigraphic cross section through five paleomagnetic sections in southwestern San Juan Basin (modified from Figure 17) using base of magnetochron C29n instead of base of Ojo Alamo Sandstone as a datum. Column localities shown on Figures 3 and 4. Column headings and figure references described on figure 17. Section HW from Fassett and Steiner (1997), four other sections from Lindsay et al. (1981); labels of magnetochrons are as shown by those authors. Alignment of column BTW based on field measurements of distance from lowermost C29n data point to base of Ojo Alamo Sandstone at BTW locality. (Some magnetochron labels shown are now known to be incorrect as discussed in section of this paper labeled “Identification of Kirtland Formation–Ojo Alamo Sandstone Magnetochrons.”)

prove the presence of normal-polarity interval C29n in the lower part of the Ojo Alamo was not provided in Butler and Lindsay (1985).

Butler and Lindsay (1985), in their reexamination of the paleomagnetic-normal interval in the Ojo Alamo Sandstone at South Mesa, Barnum Brown Amphitheater, and Barrel Spring Arroyo, concluded that their earlier determinations that this normal represented true remanent magnetism were in error. Instead, they stated that this normal interval represented a present-day, normal-field overprint that should be removed from their paleomagnetic sections in the southern San Juan Basin. They offered no mechanism for how present-day normal overprinting might have occurred at these three separate localities. Photographs of the Ojo Alamo Sandstone at these localities (Figures 6, 7, 10) show that the exposures are all in barren badlands that are eroding at a relatively rapid rate. Because samples for paleomagnetic analysis by Lindsay et al. (1981) and Fassett and Steiner (1997) were collected from fresh bedrock, never more than 1 m below the surface, any present-day normal overprinting would have had to occur within the last thousand years or so, at most. Thus, there is no conceivable mechanism for such overprinting of a

normal-polarity interval in the lower Ojo Alamo, with virtually identical thicknesses, at three topographically different and separate localities. Moreover, normal intervals at two localities are overlain and underlain by reversed-polarity sites making it extremely unlikely that an 11 m thick interval in the lower part of the Ojo Alamo could have been overprinted by the present-day normal magnetic field while the overlying and underlying rocks, also containing titanohematite, were not similarly overprinted. Thus, the Butler and Lindsay (1985) contention that the Ojo Alamo normal interval at the three South Mesa localities is a present-day normal overprint is rejected.

Lindsay et al. (1981) also identified a paleomagnetic normal interval in the lower Ojo Alamo Sandstone at the Bettonie Tsosie Wash locality. The presence of this normal interval was not questioned in the Butler and Lindsay (1985) paper, thus it can only be concluded that these authors believed that the Ojo Alamo normal interval at this locality, at least, did represent true Paleocene remanent magnetism. All available evidence shows that the paleomagnetic-normal interval present within the Ojo Alamo Sandstone at the five localities discussed herein, must represent true

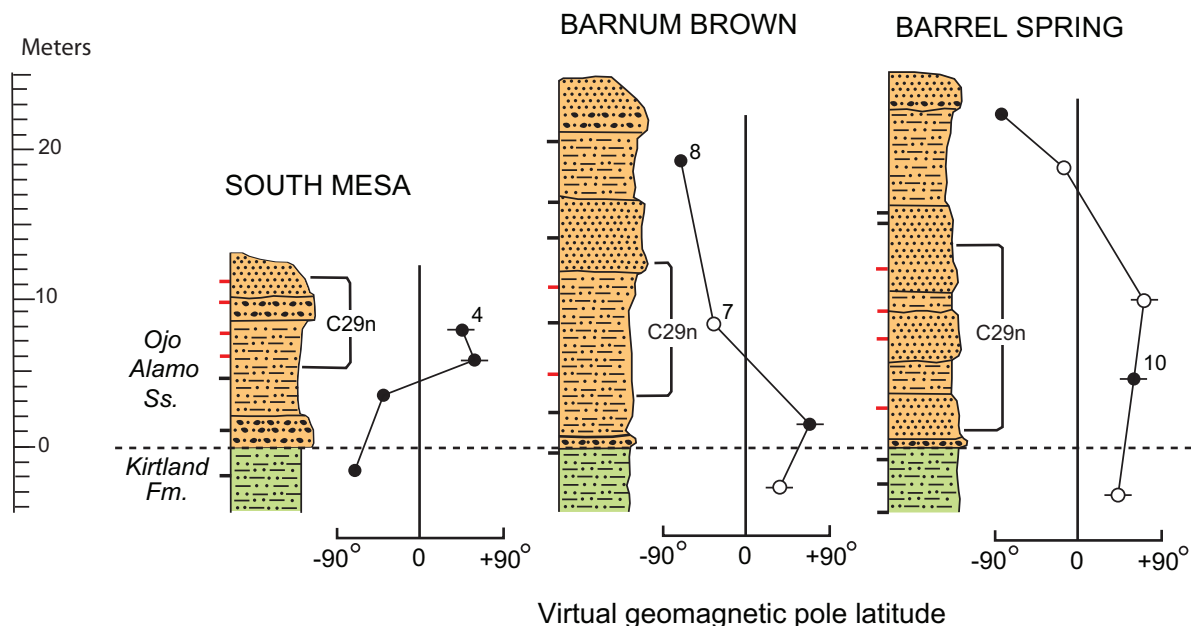


Figure 20. Stratigraphic columns and paleomagnetic plots at South Mesa, Barnum Brown Amphitheater, and Barrel Spring Arroyo (Figure 4), modified from Butler and Lindsay (1985). Figure shows positions of original paleomagnetic normal intervals (C29n) of Lindsay et al. (1981). Tick marks on left side of columns show levels of original sample sites of those authors; red tick marks indicate sites with normal polarity.

Paleocene remanent magnetism. Thus, the presence of paleomagnetic normal interval C29n in the lower part of the Ojo Alamo Sandstone confirms its Paleocene age. In addition, because the base of magnetochron C29n has an age of 65.12 Ma (Gradstein et al. 2004) and because the base of this chron is near the base of the Ojo Alamo, the age of the base of the Ojo Alamo can be estimated to be about 65.2 Ma. These findings are further supported by paleomagnetic data obtained at Mesa Portales, as discussed below.

Mesa Portales Study Area

Geography and Stratigraphy. Mesa Portales is about 17 km southwest of Cuba, New Mexico (Figures 3 and 21). The mesa is capped by the Paleocene Ojo Alamo Sandstone, which forms a gentle dip slope (from 1 to 1.5 degrees) dipping to the north; the south edge of the mesa is a steep, south-facing, 130 m high cliff face. The Upper Cretaceous Lewis Shale, Pictured Cliffs Sandstone, and the undivided Fruitland and Kirtland Formations underlie the Ojo Alamo and are well exposed at this locality. These exposures are within the Mesa Portales study area (Figure 21). Fassett (1966) mapped the Ojo Alamo Sandstone on Mesa Portales and observed that it consisted of discontinuous, sheet-like, “overlapping massive beds of

light- to rusty-brown fine- to coarse-grained sandstone that contain scattered silicified wood and conglomerate and are separated by light- to dark-gray and green shale.”

In the photograph of the Mesa Portales study area (Figure 22), the Ojo Alamo Sandstone is seen to consist of two sandstone benches; the upper bench is continuous whereas the lower bench pinches out to the east about one-third of the distance from the east edge of the photograph. On the geologic map of the Mesa Portales quadrangle (Fassett 1966), the base of the Ojo Alamo shifts from the base of the lower bench to the base of the upper bench where the lower bench pinches out. At other places on Mesa Portales, there are as many as five distinct sandstone benches included in the Ojo Alamo (Fassett 1966). Below the lowest sandstone bench (Figure 22) there is a discontinuous sandstone interval. This interval pinches out east and west of the area shown on Figure 22. Even though the base of this sandstone interval clearly marks the Cretaceous-Tertiary interface at this locality, in other areas where this lower sandy interval is not present, there is a shale-on-shale contact marking that interface. Because this lower sandy interval is not a distinct, continuous, mappable unit, it was not included in the rock-stratigraphic Ojo Alamo Sandstone on Mesa Portales of Fassett

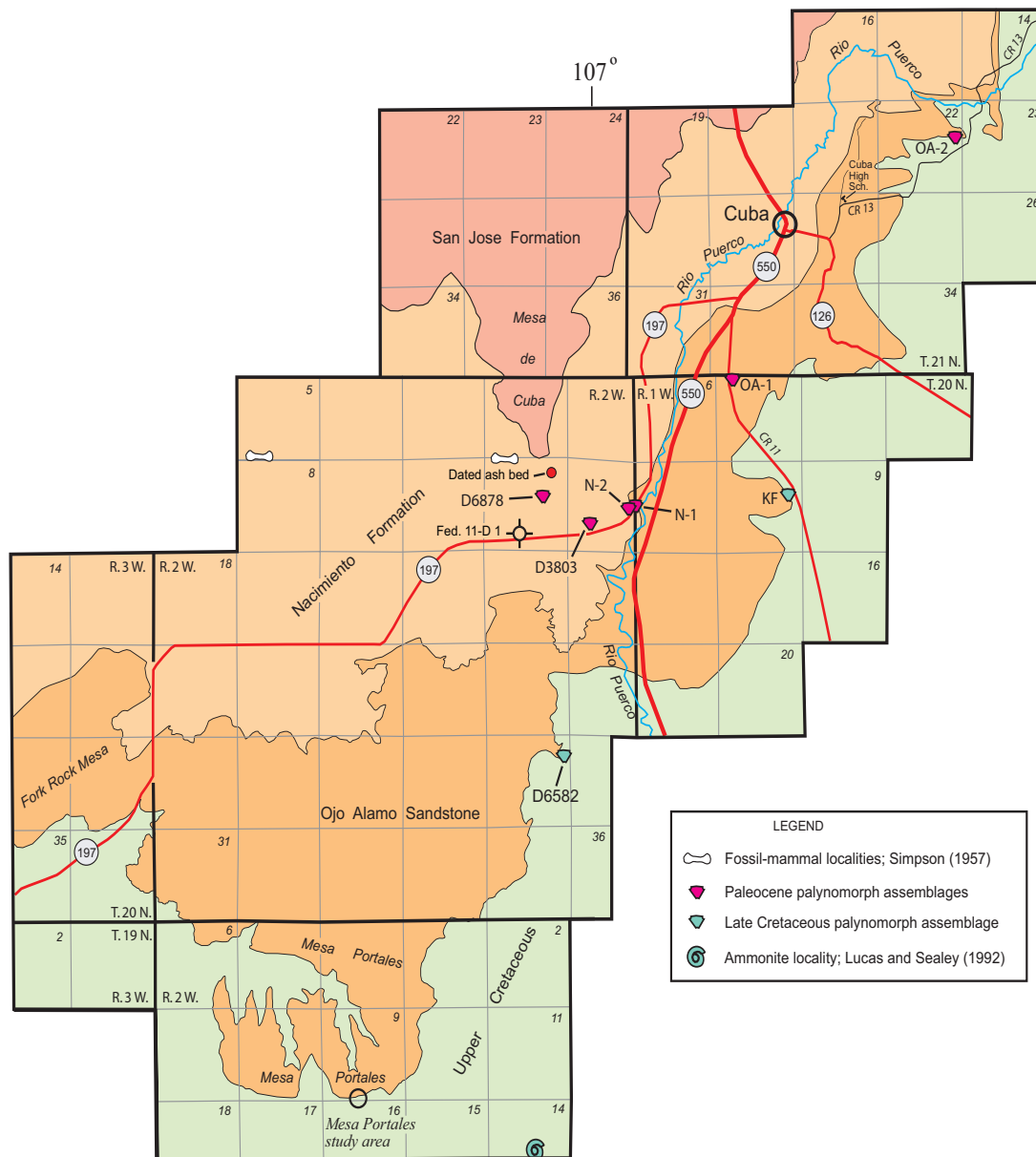


Figure 21. Geologic map showing outcrop of Ojo Alamo Sandstone in southeastern San Juan Basin (Figure 3). Mesa Portales study area contains paleomagnetic section across Cretaceous-Tertiary boundary and multiple USGS paleobotany localities through the same strata. OA-1, OA-2, KF, and N-1, N-2 (southwest and northeast of Cuba) are palynologic-collection localities of Anderson (1960). D6878, D3803, and D6582 are USGS paleobotany localities; palynomorphs from these sites are listed in the Appendix. Geology west of long. 107° W. and south of the northern boundary of T. 20 N. from Fassett (1966); geology for the rest of area from Baltz (1967).

(1966). A detailed discussion of the Ojo Alamo Sandstone on Mesa Portales is in Fassett and Hinds (1971, p. 29-31). The Fruitland-Kirtland interval is only 100 m thick in the Mesa Portales study area (Figure 23), whereas this interval is 400 m thick in the Hunter Wash area to the northwest (Figures 3, 14). The thinning of this interval south-

eastward along the south rim of the San Juan Basin is discussed in detail in a separate section of this report.

Paleomagnetic Analysis. Paleomagnetic sampling at Mesa Portales was conducted along a diagonal traverse (from lower left to upper right) up the face of the exposure shown on Figure 22. Sam-

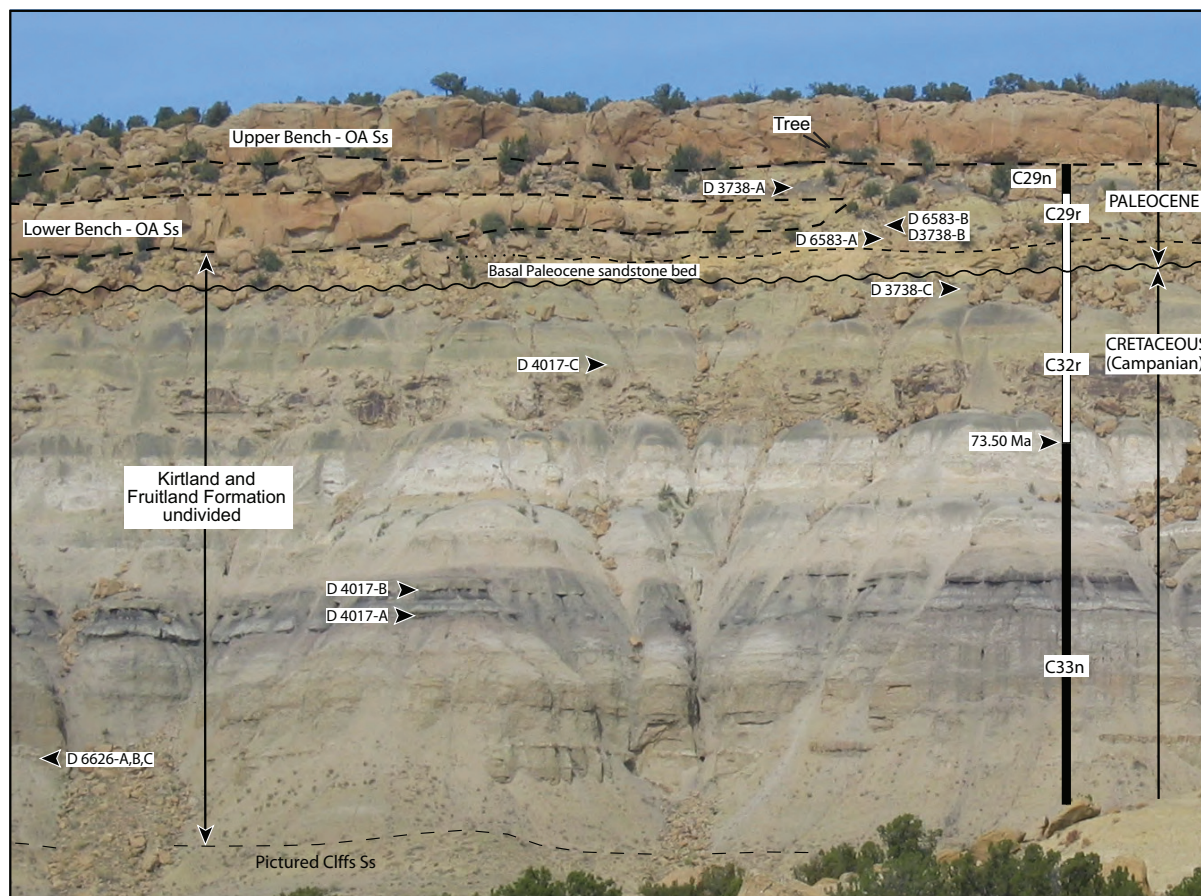


Figure 22. Photograph of south-facing cliff of Mesa Portales (Figures 1, 3, 21). Photograph annotated to show relevant chronostratigraphic data, sample-collection localities, geologic contacts, and names of geologic rock units. A paleomagnetic traverse was made up the face of this exposure, angling from the lower left to just below base of upper Ojo Alamo Sandstone bench in shadowed area just left of labeled tree. Palynologic sample-collection sites and USGS paleobotany locality numbers, such as D 4017-A, are shown with arrowheads. Sample locations are approximate; however, stratigraphic levels are accurately placed. Palynomorphs identified from these collection localities are listed in the Appendix.

ple collection was conducted by E.M. Shoemaker (USGS), M.B. Steiner (U. Wyoming), and the author in 1983; in 1988, Steiner and the author collected additional samples to fill in gaps in the original 1983 sampling. The only publication resulting from this work was an abstract by Shoemaker et al. (1984) summarizing the paleomagnetic data obtained at Mesa Portales in 1983. Figure 23 shows the paleomagnetic data plot and a stratigraphic column for the Mesa Portales locality. Digging through the weathered-rock rind down to unweathered bedrock was required at many sample sites, generally to depths of about 0.1 m or so, but in some places to a meter or more. Samples of the freshly exposed bedrock were obtained by core drilling.

The following discussion of the paleomagnetic analysis of Mesa Portales samples is slightly modified from a report by M.B. Steiner (personal commun., 1989).

Natural remanent magnetism (NRM) directions for Mesa Portales samples varied between Cretaceous normal, axial field, present field, and Late Cretaceous and early Paleocene reversed and normal directions. A reversal from normal polarity to reversed polarity was found in the NRM directions in the Cretaceous part of the section (Fruitland-Kirtland Formations) between 60 m and 68 m above the base of the sampled section (Figure 23); this reversal is estimated to be at the 64 m level (Figure 23). Another reversal, from reversed to normal polarity, was discovered in the Paleocene Ojo Alamo Sandstone between the 119 m

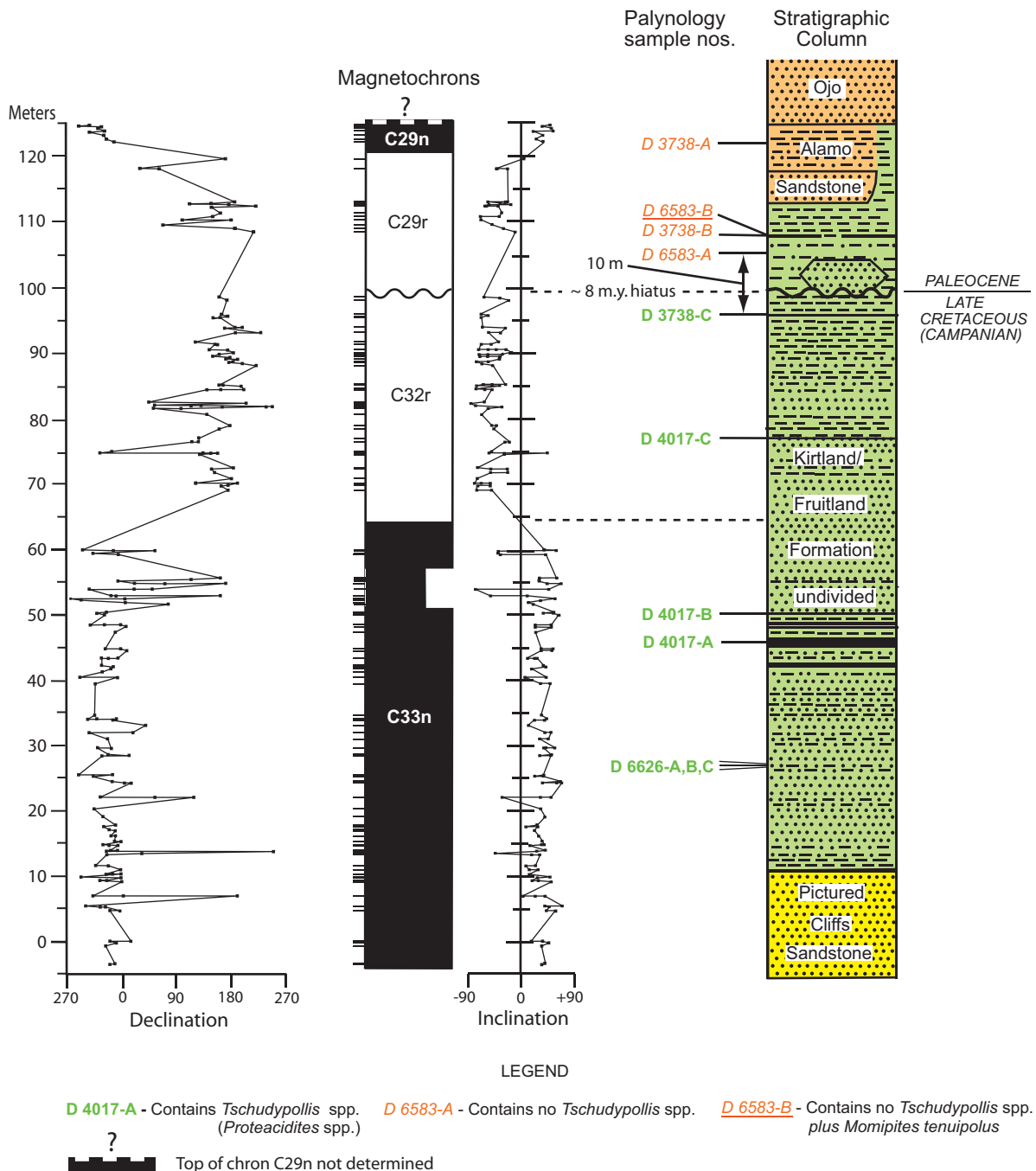


Figure 23. Paleomagnetic data plot and stratigraphic column at Mesa Portales, southeastern San Juan Basin, New Mexico (locality on Figure 21). Stratigraphy of section from Fassett (1966) and Fassett and Hinds (1971). Palynomorphs from rock samples from this section identified by R.H. Tschudy (personal commun., 1966, 1967, 1968, 1983, 1984); palynomorphs identified in tables in the Appendix. Paleomagnetic data plot provided by M.B. Steiner (personal commun., 1992). Samples for Mesa Portales paleomagnetic study were collected by E. M. Shoemaker, M.B. Steiner, and the author in 1983 and 1989; lab analyses of samples were conducted by Steiner and Shoemaker. On paleomagnetic column, full column width indicates latest Cretaceous-earliest Paleocene magnetization; two-thirds column width indicates probable latest Cretaceous-earliest Paleocene magnetization. An annotated photograph of section is Figure 22. Cretaceous index palynomorph *Tschudypollis* was originally named *Proteacidites*.

and 122 m levels (Figure 23); this reversal is placed at the 121 m level.

NRM intensities were typically 1×10^{-3} AIM (1×10^{-6} emu/cc). A small number of samples from both sandstone and mudstone beds had intensities of 1×10^{-2} AIM (10^{-5} emu/cc) and some ranged down to 1×10^{-4} AIM (10^{-7} emu/cc). Intensities of heavy-mineral laminae were as much as 2×10^{-1} AIM (2×10^{-4} emu/cc). NRM directions of these layers were clearly of Late Cretaceous-earliest Paleocene origin.

Pilot samples were demagnetized using alternating field (AF) and thermal demagnetization. Ten samples were AF demagnetized to 100 mT (1000 oe). Thirty samples were thermally demagnetized in steps of 25 degrees between 150° C and 400° C. Another 32 samples were thermally demagnetized to 200° C and then AF demagnetized to 15 mT. The remainder of the samples was thermally demagnetized in five steps between 170° C and 325° C. Subtracted vectors were computed between demagnetization steps, and characteristic directions were determined by a least-squares analysis of lines fit to the demagnetization trajectories.

AF demagnetization indicated a median demagnetizing field of between 12.5 and 20 mT. Demagnetization to as high as 100 mT, however, did not always engender stable directions and (or) decay to the origin of orthogonal axes plots. Thermal demagnetization was performed on specimens cut from the same core as the samples that were AF demagnetized. These data displayed the same direction as AF treatment for those samples for which AF caused decay to the origin; for those specimens that did not, thermal demagnetization revealed a trend (generally incomplete) toward an apparent reversed-polarity magnetization. Thermal demagnetization indicated a magnetization component stable between 200° C and 300° C, having antipodal directions.

Another group of samples was thermally demagnetized to 200° C and then AF demagnetized to 15 mT. The directions at 200° C are generally representative of the normal or reversed directions later shown to be characteristic from wholesale thermal demagnetization. Further demagnetization of the 200° C thermally demagnetized samples by AF demagnetization to 15 mT did not reduce intensities further nor induce any appreciable continuation of the demagnetization trend begun by thermal demagnetization. Further thermal demagnetization above 200° C generally removed an additional amount of magnetization

and continued the demagnetization trend begun below 200° C. In most cases, this demagnetization revealed a direction closer to the characteristic mean, but above 300° C an increasing dispersion of directions was observed. These findings indicate an antipodal magnetization with coercivities around 16 mT and unblocking temperatures between 200° C and 300° C and the presence of secondary magnetization(s) having higher coercivity and unblocking temperatures.

The greater effectiveness of thermal demagnetization dictated that the majority of samples be demagnetized by thermal means. As mentioned, the characteristic directions appeared to be held between 200° C and 300° C as is indicated in several ways: above 300° C, directions generally became erratic or diverged from a trend toward the origin. Moreover, visual inspection of the directions of the sample population at each temperature step indicated that the dispersion among directions began to increase at 300° C, and continued to increase with each succeeding temperature step. A 50% reduction in NRM intensity occurred between 200° C and 300° C for most normal, and some reversed, samples. Finally, the polarity sequences indicated by directions below 325° C is very simple, showing a well-defined change from normal to reversed polarity at 64 m above the base of the section in Cretaceous strata and from reversed to normal polarity at 121 m (Figure 23). The polarity sequences became more complex and stratigraphically inconsistent when directions above 300° C were considered.

Heavy mineral laminae in massive sandstone beds between about 70 and 84 m (Figure 23) were sampled extensively (21 samples). (These sandstone beds are the buff-colored beds seen just above the "C32r" label on Figure 22.) The samples generally had clearly defined reversed directions with only minor influence of secondary magnetization on the NRM and remanence held below 300° C. As in the other samples from Mesa Portales, the characteristic magnetization is held between 200° C and 300° C, above which the intensities diminish rapidly, and directions become more erratic. Several of the samples indicated the presence of two slightly different directions, one generally held below 300° C and the other above. The demagnetization trajectories of the heavy-mineral samples are more ragged than many other heavy-mineral laminae (Steiner 1983), which may reflect the superposition of the reversed overprint observed in the Mesa Portales section in general onto a pri-

mary reversed detrital or post-depositional remanence in these concentrates.

Curie temperatures were measured on the heavy mineral laminae collected at about 78 m above the base of the section. These displayed nearly reversible thermomagnetic curves with Curie/Neel temperatures of about 210° C. In a large-scale study of San Juan Basin sections, Lindsay et al. (1981) stressed the necessity of collecting mudstones to ensure that good magnetic remanences are obtained. The Cretaceous part of the Mesa Portales sequence (Figures 22 and 23) consists of mixed sandstone-mudstone lithologies and contains several massive sandstone beds in its upper part (Figure 22). To obtain an adequate sample-spacing pattern, large numbers of sandstone samples were collected in the section. Most of these samples were from the normal-polarity part of the section in the undivided Fruitland-Kirtland Formation. A comparison of directions and intensities of paleomagnetism of the mudstones and sandstones throughout the Mesa Portales stratigraphic section showed no differences in mean direction or polarity between the two lithologies. The uppermost (Paleocene) part of the Mesa Portales section is dominated by massive, cliff-forming sandstone beds (Figures 22 and 23); these beds were not sampled for paleomagnetic analysis.

Sample-site density for the entire section averaged about one site per meter except for two significant gaps between the 60 and 69 m level and the 98 to 108 m level (Figure 23). The lower 9 m gap is in the prominent white sandstone bed (Figure 22) that is above the coaly interval where the D-4017A, B palynologic samples were collected; the magnetic-polarity reversal from C33n to C32r falls within this white sandstone. The upper 10 m gap is mostly in the lower, sandy, Paleocene strata above the unconformity at the Cretaceous-Tertiary interface (Figure 22). When these two gaps are subtracted from the total-section thickness, sample-site spacing is about 0.80 m. Generally, three or more samples per site were collected.

The bulk of the paleomagnetic sample analysis was conducted by M.B. Steiner at the University of Wyoming paleomagnetism lab. Samples from selected intervals were also processed at the Caltech paleomagnetism lab by Joe Kirschvink for E.M. Shoemaker. Shoemaker stated (personal commun., 1984):

Enclosed is a listing of results on the Mesa Portales samples run at Caltech in Joe Kirschvink's laboratory. All samples

were thermally damaged [demagnetized] first at 150° C, so we have a good record for this temperature. All of these (except KMP 0.01) were also damaged at 200° C; in all cases the shift in direction from 150° to 200° C is relatively small and the loss of magnetization less than 50%, usually much less than 50%. Hence, demagnetization to 200° C does not appear to be pushing too deep to retain the stable component of primary magnetization (Curie T = 180° C to 300° C according to Butler["Butler" refers to Butler and Lindsay 1985]). All samples were also AF demagnetized in steps to 150 Oe. Only samples 175.61 [54 m] and 183.0 [56 m] seemed to shift significantly toward the opposite polarity at these low fields.

The two samples at 54 m and 56 m (Figure 23) that "seemed to shift significantly toward the opposite polarity" are at about the same level below the top of C33n as the thin reversed-polarity interval seen at the Hunter Wash section (Figure 18).

Paleomagnetic Data Plot. The final plot of the magnetic polarity of the samples from Mesa Portales (Figure 23) incorporates both Steiner's and Shoemaker's data. This plot shows the presence of a normal-polarity interval from the base of the section in the Pictured Cliffs Sandstone to the 64 m level in the Fruitland-Kirtland sequence (Figure 23). This normal-polarity interval is overlain by a reversed-polarity interval extending to the K-T interface at the 100 m level. Another reversed-polarity interval extends from the K-T interface to just above the 120 m level; this reversed-polarity interval is overlain by a normal-polarity interval about 5 m thick that extends to the top of the paleomagnetic section. The normal and reversed intervals in the Cretaceous strata are identified as C33n and C32r as discussed in the "Fassett and Steiner (1997) - Hunter Wash Paleomagnetic Section" section of this report. The Cretaceous part of the Mesa Portales paleomagnetic section bears a remarkable similarity to that part of the Lindsay et al. (1981) Cretaceous section at their Hunter Wash/Alamo Wash locality and the Fassett and Steiner (1997) section at Hunter Wash (Figure 18). The main difference is that the reversed-interval C32r is 61 m thick in the Ojo Alamo type area vs. 35 m thick at Mesa Portales. A zone of thin, reversed-polarity intervals in the upper part of C33n also is

common to the Mesa Portales and Hunter Wash sections (Figures 18, 23).

The Paleocene part of the Mesa Portales data plot is shown at larger scales on Figure 24. The distances, in meters, of paleomagnetic sample sites below the base of the upper Ojo Alamo Sandstone bench are shown on Figure 24.2. The reversed and normal magnetochrons above the Campanian-Paleocene interface are labeled C29r and C29n, respectively. (The identification of these chrons is discussed in the following section of this report.) Figure 25 is an annotated photograph of the upper part of the Ojo Alamo Sandstone at Mesa Portales showing the locations of paleomagnetic sample sites on the upper cliff face. This figure shows that the paleomagnetic samples from the upper Ojo Alamo were collected from a relatively steep slope. Sample 5.3 was from a dark-gray mudstone, samples 2.7, 2.3, and 1.8 were from light-gray, silty mudstones, and the uppermost four samples were collected from a greenish-brown siltstone beneath the overhang of the upper Ojo Alamo Sandstone bench; sample numbers are keyed to Figure 24.2.

Revision of Paleocene-Magnetochron Designations

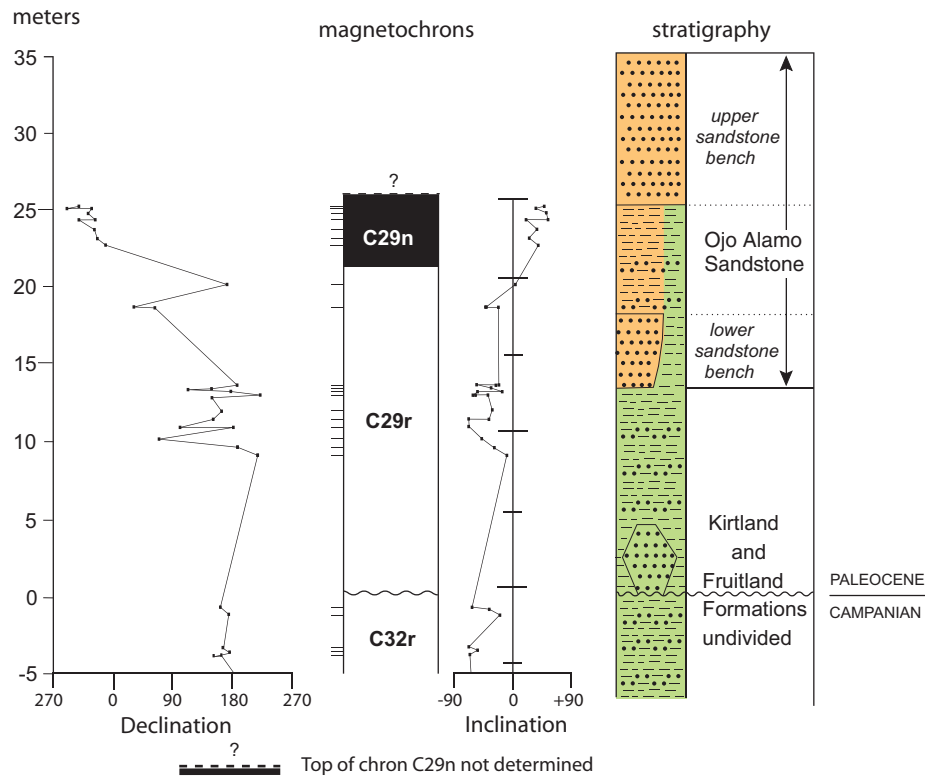
Figure 26 contains two cross sections that show paleomagnetic sections in the southern San Juan Basin that included the Ojo Alamo Sandstone. Figure 26.1 shows the magnetochron labels of Lindsay et al. (1981) and Fassett and Steiner (1997). Figure 26.2 shows the revised labeling of these magnetochrons of this report. The datum for these cross sections is the pre-Ojo-Alamo-Sandstone unconformity (Cretaceous-Paleocene interface).

Figure 27 shows the magnetic polarity of the lowermost Paleocene using all available data and using the base of chron C29n as a datum. HW data are from Fassett and Steiner (1997), MP data are from this report, and all other paleomagnetic data are from Lindsay et al. (1981). The labeling of the magnetochrons on Figure 27 is different from publications by Lindsay et al. (1981), Butler and Lindsay (1985), and Fassett and Steiner (1997). The lowermost normal-polarity interval in the Ojo Alamo Sandstone is here labeled C29n.2n. This chron was labeled C29n in Lindsay et al. (1981), was deleted from the section in Butler and Lindsay (1985), and was labeled C29n in Fassett and Steiner. The overlying reversed-polarity interval is labeled C29n.1r; this chron was called C28r in Lindsay et al. (1981), was the upper part of C29r in

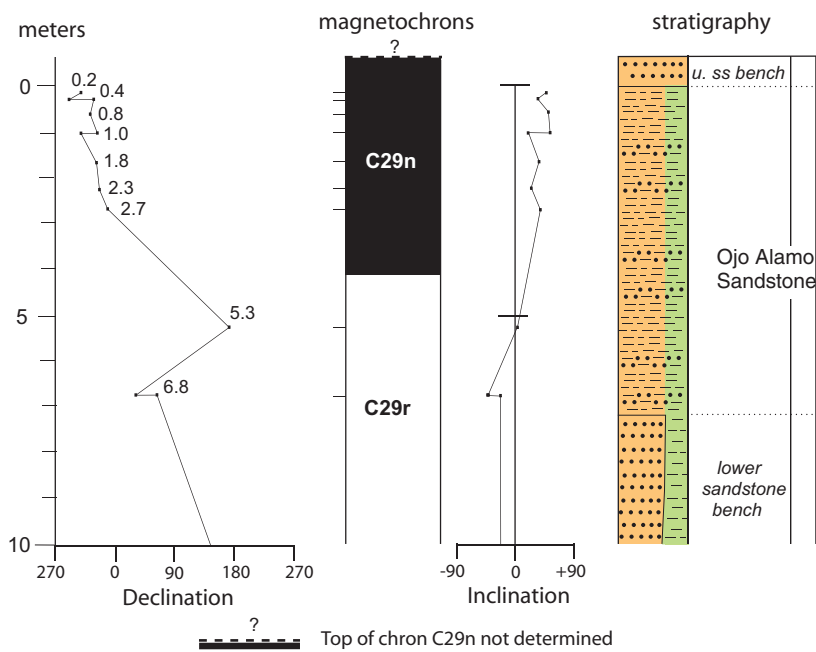
Butler and Lindsay (1985), and was C28r in Fassett and Steiner. C28r of Figure 27 was C27r of Lindsay et al. (1981), was C28r of Butler and Lindsay (1985), and was not discussed in Fassett and Steiner (1997). Chron C28n of Figure 27 was C27n of Lindsay et al. (1981) and C28n of Butler and Lindsay (1985).

The magnetochron-numbering scheme shown on Figure 27 is very similar to that of Butler and Lindsay (1985), with one important difference. The lowermost normal interval in the Paleocene; C29n.2n of Figure 27, was deleted from the Butler and Lindsay (1985) paleomagnetic section in the southern San Juan Basin, however, this thin normal interval has been found to be ubiquitous and virtually of the same thickness at all localities where paleomagnetic data have been obtained from the Ojo Alamo. The reversed-polarity interval: C29n.1r (Figure 27) is a newly identified reversed interval in the lower part of chron C29n. This interval, with a duration of about 0.07 m.y., has not been recognized in the basal part of C29n heretofore. The inclusion of chrons C29n.1r and C29n.2n in magnetochron C29n gives this chron an average thickness of about 70 m in the San Juan Basin (Figure 27). With a duration of 0.685 m.y. (Gradstein et al. 2004), the rock strata encompassing C29n has a sedimentation rate of 102 m/m.y. (not decompacted). This rate seems reasonable when compared to the sedimentation rate calculated for uppermost Cretaceous strata of 142 m/m.y. (Fassett 2000). Previous studies by Lindsay et al. (1981) and Fassett and Steiner (1997) assumed that the 11-m thick normal magnetochron in the lower Ojo Alamo Sandstone represented all of chron C29n. Using that thickness for C29n would yield a sedimentation rate of 16 m/m.y.; a rate that is unrealistically too low.

The labeling of Paleocene magnetochrons shown on Figure 27 is considered to be a best-fit interpretation of existing data. Other interpretations are possible, such as placing the lowermost Ojo Alamo Sandstone normal interval in magnetochron C29r and labeling it C29r.1n. Because the average thickness of C29n.2n is 11 m, and the thickness of C29n.1r is only about 7 m, it was thought that the placement of C29n.2n within C29n was the most parsimonious solution. It is clear that supplementary paleomagnetic studies of lowermost Paleocene strata in the San Juan Basin would be extremely useful in clarifying these relations. Most useful of all would be the precise dating of lower Paleocene strata in the basin using $^{40}\text{Ar}/^{39}\text{Ar}$ sin-



24.1



24.2

Figure 24. Large-scale views of upper part of paleomagnetic section at Mesa Portales (from upper part of paleomagnetic section of Figure 23). **24.1** Blow-up of entire Ojo Alamo Sandstone part of section; **24.2** Expanded view of paleomagnetic collection sites in upper part of magnetostratigraphy C29r and C29n. Numbers of sample levels are in meters below base of upper massive sandstone bed of Ojo Alamo Sandstone.

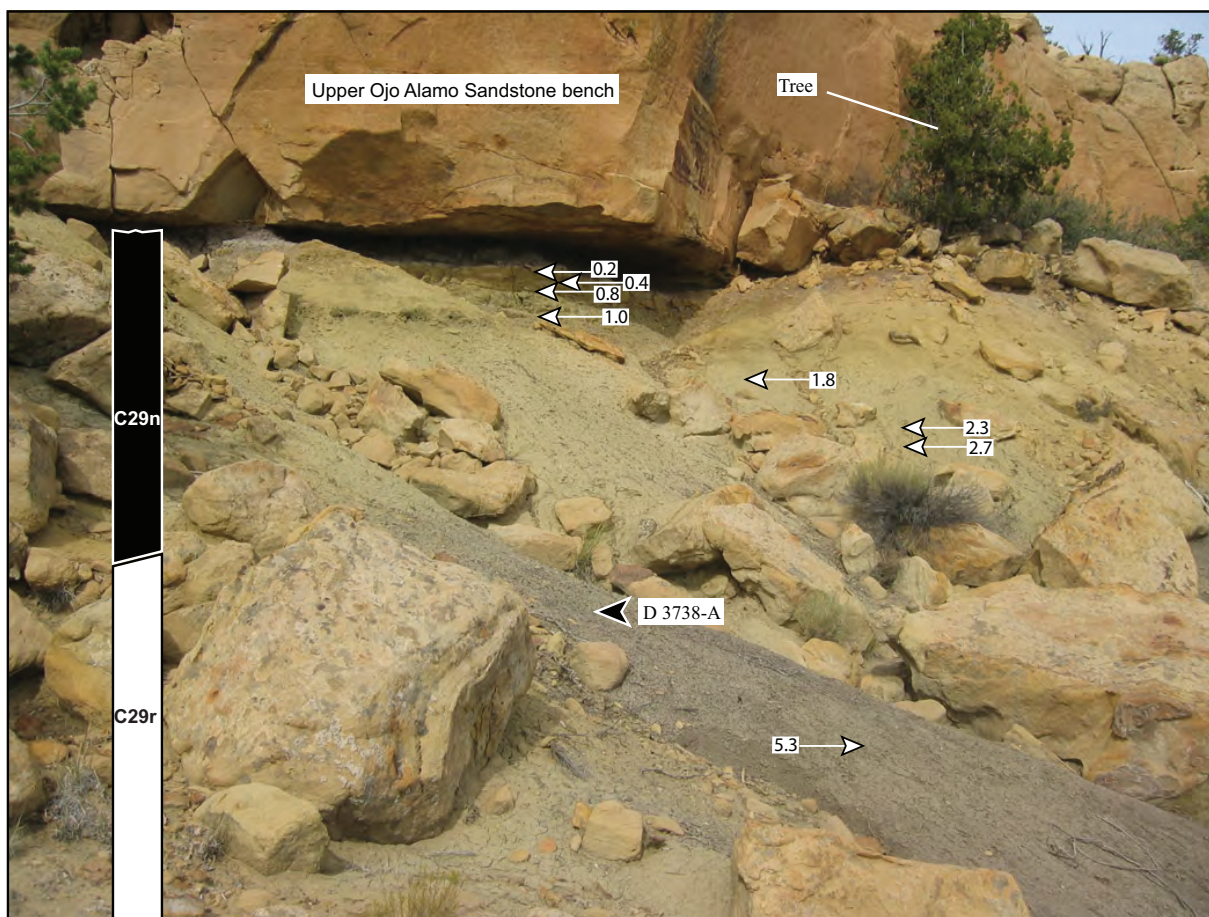


Figure 25. Photograph of upper part of Mesa Portales paleomagnetic section showing approximate locations of seven sample-collection sites of normal polarity (white arrows pointing left) and one sample of reversed polarity (white arrow pointing right). Numbers at arrows are distances in meters below the base of upper Ojo Alamo Sandstone bench (Figure 22). Palynologic collection locality for sample D 3738-A is also shown. Tree in upper right of photograph is also labeled on Figure 22 to indicate location of this photograph.

gle-crystal-sanidine or other state-of-the-art radiometric-dating methods.

Figure 27 shows an irregular erosion surface at the base of the Paleocene across the basin with a 21 m topographic low on the pre-Paleocene land surface in the Mesa Portales area. Fassett and Hinds (1971, figure 13) showed an isopach map of the interval from the Huerfanito Bentonite Bed of the Lewis Shale to the base of the Ojo Alamo Sandstone (reproduced herein as Figure 1.1); those authors suggested that because the Huerfanito Bed is a time plane (a volcanic ash fall into the Western Interior Seaway), this isopach map should represent the approximate topography of the land surface prior to deposition of the Ojo Alamo Sandstone. Fassett (1985) discussed the evolution of the pre-Ojo Alamo Sandstone erosion surface and offered illustrations (figures 3, 4) showing possible drainage patterns on that surface

at the end of the pre-Ojo-Alamo-Sandstone erosion cycle. Fassett suggested in that paper that the strong perturbations (bulges to the east) of the 600 and 700 ft contour lines in the southeast part of the basin (Figure 1.1) represented erosion channels on the pre-Ojo-Alamo surface suggesting relatively high relief near the Mesa Portales area. Thus, the presence of 20 m of relief on the erosion surface in the Mesa Portales area is not unreasonable.

Moncisco Mesa and Eagle Mesa Localities

Butler and Lindsay (1985) presented new paleomagnetic data from uppermost Cretaceous strata at two widely separated localities Moncisco Mesa and Eagle Mesa (Figure 1). The data plots for these two localities are shown on Figure 28. At Moncisco Mesa, the sampled section is 140 m long and contains 16 sample sites; a sample spacing of about 9 m. At Eagle Mesa the section is about 80

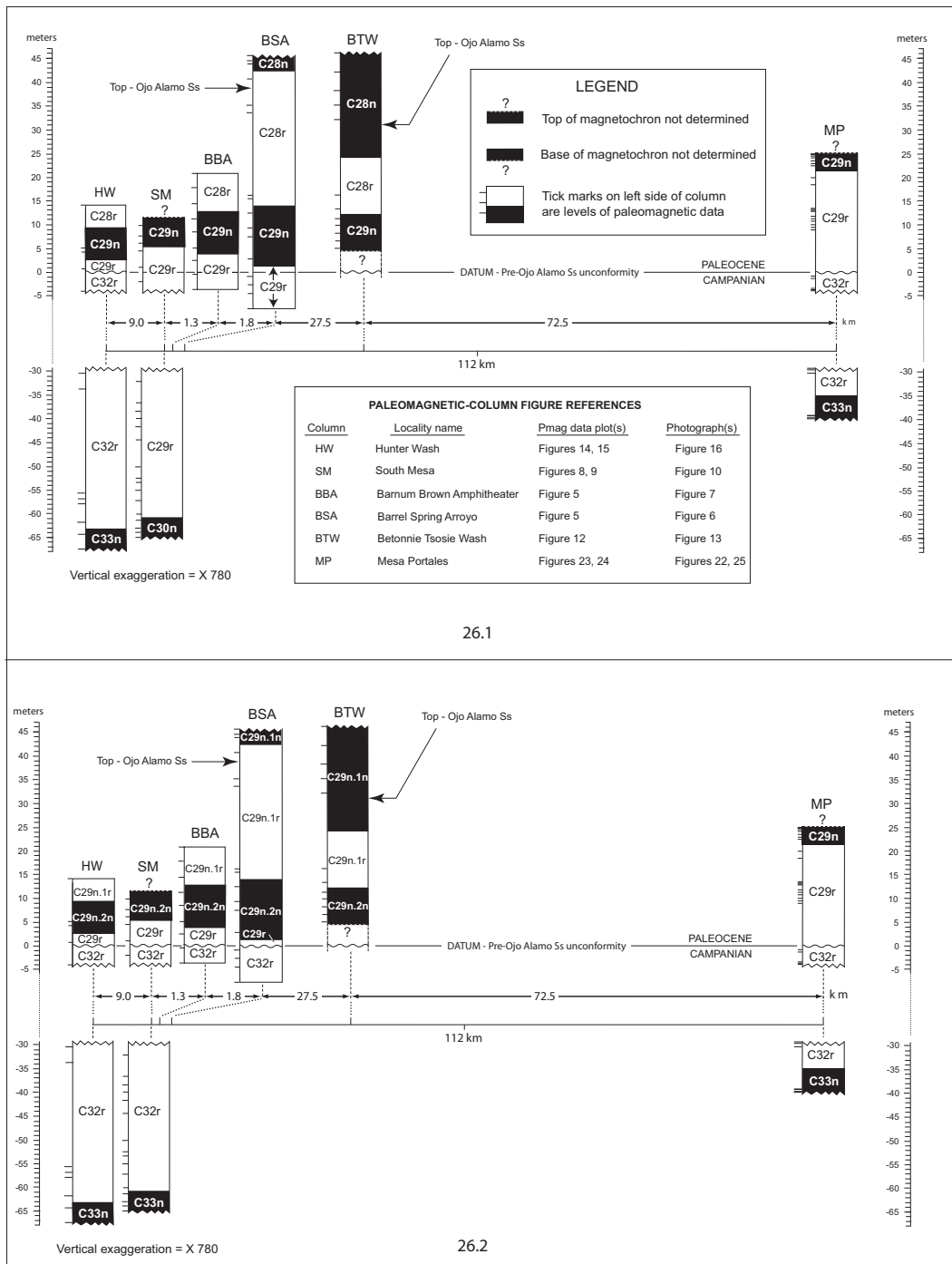


Figure 26. Cross sections through six paleomagnetic sections in southern San Juan Basin. (Section localities are shown on Figure 1; full data plots for all sections are on the figures indicated.) Only paleomagnetic sections through all or part of the Ojo Alamo Sandstone are shown. Columns are broken by a gap of 25 m to show positions of top of chron C33n at the HW, SM, and MP localities at a reasonable scale. Alignment of column TW based on field measurements of distance from lowermost C29n data point to base of Ojo Alamo Sandstone. Magnetochron boundaries are placed at mid-point between nearest-to-the-reversal data sites. **26.1** Published Paleocene magnetochron labels of Lindsay et al. (1981) and Fassett and Steiner (1997) for all but the Mesa Portales (MP) column. **26.2** Revised magnetochron labels of this report.

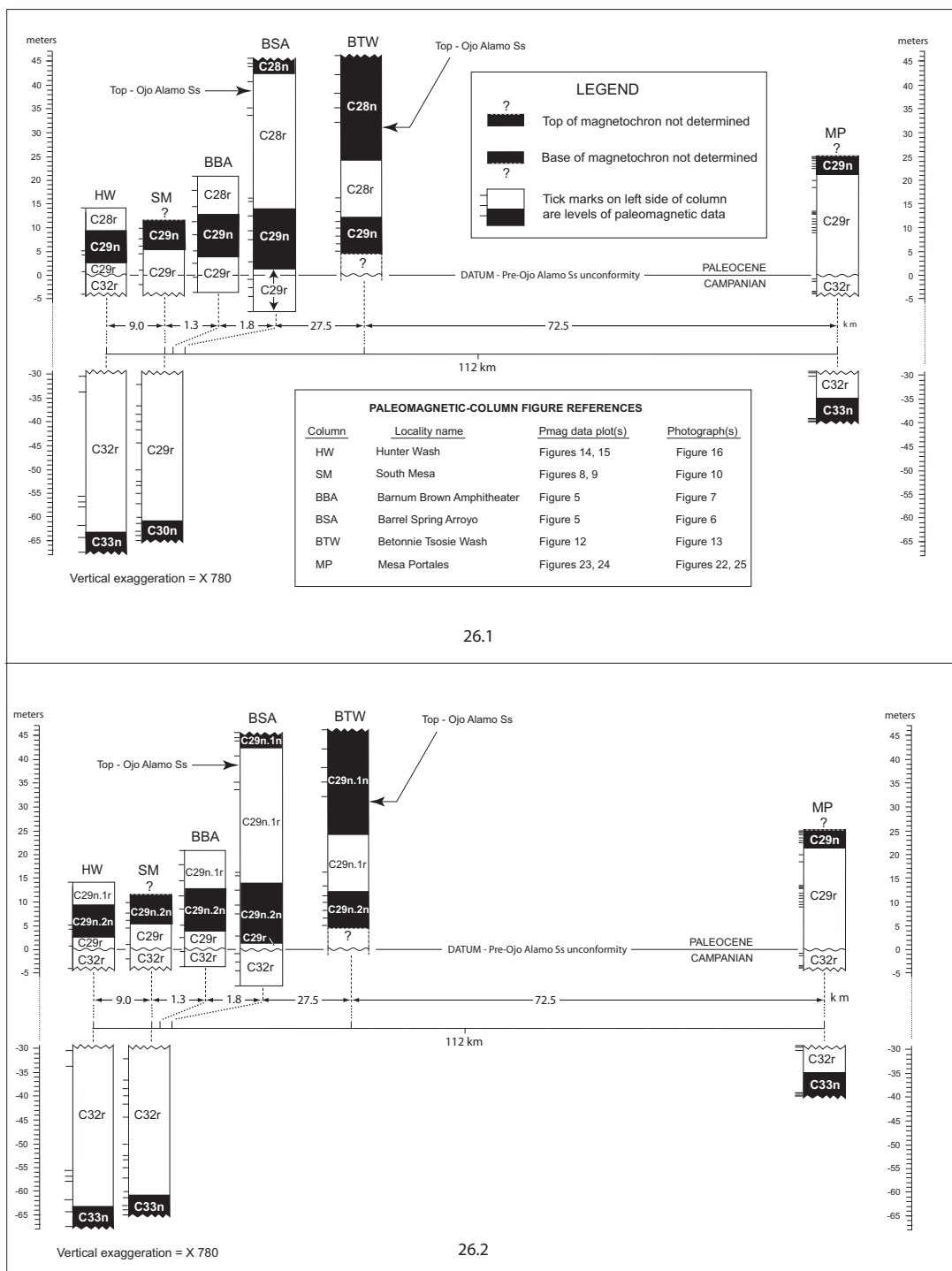
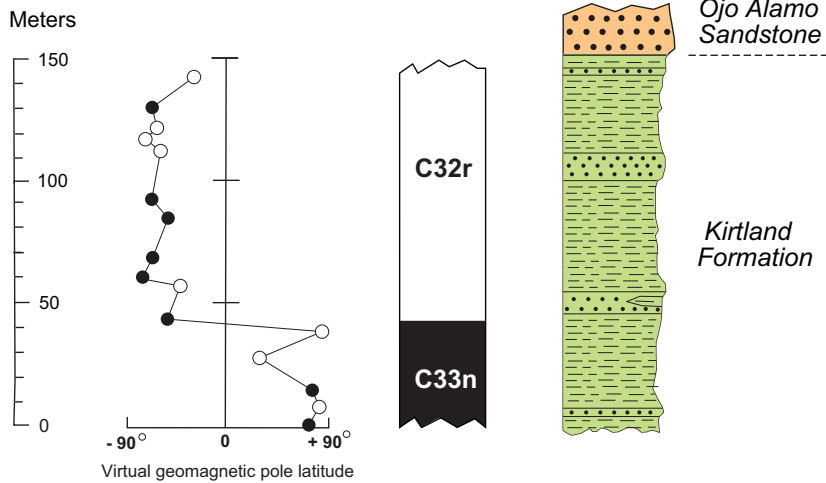


Figure 27. Cross section through six paleomagnetic sections of Paleocene and uppermost Cretaceous (Campanian) strata in southwest San Juan Basin using base of magnetochron C29n as a datum. Boundaries for chrons C28r, C29n.1r, and C29n.2n are adjusted to make the thicknesses of these chrons as close to the same as possible at each locality, while still honoring the magnetic-polarity-site data. The resulting average thickness of C29n.1r is about 7 m.; for C29n.2n average thickness is about 11 m. Thickness of chron C28r and position of base of Ojo Alamo Sandstone on column BSA are corrected from thickness and position shown in Lindsay et al. (1981, figure 7) based on field studies in this area. Figures containing paleomagnetic data plots and photographs at these localities (except for KW section) listed on Figure 26.

MONCISCO MESA



EAGLE MESA

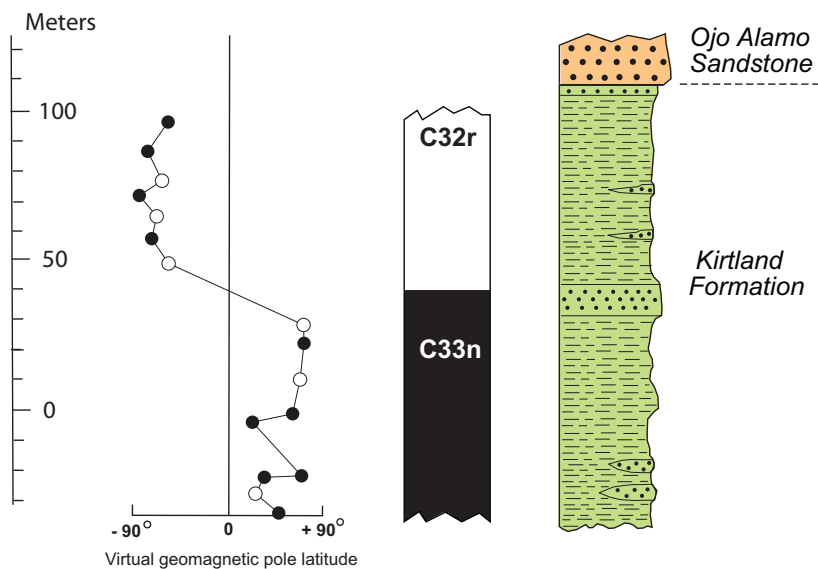


Figure 28. Paleomagnetic data plots at the Moncisco Mesa and Eagle Mesa localities (Butler and Lindsay 1985, figures 10, 11). Polarity chron C32r was labeled B- and C30n; chron C33n was labeled A+ and C30n on figures 10 and 11 of these authors. These polarity intervals are now known to be C32r and C33n (as labeled hereon). Note the significantly different vertical scales for these two sections.

m long and contains 16 sample sites for a spacing of 5 m. Apparently, the intent of Butler and Lindsay (1985) at these two sections was to locate the boundary between the normal and reversed polarity intervals in Cretaceous Kirtland Formation strata underlying the Ojo Alamo Sandstone. The wide

spacing of samples at these two localities precluded the detection of the thinner normal and reversed polarity intervals seen in the Hunter Wash and Mesa Portales paleomagnetic sections.

Figure 29 is a cross section across the southwestern part of the San Juan Basin showing all of

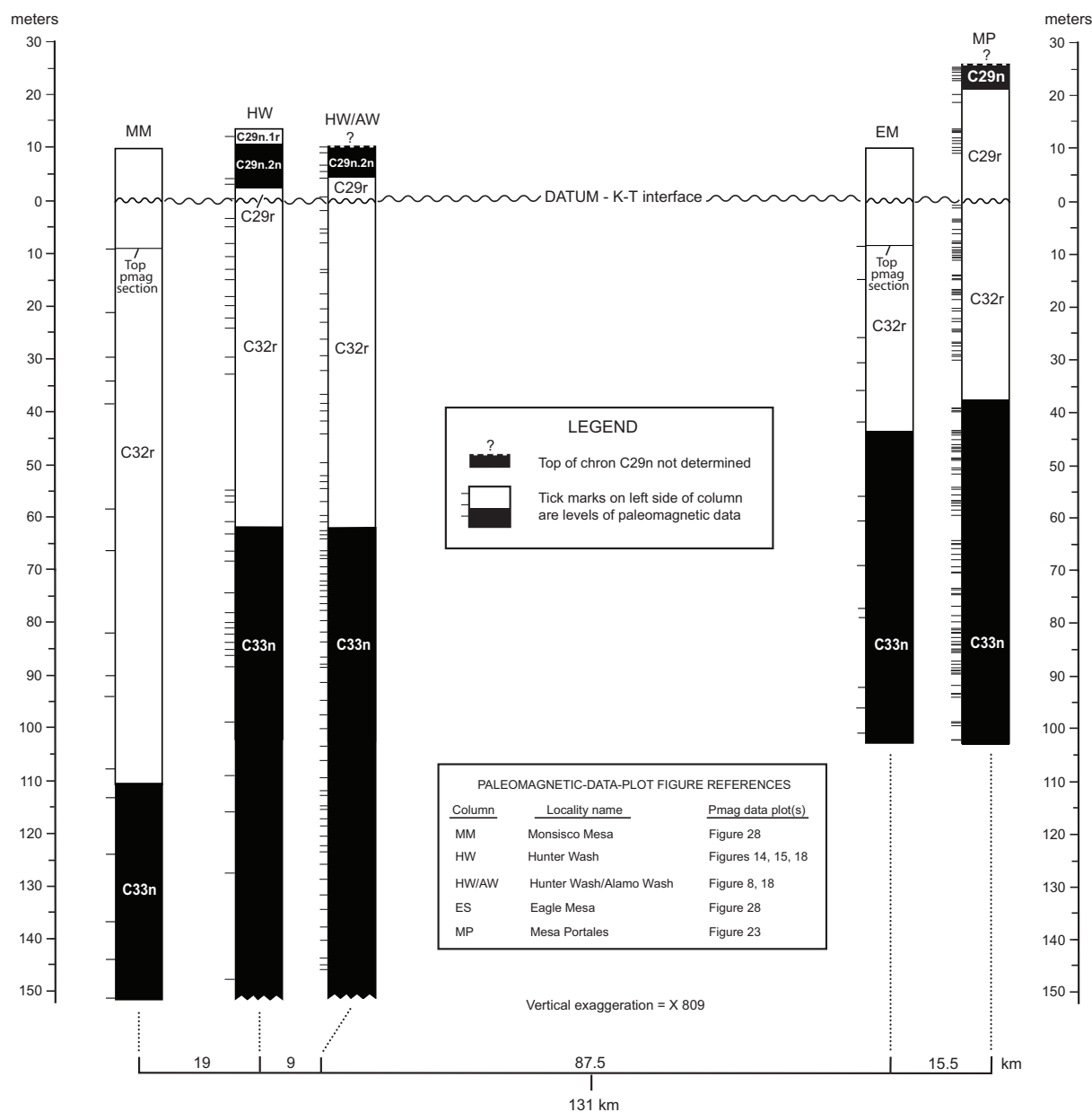


Figure 29. Cross section showing five magnetic-polarity columns containing chrons C33n and C32r in southern San Juan Basin; datum K-T interface. Figure 1 shows column localities. Column HW/AW from Lindsay et al. (1981), columns MM and EM from Butler and Lindsay (1985), column HW from Fassett and Steiner (1997), column MP is published herein for first time.

the paleomagnetic sections that extended deep enough into the Kirtland and Fruitland Formations to include chrons C32r and C33n (see Figure 1 for locations of these sections). The complete paleomagnetic sections at the Monisisco Mesa, Eagle Mesa, and Mesa Portales localities are shown on Figure 29. The lower parts of the Hunter Wash and Hunter Wash/Alamo Wash sections are not shown on this figure, but only contain more normal polarity (including the thin reversed-polarity interval dis-

cussed earlier) below the truncation points on the original data plots (Figure 18). Figure 29 shows that the C32r interval thins from the MM to the MP column by 73 m, but that the thinning is not uniform. For example, C32r thins by 48 m from column MM to HW over a distance of 19 km (2.5 m/km), whereas the C32r interval only thins by another 25 m over a distance of 112 km (0.22 m/km) from column HW to MP. Figure 30 is a reconstruction of Figure 29 using the top of polarity

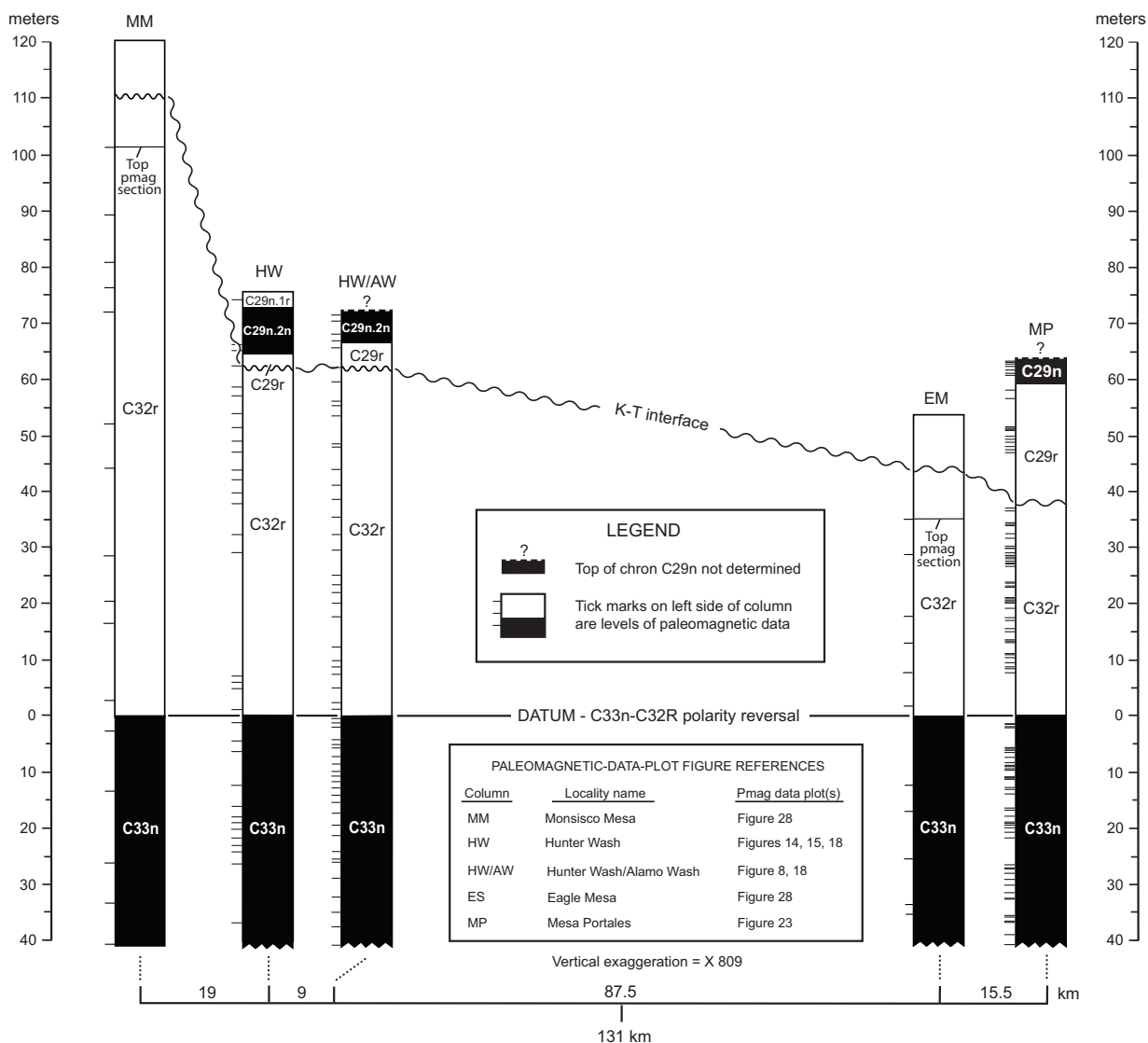


Figure 30. Cross section showing five magnetic-polarity columns containing chrons C33n and C32r in the southern San Juan Basin; datum is C33n-C32r reversal. Figure 1 shows column localities. Column HW/AW from Lindsay et al. (1981), columns MM and EM from Butler and Lindsay (1985), column HW from Fassett and Steiner (1997), and column MP is published herein for the first time. This figure is modification of Figure 29.

chron C33n as a datum. This figure more accurately shows the southeastward truncation of the strata underlying the Cretaceous-Tertiary interface that preceded deposition of the Ojo Alamo Sandstone.

A detailed discussion of the thinning of Upper Cretaceous rocks across the San Juan Basin (Figure 1) is presented in the following section of this report. Radiometric ages and palynologic data clearly indicate that the Maastrichtian and part of the uppermost Campanian are not present throughout most of the southern San Juan Basin

representing a hiatus of nearly 8 m.y. at the K-T interface. Much of the missing strata was probably removed by erosion, however, there may also have been a reduced rate of deposition of uppermost Upper Cretaceous rocks in parts of the basin in latest Cretaceous (Maastrichtian) time.

In their discussion of the Monisco Mesa and Eagle Mesa paleomagnetic sections (neither of which included the Ojo Alamo Sandstone) Butler and Lindsay (1985, p. 548) again state that the C29n normal chron (C29n.2n of Figure 27) is in the Kirtland Formation. As discussed above, state-

ments that chron C29n is in the Kirtland Formation differ from these author's previous placement of chron C29n within the Ojo Alamo Sandstone. Chron C29n was not found at Moncisco Mesa or Eagle Mesa because the Ojo Alamo Sandstone was clearly not sampled at those localities. This normal chron—C29.2n of this report—is clearly present within the Ojo Alamo Sandstone at Mesa Portales, only about 16 km east of Eagle Mesa.

Summary of San Juan Basin Paleomagnetism

Paleomagnetic studies of rock strata adjacent to the Cretaceous-Tertiary interface have been conducted at eight localities in the southern part of the San Juan Basin (Figure 1). At three of these localities—Hunter Wash, Hunter Wash/Alamo Wash, and Mesa Portales—the paleomagnetic sections include the lower part of the Paleocene Ojo Alamo Sandstone and as much as 150 m of underlying Cretaceous strata that include magnetochrons C32n and C33n (Figures 29, 30). In addition, chron C32r.1n may be present above the top of chron C33n at the Hunter Wash and Hunter Wash/Alamo Wash localities. At two other localities—Moncisco Mesa and Eagle Mesa—where only Cretaceous strata below the base of the Ojo Alamo were sampled, chrons C32r and C33n were identified (Figure 29). Chron C32r.1n was not identified at those places, probably because of the wide spacing of sample sites in those two sections.

At six localities (Figures 26, 27), a normal-polarity interval was found to be present in the lower part of the Ojo Alamo Sandstone. In the four sections where this normal interval was bracketed by reversed-polarity sites (Figures 26, 27), it is about 11 m thick. Biochronologic evidence (discussed below) unequivocally shows that the Ojo Alamo Sandstone is Paleocene, thus the normal-polarity interval in the lower Ojo Alamo is the lowermost part of chron C29n (herein labeled C29n.2n). Butler and Lindsay (1985) recommended deleting the normal-polarity interval in the lower part of the Ojo Alamo (labeled chron C29n by Lindsay et al. 1981, 1982) at three closely spaced localities—South Mesa, Barnum Brown Amphitheater, and Barrel Spring Arroyo. These authors stated that their original studies were in error because these normal intervals did not represent true Paleocene remanent magnetism but were present-day-normal overprints. However, because this normal-polarity interval is also present in the Ojo Alamo Sandstone at three other widely spaced localities, it is not credible that these normal-polarity intervals in the lower Ojo Alamo at these six localities could all

have been the result of present-day, normal-field, overprinting. The presence of chron C29n in the lower part of the Ojo Alamo Sandstone thus provides independent evidence that this formation, including its dinosaur-bearing parts at several localities, is Paleocene in age.

The Paleocene magnetochrons identified in the southern San Juan Basin have been reevaluated and relabeled as shown on Figures 26 and 27. Magnetochron C29n is about 70 m thick and contains a persistent, 7 m thick reversed-polarity interval in its lower part, thus, C29n in the San Juan Basin consists of three subchrons: C29n.1n, C29n.1r, and C29n.2n (Figure 27).

Revised Magnetic-Polarity Calibration

Figure 31 portrays a recalibration of paleomagnetic-reversal ages between the top of chron C33n and the base of chron C29r based on interpolation between two tie points: the precisely dated polarity reversal between chrons C33n and C32r (73.50 ± 0.19 Ma, Fassett and Steiner 1997 and Fassett 2000), and the age of the Cretaceous-Tertiary boundary (65.51 ± 0.01 , Hicks et al. 2002). The age of the C33n-C32r reversal was calculated on the basis of eight $^{40}\text{Ar}/^{39}\text{Ar}$ ages determined by J.D. Obradovich (USGS, retired) using the Taylor Creek Rhyolite as a standard with an assigned age of 28.32 Ma. Figure 32 (from Fassett 2000, figure 13) is a northeast-trending stratigraphic cross section across the San Juan Basin showing the positions of the eight dated ash beds from the Upper Cretaceous Lewis Shale, Fruitland, and Kirtland Formations. The stratigraphic positions of Western Interior ammonite zones and the Hunter Wash and Chimney Rock magnetic-polarity columns are also shown.

The age of the K-T boundary was determined by Hicks et al. (2002, p. 43) by normalizing "all available $^{40}\text{Ar}/^{39}\text{Ar}$ isotopic dates as published for the K-T boundary interval . . . based on the monitor age of 28.02 Ma for Fish Canyon Tuff and 28.32 Ma for Taylor Creek Rhyolite, which yields an average age of 65.51 ± 0.01 for the K-T boundary." The two tie points used to construct the calibrated magnetic-polarity column (Figure 31) are thus based on the same standards.

The global geologic time scale of Gradstein et al. (2004) shows the correct age of 65.50 Ma for the K-T boundary but an incorrect age of 73.0 Ma for the C33n-C32r reversal—the correct age of this reversal is 73.50 Ma. The use of an incorrect age for the C33n-C32r reversal resulted in incorrect age assignments in Gradstein et al. (2004) for the

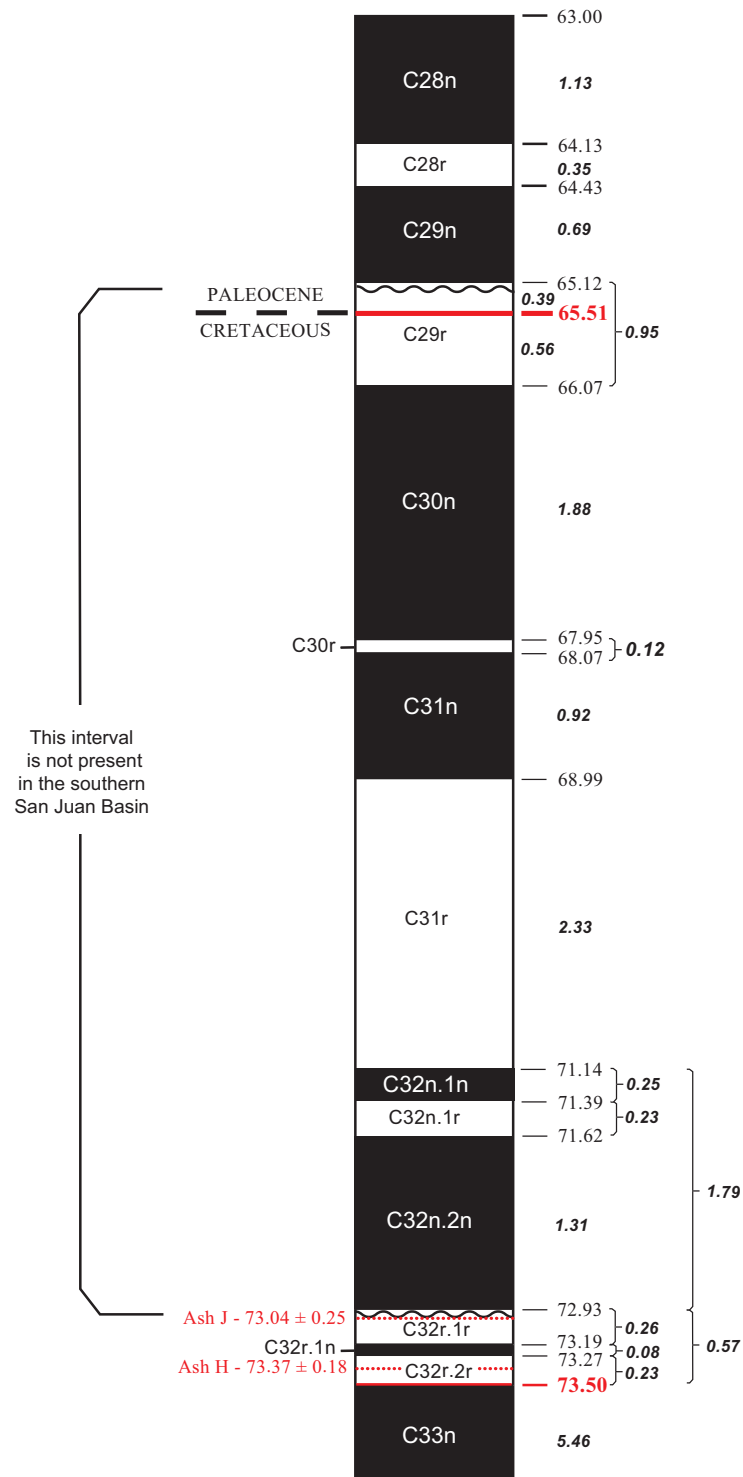


Figure 31. Paleomagnetic-polarity column showing ages of polarity reversals and durations of polarity chrons for latest Cretaceous strata based on data from San Juan Basin, New Mexico. Polarity-chron durations and reversal ages for Cretaceous magnetochrons were determined by proportionalizing chron durations of Cande and Kent (1992, 1995) between ages of 65.51 Ma for the Cretaceous-Tertiary (K-T) boundary (Hicks et al. 2002) and 73.50 Ma for the C33n-C32r reversal (Fassett and Steiner 1997; Fassett 2000). Polarity-chron ages above K-T boundary are from Gradstein et al. (2004). Ages of ash beds J and H in polarity chron C32r from Fassett and Steiner (1997).

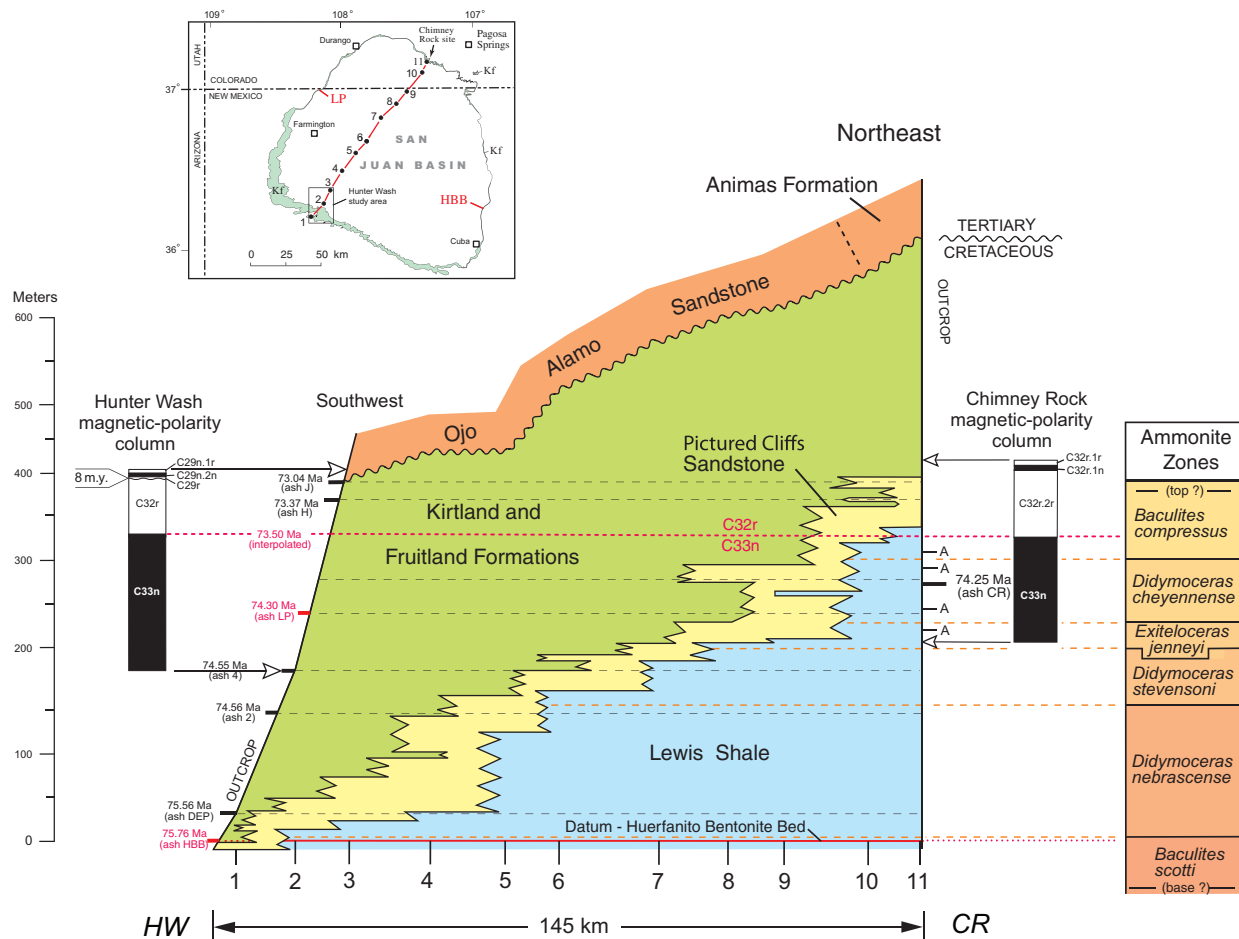


Figure 32. Stratigraphic cross section from Hunter Wash to Chimney Rock (modified from Fassett 2000). Contacts of geologic formations are from geophysical logs at localities shown (log-data are provided in Fassett and Steiner 1997). Ash-bed sample localities are shown on index map. Ash-bed ages are shown; those in red are projected into the Hunter Wash section. Letters A at right side of section show levels of ammonite collection sites. Lower ammonite-zone boundaries modified from Fassett (1985) and Fassett et al. (1997). On magnetic-polarity columns, black is normal polarity, white is reversed polarity. Vertical exaggeration = 200 X. Age of C33n-C32r magnetic-polarity reversal of 73.50 Ma is mean of 12 interpolated reversal ages based on dated ash beds bracketing reversal as discussed in Fassett and Steiner (1997) and in Fassett (2000).

reversal ages between this reversal and the K-T boundary. Ages for the paleomagnetic reversals shown on Figure 31 are calibrated based on more precisely dated tie points and thus are considered to be the most accurate currently available for this time interval. It is recommended that the reversal ages for the Upper Cretaceous of Figure 31 replace those of Gradstein et al. (2004).

The ages of uppermost Upper Cretaceous Western Interior ammonite zones of Gradstein et al. (2004, table 19.3) are also not in agreement with the ages of these faunal zones in the San Juan Basin. Figure 32 shows the positions of the Western Interior ammonite zones from *Baculites scotti* to *Baculites compressus* relative to a strati-

graphic cross section encompassing the Lewis Shale, Pictured Cliffs Sandstone, and the Fruitland and Kirtland Formations. These ammonite-zone placements are from Fassett (1987), based on the work of Cobban (1973) and Cobban et al. (1974). Time lines opposite ash-bed ages and ammonite-zone boundaries determined at outcrops in the San Juan Basin are projected into the subsurface of the basin. The highest ammonite-zone boundary shown on Figure 32 is between the *Didymoceras cheyennense* and *B. compressus* zones. This boundary was located on the outcrop in the vicinity of Chimney Rock (Figure 32) by W.A. Cobban as discussed in Fassett and Steiner (1997, p. 245). As seen on Figure 32, the base of *B. compressus* is

bracketed by the top of polarity chron C33n, with an age of 73.50 Ma and altered volcanic ash bed CR (in the underlying *D. cheyennense* zone) with an age of 74.25 Ma; these bracketing ages are from the same, continuous, stratigraphic section at a single locality. The base of *B. compressus* falls about halfway between these levels, thus the age of the base of *B. compressus* is estimated to be 73.90 Ma. The *B. scotti*-*D. nebrascense* ammonite-zone boundary was also located very precisely on the outcrop by Cobban, as reported in Fassett et al. (1997) north of Cuba, New Mexico at the HBB (Huerfanito Bentonite Bed) locality shown on the inset map on Figure 32. This ammonite-zone boundary is virtually at the same level as the Huerfanito Bentonite Bed of the Lewis Shale (Figure 32). The age of the Huerfanito Bed of 75.76 Ma was determined on the basis of samples collected at the same outcrop locality where the *B. scotti*-*D. nebrascense* boundary was located, thus the ammonite-zone boundary has been directly dated there. The duration of the interval from the base of the *D. nebrascense* zone to the base of the *B. compressus* zone is 1.86 m.y.

Gradstein et al. (2004, table 19.3) show the age of the base of *B. compressus* as 73.50 Ma and the base of *D. nebrascense* as 76.38 Ma for a duration of 2.88 m.y., or about 1 m.y. longer than the San Juan Basin interval. The base of the *B. compressus* zone of Gradstein et al. is 0.4 m.y. younger than the base of this zone in the San Juan Basin and the base of the *D. nebrascense* zone according to those authors is 0.62 m.y. older than in the San Juan Basin. Because the San Juan Basin ammonite-zone ages were determined at the

same outcrops where the ammonite-zone boundaries were located (Figure 32), it is suggested that the San Juan Basin ages for these ammonite-zone boundaries are more precise.

The ages of the intervening ammonite-zone boundaries between the base of *D. nebrascense* and the base of *B. compressus* were calibrated by interpolation between the ages of ash bed CR and HBB in the Chimney Rock section (Figure 32). Table 1 shows the ages and durations of the Western Interior ammonite zones determined in this report compared to the ages and durations of these same ammonite zones published in Gradstein et al. (2004). The more precise ages here reported for these boundaries supersede those of Gradstein et al. (2004). The base of the *B. scotti* zone in the Lewis Shale has not yet been located in the San Juan Basin.

Lucas et al. (2006, p. 5) discussed the identification by Lucas and Sealey (1992) of “ammonites of the *D. cheyennense* zone in the upper Lewis Shale near Cuba [NM].” This fossil locality is south of Mesa Portales (Figure 21) and is below the level of the Huerfanito Bentonite Bed there. Figure 32 shows that the Huerfanito Bed is 75.76 Ma, as determined by Fassett et al. (1997) who found that the Huerfanito Bed is almost exactly at the base of the *D. nebrascense* ammonite zone. Table 1 shows that the base of the *D. nebrascense* zone is about 2 m.y. older than the *D. cheyennense* zone in the San Juan Basin. As discussed above, the ammonite-zone boundaries shown on Table 1 have all been precisely dated on the outcrop in the San Juan Basin. It is therefore not physically possible for the ammonite collections of Lucas and Sealey

TABLE 1. Ages of some late Cretaceous western interior ammonite-zone boundaries of Gradstein et al. (2004) and this report.

W. Interior Ammonite Zone	Gradstein et al. (2004)		This report	
	Age (Ma)	Duration (m.y.)	Age (Ma)	Duration (m.y.)
<i>Bacutes compressus</i>	73.50	0.72	73.90	?
<i>Didymoceras cheyennense</i>	74.28	0.78	74.50	0.60
<i>Exiteloceras jenneyi</i>	75.05	0.77	74.65	0.15
<i>Didymoceras stevensoni</i>	75.74	0.69	74.98	0.33
<i>Didymoceras nebrascense</i>	76.38	0.64	75.76	0.78

Note: Ages are for base of ammonite zones.

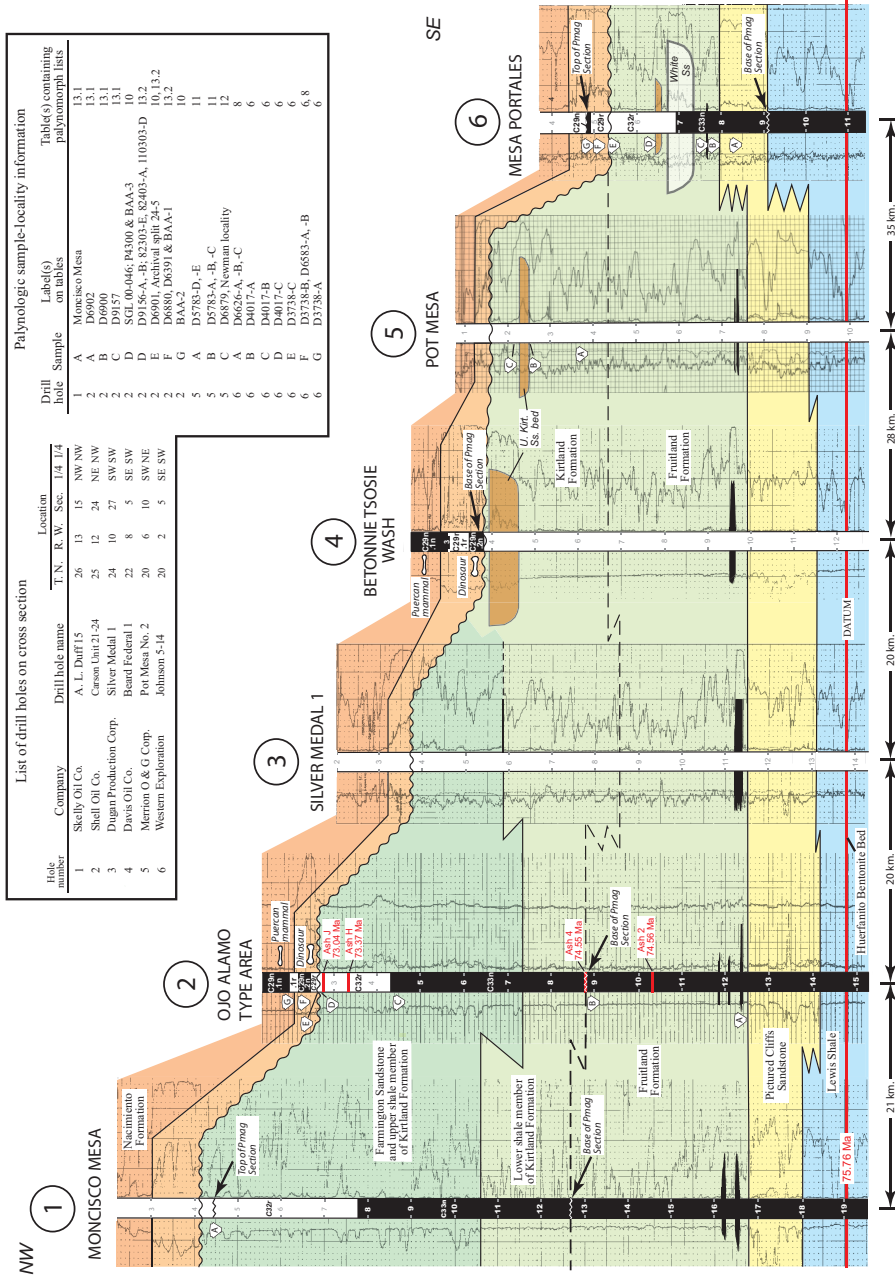


Figure 33. Stratigraphic, geophysical-log cross section along southwest margin of San Juan Basin (line of section on Figure 3). Drill-hole depths in hundreds of feet (100 feet approximately 30 m). Cross section shows thinning of Fruitland and Kirtland Formations from northwest to southeast. Coal beds in lowermost Fruitland Formation (near top of Pictured Cliffs Sandstone) are shown. Paleomagnetic data in drill holes 1, 2, 4, and 6 are projected from nearby outcrop localities (Figure 3); paleomagnetic data plots on Figures 8, 12, 14, 18, 23, and 28. Palynologic sample-collection levels in drill holes 1, 2, 5, and 6 are projected from nearby outcrop localities; palynomorphs identified from samples listed on the Appendix tables, as shown. Top of Fruitland Formation is defined by highest coal bed or carbonaceous shale bed in section (Fassett and Hinds 1971); contact is shown as dashed line because of difficulty locating it with certainty on geophysical logs. Radiometric ages of sandstone crystals from altered volcanic ash beds in Ojo Alamo type area from Fassett and Steiner (1997) and Fassett (2000); stratigraphic levels of dated ash beds are projected into log of drill-hole 2 from measured outcrop localities at or near Hunter Wash (Figure 3). Stratigraphic levels of Puercan mammal sites in lowermost Nacimiento Formation shown in drill-hole logs 2 and 4 from nearby outcrop localities from Williamson (1996) and Lindsay et al. (1981). Vertical exaggeration = 130 x. Distances between drill-hole localities not scaled horizontally.

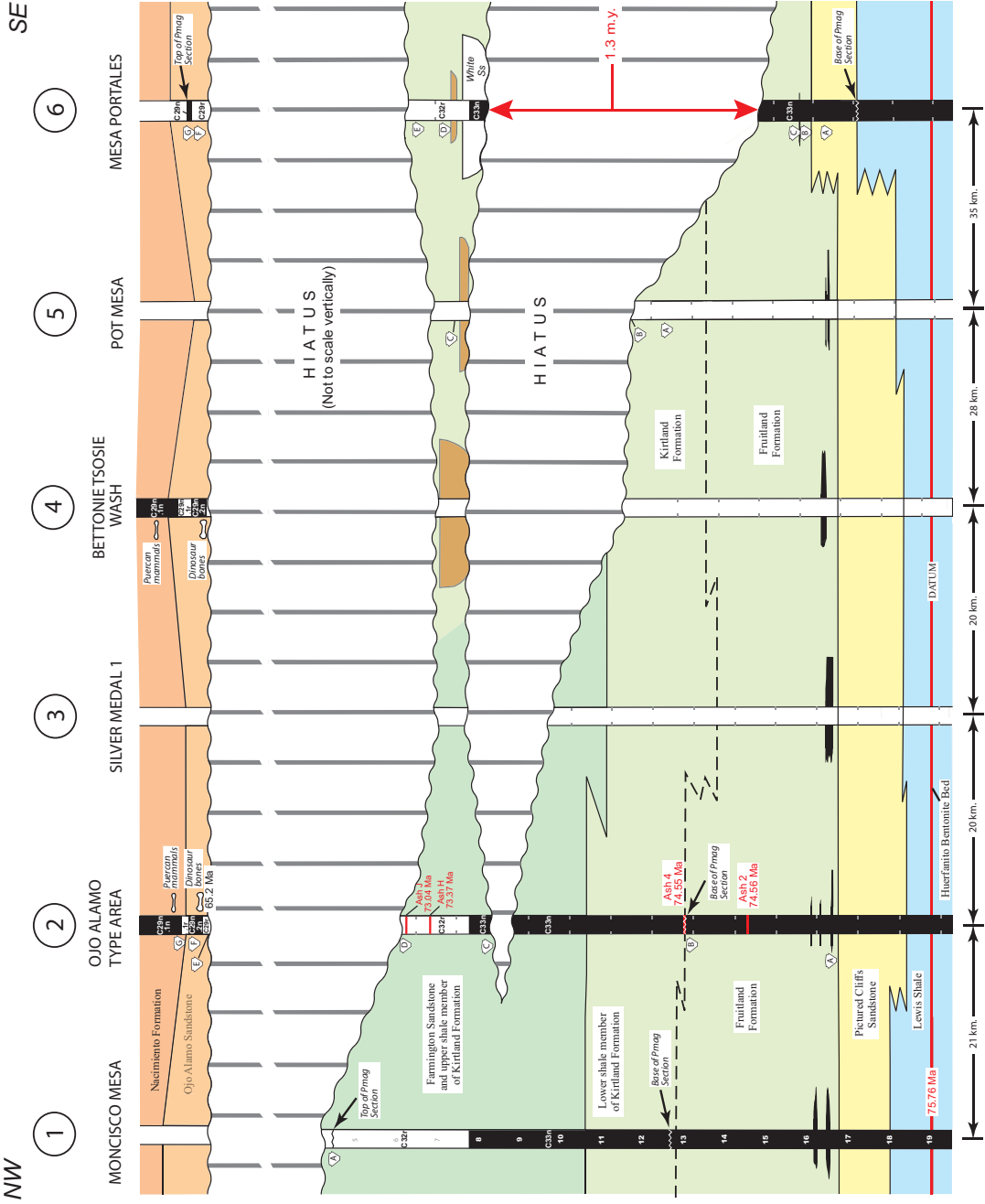


Figure 34. Time-stratigraphic cross section along southwest margin of the San Juan Basin (line of section on Figure 3). Cross section modified from Figure 33 to show presence of hiatus in Fruitland-Kirtland section between Mesa Portales area and Ojo Alamo type area; pre-Ojo Alamo Sandstone hiatus also shown. (See Figure 33 for drill-hole identifications and palynologic-sample data.) About 215 m of section missing from the Fruitland-Kirtland section in Mesa Portales area represents about 1.3 m.y. Pre-Ojo Alamo Sandstone hiatus represents nearly 8 m.y. in Ojo Alamo Sandstone type area. Vertical exaggeration = 130 x.

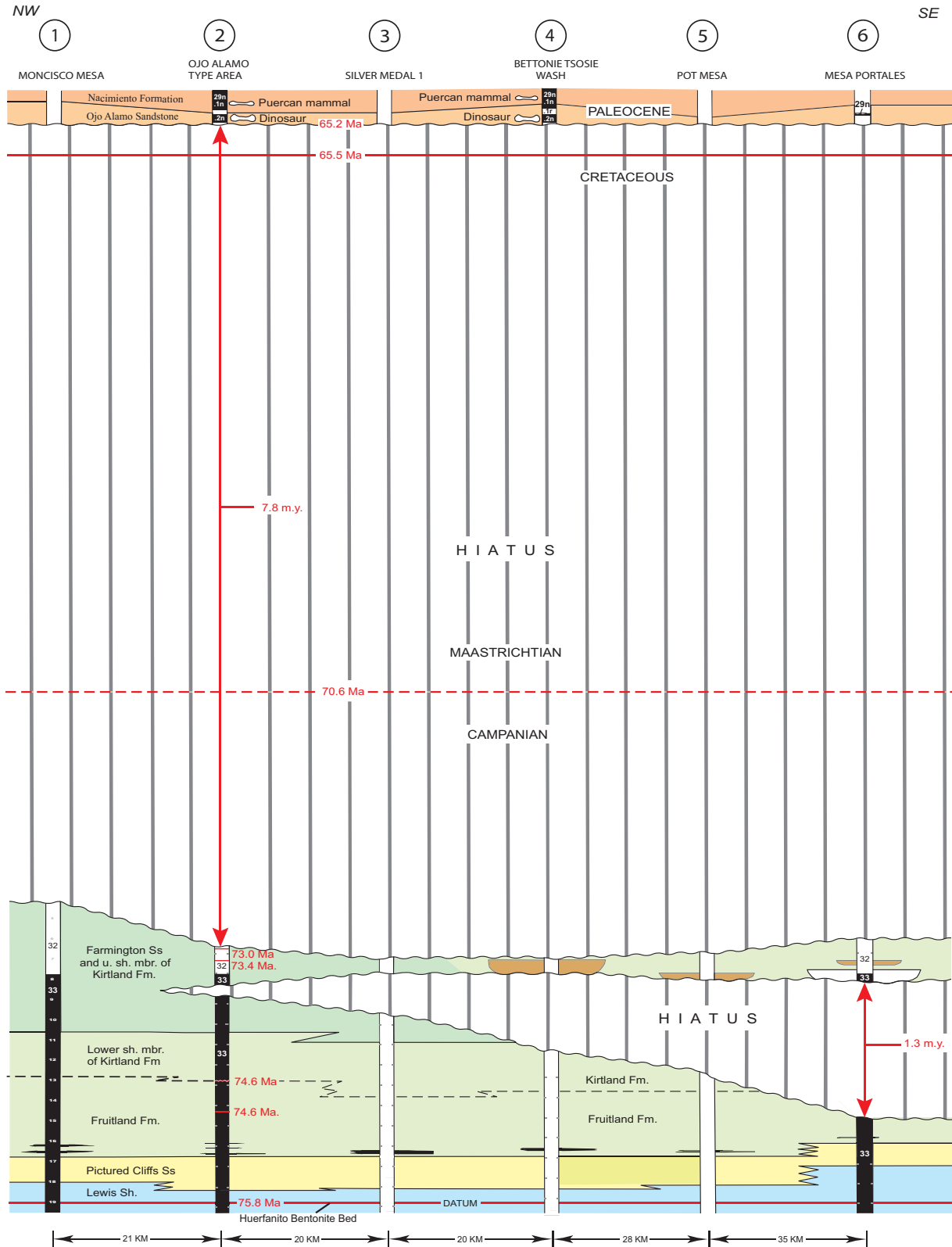


Figure 35. Time-stratigraphic cross section along southwest margin of San Juan Basin (line of section on Figure 3). Modified from Figure 34 to show magnitude of Fruitland-Kirtland and pre-Ojo Alamo Sandstone hiatuses at same scale. (See Figure 33 for drill-hole identifications.) Vertical exaggeration = 85 x.

(1992, and discussed in Lucas et al. 2006) found south of Mesa Portales to be in the *D. cheyennense* zone. Moreover, USGS paleontologist W.A. Cobban visited this locality in 1997 accompanied by the author, Lucas, and Sealey and concluded that the fossil assemblage there was in the *B. scotti* Western Interior ammonite zone. Thus, it can only be concluded that the ammonite fossils found by Lucas and Sealey (1992) at this locality were incorrectly identified.

NW TO SE THINNING OF CRETACEOUS STRATA IN SW SAN JUAN BASIN

Figure 1 shows that the Fruitland Formation-Kirtland Formation interval thins by 2,100 feet (640 m) from the northwestern to the southeastern part of the San Juan Basin. This interval also thins dramatically in the southern part of the basin from Moncisco Mesa to Mesa Portales. The isopach map (Figure 1.1) of the interval between the Huerfanito Bentonite Bed and the base of the Ojo Alamo Sandstone shows thinning of this interval of about 1,000 feet (300 m) between these two localities. To better understand and illustrate the nature of this thinning, northwest-trending stratigraphic and time-stratigraphic cross sections (Figures 33-35) were constructed across the southern part of the basin to illustrate the stratigraphy of the interval from the uppermost part of the Upper Cretaceous Lewis Shale to the lowermost part of the lower-Paleocene Nacimiento Formation; the line of these cross sections is shown on Figure 3. (Note: The following discussion of these cross sections uses feet, followed by the parenthetical thicknesses in meters, because the depth track for the geophysical logs referred to are calibrated in feet.)

The stratigraphic, geophysical-log cross section (Figure 33) was constructed using drill-hole logs at localities numbered 1 through 6 on Figure 3. Contacts of most of the geologic formations included in the interval studied are easily located on these logs, with the possible exception of the top of the Fruitland Formation whose contact has been defined as being at the top of the highest coal or carbonaceous shale bed in the formation (Fassett and Hinds 1971). This contact cannot be continuously mapped, either on the surface or on geophysical logs, because of the discontinuous nature of thin, uppermost-Fruitland coal or carbonaceous mudstone beds. Because the lithologies of the Fruitland and lower shale member of the Kirtland are virtually identical, the presence of these carbon-rich beds provides the only criterion to separate these formations. The next-highest

geologic contact between the lower shale member of the Kirtland Formation and the overlying Farmington Sandstone Member is quite distinctive because the Farmington Sandstone consists of a series of closely spaced and discontinuous channel-sandstone beds (Figure 33) that are clearly visible on geophysical logs and on the outcrop. The lowermost sandstone bed of the Farmington Sandstone Member is not always at the same stratigraphic level at different localities. This contact shifts up and down from location to location, usually within a vertical range along depositional strike of at most tens of meters (Fassett and Hinds 1971). The contact between the Kirtland Formation and the Ojo Alamo Sandstone (Figure 33) is clear-cut and easily located on geophysical logs (and on the outcrop) because the Ojo Alamo contains from one to several massive, coarse-grained, conglomeratic sandstone benches with distinctive geophysical-log characteristics.

The locations of five of the six geophysical logs on the stratigraphic cross section (Figure 33) were selected close to important outcrop localities in the southwestern San Juan Basin where paleomagnetic, palynologic, and fossil-vertebrate data were obtained. The log of drill-hole 3 was inserted in the section to maintain even spacing of subsurface control along the line of section. The datum for this cross section is the Huerfanito Bentonite Bed of the Lewis Shale. Because the Huerfanito Bed is an altered volcanic ash bed that represents an ash fall into the Lewis-Shale sea in Late Cretaceous (Campanian) time, this marker bed represents a time horizon throughout the San Juan Basin. The Huerfanito Bed is an easily recognizable marker bed on geophysical logs in the subsurface throughout most of the San Juan Basin.

Radiometric ages of sanidine crystals from the altered volcanic ash beds shown on Figures 32 and 33 were acquired using $^{40}\text{Ar}/^{39}\text{Ar}$ methodology (Fassett and Steiner 1997, Fassett et al. 1997, Fassett 2000). Four of these ages are projected into the log of drill-hole 2 of Figure 33 from their outcrop locations in or near Hunter Wash, about 9 km to the southwest. Magnetochrons identified near drill holes 1, 2, 4, and 6 (discussed in detail above) have also been projected into the geophysical logs. The magnetic-polarity column of drill-hole 2 is a composite of the two (virtually identical) columns of Lindsay et al. (1981) and Fassett and Steiner (1997) of Figure 18. The magnetic-polarity column at drill-hole 6 is from Mesa Portales (Figure 23). The nearby Eagle Mesa magnetic-polarity column of Butler and Lindsay (1985) depicted on Fig-

ures 28 and 29 places the C33n-C32r reversal at virtually the same level as at Mesa Portales. The levels of palynologic samples collected from nearby outcrop localities are shown on drill-hole logs 1, 2, 5, and 6; the palynology of these strata is summarized in the "Palynology" section of this report and is discussed in greater detail in the Appendix. Dinosaur- and mammal-bone localities shown in the Ojo Alamo Sandstone at drill holes 2 and 4 are at nearby outcrops and are discussed in the "Vertebrate Paleontology" section of this report.

The lowest unit shown on the stratigraphic cross section of Figure 33, the Lewis Shale, was deposited as marine muds and silts on the western edge of the Western Interior Seaway in late Campanian time. Overlying the Lewis Shale is the Pictured Cliffs Sandstone, a time-transgressive, shoreface-marine sandstone, deposited during the final regression of the Western Interior Seaway from southwest to northeast across the San Juan Basin area. The fact that the top of the Pictured Cliffs is essentially parallel to the Huerfanito Bentonite Bed on the logs of drill holes 1 through 5 (Figure 33) indicates that the line of cross section is directly along the depositional strike or paleo-shoreline of the Pictured Cliffs sea. Between holes 5 and 6, the Pictured Cliffs is seen to rise stratigraphically; this is because the trend of the line of section between these two holes is eastward, diverging from the Pictured Cliffs shoreline's southeast trend, and is thus reflecting the northeastward stratigraphic rise of the Pictured Cliffs Sandstone. The 400 m stratigraphic rise of the Pictured Cliffs across the entire San Juan Basin is illustrated on Figure 32.

The thickness of the Fruitland Formation ranges from about 300 feet (90 m) in drill hole 3 to 400 feet (120 m) in drill hole 1 on this cross section. The Fruitland-Kirtland contact is virtually parallel to the top of the Pictured Cliffs in drill holes 1 through 5 (Figure 33). Coal beds, representing back-shore swamp deposits in the lower Fruitland Formation, are present in all six drill holes. The contact of the lower shale member of the Kirtland Formation and the Farmington Sandstone Member of the Kirtland is about 600 feet (180 m) above the top of the Pictured Cliffs in holes 1 through 3, however in holes 4 through 6, the Farmington Sandstone is absent and large channel sandstones appear in the upper part of the section. Above the Farmington Sandstone and upper shale member of the Kirtland Formation, undivided, the Ojo Alamo Sandstone is seen to be stepping down from drill hole 1 to drill hole 6; the base of the Ojo Alamo is

950 feet (290 m) lower in drill hole 6 than in drill hole 1. All of this thinning is apparently at the expense of the underlying Kirtland Formation, which appears to be totally cut out in drill hole 6.

There is a problem with the simple interpretation of the geophysical-log section depicted on Figure 33, apparently showing progressive truncation of the Fruitland-Kirtland interval from northwest to southeast. Note that the polarity reversal from C33n to C32r (within the Fruitland-Kirtland interval) is also stepping down from drill hole 1 to drill hole 2, and from drill hole 2 to drill hole 6 (Figure 33). Paleomagnetic reversals are isochrons, therefore, if deposition of the Fruitland-Kirtland interval strata had been continuous and even across the area of the Figure 33 cross section, the C33n-C32r reversal would be parallel with the underlying Huerfanito Bentonite Bed isochron. If the progressive truncation of Kirtland strata from northwest to southeast were as simple as apparently shown on Figure 32, resulting only from a pre-Ojo-Alamo-Sandstone erosion cycle, that truncation would have totally cut out magnetochron C32r and several hundred feet (about 200 m) of the upper part of chron C33n in drill hole 6, which is clearly not the case. Why then is the C33n-C32r reversal present in the Mesa Portales area? There is an elegant, straightforward solution to this problem.

Figure 34 is a time-stratigraphic cross section on which the stratigraphic section of Figure 33 has been reordered so that the two isochrones, the C33n-C32r reversal and the Huerfanito Bentonite Bed, are parallel. Raising the top of C33n to the same level in drill holes 2 through 6 as in drill hole 1 reveals the presence of a wedge-shaped hiatus present in the Fruitland-Kirtland interval on Figure 34 (it is assumed there is no hiatus in this interval in drill hole 1, although this is not known for certain). The top of polarity chron C33n was raised 75 feet (23 m) in drill hole 2 to bring it to the same level as in drill hole 1. In drill hole 6, however, the top of chron C33n had to be raised 600 feet (185 m) to bring it up to the level of the top of this chron in drill-hole 1. Because the rate of deposition of the rock strata between the Huerfanito Bentonite Bed and Ash J averages 142 m/m.y. (384 m/2.72 m.y.) the duration of the hiatus at drill-hole 2 must be about 160,000 years whereas at drill hole 6 it is about 1.3 m.y.

The stratigraphic level of the unconformity within the Fruitland-Kirtland interval is not known with certainty, because it has never been discovered on the outcrop and it cannot be detected on geophysical logs. In drill hole 6 (Figure 34), the

unconformity has to be below the top of chron C33n and above the coal bed in the lower part of the Fruitland. Because the top of C33n is within the prominent white sandstone bed at Mesa Portales (Figures 22, 23), a reasonable placement is at the base of the white sandstone (Figures 33-35). In drill holes 4 and 5, the unconformity would logically be at the base of the conspicuous channel-sandstone beds that are present in the uppermost part of the Kirtland Formation. In drill hole 3, where there is no obvious lithologic level at which to place the unconformity, it is projected horizontally westward from hole 4, within the Farmington Sandstone Member of the Kirtland Formation (Figure 34). And in drill hole 2, the unconformity is placed below the top of chron C33n, also within the Farmington Sandstone.

Figure 35 is a time-stratigraphic cross section along the same line of section as Figures 33 and 34, but with the vertical exaggeration changed from 130 X to 85 X to make possible the portrayal of the 7.8-m.y. hiatus separating Campanian Kirtland Formation strata from the overlying Paleocene Ojo Alamo Sandstone strata. The age of the base of the Ojo Alamo Sandstone is estimated to be 65.2 Ma based on an age of 65.112 Ma (Gradstein et al. 2004) for the base of magnetochron C29n located just above the base of the Ojo Alamo. Palynologic data also confirm that earliest Paleocene strata are absent in the San Juan Basin (Newman 1987, p. 158). In addition, the K-T boundary asteroid-impact fall-out layer or the iridium-enriched layer found at the K-T boundary at many localities in the Western Interior of North America, have not been found at or near the K-T interface in the San Juan Basin despite concerted attempts to locate them at several localities in the southern San Juan Basin (Orth et al. 1982). It is thus estimated that about 0.3 m.y. of earliest Paleocene time is not represented by rock strata in the southern San Juan Basin (Figure 35). Palynologic data (discussed below) support the absence of lowermost Paleocene strata below the base of the Ojo Alamo Sandstone.

PALEOBOTANY

Leaf Fossils

Knowlton (1917, 1924) discussed leaf fossils he identified from the Fruitland and Kirtland Formations in the San Juan Basin and also discussed the significance of leaf fossils he identified from the Ojo Alamo Sandstone at several localities. Knowlton stated that Ojo Alamo Sandstone fossils were completely different from those found in underlying

beds and even though these fossil leaves did not definitively fix the age of the Ojo Alamo as Tertiary, Knowlton found them to be more Tertiary-like than Cretaceous. As far as is known, Knowlton's work is the only published report on leaf fossils from the Ojo Alamo Sandstone. Reeside (1924) addressed the age of the Ojo Alamo Sandstone and cited the paleobotanical studies of Knowlton (1917, 1924) as tentatively supporting the Paleocene age of this formation.

Palynology

The palynology of the rocks adjacent to the Cretaceous-Tertiary boundary in the San Juan Basin is discussed in detail in the Appendix of this report. All palynomorphs identified from these rocks are listed in the Appendix tables and the paleochronologic significance of these fossils is discussed therein in detail. The following section of this report summarizes the palynologic data presented in the Appendix.

Palynology has been a valuable and precise biochronologic tool for defining the Cretaceous-Tertiary boundary in continental strata of the Western Interior of North America. For nearly 50 years, index palynomorphs such as *Proteacidites* spp. and many species of *Aquillapollenites*, for example, have been the primary Cretaceous index fossils in the Western Interior with the last occurrence of these key taxa unequivocally marking the end of the Cretaceous Period (Anderson 1960, Tschudy 1973, Nichols and Johnson 2002, among others). (*Proteacidites* was renamed *Tschudypollis* in Nichols 2002.) The K-T boundary was located within centimeters in the Raton Basin of New Mexico and Colorado by R.H. Tschudy (USGS) on the basis of the last occurrence of *Tschudypollis* spp. That work enabled Orth et al. (1981) to find the iridium-enriched, end-Cretaceous, asteroid-impact, fall-out layer within that same centimeters-thick interval. Because the fall-out layer is only about 25 mm thick and not conspicuous in most exposures, the use of palynology to narrow the stratigraphic interval of interest has been critical in locating this bed at numerous sites in the Western Interior. The identification of the end-Cretaceous fall-out layer in the Raton Basin (Orth et al. 1981, 1982) was the first discovery of this important geochron in continental rocks anywhere in the world. Subsequently, the fall-out layer has been found at numerous other localities in continental strata in the Western Interior using palynology to zero in on the appropriate rock strata. The discovery of the asteroid-impact fall-out layer has not only established for the first

time the presence of a physical rock layer marking the Cretaceous-Tertiary boundary, but equally importantly, has also validated the precise age significance of Late Cretaceous and Paleocene index palynomorphs found below or above it in the Western Interior of North America.

The use of fossil pollen to fine tune ages *within* Upper Cretaceous or lower Paleocene strata, however, has proved to be useful, but less precise. As the discussion in the Appendix indicates, palynologic data in the San Juan Basin suggests that the Maastrichtian Stage is missing throughout most of the basin, however, this Stage lasted 5 m.y. (Gradstein et al. 2004); thus, this finding did not have the precision of the end-Cretaceous-boundary determination. (In actuality, as Figure 35 shows, the Cretaceous-Tertiary hiatus in the southern San Juan Basin spans 7.8 m.y.; a time period that includes about 2.5 m.y. of late Campanian time, all of Maastrichtian time, and about 0.3 m.y. of earliest Paleocene time.) The first appearance of Paleocene index palynomorphs, such as *Momipites tenuipolus* and *Brevicolporites colpella*, in the southern part of the Western Interior (Anderson 1960, Tschudy 1973, Nichols and Johnson 2002, Nichols 2003) has also been useful in determining the ages of strata adjacent to the K-T interface in the San Juan Basin. Palynologists agree (Nichols, personal commun., 2005) that rock samples that yield diverse palynomorph assemblages, contain no specimens of Cretaceous index fossils (such as *Tschudypollis* spp.), and contain Paleocene index palynomorphs (such as *B. colpella* or *M. tenuipolus*), are “unquestionably” Paleocene in age.

The palynology of rock strata in the San Juan Basin adjacent to the K-T interface has been addressed in a number of publications beginning with Anderson (1960). In addition, a large amount of palynologic data exists for these same strata in the form of unpublished USGS “Reports on Referred Fossils” in the files of the author. The appendix of this report contains a detailed discussion and synthesis of all of these palynologic data.

Palynology has fixed the Cretaceous-Tertiary (K-T) interface at (or just below) the base of the Ojo Alamo Sandstone at five principal localities in the New Mexico part of the San Juan Basin: 1) the Cuba, New Mexico area; 2) the Gasbuggy core; 3) the Mesa Portales area; 4) the Ojo Alamo Sandstone type area; and 5) the San Juan River site (see Figure 1 for locations). At one locality in the Colorado part of the basin, near Durango (Figure 1), palynology has bracketed the K-T interface at

the contact between the Cretaceous Kirtland Formation and the Paleocene Animas Formation.

Cuba, New Mexico Area. Anderson (1960) was the first geologist to use palynology to determine the location of the Cretaceous-Tertiary boundary in the San Juan Basin. He collected rock samples from the uppermost Kirtland Formation and from within the Ojo Alamo Sandstone in the southeast part of the basin near Cuba, N.M. (Figure 1) and concluded that the palynomorph assemblages from the Ojo Alamo Sandstone were all Tertiary in age and the assemblages from the underlying Kirtland Formation were Cretaceous in age. Based on these data, Anderson (1960) placed the K-T boundary at the base of the Ojo Alamo Sandstone. Anderson was aware that the Ojo Alamo contained abundant dinosaur bone in other parts of the basin and concluded that (p. 13) either those dinosaur fossils had been reworked or misidentified or that: “Alternatively, pre-Lance-type dinosaurs persisted into a Tertiary environment.”

Gasbuggy Core. Core chips from 52 levels were collected from the Gasbuggy core (Figure 1) in 1967 by the author from a drill hole in the east-central part of the San Juan Basin (Fassett 1968a, b). These samples were from the Lewis Shale, Pictured Cliffs Sandstone, Fruitland Formation, Ojo Alamo Sandstone, and Nacimiento Formation (depths of 4,263 to 3,437 ft). These samples were submitted to R.H. Tschudy (USGS) for palynologic analysis, and he reported (1973, p. 131) that 30 samples yielded sufficient specimens for a percentage count. Tschudy found that all of the Fruitland Formation samples contained abundant specimens of *Proteacidites* spp. (*Tschudypollis*) and, that the overlying Ojo Alamo Sandstone contained the Paleocene index fossil *Maceopolipollenites tenuipolus* (*Momipites tenuipolus*) and a few reworked specimens of *Proteacidites* spp. On the basis of these palynologic data, Tschudy placed the Cretaceous-Tertiary boundary in the GB-1 core at the base of the Ojo Alamo Sandstone.

Tschudy (1973) also compared the palynomorph assemblages from the Gasbuggy core with those of other Western-Interior basins, including, the nearby Raton Basin of northeastern New Mexico and southwestern Colorado. On the basis of those comparisons, Tschudy concluded that uppermost Campanian-age and all Maastrichtian-age rocks were missing in the Gasbuggy core indicating the presence of a significant hiatus separating the Paleocene Ojo Alamo Sandstone from the underlying Campanian Fruitland Formation in the San Juan Basin.

Mesa Portales. The palynology of strata adjacent to the K-T interface at Mesa Portales was discussed in Fassett and Hinds (1971). These authors collected rock samples for palynologic analysis from the uppermost Kirtland-Fruitland Formation (undivided) and from the Ojo Alamo Sandstone on Mesa Portales (Figures 1, 21). R.H. Tschudy analyzed the samples and found (in Fassett and Hinds 1971, p. 31,33, and table 1) that the K-T interface at Mesa Portales was in the uppermost part of the Kirtland-Fruitland interval, 13 m below the base of the Ojo Alamo Sandstone (Figure 23). Tschudy concluded that the uppermost 13 m of the Kirtland-Fruitland Formation and all of the Ojo Alamo Sandstone at Mesa Portales were Paleocene in age (Figures 22-25). Additional samples were subsequently collected at Mesa Portales from other parts of the Fruitland-Kirtland Formation and from the Ojo Alamo Sandstone and palynomorph lists identified by Tschudy from those samples are published for the first time in the Appendix of this paper. These new data confirmed that the K-T interface at Mesa Portales is 14 m below the base of the Ojo Alamo Sandstone in uppermost Fruitland-Kirtland strata (Figure 23). All samples from below this interface yielded large numbers of *Proteacidites* spp., and no specimens of this Cretaceous index fossil were found above this level. One sample 5 m below the base of the Ojo Alamo (D6583-B of Figure 23) yielded the Paleocene index fossil *M. tenuipolus*. Thus the Ojo Alamo Sandstone is unequivocally Paleocene in age in its entirety at Mesa Portales.

Ojo Alamo Sandstone Type Area. The Ojo Alamo Sandstone type area is between Hunter Wash and De-na-zin Arroyo in the southwest part of the San Juan Basin (Figures 1, 4). The Ojo Alamo Sandstone contains abundant dinosaur fossils in this area. As discussed in the Appendix, palynologic data from strata adjacent to the K-T interface in the Ojo Alamo Sandstone type area have been presented in several publications. In addition, the Appendix also presents unpublished palynomorph lists for this area from the files of the author. These data show that all of the many rock samples from the Cretaceous Fruitland and Kirtland Formations in this area have yielded abundant specimens of *Tschudypollis* spp. One sample from the uppermost Kirtland Formation (less than 1-m below the base of the Ojo Alamo) has yielded the Paleocene index palynomorph *M. tenuipolus* and a few reworked specimens of *Tschudypollis* spp. Several samples from mudstone interbeds in the upper part of the Ojo Alamo in this area have also yielded

Paleocene index palynomorphs and no specimens of *Tschudypollis* spp.

On the basis of these data, the K-T interface is placed just below the base of the Ojo Alamo Sandstone in the Ojo Alamo Sandstone type area.

San Juan River Site. Rock samples collected for palynologic analysis from the Ojo Alamo Sandstone at the San Juan River site from a coaly, carbonaceous shale interbed, 13 m above the base of the Ojo Alamo Sandstone, have yielded the Paleocene index fossil *M. tenuipolus*; in addition one sample also yielded the Paleocene index fossil *Brevicolporites colpella*. The carbonaceous shale yielding these Paleocene palynomorphs is 3.5 m below the level of a large hadrosaur femur collected from this locality. Some, but not all of these samples, also yielded rare, reworked specimens of *Tschudypollis* spp. The presence of two Paleocene index palynomorphs from the Ojo Alamo Sandstone at the San Juan River site provides conclusive evidence that the Ojo Alamo Sandstone is Paleocene in age at this location.

Durango Area. Studies of the palynology of rock strata adjacent to the K-T interface were conducted by Manfrino (1984) and Newman (1987) in an area in the northern San Juan Basin near Durango, Colorado (Figure 1). The results of those studies are summarized in Newman (1987). The rock strata adjacent to the K-T interface in the Durango area are different from those in the New Mexico part of the San Juan Basin because: 1) The Animas Formation rather than the Ojo Alamo Sandstone overlies the K-T interface in the northern San Juan Basin (Figure 1.1), and 2) The McDermott Formation is the stratigraphically highest Cretaceous rock unit in that area. The lower part of the Animas Formation is the same age as the Ojo Alamo Sandstone, even though the two formations are distinctly different, lithologically, and the Animas is much thicker: about 335 m in the Durango area. The upper part of the Animas Formation in the northern San Juan Basin is time equivalent to the Nacimiento Formation in the southern part of the basin even though the two formations are lithologically distinct (Fassett 1985).

The Appendix contains a summary of Newman's (1987) findings regarding the biochronologic significance of the palynomorphs identified from rock samples collected from uppermost Cretaceous and lowermost Paleocene strata in the Durango, Colorado area. Newman showed that the palynomorph assemblages from the uppermost Lewis Shale, Pictured Cliffs Sandstone, and most of the Fruitland Formation are late Campanian in

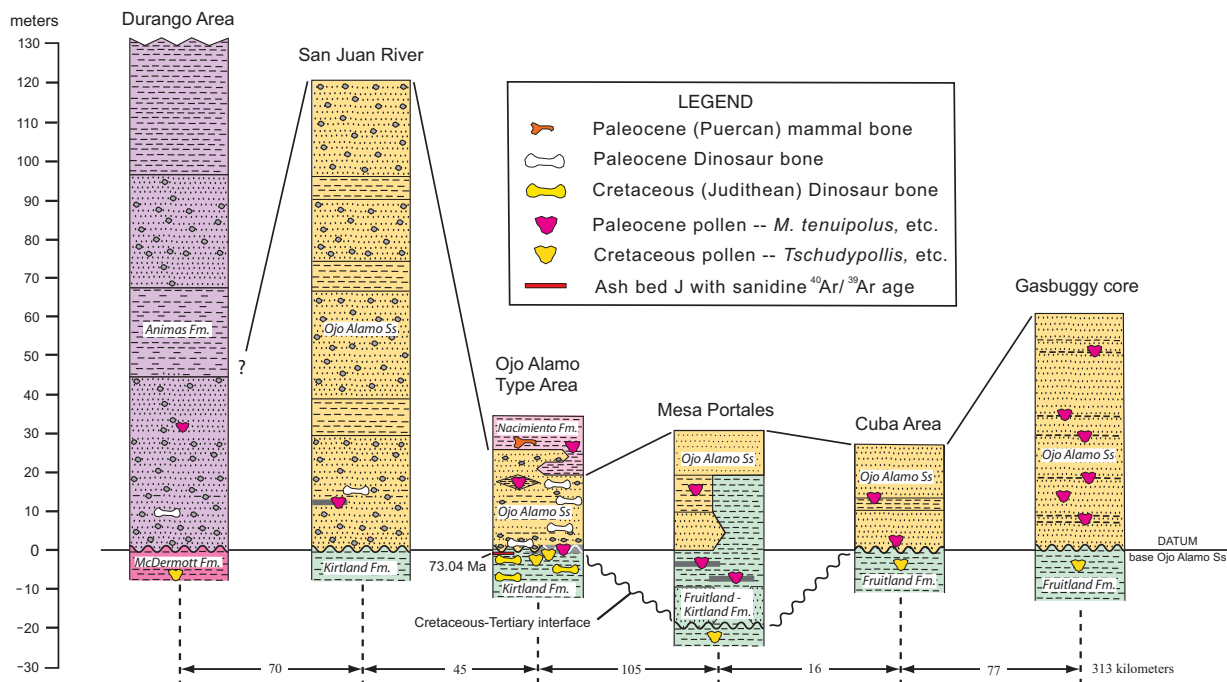


Figure 36. Stratigraphic columns showing formations adjacent to Cretaceous-Tertiary (K-T) interface at six localities in San Juan Basin (Figure 1) where palynologic data have precisely fixed its stratigraphic position. Interface is palynologically bracketed at all localities except San Juan River site. K-T interface coincident with base of Ojo Alamo Sandstone or Animas Formation except at Mesa Portales and possibly locally in Cuba area. Complete palynomorph lists in the Appendix.

age, and that most of the Kirtland Formation and the lower half of the McDermott Formation yielded palynomorphs of early Maastrichtian age. He also showed that the Animas Formation contains palynomorphs of early Paleocene age. Newman (1987) placed the K-T interface at the base of the Animas Formation in the Durango, Colorado area. Newman also concluded (p. 158) that based on his palynologic studies in this area: "Approximately the upper half of the Maastrichtian Stage is not represented, and perhaps some earliest Paleocene is missing as well between McDermott and Animas strata."

Newman's finding that the Animas Formation is Paleocene in the northern San Juan Basin supports earlier conclusions by Knowlton (1924) who conducted an extensive study of leaf fossils in the Animas Formation. Knowlton stated (p. 71) that the Animas is:

... undoubtedly Tertiary. Not a single species is known to be common to the Animas formation and the Cretaceous exclusively—in fact, there are only five species that extend into the

acknowledged Cretaceous anywhere.

Summary

Figure 36 summarizes the palynologic biochronology of strata adjacent to the K-T interface in the San Juan Basin. The six columns show the localities where palynology definitively establishes the age of the Ojo Alamo Sandstone (or lowermost Animas Formation) in the San Juan Basin. The column headed "Durango Area" shows that the Cretaceous-Tertiary (K-T) interface is at the base of the Animas Formation—top of the McDermott Formation based on palynology. The McDermott rests conformably on top of the Kirtland Formation and is only found in a small area in the northwest part of the San Juan Basin (Fassett 1985).

At the San Juan River locality (Figure 36), two Paleocene index palynomorphs *M. tenuipolus* and *B. colpella* were identified from samples about 13 m above the base of the Ojo Alamo Sandstone where it rests unconformably on the Kirtland Formation. No samples have been collected from the Kirtland for palynologic analysis at this locality, thus the K-T interface is not bracketed by palynomorph assemblages here. At the Ojo Alamo type area, the

basal contact of the Ojo Alamo Sandstone with the top of the Kirtland Formation is closely bracketed by palynologic assemblages indicating that all Ojo Alamo strata are Paleocene in age there.

At Mesa Portales, palynologic data show that not only is the Ojo Alamo Sandstone Paleocene in its entirety, but about 14 m of the underlying Fruitland-Kirtland Formation is Paleocene as well. In the Cuba area and in the Gasbuggy core, Paleocene and Cretaceous palynomorph assemblages closely bracket the basal contact between the base of the Ojo Alamo Sandstone and the top of the Fruitland Formation providing conclusive evidence that the Ojo Alamo at those places is Paleocene in its entirety.

In summary, at all localities where palynomorphs have been identified bracketing the base of the Ojo Alamo Sandstone or Animas Formation, Cretaceous palynomorphs such as *Tschudypollis* spp. are found in large numbers in underlying Cretaceous strata and Paleocene palynomorphs such as *M. tenuipolus* and (or) *B. colpella* are found in the Ojo Alamo and lowermost Animas or Nacimiento Formations. At three localities San Juan River, the Ojo Alamo type area, and the Gasbuggy core hole (Figure 36) rare, reworked specimens of the Cretaceous index palynomorph *Tschudypollis* have been identified in some samples in the lowermost part of the Ojo Alamo Sandstone but at the other localities shown on Figure 36, *Tschudypollis* has not been identified in the Ojo Alamo or Animas Formations. The weight of the palynologic evidence thus supports the conclusion that the Ojo Alamo Sandstone and the Animas Formation are Paleocene in age in their entirety throughout the San Juan Basin.

In addition, because *M. tenuipolus* has been shown to be present only in the upper part of biozone P1 in many Western Interior basins (including the nearby Raton Basin) and absent in lowermost Paleocene strata (Nichols 2003), the presence of this guide fossil in lowermost Paleocene strata in the San Juan Basin suggests that strata representing the lower part of biozone P1 is not present in the San Juan Basin (see discussion in the Appendix). This finding supports paleomagnetic evidence (discussed above) suggesting that the lowermost Paleocene strata in the San Juan Basin are 63.2 Ma (Figures 34, 35).

VERTEBRATE PALEONTOLOGY

Vertebrate fossils have been known to exist in strata adjacent to the Cretaceous-Tertiary (K-T) boundary in the San Juan Basin since the work of

Cope (1881). Subsequently, many vertebrate paleontologists visited the southern San Juan Basin and collected large numbers of vertebrate fossils in K-T strata that have been discussed and described in numerous publications up to the present day; for a list of the principal references to those publications see Williamson (1996), Fassett et al. (2002), and papers in Lucas and Heckert (2000). A detailed discussion of the history of vertebrate paleontology in the San Juan Basin is beyond the scope of this report but such discussions may be found in papers by Clemens (1973b), Fassett (1973), Powell (1973), Simpson (1981), and in Williamson (1996). This report focuses on the biochronologic significance of vertebrate fossils from the Paleocene Ojo Alamo Sandstone, Animas Formation, and the lowermost part of the Nacimiento Formation, with brief discussions of vertebrates from underlying Cretaceous strata.

Vertebrate paleontology has had limited biochronologic value in determining the age of strata adjacent to the K-T interface in the San Juan Basin. However, with the publication of a series of six radiometric ages throughout the Cretaceous Fruitland and Kirtland Formations (Fassett and Steiner 1997; Fassett 2000), the precise ages of the vertebrate assemblages in these strata have now been established. This temporal calibration of Late Cretaceous (Campanian) vertebrates in the San Juan Basin provides a standard to correlate faunal zones of the San Juan Basin to other Western Interior basins where such data sets may be less complete.

Dating of the Paleocene Ojo Alamo Sandstone on the basis of robust palynologic data and, independently, on the basis of paleomagnetism (Fassett and Lucas 2000, Fassett et al. 2002, and this report) has now established the Paleocene age of this formation and its contained vertebrate-fossil assemblage: the "Alamo Wash local fauna.. Correlation of these Paleocene vertebrates to other North American basins may improve our understanding of the survival of various "Lancian"-aspect vertebrates across the Cretaceous-Tertiary interface.

Dinosaurs

Cretaceous Kirtland and Fruitland Formations. Dinosaurs of the Fruitland and Kirtland Formations in the San Juan Basin were summarized in Lucas et al. (2000, p. 87, 88). Sullivan and Lucas (2006, p. 18-20) also presented a detailed analysis of the dinosaur taxa identified from these formations and defined their new "Kirtlandian" land vertebrate age

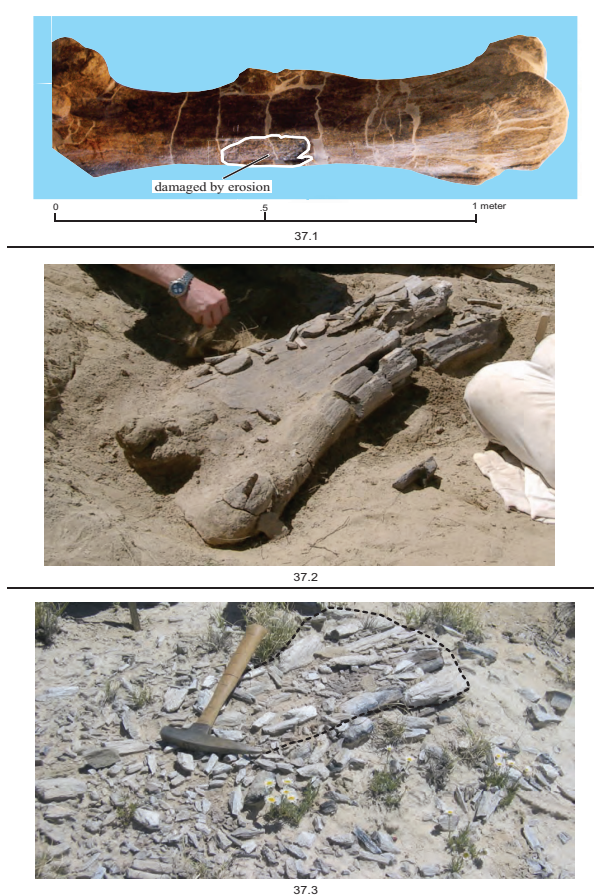


Figure 37. Photographs of three dinosaur bones from Ojo Alamo Sandstone showing different degrees of preservation. Bone in 37.1 is right hadrosaur femur from San Juan River site; bone is almost perfectly preserved (photo from Fassett et al. 2002). Bone in 37.2 is sauropod femur from Barrel Spring area (letter O on Figure 4); well preserved where encased in bed rock, but end in upper right has been subjected to subaerial erosion, become fragmented, and part is missing (Photograph from R.M. Sullivan). Bone in 37.3 is also from Barrel Spring area (letter N on Figure 4); bone is badly fragmented, however shape of large limb bone still discernible (dashed outline). Hammer 0.33 m long; hammer handle scaled in tenths of foot.

as being “equivalent to 2.2 m.y. of Campanian time” falling between the Judithian and Edmontonian land-vertebrate ages of the northern part of the Western Interior of North America. Sullivan and Lucas (2006) is an amplification of the Sullivan and Lucas (2003) paper in which the “Kirtlandian” name was first proposed.

Paleocene Ojo Alamo Sandstone. In 1983, a large—1.3 m long—right hadrosaur femur was discovered about 15 m above the base of the Ojo

Alamo Sandstone at the San Juan River locality (Figure 1.1). This bone was imbedded in the lower part of a vertical cliff face of coarse-grained, conglomeratic sandstone; only one surface of this fossil was partially exposed when it was discovered (Fassett and Lucas 2000, figure 3A). This fossil was subsequently excavated and prepared and is now on display at the University of New Mexico, Earth and Planetary Sciences Department in Albuquerque. This specimen is described in detail in Fassett and Lucas (2000); Figure 37.1 is a color photograph of this bone.

Fassett and Lucas stated that because this fossil was so massive and its outer surface so pristine (Figure 37.1), this bone could not possibly have been reworked from underlying Cretaceous strata into the high-energy, conglomeratic, Ojo Alamo Sandstone, and they wrote (p. 228): “We suggest that the hadrosaur represented by this femur lived in early Paleocene time and died near the place where this specimen was found.” The Paleocene age of the Ojo Alamo Sandstone at the San Juan River site (reported in Fassett and Lucas 2000) was established by the presence of Paleocene index palynomorphs in the lower Ojo Alamo, below the level of the hadrosaur femur. A sample of this hadrosaur femur was chemically analyzed and found to have distinct elemental concentrations characteristic of Paleocene dinosaur bone in the San Juan Basin. (The chemistry of Cretaceous vs. Paleocene dinosaur-bone samples from the San Juan Basin is discussed in detail in a subsequent section of this report.)

Sullivan et al. (2005, p. 401) discussed the hadrosaur femur from the Ojo Alamo Sandstone at the San Juan River site, as follows:

However, despite the bone’s near-pristine appearance, we argue here, largely based on parsimony [my emphasis], that the bone has been reworked, and not transported any significant distance, thereby preserving the integrity of the bone’s outer surface.

Three points are relevant to this suggestion that this specimen is “reworked”: 1) The femur was found 15 m above the base of the Ojo Alamo Sandstone in an area where the contact of the Ojo Alamo Sandstone and the underlying Kirtland Formation is essentially a planar surface; there is no conceivable way this bone could have been weathered out of the underlying Cretaceous strata and been redeposited 15 m above the base of the Ojo Alamo without moving it a “significant distance”; 2) The word “parsimony”, as used above apparently

means adherence to the concept that dinosaurs are defacto Cretaceous index fossils; it is suggested that adherence to this precept, in the face of overwhelming physical evidence to the contrary, is not parsimonious; 3) The hadrosaur femur's chemistry strongly suggests that it is a Paleocene bone (see the "Geochemistry of Vertebrate Bone Sample" section of this report). Sullivan, Lucas, and Braman (2005) offer no new evidence contravening these facts.

With the exception of the San Juan River locality, all dinosaur remains from the Ojo Alamo Sandstone are from the southwestern part of the San Juan Basin between Hunter Wash and Betonnie Tsosie Wash (Figures 1, 3). Within this region, the highest concentration of dinosaur bone is in the Ojo Alamo Sandstone type area: from just west of Hunter Wash to just east of De-na-zin Wash (Figure 4). Dinosaur fossils have also been found relatively recently in the Ojo Alamo Sandstone southeast of the type area near Betonnie Tsosie Wash (Figure 11). Fassett et al. (2002) discussed and referenced all significant published reports of dinosaur fossils from the Ojo Alamo Sandstone and listed the following dinosaurs from that formation (as reported by Lucas et al. 2000, p. 88): *Alamosaurus sanjuanensis*; ?*Albertosaurus* sp., cf *Tyrannosaurus* sp.; ankylosaurid, indeterminate; dromaeosaurid, indeterminate; hadrosaurids, indeterminate; nodosaurids, indeterminate; ornithomimid, indeterminate; *Pentaceratops*; saurornithoidids, indeterminate; *Torosaurus* cf. *T. latus*.

The "*Pentaceratops*" specimen was reexamined (Sullivan et al. 2005, p. 567), and these authors determined that this fossil should be relabeled "chasmosaurine, indeterminate." *Glyptodontopelta mimus*, according to R.M. Sullivan (personal commun., 2006) should be added to the list along with Tyrannosauridae, indeterminate. Sullivan et al. (2005) indicated that all specimens from the Ojo Alamo originally named *Torosaurus* were incorrectly identified and suggested that the name *Torosaurus* be replaced by "chasmosaurine, indeterminate." Farke (2002), however, indicated that specimen NMMNH P.22884 from the Ojo Alamo is the ceratopsian *Torosaurus* cf *T. utahensis*, thus this name is retained in the list of Ojo Alamo dinosaurs. Specimen NMMNH P.25074 was originally reported to be from the Ojo Alamo Sandstone) and was referred to *Torosaurus* sp. by Farke (2002). Sullivan et al. (2005), however, stated that this specimen was from the uppermost Kirtland Formation, not the Ojo Alamo Sandstone, and

moreover determined that this specimen was not *Torosaurus* and should thus be labeled "chasmosaurine, indeterminate." Sullivan (personal commun., 2006) suggested that the name "saurornithoidids, indeterminate" be removed from the dinosaur-fossil list of Lucas et al. (2000) reproduced above.

Williamson and Weil (2001) listed additional dinosaurs identified from vertebrate microfossil sites in the Ojo Alamo Sandstone (their "Naashobito Member" of the Kirtland Formation), as follows:

At the top of the Kirtland Formation, the Naashobito Member (Alamo Wash local fauna) has yielded teeth of, in decreasing order of abundance, ceratopsids, titanosaurids, hadrosaurids, tyrannosaurids including cf. T. rex, and species of Troodon and Richardoestesia distinct from those of from (sic) the Fruitland and lower Kirtland Formations.

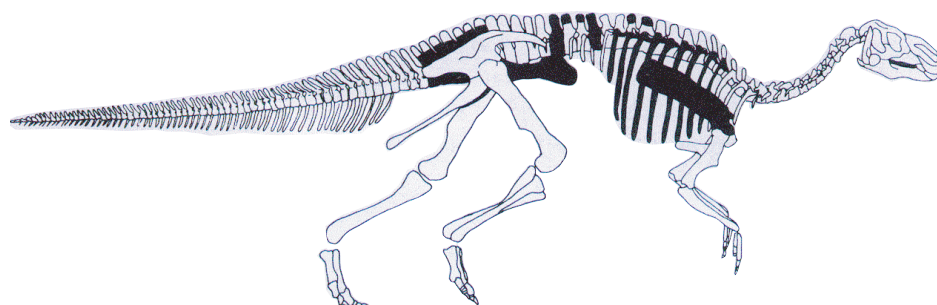
Thus, a revised list of dinosaur specimens identified from the Ojo Alamo Sandstone is: *Alamosaurus sanjuanensis*; ?*Albertosaurus* sp., cf *Tyrannosaurus* sp.; ankylosaurid, indeterminate; dromaeosaurid, indeterminate; *Glyptodontopelta mimus*; hadrosaurids, indeterminate; nodosaurids, indeterminate; ornithomimid, indeterminate; *Richardoestesia* sp.; cf titanosaurids, indeterminate; *Torosaurus* cf *T. utahensis*; *Troodon* sp.; *Tyrannosaurus rex*; and tyrannosaurid, indeterminate.

Many of the dinosaur fossils identified from the dozens of known occurrences in the Ojo Alamo Sandstone in the Ojo Alamo type area and elsewhere in the San Juan Basin are labeled "indeterminate" because nearly all specimens are single limb bones or parts of bones that cannot be identified as to genus and species. Some of these single bones are pristine and beautifully preserved, such as the hadrosaur femur from the San Juan River locality (Figure 37.1). Figure 37 shows three Ojo Alamo Sandstone dinosaur fossils in various stages of preservation ranging from being virtually perfectly preserved (Figure 37.1) to partially or nearly totally fragmented (Figure 37.2, 37.3); much of the dinosaur bone found in the Ojo Alamo is in the latter category. In at least one locality (sample 020103, locality H, Figure 4), bone fragments from several animals are preserved in a paleo channel-lag deposit.

The disintegration of dinosaur bone, as it weathers from its matrix, subaerially, (Figure 37) offers a compelling argument against the reworking of intact dinosaur bones from underlying strata into higher strata. Such reworking would require the



38.1



38.2

Figure 38. Photograph and drawing of hadrosaur-bone assemblage in lower part of Ojo Alamo Sandstone at Alamo Wash locality of Hunt and Lucas (1991). Locality is letter I of Figure 4. Bone-sample from scapula was chemically analyzed (sample P-19147 of the Appendix tables). Hammer 0.25 m long. Photograph by S.G. Lucas, New Mexico Museum of Natural History and Science, Albuquerque, New Mexico **38.1** Partially excavated bone assemblage before jacketing and removal. **38.2** Drawing of hadrosaur skeleton (from Hunt and Lucas 1991, figure 3) showing positions of bones (shaded) identified in bone assemblage of photograph 38.1. Length of skeleton is 13.5 m. Figure is from Fassett et al. (2002).

weathering-out of such bones, intact and unabraded, from their original matrix, millions of years after their original entombment, and then require that they be transported long distances laterally to a place topographically lower but stratigraphically higher than the original bone site. The fragmentation and dispersal of the weathered dinosaur fossils of Figure 37.2 and 37.3 shows why such a scenario is unlikely to impossible. Even the pristine hadrosaur femur from the San Juan River site was beginning to degrade as it weathered out of the cliff face where it was found (Figure 37.1),

and its continued erosion would have resulted in the total fragmentation and destruction of this specimen.

A commonly proposed scenario for reworking fossils from older into younger strata supposes that on a high-relief surface, a channel scour might undercut a topographically higher exposure of older strata resulting in a bone encased in that strata being dropped into a channel of younger age. This very unlikely scenario, however, would result in the displaced bone's being emplaced in the younger strata within a disoriented exotic block

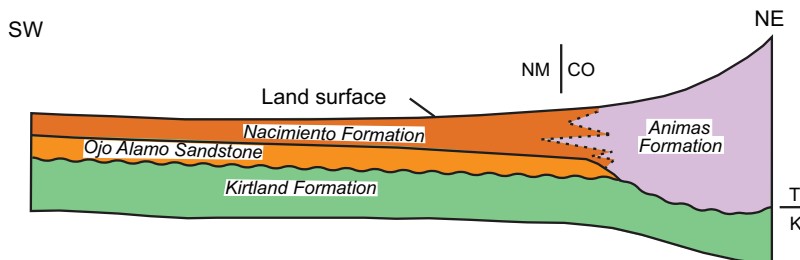


Figure 39. Diagrammatic cross section across San Juan Basin showing relations of formations near Cretaceous-Tertiary (K-T) interface. Modified from Fassett (1985).

of rock that would be clearly apparent. The large hadrosaur bone from the San Juan River site was definitely not encased in an exotic block of Cretaceous strata because, as discussed above, uppermost Cretaceous strata in the San Juan Basin are invariably fine- to medium-grained, whereas, Ojo Alamo strata are coarse-grained and conglomeratic. Figure 7 of Fassett et al. (2002) contains a photograph of the San Juan River site hadrosaur femur in place; that photograph clearly shows this fossil encased in coarse-grained conglomerate that is clearly an integral part of the surrounding rock strata. Moreover, none of the dozens of other dinosaur bones found in the Ojo Alamo in the southern part of the basin are contained in down-dropped exotic blocks. It would thus seem that the down-dropped-block scenario for all of the many dinosaur bones in the Ojo Alamo Sandstone at numerous localities in the San Juan Basin is not realistic.

The most significant, unequivocally in-place, dinosaur-bone assemblage found in the Ojo Alamo Sandstone in the San Juan Basin contained 34 skeletal elements from a single hadrosaur. Although not literally an articulated skeleton, these skeletal elements are doubtless from a single animal. This bone assemblage was described by Hunt and Lucas (1991) and was also discussed in Fassett et al. (2002) as providing clear evidence that these bones could not possibly have been reworked from underlying Cretaceous strata and thus were from an animal that lived and died in Ojo Alamo Sandstone (early Paleocene) time. The location of this site is shown on Figure 4 (locality I, sample no. P 19147). Figure 38 (reproduced from Fassett et al. 2002, figure 18, p. 327) shows this partially excavated bone assemblage.

The question of possible reworking of the many single-bone dinosaur specimens found in the Ojo Alamo Sandstone was addressed by Fassett et al. (2002). These authors presented chemical

analyses of Cretaceous and Paleocene dinosaur-bone samples showing that critical elemental concentrations in them were distinctive. An additional 14 bone samples were subsequently analyzed; six from the Ojo Alamo Sandstone, six from the Kirtland Formation, and two not in place.

These chemical analyses showed a higher abundance of uranium and a lower abundance of rare-earth elements (REE) in Paleocene bone samples and lower uranium and higher REE concentrations in Cretaceous bone samples. The distinctly different chemical “fingerprints” indicate that the Paleocene dinosaur bones were mineralized in place in the Ojo Alamo Sandstone in early Paleocene time and thus could not represent bones that had been reworked from underlying Cretaceous strata. One of the Paleocene bones chemically analyzed was a scapula from the 34-bone assemblage from a single hadrosaur, discussed above. (The geochemistry of dinosaur-bone samples from strata adjacent to the K-T interface is summarized below in the “Geochemistry of Vertebrate Bone Samples” section of this report.)

The biochronologic age of dinosaur bones from the Ojo Alamo Sandstone has been much debated over the years: Some workers have assigned a Lancian age to these fossils (Lucas et al. 1987, Hunt and Lucas 1992, Weil and Williamson 2000, and Williamson and Weil 2001, for example). Other workers (Lucas et al. 2000, p. 88), however, state that whereas the “conventional view” is that the Ojo Alamo dinosaur bones are “of Maastrichtian age, or Lancian in terms of vertebrate biochronology” a “reasonable alternative” for the age of these fossils is that they are “late Campanian”. Conclusions by Sullivan, Boere, and Lucas (2005) and Sullivan, Lucas, and Braman (2005) are far less equivocal stating that the Ojo Alamo dinosaur fossils are “early Maastrichtian” in

age or “near the Campanian-Maastrichtian boundary.”

Farke and Williamson (2006 p.1019), on the other hand, concluded that the biochronologic age of the Ojo Alamo Sandstone (their Naashoibito Member of the Kirtland Formation) based on both dinosaur and mammal fossils was Lancian. They stated:

We consider the Naashoibito Member and the Alamo Wash local fauna to be of latest Cretaceous age (Lancian land-mammal age) based on the presence of cf. T. rex (Carr and Williamson 2000) and the Lancian index mammal Essonodon browni (Lehman 1984; Williamson and Weil 2003). This correlation refutes a late Campanian or early Maastrichtian age for the Naashoibito Member (e.g., Sullivan, Lucas, and Braman [2005]).

Paleocene Animas Formation. Knowlton (1924) identified fossil leaves from Animas Formation collections from 24 numbered localities. The stratigraphic levels of these localities ranged from about 60 m above the base of the Animas to near its top more than 500 m above the base of the formation. Knowlton (p. 71) concluded that based on these fossils the Animas Formation was “undoubtedly Tertiary.”

Because of the antiquity of Knowlton’s (1924) study of fossil leaves in the Animas Formation, K. Johnson, with the Denver Museum of Nature and Science, Denver, Colorado, was asked to review Knowlton’s faunal lists from the Animas Formation and Knowlton’s conclusion that this floral assemblage was indicative of a Paleocene age for the Animas. Johnson reported (personal commun., 2008): “I would conclude that the Animas is probably early Paleocene.” Newman (1987), as discussed above, reported that the Animas Formation near Durango, Colorado, was Paleocene based on its contained palynomorphs.

Newman’s (1987) palynologic studies thus confirm Knowlton’s (1924) fossil-leaf studies indicating a Paleocene age for the Animas Formation. In addition, these studies demonstrated that the lowermost part of the Animas Formation is the same age as the Ojo Alamo Sandstone in the southern part of the San Juan Basin. (Figure 39 is a diagrammatic portrayal of Animas-Ojo Alamo relations.) Newman also confirmed the assertion by Reeside (1924) that a substantial unconformity is present between the base of the Paleocene Animas Formation and underlying Cretaceous strata. Newman’s suggestion that “perhaps some earliest

Paleocene is missing” from the lowermost Animas is in agreement with the same findings for the basal Ojo Alamo Sandstone in the southern San Juan Basin on the basis of paleomagnetism and palynology, as discussed in the Paleomagnetism and Palynology sections of this report.

The principal published references to dinosaurs found in the Animas Formation in the northern San Juan Basin are in Reeside (1924; p. 32, 34, and 52-53). Unfortunately, Reeside did not provide specific localities for any of the dinosaur-bone sites he referred to, other than “near the divide between the Pine and Piedra rivers” for one of them. There is no evidence that any of the Animas Formation dinosaur fossils referred to by Reeside were ever collected.

A search was made of the USGS field notes archives at the Denver Federal Center, Denver, Colorado, in an attempt to find more specific dinosaur-bone localities in the Animas Formation. Because one of Reeside’s (1924) references to an Animas dinosaur-bone locality contained this footnote: “Gardner, J.H., unpublished data,” Gardner’s field note books were carefully examined. The only reference to Animas dinosaurs found in Gardner’s field notes is reproduced in its entirety on Figure 40. This note indicated that Gardner, in 1907, had discovered a “*Triceratops*” specimen in the Animas Formation about 35 feet (11 m) above its base. This fossil was apparently considered to be of sufficient importance that J.W. Gidley, vertebrate paleontologist at the American Museum of Natural History, made a special trip to investigate this site. Unfortunately, the specific location of this fossil site is not given, nor is it known if this specimen was ever collected. Nevertheless, this note does confirm the presence of a recognizable ceratopsian dinosaur fossil in the lowermost part of the Animas Formation in the Colorado part of the San Juan Basin.

Apparently the presence of dinosaur fossils in the Animas Formation was common knowledge among vertebrate paleontologists working in the area at that time, as indicated in a paper by Simpson (1950, p. 86). In this report, Simpson stated that “Dinosaurs have been found in middle and lower parts of the Animas in Colorado . . .” Simpson, however indicated that the “Cretaceous-Tertiary transition occurs within this formation [Animas], at an undetermined level.” Simpson clearly thought that the K-T boundary should be placed above the highest dinosaurs in spite of Knowlton’s (1924) assertion that the Animas Formation was Paleocene based on fossil leaves.

Friday Aug. 27th 09.
 Gidley + I drive east to
 see dinosaur (Triceratops) in
 Animas that I found in 1907.
 About 35 ft. above coarse, gr. blue
 igneous s.s. base Animas resting on
 Laramie drab shales some 50 ft. above
 [?word]-gray s.s. Top Laramie.

Figure 40. Copy of entry in field notes of J.H. Gardner dated Friday, August 27, 1909. Entry reads: "Gidley & I drive east to see dinosaur (*Triceratops*) in Animas that I found in 1907. About 35 ft above coarse, gr. blue igneous s.s. base Animas resting on Laramie drab shales some 50 ft. above [?word]-gray s.s. Top Laramie." J.W. Gidley was a vertebrate paleontologist with American Museum of Natural History. (Field note entry discovered and copy provided by F. Peterson (USGS, Emeritus), Denver, Colorado.)

Simpson (1950, p. 85) is known to have worked on the Paleocene in the San Juan Basin for the American Museum beginning in 1929. Simpson's colleague at the American Museum, Walter Granger, had worked in the basin in 1912 through 1914 and in 1916. And another colleague, J.W. Gidley, had visited a ceratopsian bone site with Reeside in 1909 (Figure 40). It is probable that Granger and USGS geologists Reeside and Gardner also made field trips together and may have even visited Animas-Formation, dinosaur-bone localities together in the northern part of the San Juan Basin. The reference to Gidley in Gardner's field notes (Figure 40) clearly indicated that the American Museum staff of vertebrate paleontologists was well aware of the presence of dinosaurs discovered in the Animas Formation by USGS geologists. Although no dinosaur-bone locality has been located in the Animas Formation in modern times, there can be no doubt that these localities do exist and thus remain to be rediscovered.

Reeside (1924, p. 32 and Appendix) concluded that:

In view of the wide differences in opinion expressed by various students as to the correct assignment of this whole group of related formations, the Ojo Alamo sandstone and Animas formation are herein classified as Tertiary (?).

This conclusion by Reeside (1924) was startling and not a trivial one. Reeside had done field work throughout the San Juan Basin for many years, had measured thousands of meters of section through all of the rocks adjacent to the Cretaceous-Tertiary interface, and was well aware of the abundance of dinosaur bone in the Ojo Alamo Sandstone in the southern San Juan Basin and in the Animas Formation in the northern San Juan Basin. Reeside was certainly well aware of the significance of dinosaur bone as a Cretaceous index fossil in terrestrial strata in the Western Interior of North America. In spite of this, Reeside concluded that the Animas and Ojo Alamo were "Tertiary (?) in age." (It is suggested that Reeside's query may have been added to mollify vertebrate paleontologists and/or USGS editors of his time.) Reeside's discussions of the data in his 1924 USGS Professional Paper leave no doubt that he considered the Ojo Alamo and Animas Formations to be Tertiary in age. It is thus clear that Reeside, in 1924, was the first known geologist to challenge (albeit tacitly) the thesis that all dinosaurs became extinct at the end of the Cretaceous.

This discussion of dinosaur fossils in the Paleocene Animas Formation provides powerful, additional, independent evidence that dinosaurs lived in the San Juan Basin area in early Paleocene time. These findings, that have been slumbering in the published (and unpublished) literature for more than 80 years, seem to have been over-

looked or ignored by nearly all subsequent workers in the San Juan Basin. Fassett et al. (2002) briefly referred to Reeside's (1924) mention of Animas dinosaurs, however this report amplifies Reeside's work and adds additional supporting data from Gardner's 1909 field notes and Simpson's 1950 paper.

Mammals

Cretaceous Strata. Most of the mammalian fossils discovered in Cretaceous strata in the San Juan Basin have been recovered relatively recently using screen-washing techniques to primarily recover mammal teeth. Clemens (1973b) was the first paleontologist to conduct a concerted and extensive search for fossil mammals in upper Cretaceous strata in the San Juan Basin. He worked primarily in the southwestern part of the basin in Fruitland and Kirtland Formation strata near the Bisti Trading Post (since burned down, Figure 3), and he compiled the first list of mammal fossils from these strata. Clemens considered these mammals to be part of his "Hunter Wash local fauna" writing (p. 164) that this fauna had a "unique composition" and questioned whether this fauna differed from other faunas of the same age due to ecological or biogeographic differences "or some combination of these factors?" Clemens (1973b, p. 154) concluded that the temporal significance of his Hunter Wash local fauna was uncertain because it contained genera and species "in association with animals also known from the type Lance local fauna (Clemens 1964, 1973a), the fauna of the upper part of the Edmonton Formation (Lillegraven 1969), and those recovered from the Judith River (Sahni 1972) and Milk River formations (Fox 1970)." Clemens concluded that "Differences in local faunal composition are probably the results of both biogeographic provinciality and inequality in age."

Lindsay et al. (1981) added no new mammal identifications from the Fruitland-Kirtland interval, but based on a review of Clemens (1973b) mammal list, stated (p. 422) that the Hunter Wash fauna "includes some and lacks other mammals" characterizing the Lancian Land Mammal Age and concluded that this fauna was late, but not latest Cretaceous. This reinterpretation of the temporal significance of Clemens (1973b) mammal fauna (a bolder and quite different interpretation from that of Clemens, as noted above) was one of the lines of evidence that convinced Lindsay et al. (1981) that there was no unconformity at the base of the Ojo Alamo Sandstone and thus (mistakenly) convinced

these authors that deposition had been continuous across the Cretaceous-Tertiary interface in the San Juan Basin. Fassett and Steiner's (1997) discovery of a $^{40}\text{Ar}/^{39}\text{Ar}$ single-crystal sanidine age of 73.04 ± 0.25 Ma for an altered volcanic ash bed (Ash J of Figure 4) in the uppermost part of the Kirtland Formation (less than 5 m below the base of the Ojo Alamo Sandstone) in the Hunter Wash area refuted the assertion of Lindsay et al. (1981) that uppermost Cretaceous strata in the Hunter Wash area "represent latest Cretaceous."

Flynn (1986) reported on fossil mammals collected between 1975 and 1978 in conjunction with the field studies of Lindsay et al. (1981). The Cretaceous collections came from two areas labeled on Figure 3 as: FBS (Flynn Burnham South); and FK (Flynn Kirtland). The FBS locality is in the middle to upper part of the Fruitland Formation in the southwestern part of the San Juan Basin, southeast of the Burnham Trading Post (Figure 3). The FK locality consists of sites in the lower part of the Kirtland Formation west of Alamo Wash; these sites were apparently discovered by Lindsay et al. (1978, figure 2). Flynn listed his and previously published Cretaceous mammal identifications of Clemens (1973b) in his table 3.

Flynn (1986, table 3, Figure 41 of this report), listed 19 mammal taxa from Cretaceous strata in the southwest San Juan Basin and found that on faunal grounds, the Hunter Wash local fauna was early Judithian near the Campanian/Maastrichtian boundary with an age of about 74 Ma.

Flynn's colleagues (Lindsay et al. 1981), however, had concluded that the Hunter Wash local fauna was in the upper part of paleomagnetic chron C31n and the lower part of C30n suggesting according to Flynn (1986, p. 28) that this faunal assemblage was from strata "equivalent to the late Maastrichtian with an age of about 68 Ma" Flynn (1986, p. 28) opted to side with the geophysical data, concluding that: "The most parsimonious correlation of the normal magnetozones, without the prejudice of biochronological assumptions, is with anomalies 30 and 31." (It is now known that anomalies 30 and 31 of Lindsay et al. (1981) are really magnetochrons C32r and C33n, respectively.)

Rigby and Wolberg (1987) conducted an extensive study of microvertebrates collected from a small area in the southwestern part of the San Juan Basin known as the Fossil Forest area. The Fossil Forest mammal quarry is about 18 km southeast of the Bisti area (Figure 3) where Clemens (1973b) did his collecting and about 12 km southeast of the Alamo Wash area where Flynn

San Juan Basin Cretaceous Mammal Assemblages

(1) Lower Hunter Wash horizons (source: Clemens [1973] and UALP localities 75137 and 76168); (2) Jacobs Bone Bed (UALP 7592, 25 m above 75137); (3) Burnham South, high in Fruitland Formation; (4) UALP 7599 and 8020; BUNM-77-675 (Lehman, 1984).

Taxon	LHW ¹	7592 ²	BS ³	Alamo Wash ⁴
“Plagiaulacoid”			x	
<i>Paracimexomys judithae</i>	x	x	x	
<i>Paracimexomys</i> n. sp.		x		
<i>Mesodma formosa</i>				x
cf. <i>M. senecta</i>	?	x	x	
<i>M.</i> n. sp. or cf. <i>C. antiquus</i>		x	x	
cf. <i>Kimbetohia campi</i>	x			
<i>Cimolodon electus</i>	x	x	x	
<i>Cimolodon</i> n. sp.	x	x		
<i>Meniscoessus intermedius</i>	x	x	x	
cf. <i>Meniscoessus</i> sp.				x
cf. <i>Essonodon</i> n. sp.	?		x	
<i>Essonodon browni</i>				x
Eucosmodontid	x	?	x	
<i>Alphadon marshi</i>				x
cf. <i>A. marshi</i>	x			
cf. <i>A. wilsoni</i>		x	x	
<i>Alphadon</i> sp. A			x	
<i>Alphadon</i> sp. B		x	x	
<i>Alphadon</i> ? n. sp.	x			
cf. <i>Pedionomys cooki</i>	x			
<i>Gypsonictops</i> n. sp.	x	x	x	
cf. <i>Cimolestes</i> sp.	x	x		

Figure 41. Table 3 of Flynn (1986, p. 26) showing mammal taxa identified from Fruitland and Kirtland Formations and Ojo Alamo Sandstone in southwestern San Juan Basin. Mammal-bone localities are shown on Figure 3: LHW includes localities labeled C and FK; 7592 is FK; BS is FBS; and Alamo Wash is FOA.

(1986) collected. The Fossil Forest collections came from the lowermost Kirtland Formation and thus are at about the same stratigraphic level as Clemens' and Flynn's Lower Hunter Wash collection sites. Rigby and Wolberg (1987, p. 51) determined that their collections were most closely related to faunas of Sahni (1972) from the Judith River Formation and those of Fox (1977, 1979a, 1979b, 1979c, and 1981) from the Oldman Formation—a Judith River equivalent. These authors thus concluded that “The age of the lowermost part of the Kirtland Shale must be near the Campanian-Maastrichtian boundary based on mammalian evidence.”

As discussed above, the age of the contact between the Fruitland Formation and overlying Kirtland Formation is now known to be 74.6 Ma in the Ojo Alamo Sandstone type area (Figure 33); the precise age of dated ash 4 at about this level is 74.55 ± 0.29 Ma (Fassett and Steiner 1997, Fassett 2000). The latest published global geologic time scale (Gradstein et al. 2004) puts the Campanian-Maastrichtian boundary at 70.6 Ma. Thus, the mammal assemblages of Clemens (1973b) and Rigby and Wolberg (1987), as well as the Lower Hunter Wash mammalian fauna of Flynn (1986), can now be confidently placed in the upper Campanian with an age of 74.6 Ma; about 4 m.y. older than the Campanian-Maastrichtian boundary.

Sullivan and Lucas (2006, p. 20-21) discussed the latest Cretaceous and earliest Paleocene mammals of the southern San Juan Basin, but added nothing new to the above discussion. No other studies of Cretaceous mammals from the San Juan Basin have been published since the Rigby and Wolberg (1987) paper.

Paleocene Strata. The Ojo Alamo Sandstone has yielded relatively few mammal-fossil localities in the San Juan Basin, despite extensive searches in that formation over the last three decades. Lehman (1984) was the first paleontologist to report a small collection of fossil mammals from the lowermost part of the Ojo Alamo Sandstone (his Naashoibito Member of the Kirtland Formation) in the type area (Figure 3). Lehman assigned a Lancian Age to the Ojo Alamo because his collection contained a multituberculate tooth identified as *Essonodon browni*. Flynn (1986) identified microvertebrates from the Ojo Alamo (his Naashoibito Member of the Kirtland) less than 2 km southeast of the Lehman (1984) site (Figure 3). Flynn named this assemblage the Alamo Wash fauna and included in it Lehman's *Essonodon browni* (Figure 41). Flynn (1986, p. 26-27) concluded that: “Mammals from these high Kirtland strata appear to represent the Lancian age, based on co-occurrence of *Essonodon browni* (see Lehman 1984), *Alphadon marshi*, and *Mesodma formosa*.”

Weil and Williamson (2000) presented preliminary data from an Ojo Alamo Sandstone microvertebrate site about 1 km north of the Lehman (1984) mammal site (Figure 3). They discussed the total vertebrate assemblage from this site, including dinosaurs, and stated that the Lancian index fossil *Essonodon* was the most common mammal found in the Ojo Alamo. They also noted that *Essonodon* was “relatively rare in localities of the northern Western Interior, and the striking difference in rela-

tive abundance confirms speculation that latest Cretaceous southern mammalian faunas differ markedly from those of the northern Western Interior, as do dinosaurian assemblages.”

Clemens and Williamson (2005, p. 212) cautioned that the geochronologic value of fossil mammals in Western North America is in a state of flux. They stated that the record of mammalian evolution in the North American Western Interior is not yet complete as evidenced by “Fox and Naylor’s (2003) recent description of a new taeniodont from Alberta [that] extended the range of this eutherian lineage from the Puercan (Pu2) back into the Lancian.” These authors also noted that the multituberculate *Stygimys* that first appears in the northern part of the Western Interior at the beginning of the Puercan (Pu1) “is a member of a local fauna of Judithian age in Baja California del Norte (Weil 2002).” The cautionary statements of these authors regarding the current state of uncertainty about the biochronologic status of various fossil mammals because of the “incompleteness of the fossil record” are well advised. Moreover, these uncertainties tend to make less incredible the findings in this paper that the fossil mammals of the Ojo Alamo Sandstone (previously thought to be “Lancian”) are Paleocene in age. These mammal assemblages thus represent lineages that survived across the K-T boundary.

It seems clear that the use of fossil mammals as index fossils for dating lower Paleocene strata in the Western Interior of North America is premature at this time because of: 1) limited numbers of collection sites; 2) biogeographic diversity of taxa; and 3) limited knowledge of the evolution and radiation of mammals in earliest Paleocene time. The use of more robust geochronologic tools, such as palynology and isotopic and paleomagnetic dating of strata, as done in this study to confirm the Paleocene age of the Ojo Alamo Sandstone in the San Juan Basin, will ultimately help us to better understand the biogeographic and temporal diversity of mammals found near the K-T boundary throughout the Western Interior.

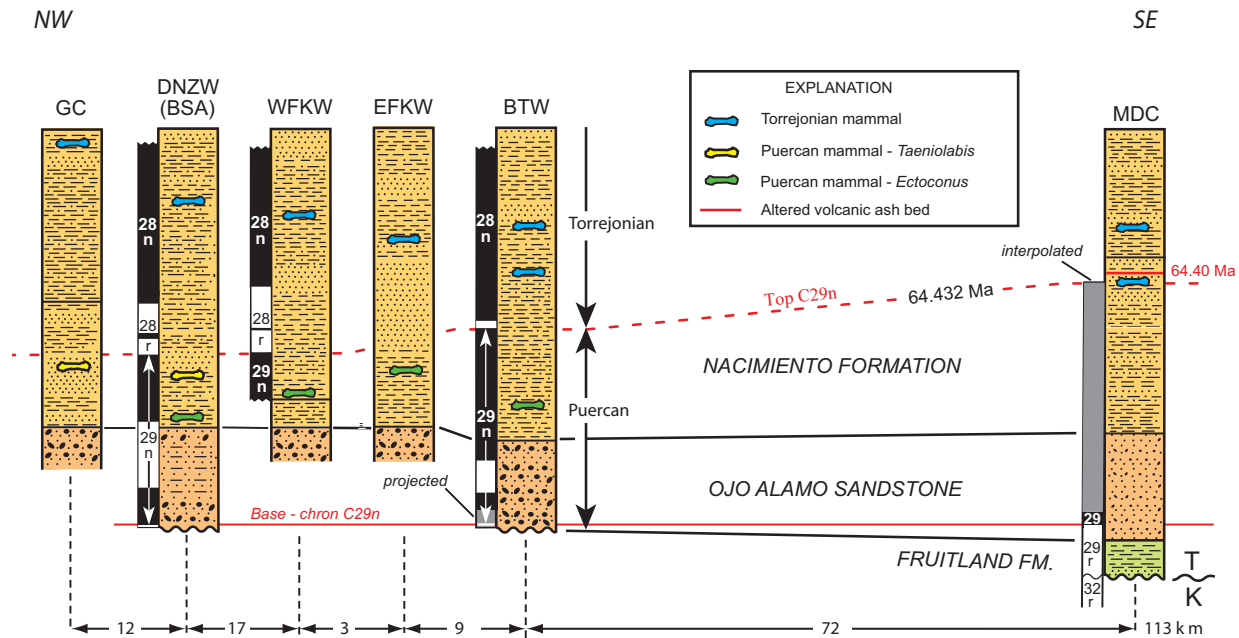
Lowermost Nacimiento Formation. As discussed above, the Nacimiento Formation intertongues with the underlying Ojo Alamo Sandstone; thus, on the basis of physical stratigraphy, it appears that deposition was continuous across this formation boundary. These formations are, however, distinctly different lithologically: the Ojo Alamo is characterized by massive, coarse-grained, conglomeratic sandstone beds deposited by high-energy braided streams flowing south to southeastward across the

San Juan Basin in early Paleocene time (Fassett 2000, Fassett et al. 2002). The Nacimiento Formation, however, at least in its lowermost part, consists of relatively finer-grained sediments deposited in a low-energy environment of low-gradient streams interspersed with lakes and swamps. This difference suggests that the pulse of high-energy stream flow represented by the Ojo Alamo Sandstone began suddenly about 65.2 Ma -300 k.y. into Paleocene time - and ended abruptly a few hundred thousand years later. Such a pulse must have been driven by a corresponding rapid uplift and then subsequent subsidence of a northern source area.

Williamson (1996) published a detailed paper on the stratigraphy and mammalian biostratigraphy of the Nacimiento Formation in the southern San Juan Basin that included a series of detailed measured sections through the Nacimiento at selected localities (Williamson 1996, appendix 1, p. 110-126). Williamson reported that Puercan (earliest Paleocene) mammals had been found in the lowermost part of the Nacimiento Formation at five localities in the southwestern part of the San Juan Basin between Gallegos Canyon and Betonnie Tsosie Wash (Figure 3).

Figure 42 is a stratigraphic cross section showing the five Puercan mammal-fossil localities and six Torrejonian localities in the lowermost part of the Nacimiento Formation; this figure is a modification of part of figure 9 of Williamson (1996). The fossil-mammal levels shown by Williamson for the DNZW, WFKW, and BTW localities differ slightly from those shown by Lindsay et al. (1981). At the DNZW and WFKW localities, the stratigraphic levels of Puercan mammals are from Lindsay et al. (1981). At the BTW locality, the levels of the Puercan and uppermost Torrejonian fossils are from Lindsay et al. (1981, figure 10) and the lower Torrejonian fossil level is from Williamson (1996, figure 9). The fossil levels at the MDC section are from Simpson (1959, figure 1) as explained below.

On Figure 42, the DNZW, BTW, and MDC columns are aligned on the base of magnetochron C29n (base projected for the BTW column). Column GC is aligned with column DNZW on the top of the Ojo Alamo Sandstone. Column WFKW is aligned with the DNZW column on the top of chron C29n. Column EFKW is aligned with the WFKW column on the top of the Ojo Alamo Sandstone. These alignments of the six columns appear to be quite reasonable in terms of the good correlation of the Puercan and Torrejonian fossil levels reported at the six localities.



NOTES: 1. GC = Gallegos Canyon, DNZW = De-na-zin Wash (same locality as BSA - Barrel Spring Arroyo of Lindsay and others, 1981), WFKW = West Fork Kimbeto Wash, EFKW = East Fork Kimbeto Wash, BTW = Betonnie Tsosie Wash, MDC = Mesa de Cuba

Figure 42. Stratigraphic cross section showing levels of Paleocene mammal fossils identified in lowermost part of Nacimiento Formation, southern San Juan Basin, modified from Williamson 1996. Magnetic-polarity columns and fossil levels for DNZW, WFKW, and BTW localities scaled directly from illustrations in original source: Lindsay et al. (1981), thus differ slightly from figure 9 of Williamson (1996). Fossil levels in GC and EFKW columns from Williamson (1996). Stratigraphic levels of Torrejonian mammals in MDC column from Simpson (1959, figure 1). Base of C29n not determined at BTW locality but projected to just above base of Ojo Alamo Sandstone. Top of C29n not determined at MDC locality but interpolated based on estimated rates of deposition for lower part of Nacimiento Formation. Boundary between Puercan and Torrejonian mammals (black dashed line) is placed between lowest Torrejonian fossil at MDC locality and highest Puercan fossil at GC locality. Boundary is estimated to be about 64.4 Ma because it is near top of magnetochron C29n. Column localities are shown on Figure 3.

The magnetic-polarity columns shown at the DNZW, WFKW, and the BTW localities are from Lindsay et al. (1981). (The DNZW section of Williamson is at the same locality as the Barrel Spring Arroyo (BSA) locality of Lindsay et al. 1981.) The top of magnetic-polarity chron C29n at the MDC locality was estimated based on a rate of deposition for the lower part of the Nacimiento Formation of 143 m/m.y. This rate was calculated based on the $^{40}\text{Ar}/^{39}\text{Ar}$ age of 64.40 ± 0.50 Ma for the youngest sanidine crystals from an altered volcanic ash bed found at the MDC locality (Fassett et al. 2007, Heizler personal commun., 2008). The level of this ash bed is shown on the MDC column on Figure 42. Williamson numbered the magnetic polarity chrons on his figure 9 based on the reinterpretation of these chrons suggested by Butler and Lindsay (1985). These magnetic-polarity intervals, however, are renumbered on Figure 42 in accordance

with the reevaluation of these chrons as discussed in detail in the "Paleomagnetism" section of this paper.

Williamson (1996, p. 27) stated that there are two faunal zones within the Puercan of the Nacimiento Formation in the southern San Juan Basin: a lower *Ectoconus* zone and an upper *Taeniolabis* zone. Figure 42 shows the *Ectoconus* zone present at four localities and the *Taeniolabis* zone at two localities; both zones are found together at only the DNZW locality where the *Ectoconus* zone was found only 10 m above the top of the Ojo Alamo Sandstone. These two zones appear to overlap very slightly at the DNZW and the EFKW localities (Figure 42).

At the Mesa de Cuba (MDC) locality, the two Torrejonian fossil levels shown on Figure 42 are 57 m and 71 m above the base of the exposure at the foot of Mesa de Cuba (Figure 43). Williamson

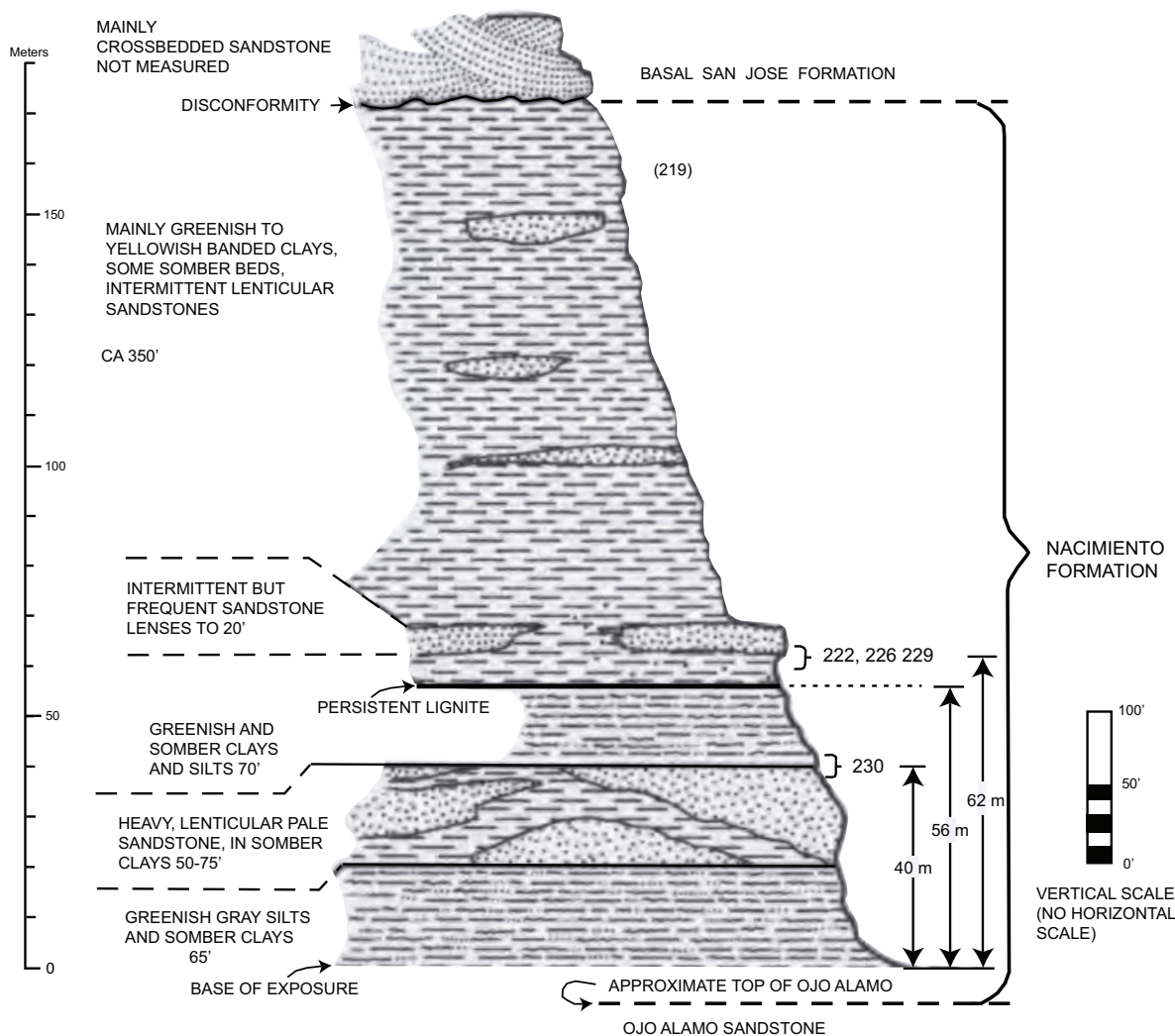


Figure 43. Stratigraphic section at Mesa de Cuba locality modified from Simpson (1959). Metric scale on left and arrows and distances above base of section to Torrejonian fossil zones and Simpson’s “persistent lignite” have been added. Numbers 230 and 222, 226, and 229 represent Simpson’s Torrejonian mammal-fossil levels at Mesa de Cuba projected into section from nearby locations.

(1996, figure 9), however, showed these faunal levels much lower in the Nacimiento at about 5 m and 30 m above the base of the exposure. In addition, whereas Simpson showed the two Torrejonian faunal zones to be about 22 m apart, stratigraphically, Williamson showed them to be 26 m apart. Apparently, Williamson (1996) misplaced these faunal zones because of a miscorrelation of the “persistent lignite” of Simpson (Figure 43). Because Simpson is the original source for the stratigraphic levels of the two Torrejonian faunal zones at Mesa de Cuba, his measurements at that locality are used in this report.

The Puercan-Torrejonian boundary can thus be placed fairly precisely in the lower part of the Nacimiento Formation (Figure 42) between the lowest Torrejonian mammal level at the MDC locality and the highest Puercan mammal level at the GC locality. The age of this boundary is estimated to be about 64.4 Ma because it is near the top of chron C29n which has an age of 64.432 Ma (Gradstein et al. 2004). Thus, the Puercan in the San Juan Basin has a duration of about 1.1 m.y., ranging from the base of the Paleocene at 65.5 Ma to the Puercan-Torrejonian boundary at 64.4 Ma (Figure 42). The Torrejonian mammals identified in the

lower part of the Nacimiento Formation in the five sections all appear to fall within magnetochron C28n. The lower of the two Torrejonian fossil localities at the MDC site, however, appears to be in chron C28r or the uppermost part of chron C29n (Figure 42). A paleomagnetic survey of the Nacimiento Formation at Mesa de Cuba would supply a valuable data set to clarify these interpretations.

The level of the interpolated top of magnetochron C29n at the MDC locality is higher than the top of this chron at the DNZW, WFKW, and BTW localities (Figure 42). This anomaly must be the result of different rates of deposition for the lower Nacimiento Formation at these widely separated localities. (The apparent rate of deposition for the part of the lowermost Nacimiento within chron C29n is estimated to be 102 m/m.y. at the DNZW locality vs. 143 m/m.y. at the MDC locality.) Chron C28r is anomalously thin at the BTW locality and Lindsay et al. (1981, p. 417) suggested that this thinness is the result of present-day-normal overprinting of the lower part of normal interval C28n due to weathering beneath recent sand dunes at the BTW locality. Additional paleomagnetic studies are clearly needed in the BTW area to help clarify this paleomagnetic pattern.

Clemens and Williamson (2005) discussed the Puercan fauna at the Betonnie Tsosie Wash (BTW) locality (Figures 11 and 42). They named a new species, *Eoconodon ginibitohia*, based on a fragment of a left dentary collected at the lowermost level for Puercan mammal fossils at that locality (Figure 42). These authors asserted that based on correlations of this taxon with other *Eoconodon* species in the northern part of the Western Interior, it, and the other mammals found in the "Ectoconus zone" of the southern San Juan Basin, belong in the "Pu2 Interval Zone" (middle part of the Puercan). They further stated that (p. 208): "Earliest Paleocene, Pu1 Interval Zone faunas are unknown in the San Juan Basin." It is here suggested that part of the missing lower "Puercan Pu1 Zone" in the San Juan Basin may be represented by the Paleocene Ojo Alamo Sandstone mammals, discussed above. And, as discussed elsewhere in this report, as much as 300 k.y. of earliest Paleocene time apparently is not represented by rock strata in the San Juan Basin, thus at least the lowermost part of the "Pu1 Interval Zone" is missing for that reason.

Clemens and Williamson (2005, p 209) placed the *Ectoconus* zone fauna in the lower part of magnetochron C29n in the San Juan Basin. However,

as Figure 42 shows, *Ectoconus*-zone mammals are present throughout the upper half of chron C29n at the four localities where it has been found in the lowermost part of the Nacimiento Formation. The presence of the middle Puercan Pu2 Interval Zone ("Ectoconus zone") in the lowermost Nacimiento Formation at the DNW locality (within 5 or 10 m of the top of the Ojo Alamo Sandstone; Lindsay et al. 1981 and Williamson 1996, respectively) suggests that the upper part of the "Pu1 Interval Zone" may be within the Ojo Alamo Sandstone providing additional strong evidence for continuous deposition across the Ojo Alamo-Nacimiento contact and in agreement with the Paleocene age of the Ojo Alamo Sandstone.

GEOCHEMISTRY OF VERTEBRATE BONE SAMPLES

Original (2002) Study

Fassett et al. (2002) presented chemical analyses of 18 vertebrate-bone samples; nine from the Cretaceous Kirtland Formation and nine from the Paleocene Ojo Alamo Sandstone. Two Kirtland samples were turtle bones; the other 16 samples were dinosaur bones. The Fassett et al. (2002) study showed that there are distinct differences in the amounts of uranium (U), the sums of the rare-earth elements (REE), and the chondrite-normalized lanthanum/ytterbium ratios (La/Yb(n)) in Paleocene Ojo Alamo Sandstone bone samples compared to Cretaceous Kirtland Formation bone samples. Uranium abundances exhibited the largest differences between the two suites of samples. The mean value for U in Ojo Alamo bone samples (447 ppm) was found to be 18 times greater than the mean for Kirtland bone samples. REE exhibited less striking, albeit consistent differences. The mean sum of REE was 1,587 for the Ojo Alamo and 3,196 for the Kirtland. The mean La/Yb(n) ratio for Ojo Alamo samples was 6.2 whereas for the Kirtland samples, the mean was 16.1. In summary, the Fassett et al. (2002) study showed that uranium is greatly enriched in Ojo Alamo bone samples relative to Kirtland samples whereas REE are more abundant and relative abundances of REE are more fractionated in Kirtland bone samples.

New Samples

Sample Descriptions. Ten of 14 new samples were collected by the author from newly discovered dinosaur-bone localities. The other four dinosaur bone samples were provided by R. B. Sullivan (The State Museum of Pennsylvania) and by S.G.

Lucas (New Mexico Museum of Natural History and Science), as discussed below and noted on Table 2 (see Table Appendix, page 113). One of the samples provided by Lucas was from a hadrosaur scapula that was one of 34 bones in the bone assemblage of Hunt and Lucas (1991; and see Figure 38). This sample is number P-19147 (Tables 2, 3 (see Table Appendix, page 114)) collected from locality I of Figure 4. The stratigraphic level of the 34-bone assemblage was measured in the field by the author in 2003 and found to be 6.1 m above the base of the Ojo Alamo. A small lag deposit of vertebrate bone was discovered near this locality 4.6 m above the base of the Ojo Alamo Sandstone and a dinosaur bone fragment from that deposit was collected and analyzed (sample number 020103 of Tables 2, 3; locality H of Figure 4). Sample number 35957-LUC (Tables 2, 3) was from a large sauropod femur (*Alamosaurus sanjuanensis*) 4.6 m above the base of the Ojo Alamo at locality D, figure 11. This bone was collected by Lucas who provided a small sample for chemical analysis; Lucas stated (personal commun., 2004) that this bone “was much too massive and pristine to have been reworked from older strata.”

Sample SMP VP-1625 was from a large *A. sanjuanensis* femur (Figure 37.2) collected by R.B. Sullivan who provided a small fragment for chemical analysis. This specimen came from locality O of Figure 4. The author determined that this locality was 4.9 m above the base of the Ojo Alamo; numerous other dinosaur bones in the Ojo Alamo were observed in the same area, including the fragmented bone shown on figure 37.3. Sample number 051504, a fragment of ceratopsian frill bone (locality N, Figure 4) was found in the same area 3.7 m above the base of the Ojo Alamo. Sample SMP VP-1494 was from a sauropod vertebra collected by Sullivan from locality G of Figure 4.

Two samples were collected from a lag deposit of abraded vertebrate-bone fragments found on the surface of the Kirtland Formation nearly 11 m below the base of the Ojo Alamo (locality C, Figure 4). At the time of collection, it was not known if these bone fragments had weathered out of the Kirtland Formation or had washed down from a higher level. The two samples analyzed from this assemblage were a fragment of turtle shell and a fragment of dinosaur bone. These samples were collected primarily to determine if there were significant differences between the chemistry of dinosaur bone and turtle shell.

New-Sample Analyses. The new set of 14 samples was prepared by R.A. Zielinski (USGS, Den-

ver, Colorado) and analyzed by instrumental neutron activation by J.R. Budahn (USGS, Denver, Colorado) using the same procedures described in Fassett et al. (2002). The samples were taken, to the extent possible, from the outermost (cortical) surface of the bones. The chemical analyses of these new vertebrate bone samples (six from the Ojo Alamo Sandstone, six from the Kirtland Formation, and two provenance uncertain) are shown on Table 3 (see Table Appendix, page 114). These samples yielded elemental concentrations similar to the original 18 samples discussed above: Ojo Alamo samples contained high levels of U and relatively low levels of REE; Kirtland samples contained low levels of U and relatively high levels of REE. Table 2 shows the concentrations of U and REE for all 32 bone samples (old and new); Figure 44 is a plot of the La/Yb(n) vs. U values for all samples.

As Tables 2 and 3 and Figure 44 indicate, the small fragments of dinosaur bone (020203-B) and turtle shell (020203-T) collected from an erosion surface on the Kirtland Formation exhibit similar chemistry. Despite their stratigraphic position, these two samples were more like Ojo Alamo bone with somewhat high U and quite low La/Yb(n). On the other hand, these samples resembled Kirtland samples with very high values for their sums of REE (Tables 2, 3). Based on their overall chemistry, it might be inferred that these samples weathered out of the Ojo Alamo Sandstone and washed down on top of the Kirtland erosion surface where they were found. Because of the uncertain provenance of these samples, they are not included in the comparison of Cretaceous and Tertiary bone chemistry.

The fragmented dinosaur limb bone from which sample 110803-B was obtained was at the contact of the Kirtland Formation and the Ojo Alamo Sandstone at the Pot Mesa locality (Figures 1, 3). The sample was a fragment of a specimen that had been collected by S.G. Lucas in 1983 designated UNM-TOA-2. This specimen is discussed and illustrated in a photograph in Fassett et al. (1987, figure 11). (The stratigraphy of the Kirtland Formation and Ojo Alamo Sandstone in this area was discussed and the formation boundary between these rock units redefined in Fassett et al. 2002). This badly fragmented bone was originally thought to be in the lowermost Ojo Alamo Sandstone (Fassett et al. 1987, p. 29, figure 11; Fassett et al. 2002, p. 324, figure 17). Table 3 shows this bone to have a relatively low concentration of uranium and a relatively high sum of REE;

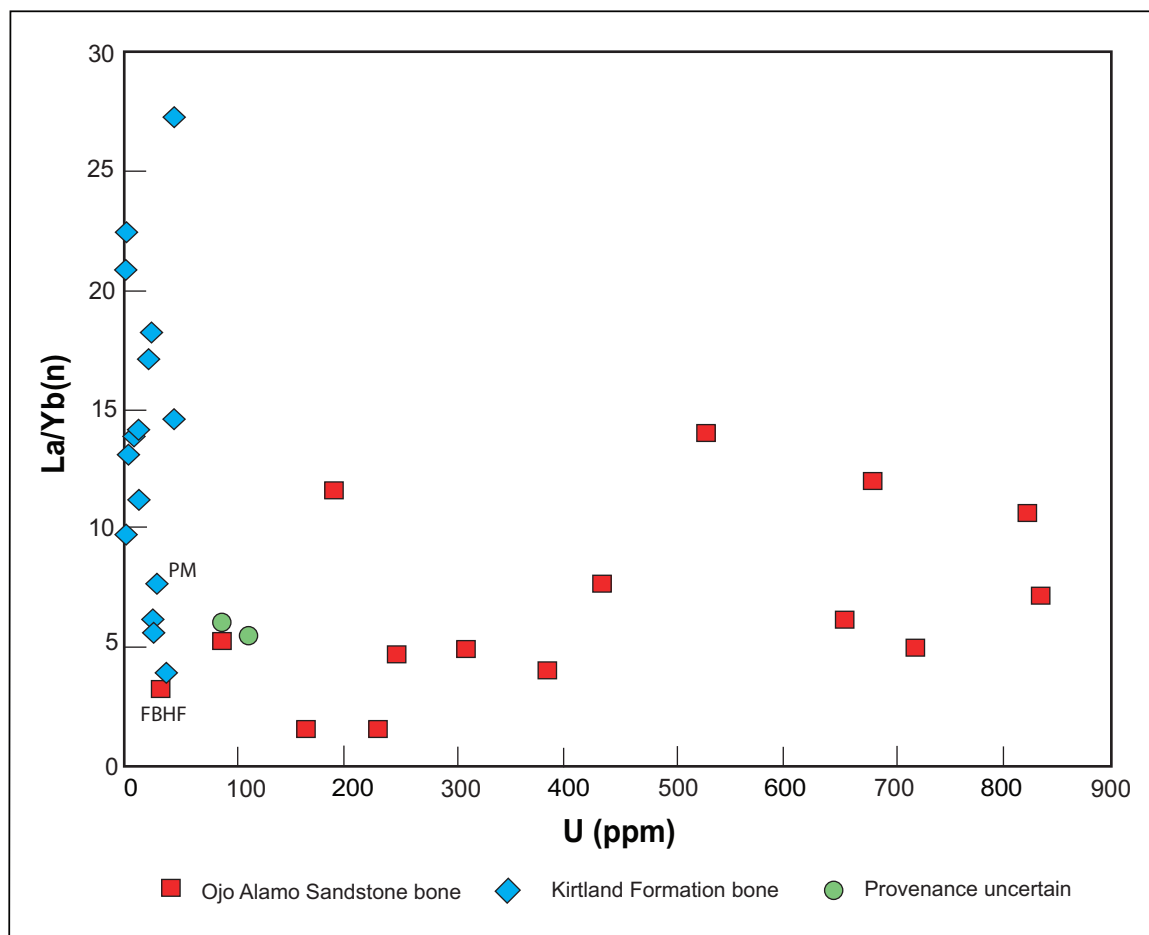


Figure 44. Plot of chondrite-normalized lanthanum/ytterbium ratios [La/Yb(n)] vs. uranium abundances (U ppm) for fossil bone samples from Ojo Alamo Sandstone and Kirtland Formation. Sample localities shown on Figures 1, 4, and 11. Elemental abundances on Tables 2 and 3. PM is bone sample from Pot Mesa, FBHF is bone sample from San Juan River locality.

chemical characteristics of a Cretaceous (Kirtland Formation) dinosaur bone. This bone was near the pre-Ojo-Alamo-Sandstone erosion surface when the Ojo Alamo was deposited on top of it. Despite its proximity to the overlying Ojo Alamo, this bone (labeled PM on Figure 44) has retained chemical characteristics of a Cretaceous bone sample; strong evidence that the U and REE concentrations were not appreciably modified when this bone was immersed in mineralizing fluids with a different chemistry nearly 8 m.y. later in Paleocene time.

The Figure 44 plot of La/Yb(n) vs. U for all of the bone samples analyzed for this study shows the significantly higher U content for Ojo Alamo samples vs. Kirtland samples. (Samples (020203-B, and 020203-T) found loose on the surface of the Kirtland Formation are shown in green.) The mean U content for all 15 Ojo Alamo samples is 422 ppm

vs. 20 ppm for 15 Kirtland samples (Table 2); more than 20 times greater. The single anomalous U value of 33 ppm is from the large hadrosaur femur collected at the San Juan River locality (Figure 1). As Figure 44 shows, the U value for this sample FBHF on this figure overlaps U values for Kirtland Formation bone samples. This was the most northerly of the Ojo Alamo bone samples and is also the stratigraphically highest 15.2 m above the base of the formation. The northern setting could have affected this sample's anomalously low U content. Uranium mineralization has been documented in the Ojo Alamo Sandstone in the southeast part of the San Juan Basin at Mesa Portales (Fassett et al. 2002, p. 330) close to possible granitic source rocks in the incipient Nacimiento Mountains. Perhaps the U content of mineralizing fluids was less in the northern part of the San Juan Basin, farther

TABLE 4. Summary statistics for chemical parameters distinguishing Kirtland Formation bones from Ojo Alamo Sandstone bones.

Chemical parameter	Ojo Alamo Sandstone (15 samples)					Kirtland Formation (15 samples)				
	Min.	Max.	Median	Mean	Standard deviation	Min.	Max.	Median	Mean	Standard deviation
U	33	834	436	447	298	2	45	25	24	16
Lan/Ybn	2	14	5	6	4	4	27	17	16	8
Sum REE	38	6174	1004	1587	1883	66	5626	2865	3196	2000

Note: n = chondrite-normalized abundance.

from that possible source area, in Ojo Alamo time. One sample, however, provides insufficient data for more than speculation regarding this sample's low U content. The chemical analyses of dinosaur bones from the Animas Formation (when they are found) in the northern part of the San Juan Basin will provide a test of this hypothesis.

Except for the FBHF bone sample from the San Juan River site, the range of U concentrations within Ojo Alamo samples is 89 to 834 ppm. In stark contrast, U values for Kirtland samples range from 2 to 45 ppm (Table 4). Large variations in U concentrations within each of these bone populations may have resulted from: 1) variations in dissolved U concentrations in mineralizing fluids, 2) variations in host lithologies affecting permeabilities and thus volumes of mineralizing fluids the bones were exposed to, and 3) the progress of bone mineralization that influenced the accessibility of U-bearing ground water during fossilization.

Analytical data indicate generally higher sums of REE in Kirtland Formation bones relative to Ojo Alamo Sandstone bones (Tables 2, 4). Three Ojo Alamo bone samples and one Kirtland sample contained particularly low "Sum REE" values (< 73 ppm, Table 2). These low abundances of REE may indicate samplings of bone further from the bone's cortical (outer) surface. When comparing samples from the outer surface with deeper-bone levels from 70 mm long cores within samples (051298-BB1 and FBHF), the sum of REE concentrations in deeper bone was lower by factors of 2-100, whereas uranium concentrations decreased only by factors < 2 (Zielinski personal commun., 2007.) and Fassett et al. (2002, p. 329). Preferential concentration of REE in outermost layers is unexplained, but may indicate enhanced uptake of REE related to early diagenetic alteration or recrystallization of outermost fossilized bone. Such uptake is apparently more pronounced in Kirtland bones and must be of limited duration in order to preserve the

apparent differences in REE patterns in the two suites of bones.

Figure 45 shows chondrite-normalized rare earth element patterns for the 21 vertebrate-bone samples that contained the greatest concentrations of REE. The newly analyzed samples (dashed lines) show the same subsets of patterns as the samples (solid lines) previously reported in Fassett et al. (2002); that is, more steeply sloped patterns for Kirtland Formation bones and flatter slopes for Ojo Alamo Sandstone bones. The steeper slope of REE patterns in Kirtland samples is primarily caused by a greater abundance of light REE (La, Ce, Nd). Steeper-sloped patterns are represented in the tables as a higher ratio of La/Yb(n).

The data plot for sample 110803-B in Figure 45.2 (Kirtland samples) is plotted in a different color because the slope for this sample is anomalous: it is noticeably flatter than the other Kirtland-sample plots and is more like an Ojo Alamo REE sample plot. As discussed above, sample 110803-B was collected less than 0.1 m below the Kirtland-Ojo Alamo contact and was originally thought to be from the Ojo Alamo Sandstone. Based on its very low U content (30 ppm) and relatively high Sum REE of 2705 (Table 2) this bone has a Kirtland geochemical signature. The anomalously flat slope of the REE plot for this bone (Figure 45.2) may be the result of its proximity to the Kirtland-Ojo Alamo contact that may have allowed for some slight alteration in REE content by Paleocene mineralizing fluids. If so, those fluids did not change the overall Kirtland chemical signature for this bone of low U and high REE (Figure 44). These data support the thesis that the U content of bone samples is fixed at the time of initial mineralization and is not subject to significant change by being immersed in mineralizing-fluids with different chemistry at a later time.

Sample 072598-6C also has a flatter slope on Figure 45 than other Kirtland bone samples and the reasons for this anomaly are unknown. This

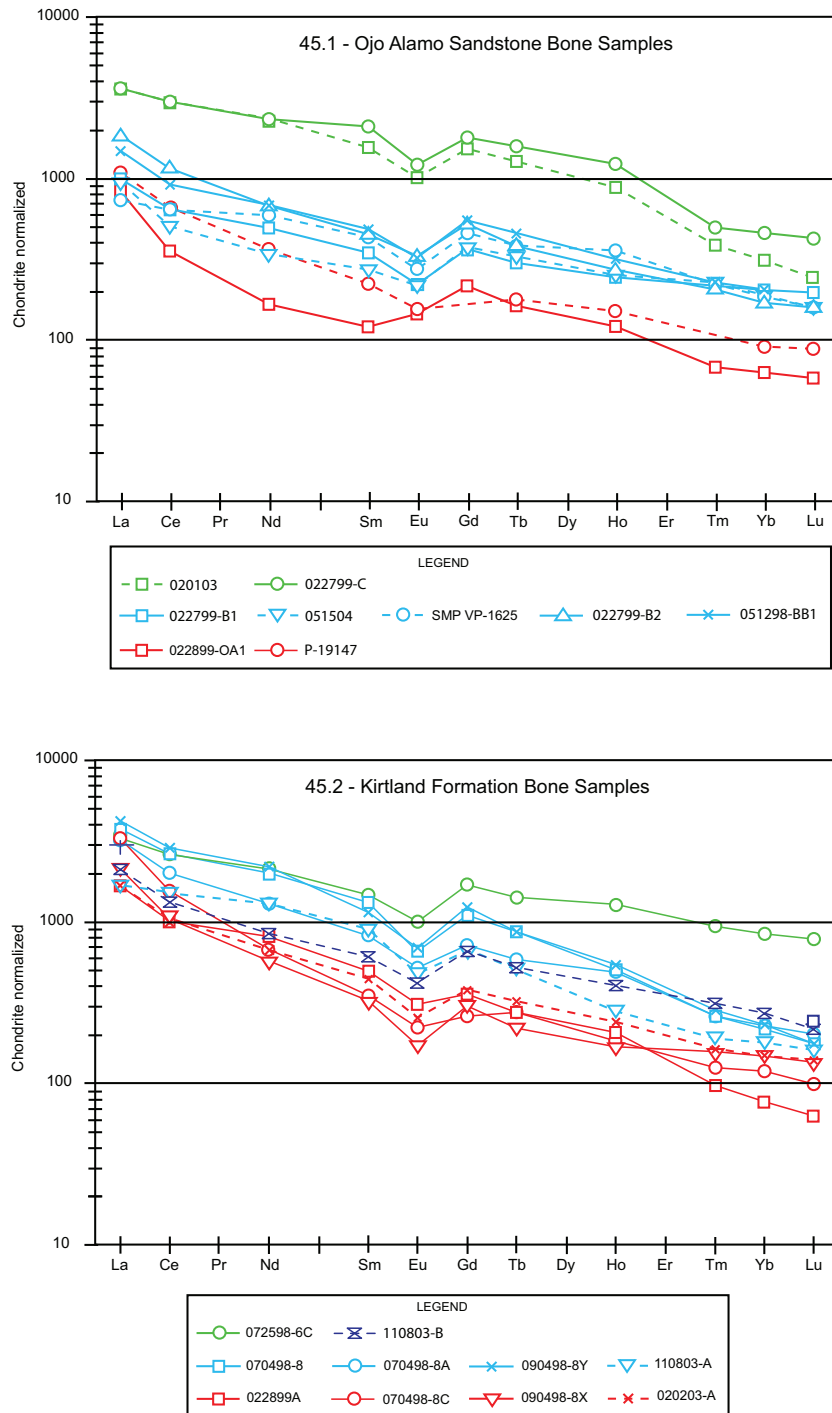


Figure 45. Chondrite normalized rare-earth-element patterns of fossil bone samples, **45.1** Ojo Alamo Sandstone, **45.2** Kirtland Formation, San Juan Basin, New Mexico. Values used in normalization: La = 0.311, Ce = 0.813, Nd = 0.603, Sm = 0.196, Eu = .074, Gd = 0.26, Tb = 0.047, Ho = 0.0718, Tm = .0326, Yb = 0.21 and Lu = 0.0323, derived from multiplying 1.32 times C1 values of Anders and Grevesse (1989) to correct to a volatile-free basis. Sample localities shown on Figures 1, 4, and 11. Specimen numbers keyed to Tables 2 and 3. Dashed lines show patterns for new samples; solid lines show patterns for samples from Fassett et al. (2002). REE patterns for samples 110803-B (purple) and 072598-6C (green) are anomalous, as discussed in text. Colors are used to improve readability and to broadly subdivide samples according to total REE content.

turtle-bone sample has a low U content (38 ppm) and very high Sum REE (Figure 2) clearly establishing it as a Kirtland bone sample.

Significance of Vertebrate-Fossil Geochemistry

The REE composition of fossil bone has been used to determine stratigraphic provenance and to identify reworked bone in the Triassic of southwest England (Trueman and Benton 1997) and in the Pleistocene in southern Kenya (Trueman et al. 2006). In this study, differences in REE and U contents between two suites of dinosaur bones (table 2) are preserved, despite their close stratigraphic proximity, and despite their largely shared post-Cretaceous alteration history (Table 4). These data strongly suggest that the chemically distinct Ojo Alamo Sandstone dinosaur bones were fossilized in place during Ojo Alamo Sandstone (Paleocene) time and thus cannot be Cretaceous bones reworked from the underlying Kirtland Formation. These facts, coupled with independent documentation of the Paleocene age of the Ojo Alamo Sandstone presented elsewhere in this paper, indicate that some dinosaurs lived, died, and were preserved in earliest Paleocene time in the San Juan Basin area.

AGE OF OJO ALAMO SANDSTONE BASED ON ALAMOSAUROS SANJUANENSIS

Sullivan, Boere, and Lucas (2005, p. 580) stated that the age of the sauropod dinosaur *A. sanjuanensis* is precisely 69 Ma throughout the Western Interior of North America, including the San Juan Basin. They stated that this finding was based on an abstract by McDowell et al. (2004) that reported a U/Pb age of 69 ± 1.0 Ma for a tuff bed found in about the middle of the Javelina Formation in the Big Bend area of Texas. This assertion that *Alamosaurus* is exactly 69 Ma (near the Campanian-Maastrichtian boundary) represents a serious challenge to the findings in this report that the Ojo Alamo Sandstone is Paleocene in age because *Alamosaurus* fossils are found at several localities within the Ojo Alamo in the San Juan Basin. Because the McDowell et al. (2004) abstract is cited by Sullivan, Boere, and Lucas (2005, p. 580), as the basis for their claim that *Alamosaurus* is 69 Ma, a careful evaluation of this abstract is critical to an assessment of their claim.

McDowell et al. (2004) stated that Maastrichtian vertebrates from the Western Interior occurred in two faunal provinces: the *Triceratops* fauna in the north and the *Alamosaurus* fauna in the south. It is thus clear that they were stating that these two

faunas are the same age: Maastrichtian, or latest Cretaceous. These authors go on to say that their dated tuff bed is from the middle of the Javelina Formation and that:

This position is within the local range of the sauropod Alamosaurus, below two sites that have yielded remains of the pterosaur Quetzalcoatlus, and above a site with petrified logs of the dicot tree Javelinoxylon. The range zones of all three taxa span the full thickness of the Javelina Formation elsewhere in the Big Bend region. The Alamosaurus Fauna is therefore Lancian to late Edmontonian in age.
[My emphasis]

It is thus clear that Sullivan, Boere, and Lucas (2005) misinterpreted the McDowell et al. abstract when they concluded that it found that the 69 Ma tuff bed represented the exact age of *A. sanjuanensis*.

Sullivan, Boere, and Lucas (2005, p. 580) continued their discussion by stating that *A. sanjuanensis* has been reported to have a long range—from late Campanian to late Maastrichtian—undermining its value as an index fossil. Following this accurate statement, these authors proceeded to present arguments purporting to show that *A. sanjuanensis* in the North Horn Formation does not really range to upper Maastrichtian but is “pre-late Maastrichtian”. These arguments are unconvincing because they contradict a large body of data supporting a late-Maastrichtian age for the *A. sanjuanensis*-bearing part of the North Horn Formation (Cifelli et al. 1999, Difley and Ekdale 1999).

In Sullivan, Lucas, and Braman (2005), the conclusions of the Sullivan, Boere, and Lucas (2005) report, regarding the 69 Ma age of *A. sanjuanensis*, were extended with the creation of the “*Alamosaurus* datum” (p. 401 and figure 7); these authors claim that this datum can be used to date the *Alamosaurus* level precisely at 69 Ma throughout the Western Interior including within the North Horn Formation of southeast Utah, the lower part of the Ojo Alamo Sandstone in the San Juan Basin, and the Javelina Formation in the Big Bend area.

Lehman et al. (2006) discussed the relations of the 69 Ma tuff bed in the Javelina Formation and their “*Alamosaurus* vertebrate fauna.. These authors stated (p. 922) that one of the reasons for publishing their paper was to clarify “misinterpretations” of the McDowell et al. (2004) abstract by recent authors, including Sullivan, Boere, and

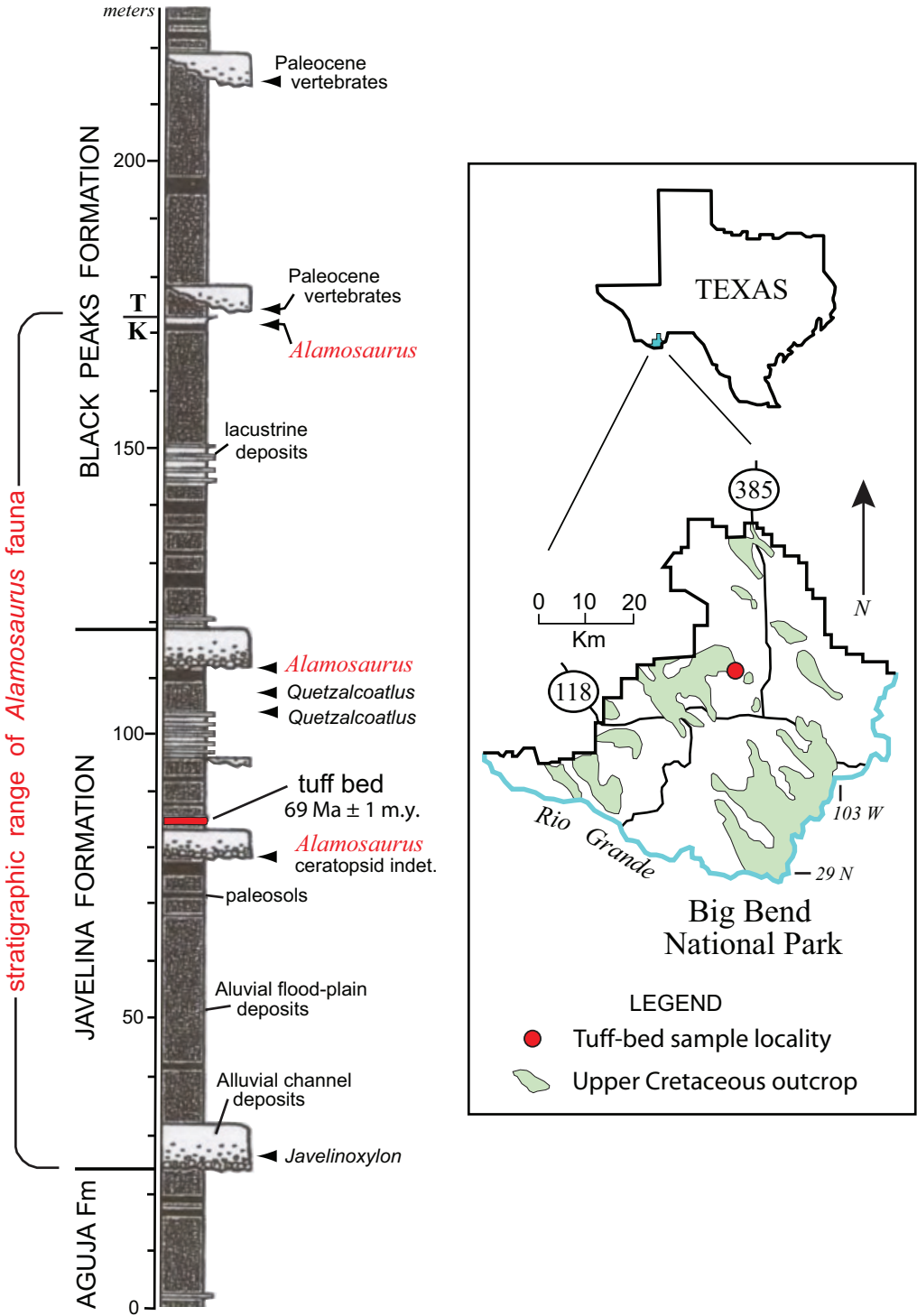


Figure 46. Stratigraphic column showing Cretaceous-Tertiary strata and stratigraphic levels of key fossils in Big Bend, Texas area, modified from Lehman et al. (2006). Red color of some items has been added for emphasis.

Lucas (2005). The stratigraphic relations of the dated tuff bed and the principal fossil levels in the Javelina and overlying Black Peaks Formation are shown on figure 1 of Lehman et al. (2006), which is reproduced herein in modified form as Figure 46. The levels of collection sites of *Alamosaurus* and other upper Cretaceous index fossils are shown; *Alamosaurus* is shown to span the interval from just below the 69 Ma tuff bed to just below the K-T boundary. The K-T boundary of Figure 46 is shown to be tightly bracketed by *Alamosaurus* just below and "Paleocene vertebrates" just above.

Lehman et al. (2006, p. 925) discussed the range of *Alamosaurus* and stated:

Hence, introduction of the Alamosaurus fauna in southern North America must have occurred sometime after about 73 Ma but before 69 Ma, and so probably not coincident with the Edmontonian-Lancian faunal transition observed in northern locales. Furthermore, although it seems likely that the Alamosaurus fauna persisted to the end of Cretaceous time (ca. 65 Ma), this has yet to be demonstrated conclusively. Some evidence suggests that the Alamosaurus fauna may have persisted into Paleocene time (Fassett et al. 2002).

The work of Lehman et al. (2006) thus contradicts the assertion of Sullivan, Boere, and Lucas (2005) and Sullivan, Lucas, and Braman (2005) that there is an "*Alamosaurus* datum" with a precise age of 69 Ma in the Big Bend area of Texas. Because the presence of *Alamosaurus* in the lower part of the Ojo Alamo Sandstone does not precisely date the base of the Ojo Alamo at 69 Ma, as suggested by Sullivan, Lucan, and Braman (2005), the presence of this dinosaur in the Ojo Alamo in no way refutes the Paleocene age of this formation.

CONCLUSIONS

This report presents new paleomagnetic and palynologic data that confirm the Paleocene age of the Ojo Alamo Sandstone and its contained dinosaurs in the San Juan Basin as reported in Fassett and Lucas (2000) and Fassett et al. (2002). In addition, chemical analyses of new dinosaur bone samples from the Cretaceous Kirtland Formation and Paleocene Ojo Alamo Sandstone expand the existing geochemical data base for such samples in the basin and confirm the findings in Fassett et al. (2002) that the dinosaur bone present in the Ojo

Alamo has not been reworked. Challenges to the Paleocene age of the Ojo Alamo by Sullivan, Lucas, and Braman (2005), when carefully analyzed, have been found to be unsupported by data.

Fassett et al. (2002) estimated that dinosaurs persisted into early Paleocene time for about 1 m.y. That estimate was based on the assumption that an 11 m thick paleomagnetic-normal interval in the Ojo Alamo Sandstone represented the entire C29n magnetochron. This report (as discussed in the "Paleomagnetism" section) extends the top of magnetochron C29n to well above the top of the Ojo Alamo Sandstone and into the lower part of the Nacimiento Formation (Figure 42). The 11 m thick magnetic-normal interval within the Ojo Alamo Sandstone is now interpreted to be only the lowermost part of chron C29n and is designated C29n.2n herein. Figure 42 shows that C29n is now known to range from about 68 to 98 m thick.

This increase in the length of magnetochron C29n required a revised estimate of how long dinosaurs lived in the Paleocene in the San Juan Basin. Dinosaur bone has been found to be 8.2 m above the base of the Ojo Alamo in the southern San Juan Basin (Table 2 and Figure 5) near the Barnum Brown Amphitheater locality (locality J of Figure 4). At that locality, the base of chron C29n is close to the base of the Ojo Alamo Sandstone. The base of C29n has an age of 65.118 Ma (Gradstein et al. 2004), thus the age of the youngest Paleocene dinosaur fossil that can be linked directly to paleomagnetic data is now estimated to be about 65 Ma. The stratigraphically highest, in-place dinosaur fossil in the entire basin was found at the San Juan River locality (Figures 1.1, 34), 15.2 m above the base of the formation, however, with no geochronologic data available at that place to quantify the time represented by this stratigraphic interval, it is not possible to say if this bone is younger than the youngest dinosaur bones in the southern part of the basin. Additional paleomagnetic studies of the Ojo Alamo Sandstone at this locality could help resolve this problem.

ACKNOWLEDGEMENTS

The preparation of this paper benefited from vigorous discussions with S.G. Lucas (New Mexico Museum of Natural History and Science, Albuquerque) and R.B. Sullivan (The State Museum of Pennsylvania, Harrisburg) over several decades. These colleagues generously provided dinosaur bone samples for chemical analyses, identified dinosaur fossils, provided copies of their and other publications, and have been invaluable sources of

information about vertebrate paleontology. Lucas graciously agreed to be one of the USGS reviewers of the manuscript, and his review is appreciated. T.E. Williamson (New Mexico Museum of Natural History and Science), New Mexico, provided help with information and publications related to fossil-mammal collection localities in the Ojo Alamo Sandstone in the San Juan Basin. Williamson also reviewed the Vertebrate Paleontology section of this report, and his comments helped to improve that section. K. Johnson (Denver Museum of Nature and Science) reviewed the paleobotany studies of Knowlton (1924) and found them to be still valid.

U. S. Geological Survey (USGS) colleagues, F. Peterson and R.B. O'Sullivan, at the Denver Federal Center, Colorado, provided invaluable assistance in researching publications in the USGS Denver Federal Center library that were critical for this report. Peterson spent hours in the USGS field-notebook archives searching for references to dinosaur bones in the Animas Formation and succeeded in locating the field-note reference to an Animas dinosaur by J.H. Gardner, reproduced on Figure 40 of this report. Peterson, R. Keefer, and E.M. Brouwers (USGS Denver) conducted technical edits of the manuscript and greatly improved the final product. USGS colleagues R.A. Zielinski and J.R. Budahn performed the chemical analyses of the additional suite of 14 vertebrate-bone samples included in this study. Zielinski's constructive comments regarding the structure of this report and his careful review of the "Geochemistry of Vertebrate Bone Samples" section of the report improved it greatly. R.H. Tschudy (1908-1986) and D. J. Nichols, USGS palynologists, analyzed many rock samples for the author over many decades and a large part of the palynologic data base presented in this report is based on their work. Nichols also reviewed the palynology sections of this report, and his suggestions were extremely helpful. USGS palynologist N. Frederiksen deserves special recognition for being the first palynologist to identify Paleocene palynomorphs in Ojo Alamo Sandstone samples at the important San Juan River locality.

M.,B. Steiner at the University of Wyoming in Laramie, provided the paleomagnetic data plot for the Mesa Portales section that has proven to be a pivotal data set for confirming the Paleocene age of the Ojo Alamo Sandstone in the San Juan Basin. E.M. Shoemaker was responsible for initiating the Mesa Portales paleomagnetic study and personally cored most of the rock samples there in

an intensive week of field work in 1984, assisted by Steiner and the author. Shoemaker's encouragement and perceptive comments about the Cretaceous-Tertiary interface problem in the San Juan Basin over the years were a constant and joyful stimulus to the author in the pursuit of more and better data to help resolve this problem. K. Zeigler, Department of Earth and Planetary Sciences, University of New Mexico, reviewed the paleomagnetism section of this paper and offered insightful suggestions that greatly improved this section.

Two anonymous reviewers for *Palaeontologia Electronica* reviewed the manuscript and provided valuable suggestions for improving the paper. C.N. Trueman reviewed the geochemistry section of the manuscript for *Palaeontologia Electronica*, and his comments and suggestions improved the clarity of that section. For permission to use figures and tables, I thank the following journals and institutions: form figures from Butler and Lindsay (1985) the *Journal of Geology*, for figures from Lindsay et al. (1981) the *American Journal of Science*, for use of table 3 of Flynn (1986) and figures of Simpson (1959) The American Museum of Natural History, for use of figures from Lehman (2006) The Society of Vertebrate Paleontology.

The initial study of the paleomagnetism, radiometric ages, palynology, and vertebrate paleontology of the rock strata adjacent to the Cretaceous-Tertiary interface in the San Juan Basin was funded by a USGS Gilbert Fellowship grant awarded to the author in 1987. Those first studies provided the foundation for the geochronologic work that has continued since then by the author and the colleagues mentioned above. Bradley Scholar grants by the USGS in 2007 and 2008 helped defray some of the expenses incurred for the review and publication of this report.

REFERENCES

- Alvarez, W. and Vann, D.W. 1979. Comment: Biostratigraphy and magnetostratigraphy of Paleocene terrestrial deposits, San Juan Basin New Mexico (Lindsay and others 1978). *Geology*, 7:66-67.
- Anders, E. and Grevesse, N. 1989. Abundances of the elements: Meteoritic and solar. *Geochimica et Cosmochimica Acta*, 53:197-214.
- Anderson, R.Y. 1960. Cretaceous-Tertiary palynology eastern side of the San Juan Basin New Mexico. New Mexico Bureau of Mines and Mineral Resources Memoir 6.
- Baltz, E.H. 1967. Stratigraphy and regional tectonic implications of part of Upper Cretaceous and Tertiary rocks east-central San Juan Basin New Mexico. USGS Professional Paper 552.

- Baltz, E.H., Ash, S.R., and Anderson, R.Y. 1966. History of nomenclature and stratigraphy of rocks adjacent to the Cretaceous-Tertiary boundary Western San Juan Basin New Mexico. USGS Professional Paper 524-D.
- Barnes, H., Baltz, E.H., Jr., and Hayes, P.T. 1954. Geology and fuel resources of the red Mesa area, La Plata and Montezuma Counties, Colorado. USGS Oil and Gas Investigations Map OM-149.
- Bauer, C.M. 1916. Stratigraphy of a part of the Chaco River valley. USGS Professional Paper, 98-P: 271-278 [1917].
- Brown, B. 1910. The Cretaceous Ojo Alamo Beds of New Mexico with description of the new dinosaur genus *Kritosaurus*. American Museum of Natural History Bulletin, 28:267-274.
- Brown, J.L. 1982. Geologic map of the Alamo Mesa East Quadrangle. USGS Miscellaneous Field Studies Map MF-1497, scale 1:24,000.
- Butler, R.F. and Lindsay, E.H. 1985. Mineralogy of magnetic minerals and revised magnetic polarity stratigraphy of continental sediments, San Juan Basin, New Mexico. *Journal of Geology*, 535-554.
- Butler, R.F., Lindsay, E.H., Jacobs, L.L., and Johnson, N.M. 1977. Magnetostratigraphy of the Cretaceous-Tertiary boundary in the San Juan Basin, New Mexico. *Nature*, 267:318-323.
- Cande, S.C. and Kent, D.V. 1992. A new geomagnetic polarity time scale for the Late Cretaceous and Cenozoic. *Journal of Geophysical Research*, 97:B10:13,917-13,951.
- Cande, S.C. and Kent, D.V. 1995. Revised calibration of the geomagnetic polarity time scale for the Late Cretaceous and Cenozoic. *Journal of Geophysical Research*, 100:6093-6095.
- Carr, T.D. and Williamson, T.E. 2000. A review of Tyrannosauridae (Dinosauria, Coelurosauria) from New Mexico. New Mexico Museum of Natural History and Science Bulletin 17:113-145.
- Cifelli, R.L., Nydam, R.L., Eaton, J.G., Gardner, J.D., and Kirkland, J.I. 1999. Vertebrate faunas of the North Horn Formation (Upper Cretaceous-lower Paleocene), Emery and Sanpete Counties, Utah, p. 377-388. In Gillette, D.D. (ed.), *Vertebrate paleontology in Utah*. Utah Geological Survey Miscellaneous Publication, Salt Lake City, Utah.
- Clemens, W.A. 1964. Fossil mammals of the type Lance Formation, Wyoming, Part I. Introduction and Multituberculata. University of California Publication Geologic Science, v. 48.
- Clemens, W.A. 1973a. Fossil mammals of the type Lance Formation, Wyoming, Part III, Eutheria and summary. University of California Publication Geologic Science, v. 94.
- Clemens, W.A. 1973b. The roles of fossil vertebrates in interpretation of Late Cretaceous stratigraphy of the San Juan Basin, New Mexico, p. 154-167. In Fassett, J.E. (ed.), *Cretaceous and Tertiary rocks of the Colorado Plateau*. Four Corners Geological Society Memoir.
- Clemens, W.A. and Williamson, T.E. 2005. A new species of *Eoconodon* (Triisodontidae, Mammalia) from the San Juan Basin, New Mexico. *Journal of Vertebrate Paleontology*, 25 no. 1:208-213.
- Cobban, W.A. 1973. Significant ammonite finds in uppermost Mancos Shale and overlying formations between Barker Dome, New Mexico, and Grand Junction, Colorado, p. 148-167. In Fassett, J.E. (ed.), *Cretaceous and Tertiary rocks of the southern Colorado Plateau*. Four Corners Geological Society Memoir.
- Cobban, W.A., Landis, E.R., and Dane, C.H. 1974. Age relations of upper part of Lewis Shale on east side of San Juan Basin, New Mexico, p. 279-282. In Siemers, C.T. (ed.) *Ghost Ranch*. New Mexico Geological Society 28th Field Conference Guidebook.
- Cope, E.D. 1881. Mammals of the lowest Eocene. *American Naturalist*, 15:829-831.
- Dane, C.H. 1936. The La Ventana-Chacra Mesa coal field. Geology and fuel resources of the southern part of the San Juan Basin, New Mexico, part 3. USGS Bulletin, 860C:81-161 (1937).
- Difley, R. and Ekdale, A.A. 1999. Stratigraphic aspects of the Cretaceous-Tertiary (K-T) boundary interval at North Horn Mountain, Emery County, Utah, p. 389-398. In Gillette, D.D. (ed.), *Vertebrate paleontology in Utah*. Utah Geological Survey Miscellaneous Publication, Salt Lake City, Utah.
- Dilworth, O.L. 1960. Upper Cretaceous Farmington Sandstone of northeastern San Juan County, New Mexico (M.S. thesis). University of New Mexico, Albuquerque, New Mexico.
- Farke, A.A. 2002. A review of "*Torosaurus*" (Dinosauria: Ceratopsidae) specimens from Texas and New Mexico, USA. *Journal of Vertebrate Paleontology*, 22 (Suppl. 3):52A.
- Farke, A.A. and Williamson, T.E. 2006. A ceratopsid dinosaur parietal from New Mexico and its implications for ceratopsid biogeography and systematics. *Journal of Vertebrate Paleontology*, 26:1018-1020.
- Fassett, J.E. 1966. Geologic map of the Mesa Portales quadrangle, Sandoval County, New Mexico USGS Geologic Quadrangle Map GQ-590.
- Fassett, J.E. 1968a. Core description from GB-1 (Gasbuggy 1) in the northeastern part of the San Juan Basin, Rio Arriba County, New Mexico. USGS open-file report 68-99.
- Fassett, J.E. 1968b. Summary of geologic data obtained from borehole GB-1, Project Gasbuggy, p. 24-27. In Shomaker, J. (ed.), *San Juan-San Miguel-La Plata Region*. New Mexico Geological Society 19th Field Conference Guidebook.

- Fassett, J.E. 1973. The saga of the Ojo Alamo Sandstone; or the rock-stratigrapher and the paleontologist should be friends, p. 123-130. In Fassett, J.E. (ed.), *Cretaceous and Tertiary rocks of the Colorado Plateau*. Four Corners Geological Society Memoir.
- Fassett, J.E. 1979. Comment: Biostratigraphy and magnetostratigraphy of Paleocene terrestrial deposits, San Juan Basin, New Mexico (Lindsay and others 1978). *Geology*, 7:2:69-70.
- Fassett, J.E. 1982. Dinosaurs in the San Juan Basin, New Mexico, may have survived the event that resulted in creation of an iridium-enriched zone near the Cretaceous-Tertiary boundary, p. 435-447. In Silver, L.T. and Schultz, P.H. (eds.), *Geological Implications of impacts of large asteroids and comets on the earth*. GSA Special Paper 190.
- Fassett, J.E. 1985. Early Tertiary paleogeography and paleotectonics of the San Juan Basin area, New Mexico and Colorado, p. 317-334. In Flores, R.M. and Kaplan, S.S. (eds.), *Cenozoic paleogeography of the west-central United States (Rocky Mountain paleogeography symposium 3)*. Rocky Mountain Section, Society of Economic Paleontologists and Mineralogists.
- Fassett, J.E. 1987. The age of the continental, Upper Cretaceous, Fruitland Formation and Kirtland Shale based on a projection of ammonite zones from the Lewis Shale, San Juan Basin, New Mexico and Colorado, p 5-16. In Fassett, J.E. and Rigby, J.K., Jr. (eds.), *The Cretaceous-Tertiary boundary in the San Juan and Raton Basins, New Mexico and Colorado*. GSA Special Paper 209.
- Fassett, J.E. 2000. Geology and coal resources of the Upper Cretaceous Fruitland Formation, San Juan Basin, New Mexico and Colorado. In Kirschbaum, M.A., Roberts, L.N.R., and Biewick, L.R.H., (eds.). *Geologic assessment of coal in the Colorado Plateau: Arizona, Colorado, New Mexico, and Utah*. USGS Professional Paper 1625-B, Chapter Q (published in digital form on CD-ROM).
- Fassett, J.E. and Hinds, J.S. 1971. Geology and fuel resources of the Fruitland Formation and Kirtland Shale of the San Juan Basin, New Mexico and Colorado. USGS Professional Paper 676.
- Fassett, J.E. and Lucas, S.G. 2000. Evidence for Paleocene dinosaurs in the Ojo Alamo Sandstone, San Juan Basin, New Mexico, p. 221-230. In Lucas, S.G. and Heckert, A.B. (eds.), *Dinosaurs of New Mexico*. New Mexico Museum of Natural History and Science Bulletin 17.
- Fassett, J.E. and Rigby, J.K., Jr. (eds.). 1987. The Cretaceous-Tertiary boundary in the San Juan and Raton Basins, New Mexico and Colorado. GSA Special Paper 209.
- Fassett, J.E. and Steiner, M.B. 1997. Precise age of C33n-C32r magnetic polarity reversal, San Juan Basin, New Mexico and Colorado, p. 239-247. In Anderson, O.J., Kues, B.S., and Lucas, S.G. (eds.), *Mesozoic geology and paleontology of the Four Corners Region*. New Mexico Geological Society 48th Field Conference Guidebook.
- Fassett, J.E., Cobban, W.A., and Obradovich, J.D. 1997. Biostratigraphic and isotopic age of the Huerfano Bentonite Bed of the Upper Cretaceous Lewis Shale at an outcrop near Regina, New Mexico, p. 229-232. In Anderson, O.J., Kues, B.S., and Lucas, S.G. (eds.), *Mesozoic geology and paleontology of the Four Corners Region*. New Mexico Geological Society 48th Field Conference Guidebook.
- Fassett, J.E., Heizler, M.T., and McIntosh, W. 2007. Geochronology of lowermost Paleocene Nacimiento and Ojo Alamo formations, San Juan Basin, New Mexico (abs.). GSA National Meeting, Denver, Colorado.
- Fassett, J.E., Lucas, S.G., and O'Neill, F.M. 1987. Dinosaurs, pollen and spores, and the age of the Ojo Alamo Sandstone, San Juan Basin, New Mexico, p 17-34. In Fassett, J.E. and Rigby, J.K., Jr. (eds.), *The Cretaceous-Tertiary boundary in the San Juan and Raton Basins, New Mexico and Colorado*. GSA Special Paper 209.
- Fassett, J.E., Zielinski, R.A., and Budahn, J.R. 2002. Dinosaurs that did not die: Evidence for Paleocene dinosaurs in the Ojo Alamo Sandstone, San Juan Basin, New Mexico, p. 307-336. In Koerble, C. and McLeod, K.G. (eds.), *Catastrophic Events and Mass Extinctions: Impacts and Beyond*. GSA Special Paper 356.
- Fleming, R.F. 1990. Palynology of the Cretaceous-Tertiary boundary interval and Paleocene part of the Raton Formation, Colorado and New Mexico (Ph.D. dissertation). University of Colorado, Boulder, Colorado.
- Flynn, L.J. 1986. Late Cretaceous mammal horizons from the San Juan Basin, New Mexico. *American Museum of Natural History Novitates*, 2845.
- Fox, R.C. 1970. Eutherian mammal from the early Campanian (Late Cretaceous) of Alberta, Canada. *Nature*, 227:630-621.
- Fox, R.C. 1977. Notes on the dentition and relationships of the Late Cretaceous insectivore *Gypsonictops* Simpson. *Canadian Journal of Earth Sciences*, 14, no. 8:1823-1831.
- Fox, R.C. 1979a. Mammals from the Upper Cretaceous Oldman Formation, Alberta; I. *Alphadon* Simpson (Marsupialia). *Canadian Journal of Earth Sciences*, 16, no. 1:91-102.
- Fox, R.C. 1979b. Mammals from the Upper Cretaceous Oldman Formation, Alberta; II *Pedionomys* Marsh (Marsupialia). *Canadian Journal of Earth Sciences*, 16, no. 1:103-113.
- Fox, R.C. 1979c. Mammals from the Upper Cretaceous Oldman Formation, Alberta; III, Eutheria. *Canadian Journal of Earth Sciences*, 16, no.1:114-125.

- Fox, R.C. 1981. Mammals from the Upper Cretaceous Oldman Formation, Alberta; *V. eodelphus* Matthew, and the evolution of the Stagodontidae (Marsupialia). *Canadian Journal of Earth Sciences*, 18, no. 2:350-365.
- Fox, R.C. and Naylor, B.G. 2003. A Late Cretaceous taeniodont (Eutheria, Mammalia) from Alberta, Canada. *Neues Jahrbuch für Geologie und Paläontologie, Abhandlungen*, 229:393-420.
- Gilmore, C.W. 1946. Reptilian fauna of the North Horn Formation of central Utah. USGS Professional Paper 210-C.
- Gradstein, F.M., Ogg, J.G., and Smith, A.G. 2004. A Geologic Time Scale 2004. Cambridge University Press, Cambridge, UK.
- Hicks, J.F., Johnson, K.J., Obradovich, J.D., Tauxe, L., and Clark, D. 2002. Magnetostratigraphy and geochronology of the Hell Creek and Basal Fort Union Formations of southwestern North Dakota and a recalibration of the age of the Cretaceous-Tertiary boundary, p. 35-55. In Hartman, J.H., Johnson, K.R., and Nichols, D.J. (eds.), *The Hell Creek Formation and the Cretaceous-Tertiary boundary in the northern Great Plains: An integrated continental record of the end of the Cretaceous*. GSA Special Paper 361.
- Hunt, A.P. and Lucas, S.G. 1991. An associated Maastrichtian hadrosaur and a Turonian ammonite from the Naashoibito Member, Kirtland Formation (Late Cretaceous: Maastrichtian), northwestern New Mexico. *New Mexico Journal of Science*, 31:1:27-35.
- Hunt, A.P. and Lucas, S.G. 1992. Stratigraphy, paleontology and age of the Fruitland and Kirtland Formations (Upper Cretaceous), San Juan Basin, New Mexico, p. 217-239. In Lucas, S.G., Kues, B.S., Williamson, T.E., and Hunt, A.P. (eds.), *San Juan Basin IV. New Mexico Geological Society Guidebook 43*.
- Jentgen, R.W. and Fassett, J.E. 1977. Sundance-Bististar Lake 1976 drilling in McKinley and San Juan Counties, northwestern New Mexico. USGS Open-File Report 77-369.
- Knowlton, F.H. 1917. Flora of the Fruitland and Kirtland Formations. USGS Professional Paper, 98-S:327-354 [1917].
- Knowlton, F.H. 1924. Flora of the Animas Formation. USGS Professional Paper, 134:71-114.
- Lehman, T.M. 1984. The Multituberculata *Essonodon browni* from the Upper Cretaceous Naashoibito Member of the Kirtland Shale, San Juan Basin, New Mexico. *Journal of Vertebrate Paleontology*, 4:602-603.
- Lehman, T.M., McDowell, F.W., and Connelly, J.N. 2006. First isotopic (U-Pb) age for the Late Cretaceous *Alamosaurus* vertebrate fauna of West Texas, and its significance as a link between two faunal provinces. *Journal of Vertebrate Paleontology*, 26:922-928.
- Lillegraven, J.A. 1969. Latest Cretaceous mammals of upper part of Edmonton Formation of Alberta, Canada, and review of marsupial-placental dichotomy of mammalian evolution. University of Kansas, Paleontologic Contributions, Article 50 (Vertebrates 12).
- Lindsay, E.H., Butler, R.F., and Johnson, N.M. 1981. Magnetic polarity zonation and biostratigraphy of Late Cretaceous and Paleocene continental deposits, San Juan Basin, New Mexico. *American Journal of Science*, 281:390-435.
- Lindsay, E.H., Butler, R.F., and Johnson, N.M. 1982. Testing of magnetostratigraphy in Late Cretaceous and early Tertiary deposits, San Juan Basin, New Mexico, p. 435-447. In Silver, L.T. and Schultz, P.H. (eds.), *Geological Implications of impacts of large asteroids and comets on the earth*. GSA Special Paper 190.
- Lindsay, E.H., Jacobs, L.L., and Butler, R.F. 1978. Biostratigraphy and magnetostratigraphy of Paleocene terrestrial deposits, San Juan Basin, New Mexico. *Geology*, 6:425-429.
- Lucas, S.G. and Heckert, A.B. 2000. Dinosaurs of New Mexico. New Mexico Museum of Natural History and Science Bulletin 17.
- Lucas, S.G. and Rigby, J.K., Jr. 1979. Comment: Biostratigraphy and magnetostratigraphy of Paleocene terrestrial deposits, San Juan Basin, New Mexico (Lindsay and others 1978). *Geology*, 7:2:323-326.
- Lucas, S.G. and Sealey, P.L. 1992. Preliminary report on invertebrate fossils from the Lewis Shale near Mesa Portales, Sandoval County, New Mexico, p. 24-26. In Lucas, S.G., Kues, B.S., Williamson, T.E., and Hunt, A.P. (eds.), *San Juan Basin IV. New Mexico Geological Society 43rd Field Conference Guidebook*.
- Lucas, S.G. and Sullivan, R.M. 2000. Stratigraphy and vertebrate biostratigraphy across the Cretaceous-Tertiary boundary, Bettonie Tsosie Wash, San Juan Basin, New Mexico, p. 95-103. In Lucas, S.G. and Heckert, A.B. (eds.), *Dinosaurs of New Mexico*. New Mexico Museum of Natural History and Science Bulletin 17.
- Lucas, S.G., Heckert, A.B., and Sullivan, R.M. 2000. Cretaceous dinosaurs in New Mexico, p. 83-90. In Lucas, S.G. and Heckert, A.B. (eds.), *Dinosaurs of New Mexico*. New Mexico Museum of Natural History and Science Bulletin 17.
- Lucas, S.G., Hunt, A.P., and Sullivan, R.M. 2006. Stratigraphy and age of the Upper Cretaceous Fruitland Formation, west-central San Juan Basin, New Mexico, p. 1-6. In Lucas, S.G. and Sullivan, R.M. (eds.), *Late Cretaceous vertebrates from the Western Interior*. New Mexico Museum of Natural History and Science Bulletin 35.
- Lucas, S.G., Mather, N.J., Hunt, A.P., and O'Neill, F.M. 1987. Dinosaurs, the age of the Fruitland and Kirtland Formations, and the Cretaceous-Tertiary boundary in the San Juan Basin, New Mexico, p. 35-50. In

- Fassett, J.E. and Rigby, J.K., Jr. (eds.), The Cretaceous-Tertiary boundary in the San Juan and Raton Basins, New Mexico and Colorado. GSA Special Paper 209.
- Manfrino, C. 1984. Stratigraphy and palynology of the upper Lewis Shale, Pictured Cliffs Sandstone, and lower Fruitland Formation (Upper Cretaceous) near Durango, Colorado (M.S. thesis). Colorado School of Mines, Golden, Colorado.
- McDowell, F.W., Lehman, T.M., and Connelly, J.N. 2004. A U-Pb age for the Late Cretaceous *Alamosaurus* vertebrate fauna of West Texas. GSA Abstracts with Programs, 36:4:6.
- Newman, K.R. 1987. Biostratigraphic correlation of Cretaceous-Tertiary boundary rocks, Colorado to San Juan Basin, New Mexico, p 151-164. In Fassett, J.E. and Rigby, J.K., Jr. (eds.). The Cretaceous-Tertiary boundary in the San Juan and Raton Basins, New Mexico and Colorado. GSA Special Paper 209.
- Nichols, D. 1994. A revised palynostratigraphic zonation of the nonmarine Upper Cretaceous Rocky Mountain region, United States, p. 503-521. In Caputo, M.V., Peterson, J.A., and Franczyk, K.J. (eds.). Mesozoic Systems of the Rocky Mountain Region, USA. Rocky Mountain Section, SEPM (Society for Sedimentary Geology), Denver, Colorado.
- Nichols, D.J. 2002. Palynology and palynostratigraphy of the Hell Creek Formation in North Dakota: a microfossil record of plants at the end of Cretaceous time, p. 393-456. In Hartman, J.H., Johnson, K.R., and Nichols, D.J. (eds.). The Hell Creek Formation and the Cretaceous-Tertiary boundary in the northern Great Plains: An integrated continental record of the end of the Cretaceous. GSA Special Paper 361.
- Nichols, D.J. 2003. Palynostratigraphic framework for age determination and correlation of the nonmarine lower Cenozoic of the Rocky Mountains and Great Plains region, p. 107-134. In Reynolds, R.G. and Flores, R.M. (eds.). Cenozoic systems of the Rocky Mountain region. Rocky Mountain Section, SEPM (Society for Sedimentary Geology), Denver, Colorado.
- Nichols, D.J. and Fleming, R.F. 2002. Palynology and palynostratigraphy of Maastrichtian, Paleocene, and Eocene strata in the Denver Basin, Colorado. Rocky Mountain Geology, 37:2:135-163.
- Nichols, D.J. and Johnson, K.R. 2002. Palynology and microstratigraphy of Cretaceous-Tertiary boundary sections in southwestern North Dakota, p. 95-143. In Hartman, J.H., Johnson, K.R., and Nichols, D.J. (eds.). The Hell Creek Formation and the Cretaceous-Tertiary boundary in the northern Great Plains: An integrated continental record of the end of the Cretaceous. GSA Special Paper 361.
- Nichols, D.J., Fleming, R.F., and Frederiksen, N.O. 1990. Palynological evidence of effects of the terminal Cretaceous event on terrestrial floras in western North America p. 351-364. In Kauffman, E.G. and Walliser, O.H. (eds.), Extinction events in Earth history. New York, Springer Verlag.
- Nichols, D.J., Brown, J.L., Attrep, M., Jr., and Orth, C.J. 1992. A new Cretaceous-Tertiary boundary locality in the western Powder River Basin, Wyoming: Biological and geological implications. Cretaceous Research, 13:3.
- Orth, C.J., Gilmore, J.S., Knight, J.D., Pillmore, C.L., Tschudy, R.H., and Fassett, J.E. 1981. An iridium abundance anomaly at the palynological Cretaceous-Tertiary boundary in northern New Mexico. *Science*, 214:1341-1343.
- Orth, C.J., Gilmore, J.S., Knight, J.D., Pillmore, C.L., Tschudy, R.H., and Fassett, J.E. 1982. Iridium abundance measurements across the Cretaceous/Tertiary boundary in the San Juan and Raton Basins of northern New Mexico, p. 423-433. In Silver, L.T. and Schultz, P.H. (eds.), Geological Implications of impacts of large asteroids and comets on the earth. GSA Special Paper 190.
- Powell, J.S. 1973. Paleontology and sedimentation models of the Kimbeto Member of the Ojo Alamo Sandstone, p. 111-122. In Fassett, J.E. (ed.), Cretaceous and Tertiary rocks of the Colorado Plateau. Four Corners Geological Society Memoir.
- Reeside, J.B., Jr. 1924. Upper Cretaceous and Tertiary formations of the western part of the San Juan Basin of Colorado and New Mexico. USGS Professional Paper 134:1-70.
- Rigby, J.K., Jr., and Wolberg, D. 1987. The therian mammalian fauna (Campanian) of Quarry 1, Fossil Forest Study Area, San Juan Basin, New Mexico, p. 51-79. In Fassett, J.E. and Rigby, J.K., Jr. (eds.), The Cretaceous-Tertiary boundary in the San Juan and Raton Basins, New Mexico and Colorado. GSA Special Paper 209.
- Sahni, A. 1972. The vertebrate fauna of the Judith River Formation, Montana. American Museum of Natural History Bulletin 146:321-412.
- Scott, G.R., Mytton, J.W., and Schneider, G.B. 1980. Geologic map of the Star Lake Quadrangle, McKinley County, New Mexico. USGS Miscellaneous Field Studies Map MF-1248.
- Scott, G.R., O'Sullivan, R.O., and Mytton, J.W. 1979. Geologic map of the Alamo Mesa West Quadrangle. USGS Miscellaneous Field Studies Map MF-1074.
- Shoemaker, E.M., Steiner, M.B., and Fassett, J.E. 1984. Magnetostratigraphy of Upper Cretaceous rocks at Mesa Portales, New Mexico (abs.). GSA Rocky Mountain Section Meeting, Durango, Colorado.

- Sikkink, P.G.L. 1987. Lithofacies relationships and depositional environment of the Tertiary Ojo Alamo Sandstone and related strata, San Juan Basin, New Mexico and Colorado, p. 81-104. In Fassett, J.E. and Rigby, J.K., Jr. (eds.), The Cretaceous-Tertiary boundary in the San Juan and Raton Basins, New Mexico and Colorado. GSA Special Paper 209.
- Silver, C. 1950. The occurrence of gas in the Cretaceous rocks of the San Juan Basin, New Mexico and Colorado, p. 109-123. In San Juan Basin, New Mexico and Colorado. New Mexico Geological Society 1st Field Conference Guidebook.
- Simpson, G.G. 1950. Lower Tertiary formations and vertebrate faunas of the San Juan Basin, p. 85-89. In San Juan Basin, New Mexico and Colorado. New Mexico Geological Society 1st Field Conference Guidebook.
- Simpson, G.G. 1959. Fossil mammals from the type area of the Puerco and Nacimiento strata, Paleocene of New Mexico. *American Museum Novitates* 1957:1-22.
- Simpson, G.G. 1981. History of vertebrate paleontology in the San Juan Basin, p. 3-25. In Lucas, S.G., Rigby, J.K. Jr., and Kues, B.S. (eds.), *Advances in San Juan Basin paleontology*. University of New Mexico Press, Albuquerque, New Mexico.
- Steiner, M.B. 1983. Detrital remanent magnetization in hematite. *Journal of Geophysical Research*, 88:B8:6523-6539.
- Sullivan, R.M. and Lucas, S.G. 2003. The Kirtlandian, a new land-vertebrate "age" for the Late Cretaceous of Western North America, p. 375-383. In Lucas, S.G., Semken, S.C., Berglof, W.R., and Ulmer-Scholle, D.S. (eds.), *Geology of the Zuni Plateau*. New Mexico Geological Society 54th Field Conference Guidebook.
- Sullivan, R.M. and Lucas, S.G. 2006. The Kirtlandian, land-vertebrate "age" – faunal composition, temporal position and biostratigraphic correlation in the non-marine upper Cretaceous of Western North America, p. 7-29. In Lucas, S.G. and Sullivan, R.M., eds., *Late Cretaceous vertebrates from the Western Interior*. New Mexico Museum of Natural History and Science Bulletin 35.
- Sullivan, R.M., Boere, A.C., and Lucas, S.G. 2005. Redescription of the ceratopsid dinosaur *Torosaurus utahensis* (Gilmore 1946) and a revision of the genus. *Journal of Paleontology*, 79:3:564-582.
- Sullivan, R.M., Lucas, S.G., and Braman, D.R. 2005. Dinosaurs, pollen, and the Cretaceous-Tertiary boundary in the San Juan Basin, New Mexico, p. 395-407. In Lucas, S.G., Zeigler, K.E., Lueth, V.W., and Owen, D.E. (eds.), *Geology of the Chama Basin*. New Mexico Geological Society 56th Field Conference Guidebook.
- Trueman, C.N. and Benton, M.J. 1997. A geochemical method to trace the taphonomic history of reworked bones in sedimentary settings. *Geology*, 25:3:263-266.
- Trueman, C.N., Behrensmeyer, A.K., Potts, R., and Turross, N. 2006. High-resolution records of location and stratigraphic provenance from the rare earth element composition of fossil bones. *Geochimica et Cosmochimica Acta*, 70:4343-4355.
- Tschudy, R.H. 1973. The Gasbuggy core; a palynological appraisal, p. 123-130. In Fassett, J.E. (ed.), *Cretaceous and Tertiary rocks of the Colorado Plateau*. Four Corners Geological Society Memoir.
- Weil, A. 2002. Late Cretaceous and Early Paleocene mammalian faunal exchange between Asia and North America (abs.). GSA Abstracts with Programs 34:316.
- Weil, A. and Williamson, T.E. 2000. Diverse Maastrichtian terrestrial vertebrate fauna of the Naashoibito Member, Kirtland Formation (San Juan Basin, New Mexico) confirms "Lancian" faunal heterogeneity in Western North America (abs.). GSA Rocky Mountain Section Meeting, Reno, Nebraska.
- Williamson, T.E. 1996. The beginning of the age of mammals in the San Juan Basin: Biostratigraphy and evolution of Paleocene mammals of the Nacimiento Formation. *New Mexico Museum of Natural History and Science Bulletin* 8.
- Williamson, T.E. and Lucas, S.G. 1992. Stratigraphy and mammalian biostratigraphy of the Paleocene Nacimiento Formation, southern San Juan Basin, New Mexico, p. 265-296. In Lucas, S.G., Kues, B.S., Williamson, T.E., and Hunt, A.P. (eds.), *San Juan Basin IV*. New Mexico Geological Society 43rd Field Conference Guidebook.
- Williamson, T.E. and Lucas, S.G. 1993. Paleocene vertebrate paleontology of the San Juan Basin, New Mexico, p. 105-135. In Lucas, S.J. and Zidek, J. (eds.), *Vertebrate paleontology in New Mexico*. New Mexico Museum of Natural History and Science, Bulletin 2.
- Williamson, T.E. and Weil, A. 2001. Dinosaurs from microvertebrate sites in the Upper Cretaceous Fruitland and Kirtland Formations, San Juan Basin, New Mexico (abs.). GSA Rocky Mountain and South Central Sections Joint Meeting, Albuquerque, New Mexico.
- Williamson, T.E. and Weil, A. 2003. Latest Cretaceous dinosaurs in the San Juan Basin, New Mexico. *Journal of Vertebrate Paleontology* 23 (Suppl. 3):110A.
- Williamson, T.E., Nichols, D.J., and Weil, A. 2008. Paleocene palynomorph assemblages from the Nacimiento Formation, San Juan Basin, New Mexico, and their biostratigraphic significance, p. 3-11. *New Mexico Geology* 30:01.
- Winchester, S. 2001. *The Map That Changed the World*. Harper Collins Publishers, Inc., New York, New York.
- Woodward, L.A., Anderson, L.A., Kaufman, W.H., and Reed, R.K. 1973. Geologic map and sections of San Pablo quadrangle, New Mexico. New Mexico Bureau of Geology and Mineral Resources GM-26.

Woodward, L.A., McLelland, D., Anderson, J.B., and Kaufman, W.H. 1972. Geologic map of Cuba quadrangle, New Mexico. New Mexico Bureau of Geology and Mineral Resources GM-25.

APPENDIX

SYNTHESIS OF PUBLISHED AND UNPUBLISHED PALYNOLOGIC DATA FOR CRETACEOUS-TERTIARY BOUNDARY STRATA; SAN JUAN BASIN, NEW MEXICO

INTRODUCTION

Palynology has been the most precise bio-chronologic tool for locating the stratigraphic position of the Cretaceous-Tertiary (K-T) boundary in the Western Interior of North America. In the Raton Basin, 230 km east of the San Juan Basin, the K-T boundary was located to within a few centimeters on the basis of the last occurrence of the Cretaceous index palynomorph *Tschudypollis* (formerly named *Proteacidites*). The end-Cretaceous asteroid-impact fall-out layer was subsequently discovered within that same centimeters-thick interval by Orth et al. (1981, 1982). The K-T fall-out layer has now been found at numerous localities throughout the Western Interior of North America just above the last occurrence of *Tschudypollis* and (or) other Cretaceous index palynomorphs, validating the value of these index fossils for determining the precise location of the K-T interface. Nichols and Johnson (2002, p. 100) stated that:

In southwestern North Dakota, as elsewhere in the Western Interior region of the United States and Canada, the K-T boundary is defined by the disappearance (local or total extinction) of certain palynomorph taxa. . . . In this study, the K-T boundary was determined on the basis of palynology to be between the highest sample that yielded K taxa [Cretaceous index palynomorphs] and the next sample above that lacks K taxa.

One of the key "K taxa" listed by Nichols and Johnson (2002) was *Tschudypollis*. In the following discussion, it is shown that the last occurrence of the Cretaceous index palynomorph *Tschudypollis* precisely locates the stratigraphic level of the K-T interface at the base of the Ojo Alamo Sandstone at several localities in the San Juan Basin. At a few localities, rare specimens of *Tschudypollis* have been identified from Ojo Alamo Sandstone rock samples. Nichols and Fleming (2002, p. 240) discussed the reworking of palynomorphs from older strata into younger strata and concluded that "The age of a contaminated [palynomorph] assemblage

is determined by the youngest species present, one that has a restricted stratigraphic range, and does not occur in older rocks." In every instance where rare *Tschudypollis* specimens have been found in Ojo Alamo Sandstone samples, the younger Paleocene guide fossil *Momipites tenuipolus* is also present. *M. tenuipolus* is a known Paleocene guide fossil in the Western Interior of North America (Nichols and Johnson 2002) and has never been found in Cretaceous strata in the southern part of the Western Interior, thus the presence of this palynomorph in the Ojo Alamo Sandstone confirms the Paleocene age of these "contaminated" assemblages.

Obtaining outcrop rock samples productive of palynomorphs has been a difficult challenge in the San Juan Basin. Commonly, samples that looked promising in the field that is, with evidence of abundant organic material in them proved barren, when analyzed. For that reason, palynologic sampling from Mesa Portales, the Ojo Alamo Sandstone type area, and other localities (discussed below), has been spaced out over decades. For every set of samples collected, more than half, typically, turned out to be barren of palynomorphs, so recollecting was necessary to try to find productive material to fill in gaps. This problem has been especially acute in the Ojo Alamo type area (Figure 4), where abundant dinosaur bone is present in the lower part of the Ojo Alamo Sandstone. Numerous attempts to obtain rock samples productive of palynomorphs from dinosaur-bearing strata within the Ojo Alamo Sandstone in the type area, by various workers (including the author), have still not succeeded. Productive samples yielding diverse palynomorph assemblages from dinosaur-bearing strata would contribute greatly to the biochronologic data-base for the Ojo Alamo Sandstone in the southern San Juan Basin.

Good results, however, have been relatively recently obtained at the San Juan River site, where multiple palynomorph-productive samples were obtained a few meters below a large hadrosaur femur in the Ojo Alamo Sandstone (Fassett and Lucas 2000) and at the Barrel Spring locality where

the Paleocene index palynomorph *Momipites tenuipolus* was identified from samples just below the base of the dinosaur-bearing Ojo Alamo Sandstone (Fassett et al. 2002). Excellent results have also been obtained from Cretaceous-Tertiary (K-T) strata at Mesa Portales where multiple, productive, palynologic sample sites closely bracket the Cretaceous-Tertiary interface. Even though studies of the palynology of the Ojo Alamo Sandstone and adjacent strata have been conducted at numerous localities, no synthesis of all available data has been published heretofore.

The aim of this appendix is to present, chronologically, all available published and unpublished palynologic data for rock strata adjacent to the K-T interface in the San Juan Basin.

Anderson (1960)

Anderson (1960) was the first to publish palynologic data for strata adjacent to the Cretaceous-Tertiary boundary in the San Juan Basin. In

his introduction, he summarized the conflicting paleontologic data relating to the age of the Ojo Alamo Sandstone in the southern San Juan Basin: paleobotanical data indicated that the Ojo Alamo was Paleocene and abundant dinosaur fossils indicated that this formation was Cretaceous. Anderson wrote (p. 1): "One objective of this study is to determine what bearing the pollen and spore evidence has on the controversy." Anderson (1960) collected rock samples from the Ojo Alamo Sandstone and adjacent strata at five localities in the southeastern part of the basin near Cuba, New Mexico (Figure 21): the Kirtland Shale, Ojo Alamo 1 and 2, and Nacimiento 1 and 2 localities. (Anderson's palynomorph lists from these localities are in Table 5 (see Table Appendix, page 118).)

Figure 47 is a composite stratigraphic diagram showing the relative stratigraphic positions of Anderson's Kirtland and Ojo Alamo sample sites. The sample locality for the "Kirtland shale florule" is in a badland amphitheater where the upper part of

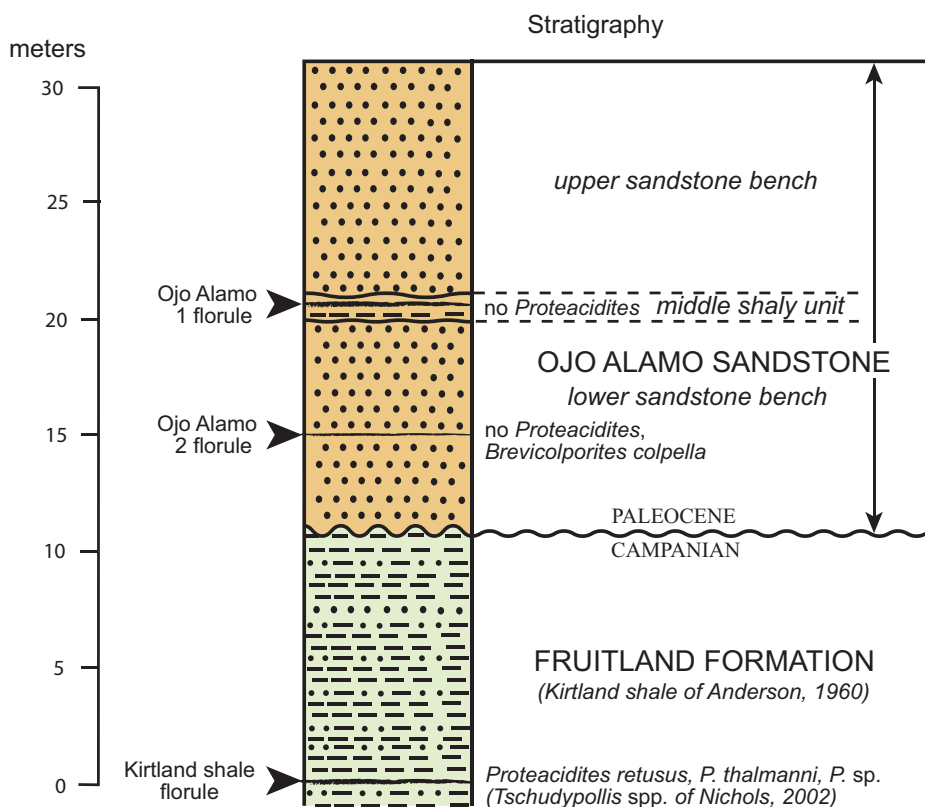


Figure 47. Composite stratigraphic column showing levels of samples collected by Anderson (1960) for palynologic analysis from Fruitland Formation and Ojo Alamo Sandstone near Cuba, New Mexico. Sample localities shown on Figure 21. Key index-palynomorph levels are shown. *Proteacidites* renamed *Tschudyipollis* by Nichols (2002).



Figure 48. Photograph of “Kirtland shale florule” locality of Anderson (1960) showing “carbonaceous zone” from which Kirtland-shale-florule sample was collected. Locality about 4 km south of Cuba, New Mexico (Figure 21).

the Kirtland Formation and Ojo Alamo Sandstone are well exposed (Figures 21, 48). This locality is 220 m west of County Road (CR) 11 (Figure 21) and is 4.0 km (2.4 mi.) south of the intersection of CR 11 and US Highway 550. Anderson’s sample was collected from “. . . the upper carbonaceous zone in a medium-gray micaceous mudstone approximately 37 feet [11.3 m] below the base of the Ojo Alamo Sandstone.” (Anderson 1960, p. 5). The key Cretaceous index palynomorphs identified by Anderson from this sample were *Proteacidites retusus*, *P. thalmani*, and *P. sp.* (his tables 2, 3). (The genus name “*Proteacidites*” was recently changed to *Tschudypollis* by Nichols, (2002, p. 443-444)). The complete list of Anderson’s palynomorphs constituting the “Kirtland shale florule” is in Table 5.

Figure 48 is a photograph of the “Kirtland shale florule” locality. The Ojo Alamo Sandstone is about 18 m thick here and consists of two ledges of white sandstone separated by a thin bed of siltstone and mudstone. The Ojo Alamo is underlain by the “Kirtland shale” of Anderson; this rock unit

was mapped as Kirtland Shale and Fruitland Formation, undivided, in this area by Baltz (1967), Fassett and Hinds (1971), Woodward et al. (1972), and Woodward et al. (1973). Fassett and Hinds (1971, figure 9, plate 2), however, show that the Fruitland-Kirtland interval is beveled at the top from northwest to southeast across the San Juan Basin, resulting in the Kirtland being absent along the east side of the basin, including the area of Anderson’s “Kirtland shale florule” (see Figure 21). Thus, the rock unit underlying the Ojo Alamo Sandstone at Anderson’s localities is more properly named the Fruitland Formation. (See Figure 1.2 for a basin-wide cross section depicting the convergence of the basal contact of the Paleocene Ojo Alamo with underlying Cretaceous strata.) The base of the lower Ojo Alamo Sandstone bench is stratigraphically higher on the right side (north) on Figure 48 than on the left (south) side. The interface between Cretaceous and Paleocene strata here is probably at the base of the sandy interval just above the top of the carbonaceous zone in the Fruitland Forma-

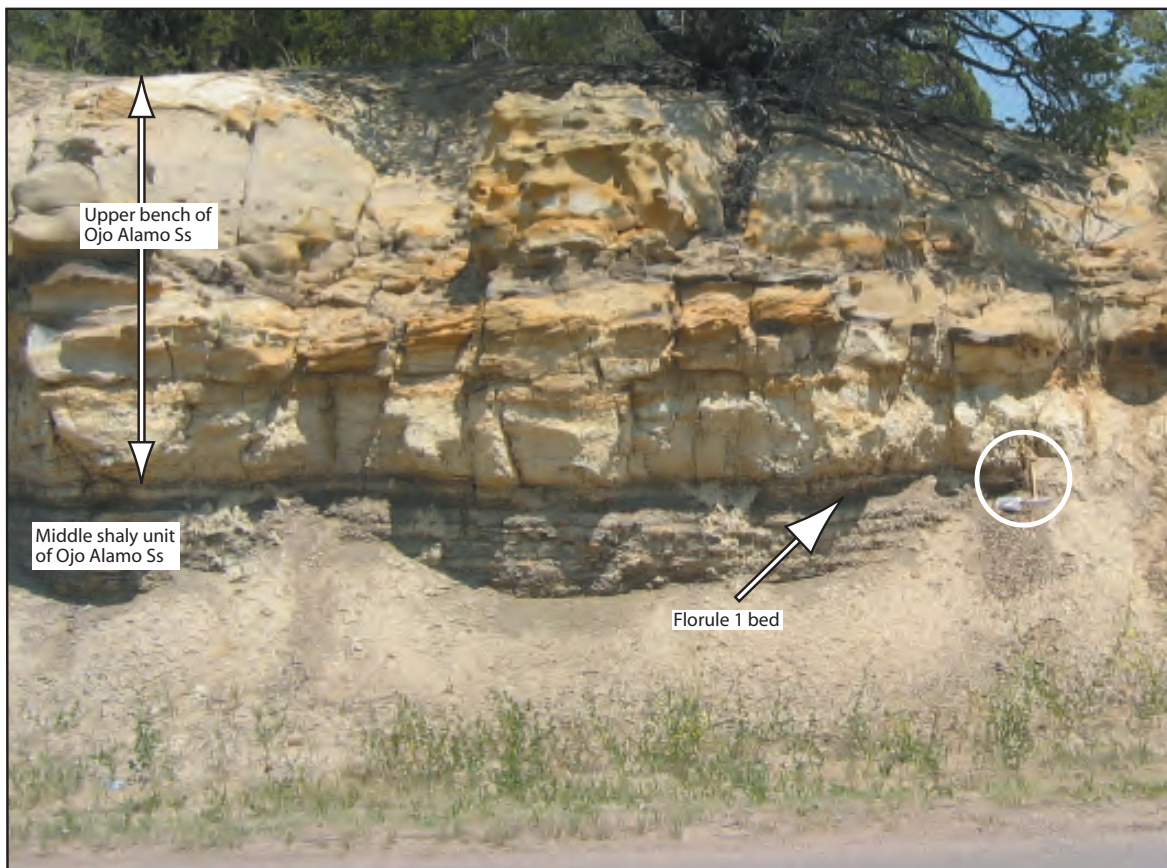


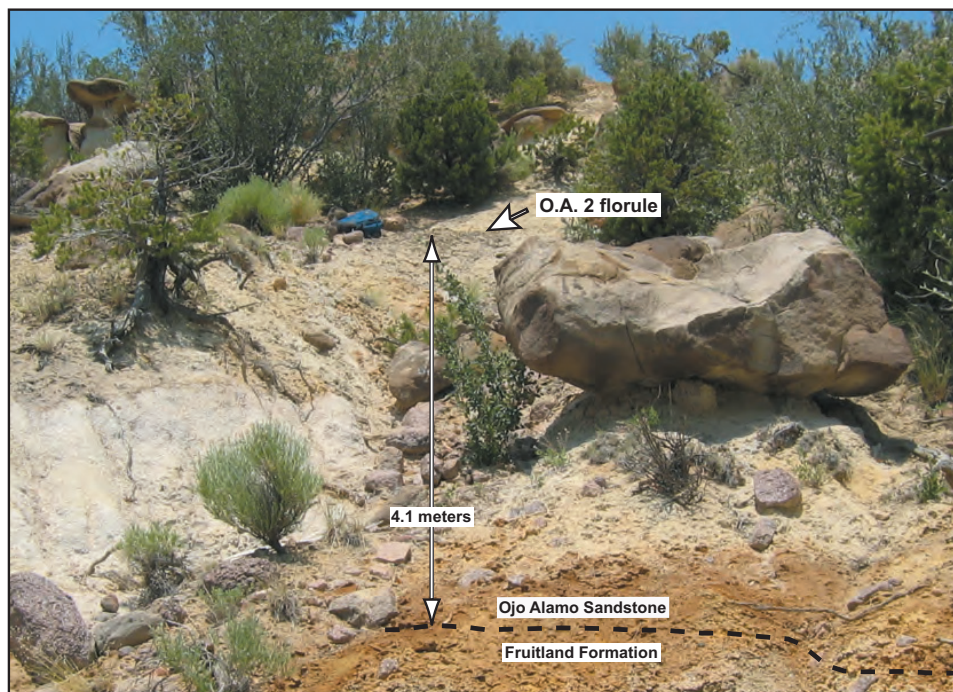
Figure 49. Photograph of “Ojo Alamo 1 florule” locality of Anderson (1960). Locality about 1.5 km south of Cuba, New Mexico (Figure 21). Geologic pick in white circle is 0.33 m. Upper bench of Ojo Alamo nearly 3 m thick. Anderson stated that this sample locality was at base of Ojo Alamo Sandstone; however, locality is now known to be in middle mudstone to siltstone bed of the Ojo Alamo as seen on Figure 21.

tion and not at the base of the rock-stratigraphic Ojo Alamo.

Anderson’s “Ojo Alamo 1 florule” was collected from “a thin carbonaceous layer within a light brownish-buff siltstone lens at the base of the Ojo Alamo sandstone.” (Anderson 1960, p. 5). He stated that “The siltstone lens from which the sample was taken could be considered a part of either the Ojo Alamo Sandstone or the Kirtland shale.” This locality is in a road cut in the Ojo Alamo just east of CR 11, 1.5 km (0.95 mi.) south of the intersection of CR 11 and US Highway 550 (Figures 21, 49). Although Anderson stated that this sample came from “the base of the Ojo Alamo Sandstone,” subsequent mapping by Baltz (1967) and Woodward et al. (1973) showed that Anderson’s Ojo Alamo 1 florule was actually collected from a mudstone and siltstone layer within the Ojo Alamo. The Ojo Alamo 1 florule from this locality does not contain the key Cretaceous index fossil: *Tschudypollis*

(*Proteacidites*). Anderson (1960, p. 5) stated that: “The florule is very different from the underlying one in the Kirtland shale . . .” but concluded (p. 9) that “The Ojo Alamo 1 florule has a ‘Tertiary’ aspect but is not necessarily Tertiary from the standpoint of common forms.” Anderson’s complete list of palynomorphs from this locality is in Table 5.

Anderson’s (1960, p. 5) “Ojo Alamo 2 florule” (Table 5) was “. . . found in a carbonaceous zone at the base of a middle shale unit within the Ojo Alamo Sandstone.” Anderson’s road directions to this locality cannot be literally followed to arrive at this collection site; however, the placement of this site on his map (figure 1) is accurate. (The map on Figure 21 of the present report clearly shows how to access this site via NM State Highway 126 and CR 13: go 0.86 km (0.54 mi) east of US Hwy 550 on NM Hwy 126 and then 3.7 km (2.3 mi) north and east on CR 13); the site is about 200 m west of CR 13. This sample site is within a lower bench of the



50.1



50.2

Figure 50. Photographs of “Ojo Alamo 2 florule” locality of Anderson (1960). Locality about 4.5 km northeast of Cuba, New Mexico (Figure 21). Photograph **50.1** shows location of florule 2 sample collection site in about center of lower sandstone bench of Ojo Alamo Sandstone (Figure 47); bench is about 9 m thick here. Photograph **50.2** shows close-up view of 75-mm-thick black carbonaceous shale layer from which sample containing “Ojo Alamo 2 florule” was collected (hammer handle is scaled in inches). Paleocene index fossil *Brevicolporites colpella* was identified from this sample.

Ojo Alamo Sandstone about 4 m above the Ojo Alamo Sandstone-Fruitland Formation contact. Figure 50 shows two photographs of the Ojo Alamo 2 florule site: Figure 50.1 shows the position of Anderson's "carbonaceous zone" within the lower bench of the Ojo Alamo; Figure 50.2 is a close-up view of the sample site. The lower bench of the Ojo Alamo Sandstone here caps an east-trending ridge, but further west, this ridge merges with the northeasterly trending Ojo Alamo Sandstone outcrop (Figure 21). There, the Ojo Alamo consists of this lower sandstone bench, a middle claystone-to-siltstone layer, and an upper sandstone bench.

Anderson did not find the Cretaceous index palynomorph *Tschudypollis* in this florule, however he did find that it contained the Paleocene index fossil *Brevicolporites colpella*. (See Nichols and Johnson 2002, for a comprehensive discussion of the palynology of Cretaceous-Tertiary boundary rocks in the Western Interior of North America.) The disappearance of *Tschudypollis* (a "K taxon" of Nichols and Johnson 2002) going upward in a stratigraphic section provides evidence that the Cretaceous-Tertiary boundary has been crossed. Moreover, also finding the Paleocene index fossil *B. colpella* (Nichols and Johnson 2002) present and K taxa absent from the same strata provides unequivocal evidence of the Paleocene age of the strata in question (Nichols, personal commun., 2005).

Figure 47 shows the stratigraphic relations of Anderson's sample-collection sites near Cuba, New Mexico. The stratigraphically lowest sample (about 11 m below the base of the Ojo Alamo Sandstone) yielded his "Kirtland shale florule" which is notable for the presence of the Cretaceous index fossil *Proteacidites thalmani* (*Tschudypollis*) "as the dominant dicotyledon" plus other *Proteacidites* species (Anderson 1960, p. 5 and tables 2, 3). Anderson's "Ojo Alamo 2 florule" is from a sample about 4 m above the base of the Ojo Alamo; this florule contains no *Proteacidites* (*Tschudypollis*) species but does contain the Paleocene index fossil *Brevicolporites colpella*. Going up section to the middle part of the Ojo Alamo and Anderson's "Ojo Alamo 1 florule," again there are no *Proteacidites* (*Tschudypollis*) species and according to USGS palynologist D.J. Nichols (personal commun., 2006): "Anderson's OA florule 1, which lacks *Tschudypollis* spp. as you note, does appear to be Paleocene in age." It thus seems clear that the Ojo Alamo Sandstone in Anderson's study area near Cuba, New Mexico, is Paleocene in age in its entirety.

Anderson (1960, p. 13) concluded that palynologic data suggest that "most of the Ojo Alamo sandstone is Tertiary, but the basal part may be either Cretaceous or Paleocene." As for the abundant Ojo Alamo dinosaur fossils in the type area, Anderson stated that they may have been reworked, or "Alternatively, pre-Lance-type dinosaurs persisted into a Tertiary environment." Anderson thus became the second geologist (after Reeside 1924) to suggest that dinosaurs may have lived on into the Paleocene in the San Juan Basin.

Anderson's Nacimiento 1 and 2 florule localities are shown on Figure 21 but are not discussed in detail in this report, because the Paleocene age of the Nacimiento Formation has never been questioned. Anderson (1960, p. 8) stated that the "Nacimiento 1 florule" was collected from a "medium-gray, micaceous, carbonaceous mudstone, 1 foot above the Ojo Alamo sandstone"; the "Nacimiento 2 florule" was from "an 8-inch coal bed about 115 feet above the Nacimiento 1 florule." Palynomorph assemblages from these localities were determined by Anderson to be Paleocene in age. Anderson's palynomorph lists from his two Nacimiento localities are included in Table 5.

Baltz et al. (1966)

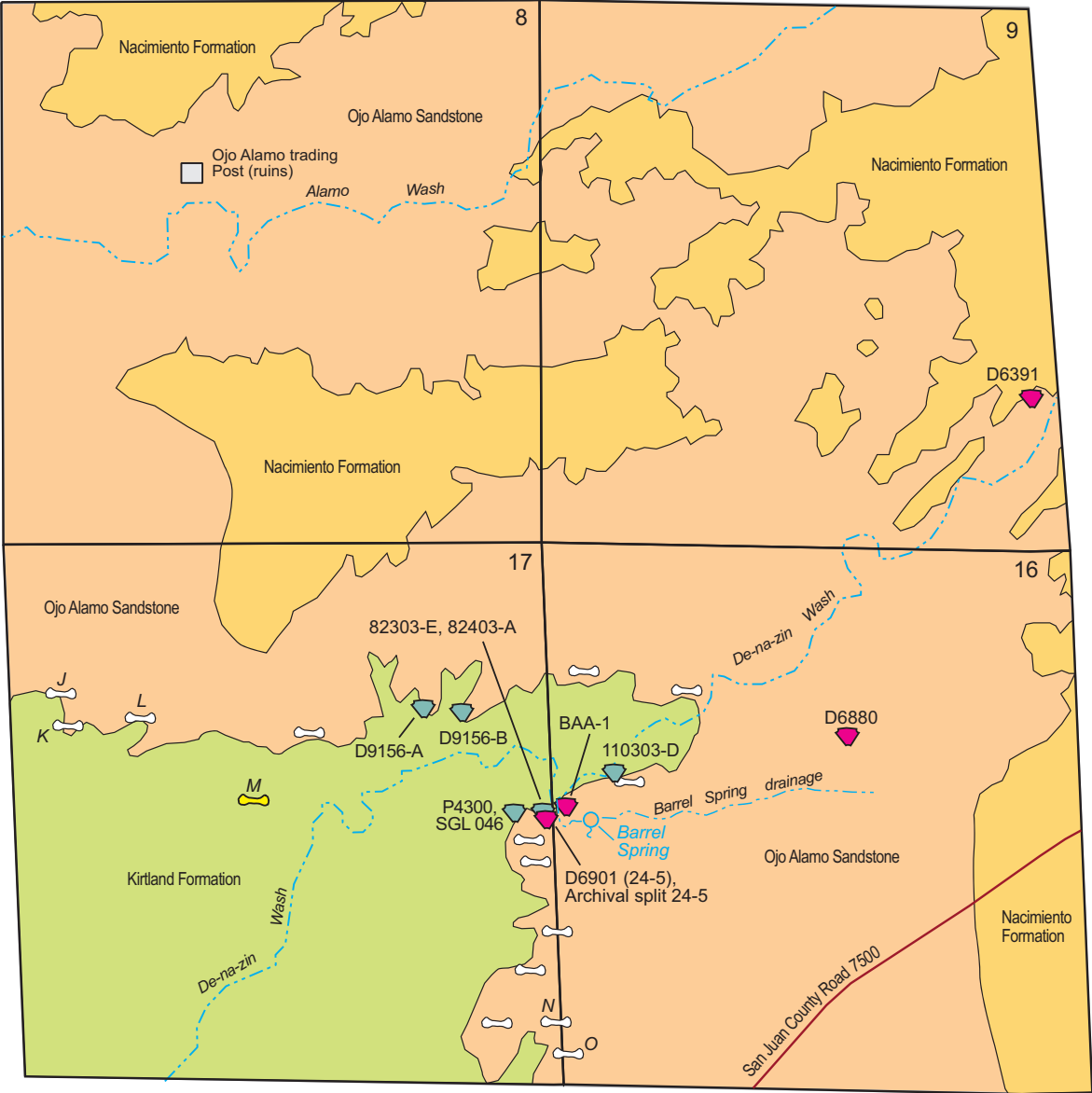
Baltz et al. (1966) conducted a detailed study of the Ojo Alamo Sandstone in the Ojo Alamo type area (Figures 3, 4, 51). This study included collecting rock-samples from the uppermost Kirtland Formation, upper part of the Ojo Alamo Sandstone, and the lowermost part of the Nacimiento Formation for palynologic analysis. These authors also redefined the Ojo Alamo Sandstone in their paper (see Figure 2). Figure 52 shows the stratigraphic levels of the three palynologic collections of Baltz et al. (1966); because these samples were collected from different localities, their placement on one column on Figure 52 is diagrammatic. The palynomorphs identified from these three collections are listed in Table 6 (see Table Appendix, page 119).

Collection 3 of Baltz et al. was obtained from a "lignite" (carbonaceous mudstone) bed in the uppermost part of the Kirtland Formation (Figure 52) just north of Alamo Wash in the extreme NW ¼ Sec. 7, T. 24 N., R. 11 W. (BAA-3 on Figure 4).

Anderson, in Baltz et al. (p. D17) stated that:

The florule of collection 3 from the Kirtland is strikingly different from collections 1 and 2 and from any of the Cretaceous and Tertiary florules described by Anderson (1960) from the

T. 24 N., R. 11 W



- LEGEND**
- | | | |
|--|--|--|
| | | |
| | | |

Figure 51. Large-scale geologic map of Barrel Spring area showing USGS and other paleobotany localities discussed in text. Dinosaur-bone localities also shown and geochemistry of bone samples from lettered localities shown on Tables 2 and 3. Geology modified from Brown (1982); base of Ojo Alamo remapped by author for this study. All of area, except south of San Juan County Road 7500, in Bisti - De-na-zin Wilderness Area.

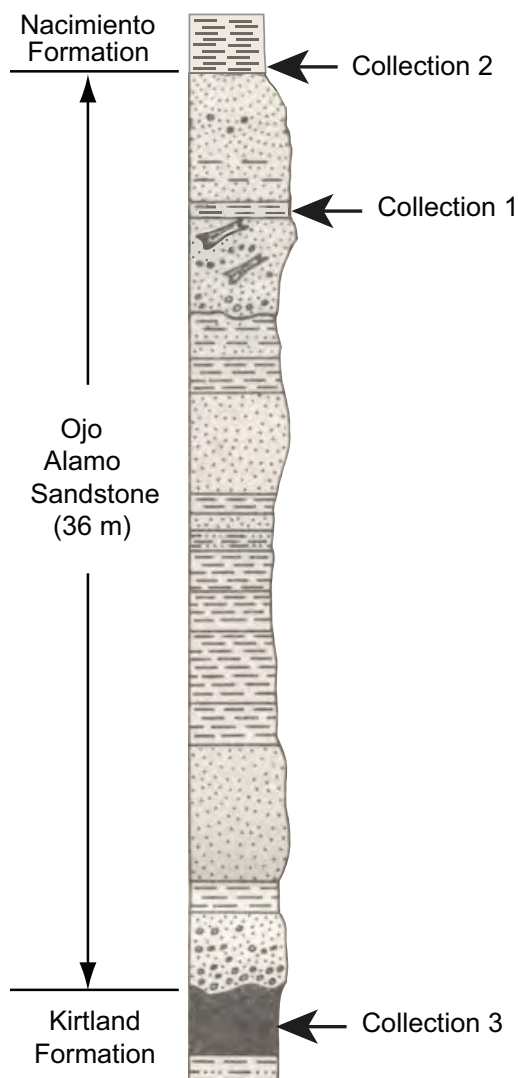


Figure 52. Stratigraphic column of Ojo Alamo Sandstone and adjacent strata near Barrel Spring in Ojo Alamo type area (Figures 3, 4). Column is modified from Baltz et al. (1966, plate I, column 11). Stratigraphic levels for collections 2 and 3 projected into column; sample collection 2 from west of Barrel Spring, sample collection 3 from north of Ojo Alamo Arroyo (Baltz et al. 1966, plate I).

eastern part of the basin. The dominant forms of collection 3 are polypodiaceous spores and a monosulcate grain with echinate-clavate sculpture. Pinaceous conifer pollen are [sic] common. Dicotyledon grains are much fewer than in any of the eastern florules, and the dominant form is a tricolpate, reticulate,

brevaxial grain with intersemiangular to intersemilobate outline. Smooth and warty trilete spores are present in collection 3, and there are many cystlike structures with hollow processes that resemble some hystrichosphaerids. The florule contains *Liliacidites leei* Anderson which occurs in the Kirtland, Ojo Alamo, and Nacimiento florules of the eastern part of the basin and *Liliacidites hyalaciniatus?* Anderson which occurs in the Kirtland and Ojo Alamo 1 florules of the eastern part of the basin.

Proteacidites thalmani Anderson is the only really distinctive form in collection 3 that is found also in an eastern florule. It occurs in Anderson's (1960) Kirtland Shale and Lewis Shale florules and suggests a Cretaceous age for collection 3.

Collection 1 was from a "lignitic shale" (carbonaceous mudstone) interbed in the upper part of the Ojo Alamo Sandstone (Figure 52). This locality was reported to be "on the mesa about one-eighth mile [200 m] north of Barrel Spring" by Baltz et al. (p. D17). The location for this sample collection cannot be correct because 200 m north of Barrel Spring is not "on the mesa" and not in the uppermost Ojo Alamo Sandstone, but rather is in the drainage-way of De-na-zin arroyo in the upper Kirtland Shale. The actual location for this locality appears to be in the west-central part of Sec. 16, T. 24 N., R. 11 W. at the edge of the mesa about 70 m north of Barrel Spring (labeled BAA-1 on Figures 4, 51).

Collection 2 was from an extensive bed of "lignite" (carbonaceous mudstone) in the lower part of the Nacimiento Formation (Figure 52) in the southwest part of Sec. 10, T. 24 N., R. 11 W. in Barrel Spring Arroyo (Figure 4). Barrel Spring Arroyo of Baltz et al. (1966) is now named De-na-zin Wash (Alamo Mesa East, 1/24,000 USGS topographic quadrangle map); the collection 2 palynologic locality is labeled BAA-2 on Figure 4.

Anderson (in Baltz et al., p. D17) stated that:

*Collection 1 from the Ojo Alamo and collection 2 from the Nacimiento are similar to each other and contain common to abundant grains of *Ulmoideipites tricostatus* Anderson and *Podocarpus* sp. These are the two dominant types of grains in Anderson's (1960) Ojo Alamo florules from the eastern part of the basin. Several kinds*

of Momipites grains are present in collections 1 and 2; these also are common in Anderson's (1960) Ojo Alamo and Nacimiento florules from the eastern part of the basin. The florule of collection 1 contains many large inaperturate semihexagonal grains, some monosulcate grains, monolete and trilete spores, triporate pollen, and pinaceous conifer pollen. The florule of collection 2 contains Quercus? sp., Arcipites cf. A. reticulatus (Van der Hammen), Cupaneidites cf. C. major Cookson and Pike, Paliurus triplicatus? Anderson, and some spores, all of which are present in Anderson's (1960) Ojo Alamo or Nacimiento florules from the eastern part of the basin.

Complete palynomorph lists for the three palynologic localities of Baltz et al. (1966) were not provided.

Baltz et al. (1966, p. D17) concluded that: "The palynology does not directly fix the age of the Restricted Ojo Alamo Sandstone . . ." but then added the somewhat contradictory statement: "In summary, the palynologic and physical-stratigraphic evidence of the [Paleocene] age of the restricted Ojo Alamo Sandstone are in agreement." As for the differences in palynomorph assemblages in the Ojo Alamo type area and in Anderson's (1960) collections near Cuba, New Mexico, on the east side of the basin, Baltz et al. (1966) suggested that the different florules:

. . . allow for the possibility that rocks equivalent in age to the upper shale member of the Kirtland (colln. 3) at Ojo Alamo may be absent from the eastern part of the basin. This interpretation would be consistent with the physical evidence for a hiatus between the deposition of the Kirtland and the Ojo Alamo.

Subsequent work, demonstrating the presence of a nearly 8-m.y. hiatus at the Kirtland-Ojo Alamo contact (Fassett and Steiner 1997; Fassett, 2000), and the thinning of Cretaceous strata by more than 650 m from northwest to southeast across the San Juan Basin (Figure 1), shows that the upper Kirtland Formation strata sampled at Ojo Alamo Arroyo indeed are not present east of Cuba, New Mexico. The stratigraphic cross sections of Figures 33-35, conclusively show that the uppermost Kirtland Formation strata in the Ojo Alamo type area (drill-hole 2) are not present in the Cuba,

New Mexico, area (drill-hole 6). Thus, the different palynomorph assemblages at the two places are the result of sampling of strata of different ages deposited in quite different environments: relatively near to the regressing Pictured Cliffs Sandstone shoreline near Cuba vs. far inland from the paleo-shoreline at the Ojo Alamo Sandstone type area.

Fassett and Hinds (1971)

Fassett and Hinds (1971, table 1) published a palynomorph list for samples from eight localities in the San Juan Basin. At a locality in the northeast part of the basin in Colorado, the lowermost Fruitland Formation was sampled; at another locality, south of Mesa de Cuba, the lower part of the Nacimiento Formation was sampled. The other six localities were in the Mesa Portales study area (Figure 21), where multiple samples were collected from the undivided Fruitland-Kirtland Formation and from the Ojo Alamo Sandstone. All these samples were collected by the author between 1964 and 1968 and were analyzed by R.H. Tschudy, U. S. Geological Survey, Denver, Colorado; Tschudy's data were provided in written communications in 1966, 1967, and 1968. Complete palynomorph lists for these localities were presented in table 1 of Fassett and Hinds (1971); that table is reproduced herein as Table 7 (see Table Appendix, page 120). (The stratigraphic positions of the Mesa Portales sample localities of Fassett and Hinds are shown on Figures 22 and 23; the other palynologic sample localities shown on these figures were collected later and are discussed in a subsequent section of this appendix.) Palynomorph assemblages in Fassett and Hinds (1971) from Mesa Portales made clear that the Cretaceous-Tertiary boundary there was located below the base of the rock-stratigraphic Ojo Alamo Sandstone in the 13 m interval between samples D3738-C and D3738-B (Figures 22, 23).

All of the Fassett and Hinds samples from the undivided Fruitland-Kirtland interval in the Mesa Portales study area contained abundant specimens of the Cretaceous index fossil *Proteacidites* (*Tschudyipollis*). Table 7 lists *Proteacidites retusus* Anderson from samples D3738-C, D4017-A, D4017-B, and D4017-C (Figures 22, 23). *Tschudyipollis* spp. has come to be universally accepted as one of the premier index palynomorphs for uppermost Upper Cretaceous rocks throughout much of the Western Interior of North America. For example, Tschudy (1973, p. 133) wrote:

The genus Proteacidites throughout the Rocky Mountain region is limited to the

Late Cretaceous. In no place, except as isolated redeposited specimens, has it been found in the Paleocene.

Samples D3738-A and D3738-B from the Ojo Alamo Sandstone (Figures 22, 23) contained no *Proteacidites* specimens. In his discussion of these samples in Fassett and Hinds (1971, p. 33) Tschudy wrote of sample D3738-A: "This assemblage is clearly of Paleocene age and is equivalent to the assemblages found by Anderson [1960] in the Ojo Alamo Sandstone." And for sample D3738-B he wrote that it was "from the Tertiary." Tschudy further wrote in Fassett and Hinds (1971, p. 33):

It is possible to postulate a hiatus between the Cretaceous and Paleocene at this locality. The genus Araucariacites (table 1) has not been found in rocks younger than Campanian in the Rocky Mountain Region. Moreover, the Cretaceous assemblages found in your samples are different from those found in the latest Cretaceous of the Raton Formation. However, it must be emphasized that we do not have enough control data from your area to do more than guess at a possible hiatus. For example, the closest area from which we have control on the occurrence of Araucariacites in the Upper Cretaceous is northern Colorado. Furthermore, we know that several floral provinces existed during Late Cretaceous time.

Thus, the palynological data of Fassett and Hinds (1971) from the Mesa Portales study area established the presence of the Cretaceous-Tertiary interface below the base of the Ojo Alamo Sandstone (Figures 22, 23), confirmed the age of the Ojo Alamo in its entirety as Paleocene, and suggested the presence of a hiatus at the K-T interface representing all of post-Campanian (Maastrichtian) time.

Tschudy (1973), the Gasbuggy Core

The Gasbuggy project was initiated in February 1967 with the drilling of the Gasbuggy 1 (GB-1) core hole in the east-central part of the San Juan Basin (Figure 1.1). The objective of the project was to explode a nuclear device in the Pictured Cliffs Sandstone about 1,200 m (4,000 ft) deep as an experiment to determine whether or not natural gas production from the Pictured Cliffs, a relatively impermeable rock unit in that part of the basin, could thereby be significantly increased. A continuous core was cut starting in the lower part of the

Nacimiento Formation, through 60 m of massive Ojo Alamo Sandstone, 73 m of the Fruitland Formation, and 192 m of Pictured Cliffs Sandstone and underlying Lewis Shale (Fassett 1968a, b). This continuous core offered an unprecedented opportunity to obtain a large number of closely spaced rock samples across the Cretaceous-Tertiary interface from unweathered core material.

Samples from core hole GB-1 were collected at about 6m intervals by the author in 1968, from the Nacimiento Formation down through the upper part of the Lewis Shale. Core chips from 52 levels were collected and submitted to R.H. Tschudy for analysis. Tschudy reported that: "Thirty-nine samples yielded some palynomorphs and thirty of these yielded sufficient specimens for a percentage count." Figure 53 is a copy of figure 1 from Tschudy (1973) showing the distribution of the GB-1 core samples. Tschudy (1973, p. 142) also included a table listing all of the palynomorphs identified from the GB-1 core samples; Table 8 (see Table Appendix, page 121) is a modified version of Tschudy's table showing palynomorphs identified from the Fruitland, Ojo Alamo, and Nacimiento Formations. It is interesting to note, that even in the unweathered core material, only slightly more than half of the samples yielded meaningful numbers of palynomorphs, and 12 samples were barren of palynomorphs.

Tschudy's GB-1 palynomorph list (Table 8) shows that the Cretaceous index fossil *Tschudy-pollis* spp. (*Proteacidites* spp. on Tschudy's list) averages nearly fourteen specimens per Fruitland Formation slide. The two lowermost samples from the Ojo Alamo Sandstone; D4665-A and D4666-K (Figure 53, Table 8) yielded (Tschudy 1973, p. 133) ". . . very sparse specimens of *Proteacidites* . . . possibly . . . due to redeposition of Cretaceous pollen in Tertiary rocks near the Cretaceous-Tertiary unconformity." Tschudy further stated that the sample at 3515.6 feet [D4665-D, Figure 53] "contained *Maceopolipollenites tenuipolus* [now, *Momipites tenuipolus*], a fossil that elsewhere in the Rocky Mountain region is limited to the Paleocene but is not present in the lowermost Paleocene."

On the basis of palynologic data, Tschudy placed the Cretaceous-Tertiary boundary in the GB-1 core between samples D4778-D and D4666-K (Figure 53, Table 8); essentially, at the base of the Ojo Alamo Sandstone.

Figure 54 (after Tschudy 1973, figure 3) shows the stratigraphic distribution of selected palynomorphs identified from samples of the Gasbuggy core. The hiatus at the Cretaceous-Tertiary

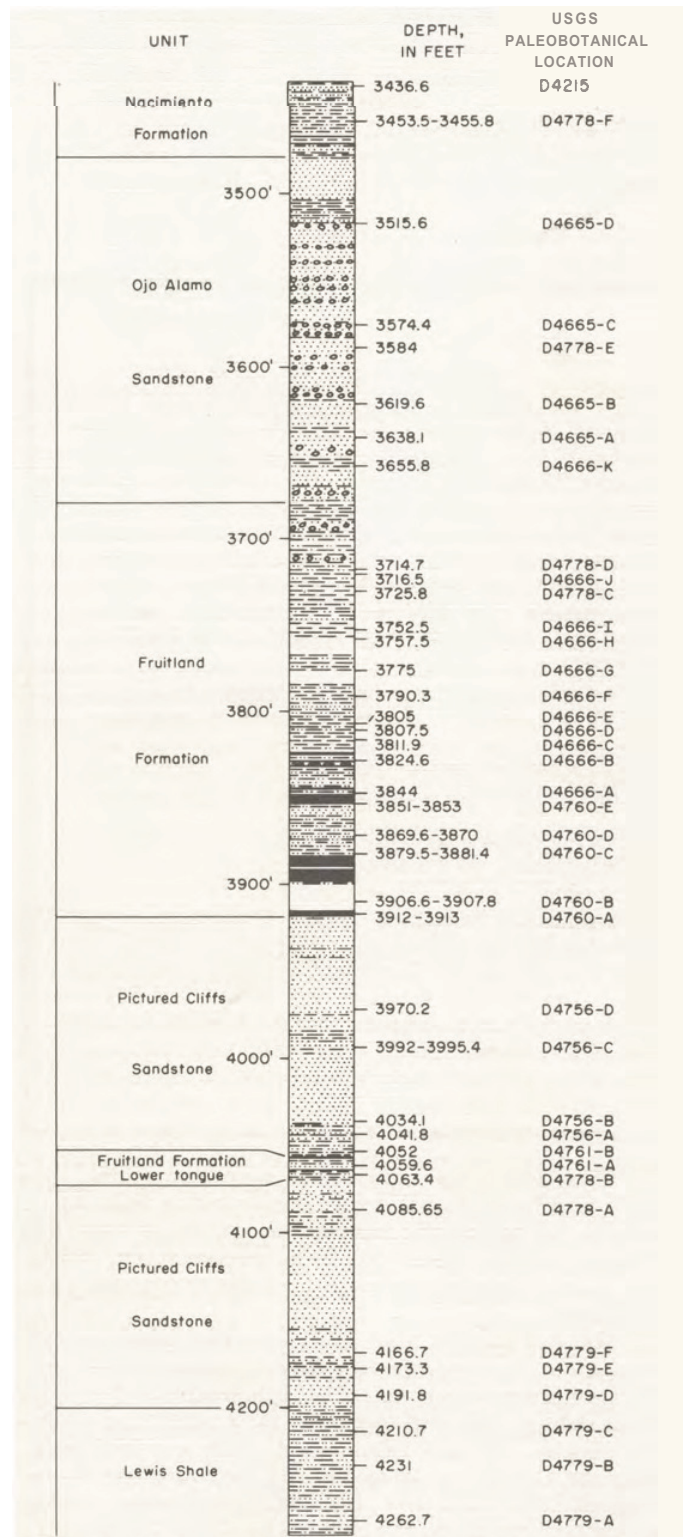


Figure 53. Stratigraphic column of Gasbuggy 1 drill core (from Tschudy 1973, figure 1). Depths on left side of column in feet below Kelly Bushing of drill rig (10 ft above ground level). Depths in feet on right side of column are levels of samples collected for palynologic analysis; USGS paleobotanic sample numbers for samples also shown.

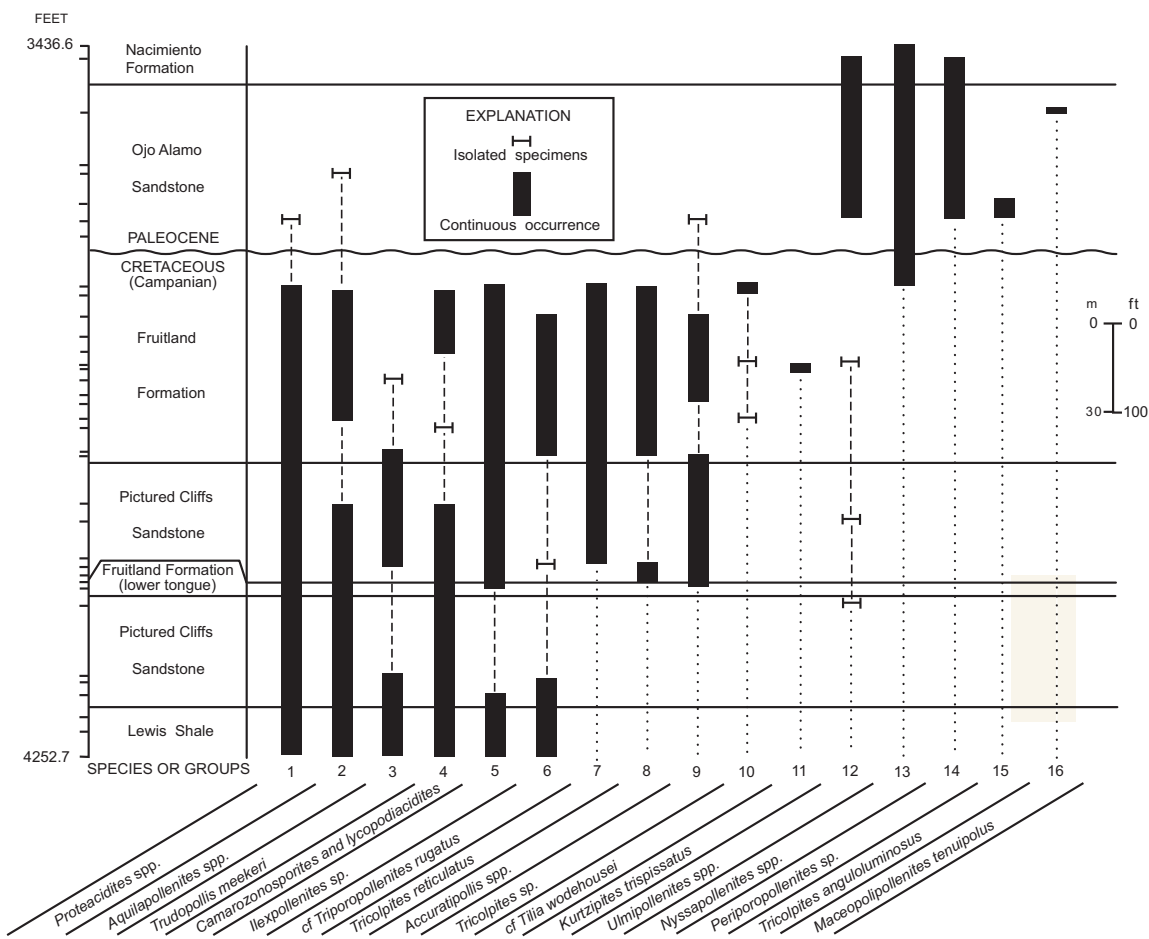


Figure 54. Stratigraphic distribution of selected palynomorphs identified in samples from the Gasbuggy core (Figure 1); modified from Tschudy (1973, figure 3). Hiatus at the Fruitland Formation-Ojo Alamo Sandstone (Cretaceous-Tertiary) contact is clearly indicated by the termination of the first 11 palynomorphs (except for probably reworked specimens) at the contact and the emergence of five new species just below or above the contact. Tick marks along left side of diagram show levels of sample collections.

(Campanian-Paleocene) boundary is marked by the termination of the first 11 palynomorphs (or groups) at the contact between the Fruitland Formation and overlying Ojo Alamo Sandstone. Isolated specimens of *Proteacidites* spp., *Aquilapollenites* spp., and *Tricolpites* sp. are present above this contact, but as articulated by Tschudy, above, the presence of these isolated specimens is probably due to “redeposition of Cretaceous pollen in Tertiary rocks.” The Ojo Alamo was deposited on a vast erosion surface that beveled Upper Cretaceous rocks across the entire San Juan Basin (Figure 1). It is thus not surprising that a few, random, Cretaceous palynomorphs redeposited from underlying Cretaceous strata are present in the lowermost part of the Ojo Alamo.

Lowermost Ojo Alamo sediments were deposited by high-energy streams flowing from the north or northwest across this widespread erosion surface, and it would indeed be more remarkable if a few, random, Cretaceous palynomorphs had not been transported by wind or water into the lowermost Ojo Alamo Sandstone’s channel-sandstone and over-bank deposits.

Figure 54 also shows the emergence of three new species in the Paleocene Ojo Alamo: *Periporopollenites* sp., *Tricolpites anguloluminosus*, and *Maceopolipollenites tenuipolus* (now *Momipites tenuipolus*). In addition, *Ulmipollenites* sp., identified in only three isolated samples in Cretaceous strata, is found to be continuously present

EAST

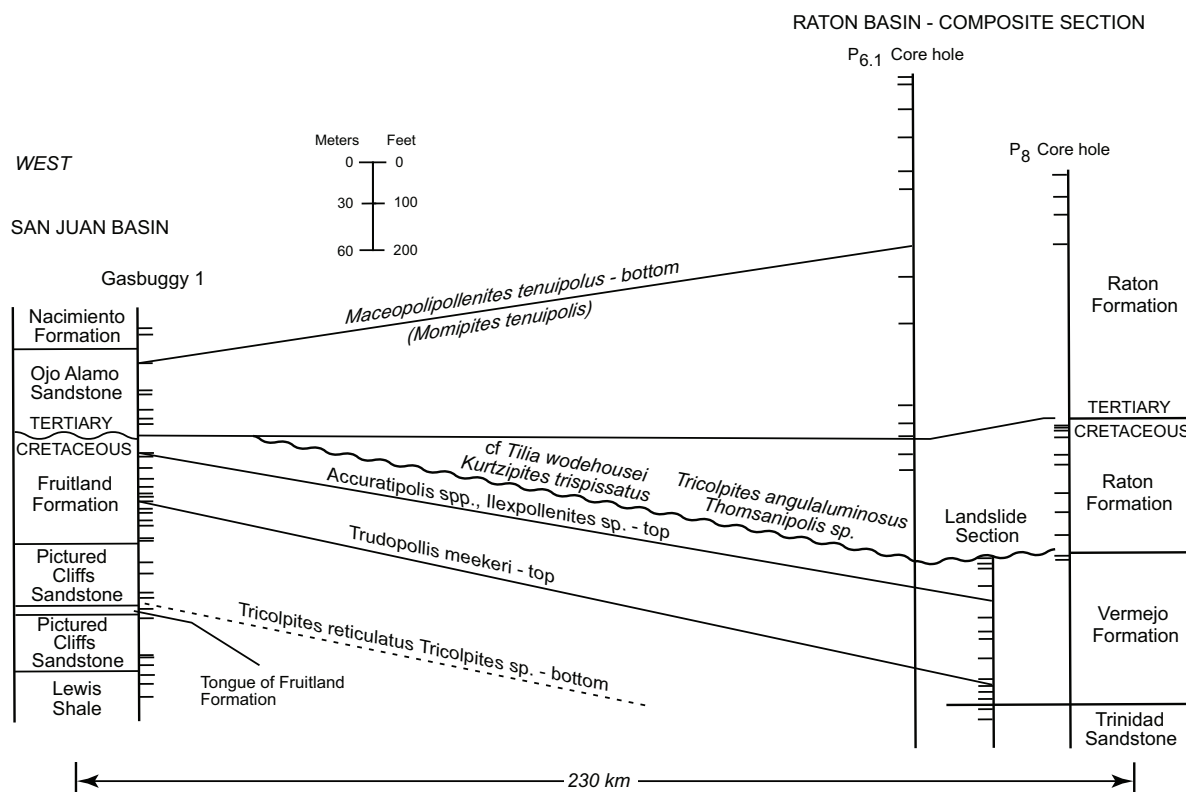


Figure 55. Palynologic correlation diagram based on core-hole data in the San Juan and Raton Basins; modified from Tschudy (1973, figure 5). Tick marks on drill-hole lines represent levels where core samples yielded identifiable palynomorphs. All of Maastrichtian stage appears to be missing in Gasbuggy 1 core. Hiatus at Cretaceous-Tertiary (K-T) interface is nearly 8 m.y. in the southern San Juan Basin; no hiatus in Raton Basin at the K-T boundary.

through most of the Ojo Alamo and into the Nacimiento Formation.

Tschudy compared the Cretaceous palynomorph assemblages in the GB-1 core with palynomorph assemblages from uppermost Cretaceous rocks in northern Montana and Wyoming. On the basis of those comparisons he concluded that uppermost Upper Cretaceous palynomorph assemblages present in that region were missing from the GB-1 core. In addition, Tschudy compared the GB-1 palynomorph assemblages with those he had identified from drill-core samples in the Raton Basin, only 230 km east of the San Juan Basin and concluded that the uppermost-Cretaceous pollen assemblages in the Raton Basin were not present in the GB-1 core hole. Tschudy (1973, p. 131) summed up this situation by stating:

A section of the Upper Cretaceous, present in the upper part of the

Cretaceous in the Raton Basin, is absent from the Upper Cretaceous of the Gasbuggy core. This confirms the presence of a marked hiatus at the top of the Cretaceous, as previously postulated in the San Juan Basin [in Fassett and Hinds 1971, p. 33].

Figure 55, modified from Tschudy (1973, figure 5), is a cross section showing the correlation of palynomorph assemblages from the Raton Basin to the San Juan Basin. This diagram shows that several palynomorph zones present in the uppermost Cretaceous strata of the Raton Basin are missing in the San Juan Basin.

Fassett et al. (1987)

Fassett et al. (1987) surveyed all of the known localities in the Ojo Alamo Sandstone where either dinosaur bone or palynomorphs had been docu-

mented. They discussed the palynomorphs that had been identified from the Ojo Alamo Sandstone by R.H. Tschudy at three places in the basin: 1) Near Barrel Spring, 2) At Mesa Portales, and 3) In the Gasbuggy 1 core.

Barrel Spring Locality. The Barrel Spring locality was sampled by C.J. Orth, Los Alamos National Laboratory, in 1982; Orth's samples were submitted to R.H. Tschudy for analysis. According to Orth et al. (1982, p. 427), this locality is 2 km east of Barrel Spring on De-na-zin Arroyo (probably in the SE1/4 SE1/4 Sec. 9, T. 24 N., R. 11 W., Figures 4, 51). The sample, labeled USGS paleobotany locality number D6391 (Tschudy, personal commun., 1982) was collected from a claystone layer about 3 m below the top of the Ojo Alamo Sandstone. Tschudy reported that:

This assemblage is clearly of Paleocene age. Several taxa including Momipites tenuipolus were not recorded by Anderson from the Ojo Alamo, but were recorded from the overlying Nacimiento. I have not seen M. tenuipolus in any basal Paleocene samples from the Western Interior. This occurrence suggests that the sample is not from the basal Paleocene but rather from the upper Lower or Lower middle Paleocene.

Mesa Portales locality. Fassett et al. (1987, p. 30, 31) referred to a new Ojo Alamo Sandstone palynologic sample locality on Mesa Portales (D6583-B, Figures 22, 23) but did not list all of the palynomorphs identified from that locality. They did state, however, that R.H. Tschudy had reported the presence of the Paleocene index palynomorph *Momipites tenuipolus* in that assemblage. (The complete list of palynomorphs from this locality is in Table 9 (see Table Appendix, page 122), and Tschudy's comments about this assemblage are given in full in the "This Paper" part of the "Palynology" section of this report.)

Gasbuggy Core. The results of Tschudy's (1973) study of the palynomorphs identified from the Gasbuggy-core samples were summarized in Fassett et al. (1987), and the Ojo Alamo Sandstone part of the core was illustrated in a stratigraphic column. Tschudy's comments to the effect that the palynomorphs from the Ojo Alamo Sandstone in the Gasbuggy core indicated that it was Paleocene in its entirety were cited. The complete list of palynomorphs identified from the Gasbuggy core samples is in Table 8.

Newman (1987)

K.R. Newman (1987) published a comparison of the palynology of several Western Interior basins with that of the San Juan Basin. Newman and C. Manfrino (1984) had conducted extensive palynological studies of uppermost Cretaceous and lowermost Tertiary strata in the northern San Juan Basin in the Animas River valley south of Durango, Colorado, and compiled a robust palynologic data set there. The Ojo Alamo Sandstone is absent in the northern part of the San Juan Basin and the lowermost Paleocene formation there is the Animas Formation, thought by Reeside (1924), and most subsequent workers, to be the same age as the Ojo Alamo Sandstone in the New Mexico part of the basin. (The Animas Formation is discussed in separate sections of this paper.) Figure 56 shows Newman's interpretation of the strata adjacent to the Cretaceous-Tertiary interface in the northern San Juan Basin based on palynology.

Newman also carried out detailed studies of the palynology of the Fruitland Formation in the southern part of the San Juan Basin. These studies were based on core samples from the Fossil Forest area (Figure 3); Newman (1987, p. 159) wrote:

*Ten samples from 51 m of cored Fruitland Formation have yielded an excellent assemblage of palynomorphs including the guide fossils *Trudopollis meekeri*, *Myrtaceipollenitius peritus*, and *Pseudoplicapollis* sp. . . . Therefore, the combination of the ammonite and palynomorph zones indicates late Campanian age for the upper Lewis, Pictured Cliffs, and Fruitland Formations in this area, just as at Durango.*

Newman did not publish a complete list of identified palynomorphs from this core.

Newman (1987, p. 159) discussed a rock sample from the upper Kirtland Formation at Pot Mesa (Figure 1) and stated that it contained the Maastrichtian palynomorphs *Proteacidites* (*Tschudypollis*), *Balmeisporites*, *Interpollis*, *Gunnera*, *Kurtizipites*, and *Ulmoideipites* spp. (Newman stated that this sample was from the Ojo Alamo Sandstone, but subsequent studies (Fassett et al. 2002) now place this sample in the uppermost Kirtland Formation.) Fassett et al. (2002) published a list of palynomorphs identified by D.J. Nichols from a separate sample from this same interval; a comparison of that palynomorph assemblage with Newman's is discussed in the "Fassett et al. (2002)" section of this appendix.

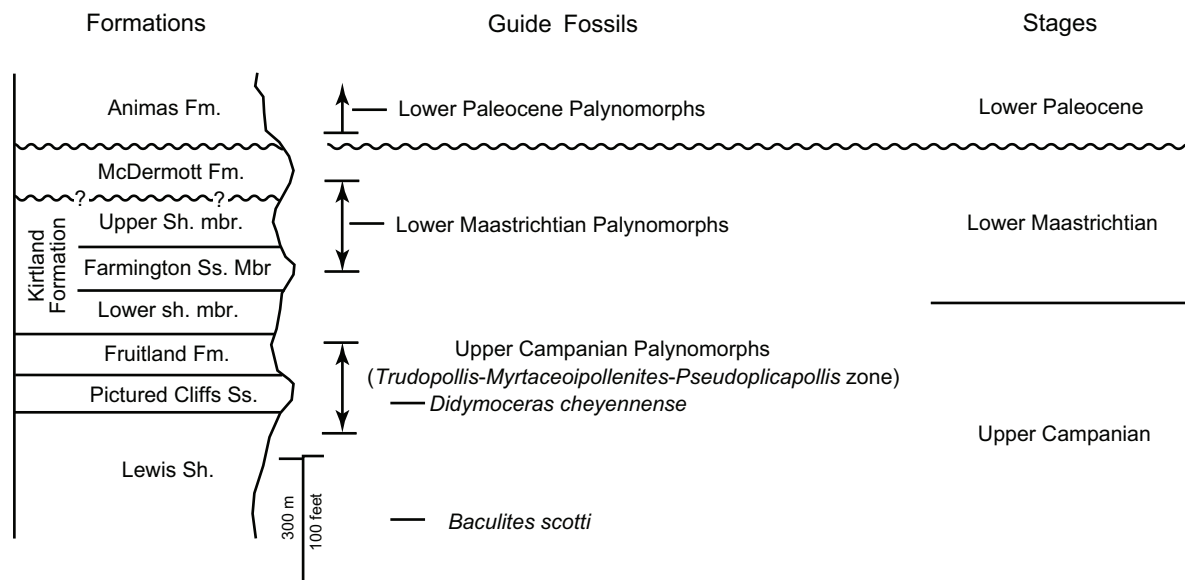


Figure 56. Biostratigraphic diagram of uppermost Cretaceous-lowermost Tertiary strata in northern San Juan Basin (south of Durango, Colorado, Figure 1); modified from Newman (1987, figure 7). Ojo Alamo Sandstone not present in northern San Juan Basin; lower part of Paleocene Animas Formation is time-equivalent of Ojo Alamo there.

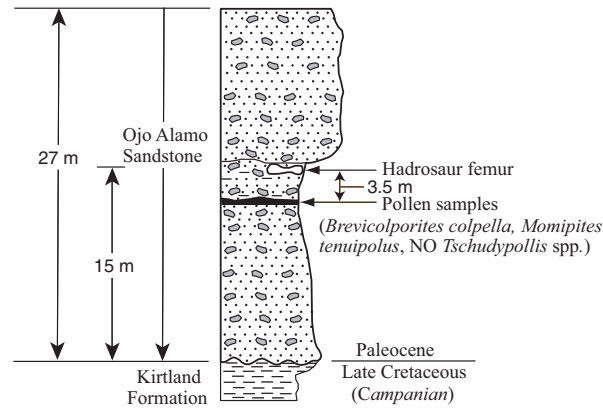
Newman also reported on a sample he claimed was from the Ojo Alamo Sandstone from a locality “near Farmington” (no more specific location was provided). The author had escorted Newman to the San Juan River Hadrosaur-bone site in 1984 and was informed by Newman at that time that he (Newman) had collected a rock sample “from a lower stratigraphic level” (well below the level of the Hadrosaur bone), but Newman was not specific as to the exact stratigraphic level of that sample. (It is assumed that Newman’s “near Farmington” locality is the San Juan River site of this report.) Newman (1987, p. 159) stated that his sample collected “near Farmington” yielded the same Maastrichtian palynomorphs that he found at Pot Mesa in the uppermost Kirtland Formation. Newman’s determination that the “Ojo Alamo” palynomorph assemblage “near Farmington” is Maastrichtian is not in agreement with the three other palynomorph lists from the Ojo Alamo at the San Juan River site (Table 10 (see Table Appendix, page 123)). Those palynomorph lists all contained the Paleocene index palynomorph *Momipites tenuipolus*, and one of them also contained the Paleocene index palynomorph *Brevicolporites colpella* (Table 10). Three of the palynologists found the Cretaceous index fossil *Proteacidites* (*Tschudypollis*) in their samples from the San Juan River site, however, D.J. Nichols did not find this index fossil in any of his three samples from that locality. The

presence of two Paleocene index palynomorphs in samples from this locality suggests that the *Proteacidites* specimens found in some of them were reworked. Fassett and Lucas (2000) and Fassett et al. (2002) concluded that the Ojo Alamo Sandstone was Paleocene in age at the San Juan River site on the basis of palynologic data.

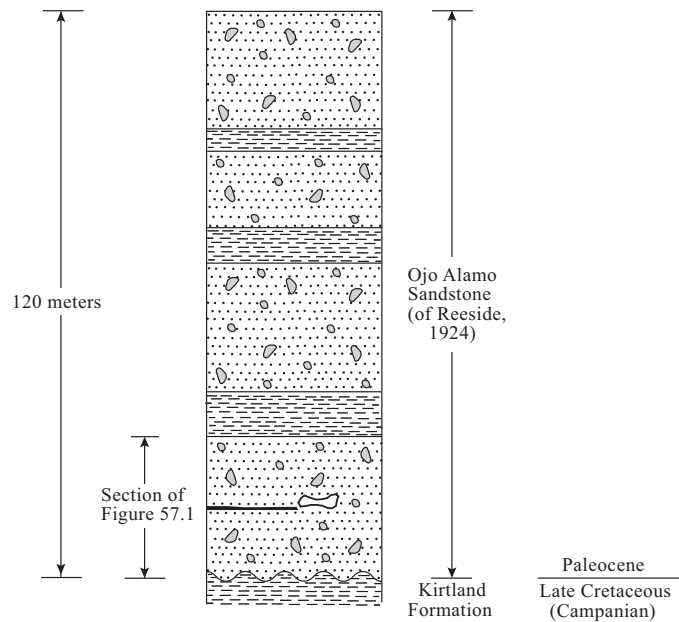
Newman (1987) concluded, (as did Tschudy 1973), that the Ojo Alamo Sandstone rests on a significant unconformity in the San Juan Basin and that a hiatus representing most, if not all, of the Maastrichtian and possibly the lowermost part of the Paleocene separated Cretaceous from Tertiary rocks throughout the San Juan Basin. Newman (1987, figure 10) also showed that more uppermost Cretaceous strata were missing in the southern part of the basin than in the northwestern part.

Fassett and Lucas (2000)

Fassett and Lucas (2000) published a paper focused on the large hadrosaur femur that had been discovered in the Ojo Alamo Sandstone at the San Juan River site (Figure 1). They reported the results of palynologic studies of three samples collected from a carbonaceous to coaly shale bed located 3.5 m stratigraphically below the level of the hadrosaur femur (Figure 57). (Those three samples are shown as a composite list of samples 6877-A, -B, and -C on Table 10.) These samples were processed and analyzed by D.J. Nichols who



57.1



57.2

LEGEND


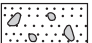


-  Hadrosaur femur
-  Conglomeratic sandstone
-  Mudstone
-  Coaly carbonaceous shale containing Paleocene pollen

Figure 57. Stratigraphic columns of Ojo Alamo Sandstone at San Juan River site (Figure 1). **57.1** is expanded-scale view of lower part of Ojo Alamo column of **57.2**. Figures show relative positions of large (1.3m long) hadrosaur femur (Figure 37.1) collected from Ojo Alamo Sandstone at San Juan River locality and rock samples collected for palynologic analyses. Paleocene index palynomorphs identified by D.J. Nichols, (USGS) are shown. Modified from Fassett and Lucas (2000, figure 8).

found that the samples contained the Paleocene index fossils *Momipites tenuipolus* and *Brevicolporites colpella* and no specimens of the Cretaceous index fossil, *Tschudypollis* spp. (Nichols, personal commun., 1994). Thus, the palynologic evidence for the age of the Ojo Alamo Sandstone at the San Juan River site showed it to be unequivocally Paleocene. On the basis of this evidence, Fassett and Lucas (2000, p. 229) stated that the hadrosaur femur found above this palynomorph assemblage must have come from a dinosaur that lived during earliest Paleocene time, and they concluded that: "some dinosaurs in the San Juan Basin survived the 'terminal' end-Cretaceous asteroid impact event only to become extinct a few hundred thousand years (at most) later, in earliest Paleocene time."

As discussed above, Newman (1987) had reported a palynomorph assemblage at his "near Farmington" locality totally different from the assemblages identified by D.J. Nichols at the San Juan River site. Table 10 shows that there are no palynomorphs in common between the Nichols list and the Newman list. Because the palynomorph assemblages of Fassett and Lucas (2000, table 1) came from three separate samples and because those results have been independently replicated two other times (Frederiksen personal commun., 1986, and Braman, personal commun., 2000 as discussed below in the "This Paper" section of this report) it seems evident that Newman's (1987) palynomorph assemblage could not have come from the Ojo Alamo Sandstone at the San Juan River site. The base of the Ojo Alamo Sandstone is covered by slope wash immediately below the hadrosaur-bone site, and thus its contact with the underlying Kirtland Formation is masked, it may be that Newman's sample containing Cretaceous palynomorphs "near Farmington" may actually have been collected from the uppermost Kirtland Shale and not from the Ojo Alamo Sandstone. Another possibility is that Newman's sample came from a rip-up clast of Kirtland mudstone imbedded in the lowermost part of the Ojo Alamo Sandstone. Such rip-up clasts are not uncommon in the lower meter or two of the Ojo Alamo Sandstone in this area. A third possibility is that if Newman's sample did indeed come from the Ojo Alamo, the Maastriichtian palynomorphs found therein were reworked from underlying Cretaceous strata. And finally, Newman's sample may have come from the Kirtland Formation at an entirely different site from the San Juan River site.

Fassett et al. (2002)

Ojo Alamo Type Area. Fassett et al. (2002) summarized the study of Fassett and Lucas (2000) and in addition discussed the palynology of Cretaceous and Tertiary strata in the Ojo Alamo type area (Figures 3, 4). These authors listed palynomorphs identified by D.J. Nichols (personal commun., 1994) from rock samples in the Ojo Alamo type area. (Figures 4 and 51 show the locations of the palynologic collection sites in the Ojo Alamo type area; Figure 51 is a larger-scale map of the Barrel Spring area showing palynologic sample localities in more detail.) One sample (no. 24-5, D6901 of Figure 51) from a carbonaceous shale bed less than 1 m below the base of the Ojo Alamo Sandstone yielded "a well-preserved assemblage of palynomorphs" including the Paleocene index fossil *Momipites tenuipolus* (Nichols, personal commun., 1994). (Table 6 contains the published palynomorph lists from the Ojo Alamo type area.) Nichols reported that the palynomorph assemblage from this sample closely resembled the Paleocene assemblage found in the Ojo Alamo at the San Juan River site (Table 10). Sample D6901 also contained the Cretaceous index fossil *Tschudypollis*, however, Fassett et al. (2002, p. 318, 319) stated that:

The Proteacidites specimens in this assemblage must be reworked from underlying Cretaceous strata: the reworking of some Cretaceous palynomorphs into this Paleocene assemblage is not unexpected because the early Paleocene swamp in which indigenous Paleocene pollen was accumulating was located on an erosion surface (peneplain) on Kirtland Formation strata of Campanian age and Cretaceous pollen could easily have been transported laterally a few, to a few tens of meters across this surface in wind-blown dust and deposited in the Paleocene swamp.

On the basis of the presence of the Paleocene index fossil *M. tenuipolus* in this palynomorph assemblage and its similarity to the palynomorph assemblage from the Ojo Alamo Sandstone at the San Juan River locality, Fassett et al. (2002) concluded that the Ojo Alamo Sandstone, including its contained dinosaur fauna in the Ojo Alamo type area, is Paleocene in age. Figure 58 is a composite stratigraphic column for the Ojo Alamo type area

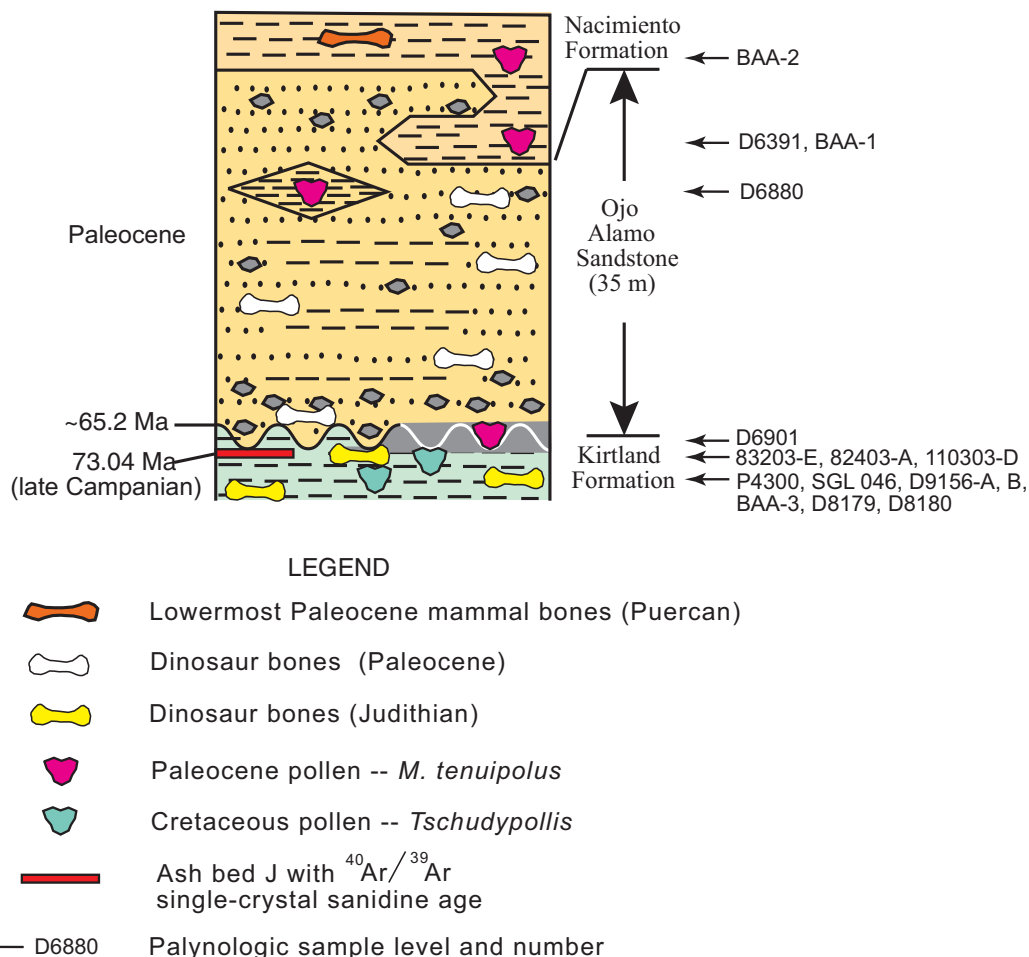


Figure 58. Composite stratigraphic column for Ojo Alamo type area showing relative stratigraphic levels of samples collected for biochronologic and $^{40}\text{Ar}/^{39}\text{Ar}$ sanidine-crystal dating from Ojo Alamo Sandstone and uppermost Kirtland Formation. Samples from different localities are projected into one column for ease of portrayal, however, localities are dispersed throughout Ojo Alamo type area as shown on Figures 4 and 51.

showing the positions of palynologic samples collected there.

Nichols (1994, written commun.) identified and discussed palynomorphs from the upper Ojo Alamo Sandstone at USGS locality D6880 (labeled sample 24-3C on table 2 of Fassett et al., 2002). This locality is about 0.6 km east of Barrel Spring (Figure 51) and about 30 m above the base and about 5 m below the top of the Ojo Alamo Sandstone. (Fassett et al. 2002, incorrectly stated that this sample was 15 m above the base of the Ojo Alamo Sandstone.) This sample was from a dark gray mudstone pod completely enclosed within the upper conglomeratic sandstone bench of the Ojo Alamo. Nichols listed the palynomorphs from this sample (Table 6) and stated that it “yielded abun-

dant cutinite as well as palynomorphs” and concluded that “Based on this assemblage, the sample is Paleocene in age.”

Fassett et al. (2002) also reported palynomorph identifications from samples collected from the uppermost Kirtland Formation in the vicinity of Barrel Spring from a coaly, carbonaceous shale bed. This sample, numbered 043002 in Fassett et al., came from 3 m below the base of the Ojo Alamo Sandstone less than 100 m west of Barrel Spring (Figure 51). D.J. Nichols (personal commun., 2000) reported that this sample (USGS number P4300, Figure 51) contained a “well-preserved assemblage of palynomorphs indicating Late Cretaceous age.” Nichols stated that:

The assemblage identified consists of 12

T. 20 N., R. 6 W.

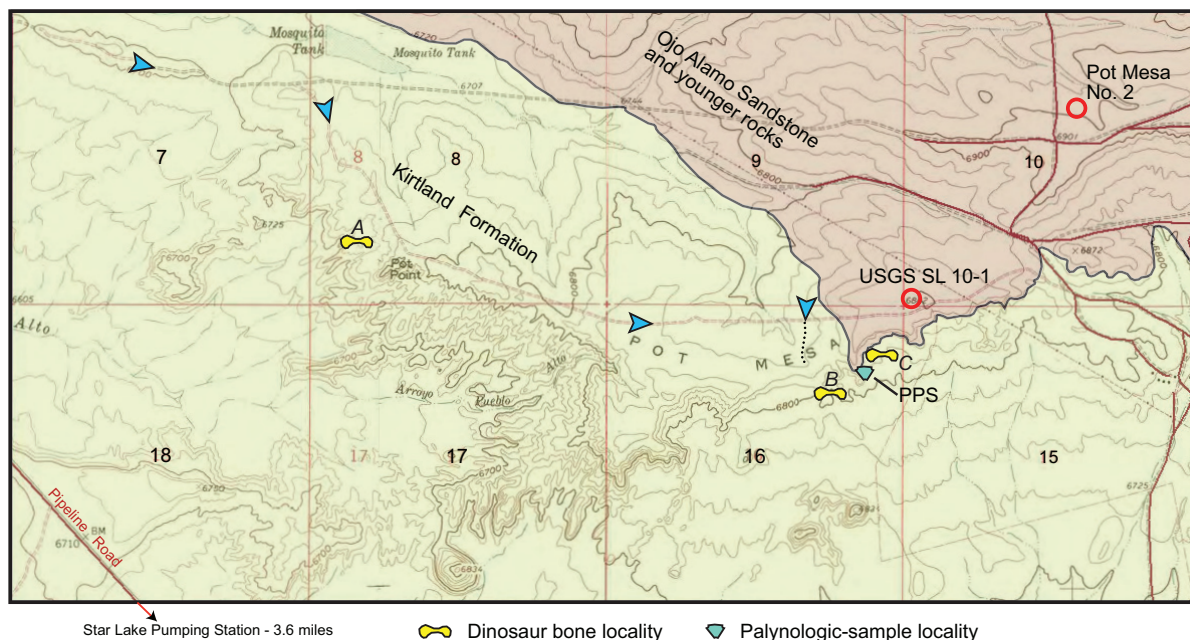


Figure 59. Geologic map of Pot Mesa area; outcrop of Ojo Alamo Sandstone modified from Scott et al. (1980). Dinosaur bone sample-site letters keyed to Tables 2 and 3 that show abundances of selected elements from samples. Dotted line near bone-sample locality B is primitive road to edge of Pot Mesa. Blue arrowheads mark access route to top of Pot Mesa. Samples from drill hole USGS SL 10-1 analyzed by USGS palynologist R.H. Tschudy; PPS is location of outcrop palynologic sample site of Fassett et al. (2002) and Newman (1987). Topographic map from USGS 1:24,000-scale Star Lake and Pueblo Alto Trading Post Topographic Quadrangle maps.

species, mostly fossil pollen, including three that are restricted to the Upper Cretaceous and none that are known to occur only in the lower Tertiary. The Cretaceous species are Tricolpites interangulus, Proteacidites retusus, and P. thalmannii. Tricolpites interangulus is the most common single species in the assemblage, and an estimated 300 specimens are present on the slide examined. This species is known from the upper Campanian-lower Maastrichtian interval in Colorado and New Mexico. The species of Proteacidites are well known Upper Cretaceous guide fossils throughout the Western Interior region.

The complete list of palynomorphs from this sample is in Fassett et al. (2002, table 2) and is shown on Table 6 of this report.

Fassett et al. (2002, p. 319) also stated that:

Additional samples from the same level in this bed (a few meters below the base

of the Ojo Alamo) a few hundred meters northwest of the 043002 sample site also yielded Campanian to lower Maastrichtian palynomorphs (Nichols, personal commun., 2000).

The locations and palynomorph lists obtained from those samples are provided in the "This Paper" section of this report.

Pot Mesa. At Pot Mesa (Figures 3, 59) the Ojo Alamo Sandstone has been considered by some investigators to consist of just one sandstone bench and by others to contain two sandstone benches, as discussed in Fassett et al. (2002, p. 324). In that report, Fassett et al. concluded that the Ojo Alamo consisted only of the uppermost of the two benches in question at Pot Mesa. A rock sample collected for palynologic analysis from about 9 m below the base of the upper bench was found to be unquestionably Cretaceous in age (Nichols personal commun., 1994). Fassett et al. (2002) did not list the palynomorphs identified at this site, but that listing is provided in the "This Paper" section of this report.

Sullivan et al. (2005)

Sullivan et al. (2005) reviewed “the stratigraphic position of the Cretaceous-Tertiary (K/T) boundary in the San Juan Basin” and included a palynomorph list from the uppermost Kirtland Formation in the vicinity of Barrel Spring from the same coaly carbonaceous shale bed as the P4300 sample of Figure 51. Their sample was given locality number SGL 00-046 (SGL 046 on Figure 51) and contained a list of palynomorphs identified by D.R. Braman (personal commun., 2006) as shown on Table 6. Braman commented as follows regarding these palynomorphs:

The above assemblage is made up of mostly species that span the Cretaceous-Tertiary boundary. The exception is Proteacidites retusus and Proteacidites thalmani which are thought to have been two species that went extinct at the boundary (Nichols 1994; Nichols et al. 1992; Nichols et al. 1990). Using this observation then would indicate that the sample is Cretaceous in age. The species occurs in Campanian and Maastrichtian deposits, but the presence of Pandaniidites typicus and Ulmoideipites krempii suggests a Maastrichtian age for the sample. The sample is dominated by bisaccate conifer pollen and the species Tricolpites reticulatus.

This Paper

This paper presents unpublished palynologic data from Mesa Portales, Pot Mesa, the Ojo Alamo type area, the San Juan River site, and other localities.

Mesa Portales. Rock samples were collected for palynologic analyses from within and below the Ojo Alamo Sandstone at Mesa Portales (Figure 21) by C.L. Pillmore (USGS) in 1983. These samples were submitted to R.H. Tschudy, and the productive samples were given USGS paleobotany locality numbers D6582, D6583-A, and D6583-B. Localities 6583-A and B, from the Ojo Alamo Sandstone are shown on Figures 22 and 23; locality D6582, from the uppermost Fruitland-Kirtland Formation, is shown on Figure 21. The stratigraphically lowest of the Ojo Alamo samples; D6583-A, was collected to try and narrow the gap in which the Cretaceous-Tertiary interface was located on Mesa Portales. Tschudy (personal commun., 1983) reported that this sample:

. . . yielded abundant finely divided organic fragments plus fusinite. The sample appears to have been oxidized. Few palynomorphs, difficult to identify, were present. The following were tentatively identified: Tricolpites, Podocarpidites cf. P. sellowiformis, Arecipites, Periporopollenites, Ulmipollenites, Alnipollenites, Lycopodiacidites, Trilete fern spores. This sample did not yield any characteristic Late Cretaceous taxa.

Sample D6583-B was collected from the same bed as sample D3738-B (Figures 22, 23) of Fassett and Hinds (1971). Tschudy reported that this sample:

. . . was very poor. Very few palynomorphs were present. . . The presence of Momipites tenuipolus strongly suggests a Paleocene age. We have not observed this taxon in other than Paleocene rocks. Sample D3738-B (Fassett and Hinds [1971] P.P. 676, p. 22) was rechecked and bore some resemblance to this sample but D3738-B although also poor, did not exhibit as much evidence of oxidation.

Sample D6582 was collected from a light-gray claystone about 100 mm below the base of the Ojo Alamo Sandstone on the east side of Mesa Portales (Figure 21). Tschudy stated that:

This sample was oxidized and very poor. Fusinite and oxidized organic material were present, but very few palynomorphs. . . The assemblage, though poor, indicates a Late Cretaceous age. Owing to the poor recovery and the condition of the sample, even though no evidence of Paleocene fossils was evident, one should consider the possibility that the Cretaceous fossils might have been redeposited in Paleocene rocks.

The palynomorphs identified from localities D6582, D6583-A, and D6583-B are listed on Table 9 for easier comparison with palynomorph lists from other localities on Mesa Portales.

E. M. Shoemaker collected additional rock samples from the lower part of the Kirtland and Fruitland Formations, undivided, for palynologic evaluation in 1983. The samples were processed by R.H. Tschudy in 1984, and the three productive samples were given USGS paleobotany locality

numbers D6626-A, -B, and -C (Figures 22, 23). Table 9 lists the palynomorphs identified at each of these localities. In his commentary regarding the significance of these palynomorph assemblages, Tschudy (personal commun., 1984) stated:

*The palynomorph assemblages from the above three samples were virtually identical. They indicate a Cretaceous age for the samples but not a latest Cretaceous age. The taxa *Pristinuspollenites*, *Rugubivesiculites*, *Trudopollis*, *Accuratipollis*, and *Pseudoplicapollis* in particular have not been observed in post-Campanian rocks from the Western Interior but are commonly found in rocks of that age. I am confident that these samples are no younger than Late Campanian. This evaluation is supported by the presence of *Aquilapollenites* spp., *Proteacidites* - large, abundant, *Araucariacites*, and *Aequitriradites*, taxa with a greater stratigraphic range, but uncommon in terminal Cretaceous rocks.*

*The presence of *Botryococcus*, *Lecaniella*, *Pediastrum* (algae) and *Balmeisporites* (a water fern) indicates lacustrine deposition. The few dinoflagellate and hystrichosphere cysts probably were redeposited from older marine rocks.*

In 1985, the author collected a sample from USGS paleobotany locality D6878 from a thin coal bed in the lower part of the Nacimiento Formation about 50 m above the top of the Ojo Alamo Sandstone (Figure 21, Table 9). D.J. Nichols (personal commun., 1994) reported that this sample "yielded abundant sapropel and inertinite along with palynomorphs." Nichols concluded that: "Based on this assemblage, the sample is Paleocene in age." Palynomorphs identified from this sample are listed on Table 9.

Pot Mesa. As discussed in a previous section of this report, palynomorphs from the uppermost Kirtland Formation were identified at the Pot Mesa locality (Figures 3, 59). One set of samples was described by Newman (1987), a second set by Nichols (in Fassett et al. 2002); and a third set was analyzed by R.H. Tschudy (personal commun., 1977). Tschudy's 1977 list of palynomorphs is published here for the first time (Table 11 (see Table Appendix, page 124)). Although Newman (1987) did not provide the stratigraphic level or exact loca-

tion of his sample site, he did indicate to the author in the field (Newman, personal commun., 1984) its approximate stratigraphic position and locality which is nearly identical to the sample locality of Fassett et al. (2002), 9 m below the base of the Ojo Alamo, and labeled PPS on Figure 59. (As stated above, Newman thought his Pot Mesa sample was from the Ojo Alamo Sandstone at the time he collected it.)

R.H. Tschudy (personal commun., 1977) provided palynomorph identifications from drill-core and cuttings samples from a drill hole on top of Pot Mesa (Figure 59). The hole USGS SL 10-1 was drilled by the USGS in 1975 to evaluate Fruitland Formation coal resources in this area. (A geophysical log and description of the lithology of the drill hole are in Jentgen and Fassett 1977.) An attempt was made to core this drill hole from the depths of 4.5 m to 30 m (15 to 97 ft), however, swelling shales between the depths of 10 m and 20 m (32 and 65 ft) prevented that part of the hole from being cored. The drill hole started in the Ojo Alamo Sandstone at the surface and ended in the Pictured Cliffs Sandstone (Figure 60). The basal contact of the Ojo Alamo was at a depth of about 10 m (32 ft). Unfortunately, samples from the Ojo Alamo Sandstone part of the core were barren, and all palynomorph-productive samples came from the Kirtland and Fruitland Formations. The author was present at the time this hole was drilled and collected the samples from this drill core, which were analyzed by Tschudy.

Table 11 lists the palynomorphs identified by Tschudy (personal commun., 1977) from samples from drill hole USGS SL 10-1; this table is in the format presented by Tschudy in his report. The five productive samples were given USGS paleobotanical locality numbers; D5783-A, -B, -C, -D, and -E (Table 11, Figure 60); sample depths are provided on table 11. Samples D5783-A, -B, and -C were from drill core; the other two samples were from drill cuttings. The two uppermost samples and the lowermost sample were the most productive of palynomorphs; the two middle samples produced sparse numbers of palynomorphs. All five of the samples were productive of the Cretaceous index fossil *Tschudypollis* (*Proteacidites* on Table 11). In his discussion of these samples, Tschudy stated:

*The genus *Proteacidites* is present in the Cretaceous but has not been found in the Paleocene in any samples from the Rocky Mountain region. On this basis I would place the Cretaceous-Tertiary boundary between 93.8 feet and 94.5*

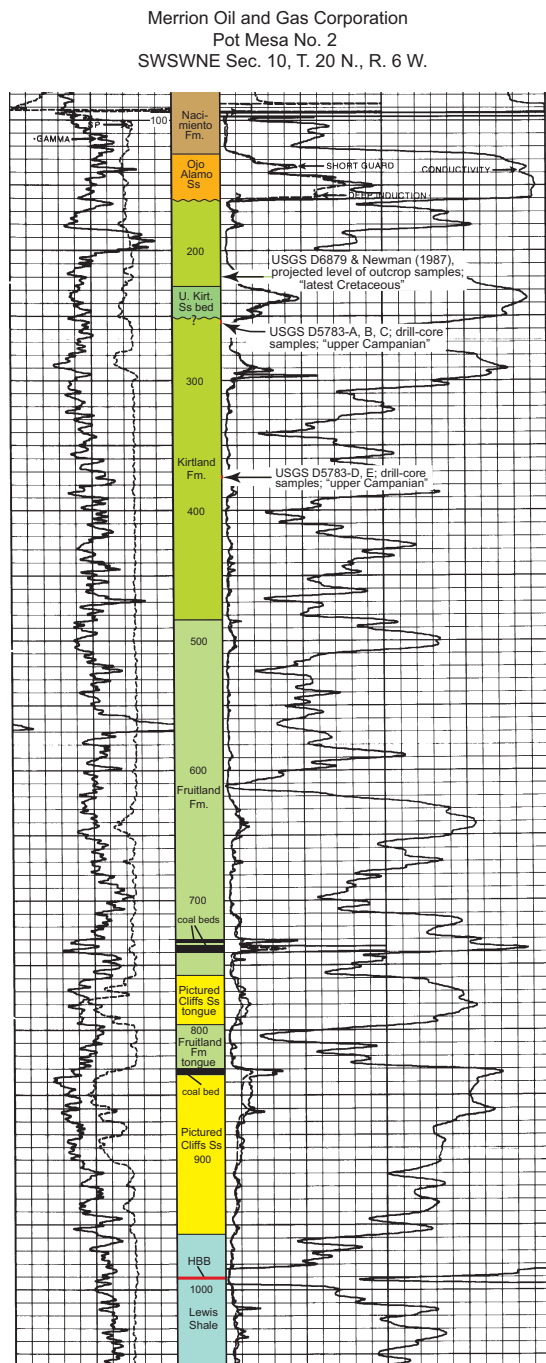


Figure 60. Geophysical log from drill hole Pot Mesa No. 2, top of Pot Mesa (Figure 59), showing formation boundaries and relative levels of samples collected for palynologic analyses; sample levels projected from actual locations. Log depths in feet. HBB = Huerfanito Bentonite Bed.

feet. However, the samples from these two levels are so similar in their palynomorph recovery, that I suspect that the sample from 93.8 feet is also of Cretaceous age. Both of these samples yielded many taxa common to the Cretaceous, but generally foreign to the Paleocene. Furthermore, no clearly Paleocene taxa were found in the sample from 93.8 feet.

At the author's request, Tschudy later re-examined his slides for the samples from the Pot Mesa drill hole and revised his earlier findings for these samples stating the following (Tschudy, personal commun., 1981):

At your request I re-examined the slides reported on in 1977 from Star Lake Drill hole 10-1. I made a serious error. On re-examination I found Proteacidites pollen on the original slides. The grains were few and light colored, but I shouldn't have missed them, however, they are definitely present for all to see. Thus the uppermost sample from 93.8 feet (D5783-A) becomes palynologically Cretaceous.

Furthermore, all but 3 taxa found in the uppermost samples were present in the next lower sample (D5783-B) which I originally designated as Cretaceous. The three taxa are Liliacidites, Azolla and Pterospermopsis, forms that we now know to exist in both the Cretaceous and Tertiary. Pollen grains that are present in the uppermost Cretaceous such as Gunnera and "Tilia wodehouseii" were not found in these samples. On the basis of the current information I believe that these samples are not near the Cretaceous-Tertiary boundary, but from lower in the Cretaceous, possibly as low as the upper Campanian.

Thus, the total palynomorph assemblage from drill-hole samples at Pot Mesa indicates that all of the Maastrichtian stage and possibly the upper part of the Campanian stage are missing from the Kirtland Formation below the upper Kirtland sandstone bed shown on Figure 60.

Table 12 (see Table Appendix, page 125) lists the palynomorphs identified by Tschudy, Nichols, and Newman from the Pot Mesa locality. Newman (1987, p. 159) stated that his Pot Mesa palynomorph assemblage indicated a "... Maastrichtian

age. So far, it has not been possible to determine whether the age is early or late Maastrichtian from these assemblages.” Nichols (personal commun., 1994) concluded that: “Based on this diverse and well-preserved assemblage, the sample is clearly of latest Cretaceous age.” Nichols and Newman identified *Gunnera* in their samples from Pot Mesa and Nichols also reported “*Tilia wodehouseii* in his sample from that locality. According to Tschudy (above) both of these forms are “uppermost Cretaceous” index fossils. In his comparison of Gasbuggy-core palynomorphs with palynomorphs identified below the K-T boundary in the Raton Basin, Tschudy (1973) showed “cf *Tilia woodhousei*” was present in the uppermost Cretaceous of the Raton Basin but absent in the highest Cretaceous strata of the Gasbuggy core (Figure 54). Thus, palynologic data at Pot Mesa indicate the possible presence of an unconformity at the base of the upper Kirtland sandstone bed (Figure 60) separating Campanian strata from Maastrichtian strata. The existence of this unconformity is further evidenced by the fact that even though the stratigraphic levels of palynomorph samples above and below the upper Kirtland sandstone bed are only 12 m apart (Figures 60, 33), only about 9 % of the palynomorph taxa are common to the palynomorph lists for these two samples. These data support the presence of the hiatus shown at the Pot Mesa locality at drill-hole 5 on Figures 34 and 35 at the base of the upper Kirtland sandstone bed.

Ojo Alamo Sandstone Type Area. Unpublished lists of palynomorphs identified by R.H. Tschudy and D.J. Nichols in and near the Ojo Alamo Sandstone type area are presented on Tables 13.1 and 13.2. These USGS paleobotany localities are shown on Figures 1, 2, 4, and 51. Samples range in stratigraphic position from the lowermost Fruitland Formation (sample D6902, about 12 m above the base) to the uppermost Kirtland Formation for the Moncisco Mesa sample (just below the Kirtland Formation—Ojo Alamo Sandstone contact); a stratigraphic spread of about 370 m (Figure 33). Samples from localities D6900 and D6902 (Table 13.1, Figure 3) (see Table Appendix, page 126) were collected by J.D. Obradovich (USGS) in 1984 and analyzed by R.H. Tschudy (personal commun., 1985). The Moncisco Mesa sample (Table 13.1, Figure 3) was collected by C.J. Orth in 1982 and analyzed by Tschudy for its palynologic content. The complete report for this sample is not available, but a summary of Tschudy’s report is contained in an undated communication from Orth (1983?, written communication); the palynomorphs

listed in that summary are shown on Table 13.1. Tschudy concluded that the palynomorph assemblage from the Moncisco Mesa sample was an: “Assemblage equivalent to those in Vermejo Fm [in the Raton Basin]. Age represented is Campanian or early Maastrichtian.”

The sample from locality D9157 (Table 13.1, Figures 4, 33) is 55 m below the Kirtland Formation—Ojo Alamo Sandstone contact. D.J. Nichols analyzed this sample and reported (personal commun., 2000) that its palynomorph assemblage was early Maastrichtian. Samples D8179 and D8180 (Table 13.1, Figures 4, 33) were collected from the uppermost Kirtland Formation. Sample D8179-A was from a carbonaceous shale bed about 0.6 m below the base of the Ojo Alamo; sample D8179-B was collected from the same bed, but about 10 m east of the D8179-A locality. Sample D8180 was collected from an organic-rich mudstone bed about 3 m below the D8179-sample level. Nichols reported (personal commun., 1995) that these samples yielded sparse assemblages of palynomorphs. Because so few palynomorphs were identified from each of these samples. They are listed in a composite list on Table 13.1. Nichols concluded that this assemblage was Late, but not latest Cretaceous in age.

The palynomorph lists on Table 13.2 were all provided by D.J. Nichols (personal commun., 2000, 2003). Samples D9156-A and D9156-B (Figure 51) were collected from the same carbonaceous mudstone bed about 2 m below the Kirtland—Ojo Alamo contact. Nichols concluded that these two assemblages indicate an early Maastrichtian age. Samples from localities 82403-A, 82303-D, and 82303-E (Figure 51) were collected from a trench excavated through the base of the Ojo Alamo Sandstone and into the uppermost Kirtland Formation; the trench locality is shown on Figures 51 and 61.

This trench was excavated to try to relocate the bed from which the D6901 palynomorph assemblage (Table 6) had been collected in 1985 in the same area. (An earlier attempt to locate that bed by trenching in the vicinity of sample sites P4300 and SGL 046 (Figure 51) was not successful, as discussed in Fassett et al. 2002, p. 318-321.) The D6901 sample locality (referred to as the 24-5 locality in Fassett et al. 2002) is important because it produced a Paleocene palynomorph assemblage that confirmed the Paleocene age of the Ojo Alamo Sandstone in the Ojo Alamo Sandstone type area. Figure 61 is an annotated photograph of the Barrel Spring area showing the

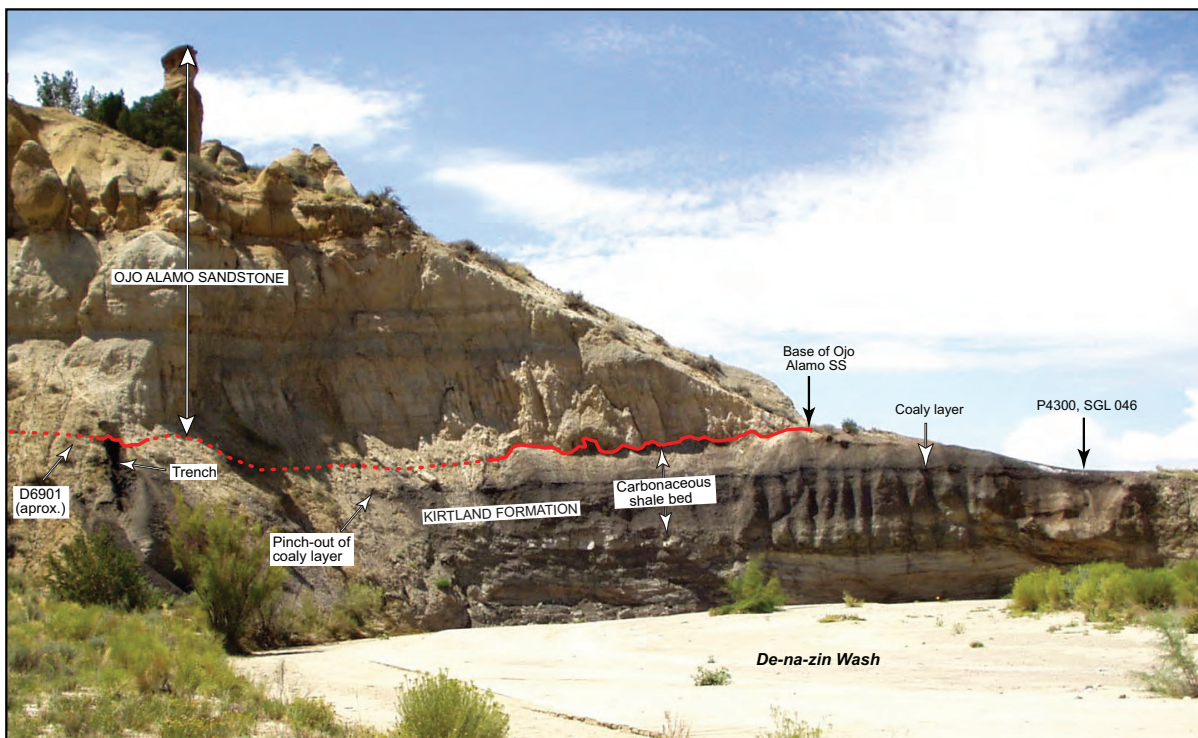


Figure 61. Photograph of Barrel Spring locality on De-na-zin Wash, looking southwest. Figure 51 shows map locations of paleobotany localities shown on photograph; localities 82303-E, 82403-A, and 110303-D are in trench on left side of photograph. Basal contact of Ojo Alamo Sandstone shown with red line (solid where clearly exposed, dotted where covered).

location of the trench on the left side of the photograph at the base of the Ojo Alamo Sandstone. The approximate location of the original D6901 sample site is shown to the left of the trench on this Figure.

Figure 62 is an annotated photograph of the entire trench, showing the stratigraphic level (4 m below the base of the Ojo Alamo Sandstone) of sample 82403-A. (Palynomorphs identified from this sample are listed on Table 13.2.) This sample is at about the same level as the coaly, carbonaceous shale bed shown on Figure 61 from which samples P4300 and SGL 046 (Table 6) were collected further to the west (Figures 51, 61). The thin, coaly layer is not present in the trench because it pinches out to the east, as shown on Figure 61. Nichols (personal commun., 2003) concluded that the palynomorph assemblage from sample 82403-A was early Maastrichtian in age.

Figure 63 is a close-up view of the upper trench of Figure 62 showing the locations of all samples that were collected for palynologic study here. Sample 82303-E, according to Nichols con-

tained a “diverse and well-preserved assemblage of fossil pollen and spores.” (Table 13.2) He concluded that this assemblage indicated an early Maastrichtian age. Nichols reported that sample 82303-D “appears to have been weathered in place such that only a few robust palynomorph species survived; species identified have no biostratigraphic value; assemblage also includes cysts of freshwater algae (also lacking biostratigraphic value).” The three palynomorphs identified by Nichols from this sample are *Ghoshispora* sp., *Pityosporites* sp., and *Taxodiaceapollenites hiatus*.

All of the other samples collected from the upper trench shown on Figure 63 were barren of palynomorphs, thus this attempt to relocate the bed from which the D6901 sample was collected was not successful. The level of that bed must be between sample 82303-E and the base of the Ojo Alamo Sandstone and is probably within the thin interval between the yellow-dashed line and the base of the Ojo Alamo. It is suggested that the Cretaceous-Paleocene interface may be located at the



Figure 62. Photograph of trench cut through base of Ojo Alamo Sandstone and uppermost Kirtland Formation at Barrel Spring locality. Figure 61 shows location of trench. Sample locality 82403-A is about 4 m below base of Ojo Alamo Sandstone at about same stratigraphic level as coaly bed that pinches out east of here (Figure 61). Contact between Ojo Alamo Sandstone and Kirtland Formation shown by red line (solid where clearly visible, dotted where covered). Geologic pick 0.33 m long.

yellow-dashed line on Figure 63. The pre-Paleocene unconformity, which, as discussed above, represents a 7.8 m.y. hiatus, is probably on an erosion surface on top of the harder and more massive blue-black strata shown beneath the yellow-dashed line on Figure 63. The squeeze-ups seen at the base of the Ojo Alamo Sandstone are a clear

indication that the sediments between the Paleocene interface and the base of the Ojo Alamo must have been unconsolidated and at least somewhat fluid at the time that the first high-energy streams carrying the gravels of the lower Ojo Alamo Sandstone flowed across the pre-Ojo Alamo erosion surface and rapidly built up to a thickness of sand

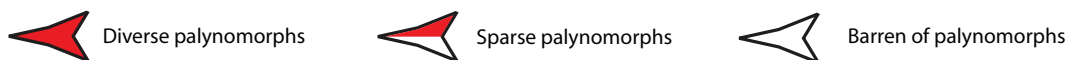
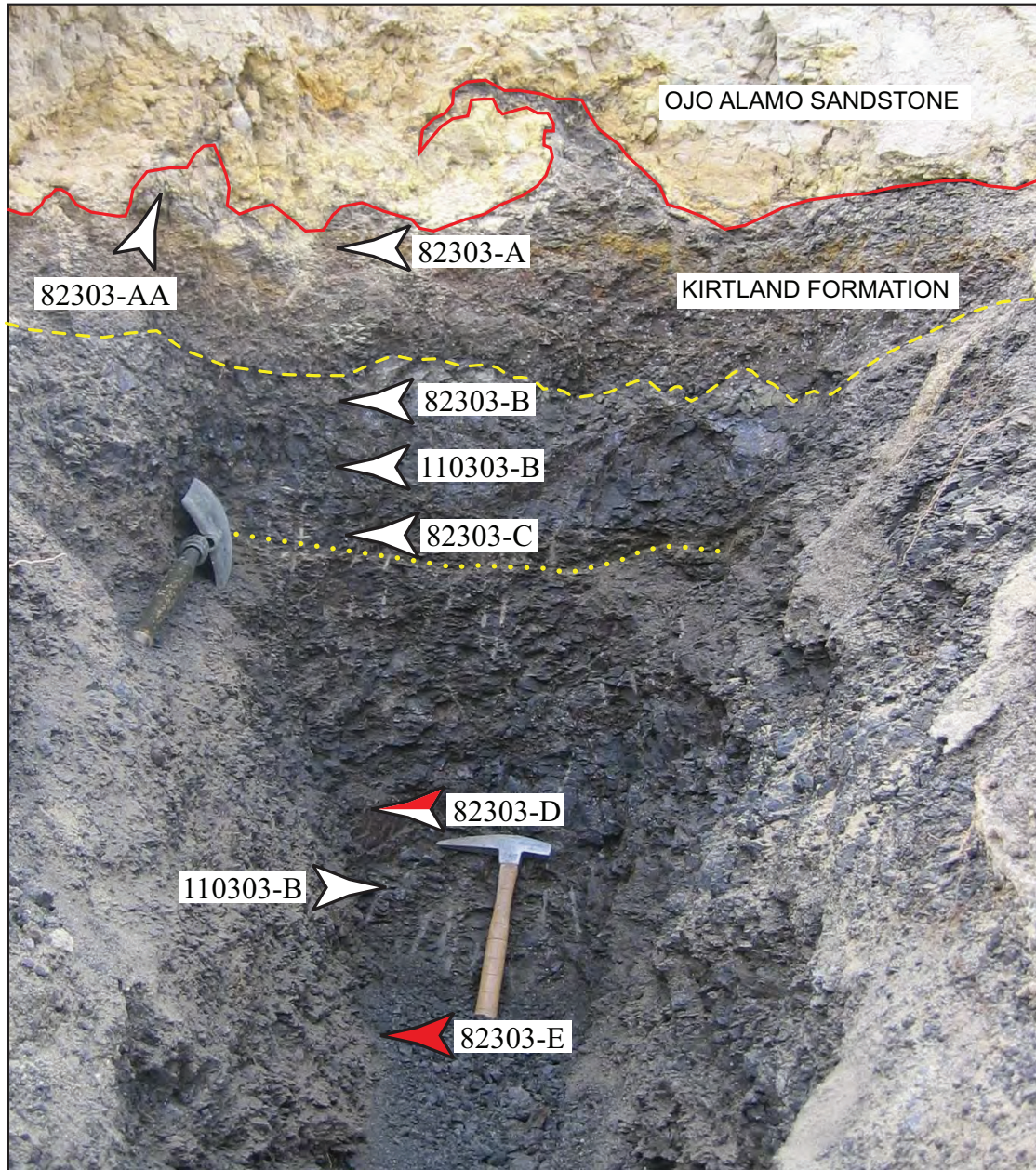


Figure 63. Photograph of upper part of trench of Figure 62; distance from base of Ojo Alamo Sandstone to sample locality 82303-E is 1.7 m.; geologic-pick length 0.33 m. Note intense, soft-sediment deformation at base of Ojo Alamo Sandstone, including distinct squeeze-up of uppermost Kirtland Formation mudstone forced up into basal Ojo Alamo Sandstone conglomerate in top-center of photograph. Such rapid-loading features are also visible below base of Ojo Alamo in center of Figure 61. Palynologic sample localities in carbonaceous mudstone bed in uppermost Kirtland are shown. All samples, except 82303-D and 82303-E, barren of palynomorphs. Yellow-dashed line is subtle contact between harder, more massive, blue-black shale below and softer, more thin-bedded, gray mudstone above. Yellow-dotted line is another subtle contact at base of blue-black shale bed. One of these contacts (probably upper one) is the Cretaceous-Paleocene interface.

and gravel of sufficient weight to cause the bed distortion seen on Figures 61, 62, and 63 at the base of the Ojo Alamo.

The thin gray unit below the base of the Ojo Alamo Sandstone (Figure 63) may be the bed from which the D6901 sample was collected in 1985 east of the trench in a place where palynomorphs were better preserved. This interval probably represents a soil layer or swamp deposit that filled a low-lying area on the pre-Paleocene erosion surface in early Paleocene time. The few Cretaceous palynomorphs found in the D6901 palynomorph assemblage could easily have been washed or blown into this layer from the adjacent Cretaceous land surface, as discussed in Fassett et al. (2002, p. 318-319). It is possible, although less likely, that the Cretaceous-Tertiary interface is at a lower level in the upper trench, somewhere above sample 82303-E (Figure 63). There is another (subtle) lithologic break at the base of the blue-black massive shale bed marked by a thin greenish-gray silty layer just below the level of sample 82303-C (yellow-dotted line on Figure 63) and perhaps the base of this unit represents the K-T interface. There are no other apparent lithologic breaks in the interval between samples 82303-C and 82303-E in the strata exposed in the trench.

Sullivan et al. (2005) disputed the presence of Paleocene dinosaurs in the Ojo Alamo Sandstone of the San Juan Basin. These authors argued that the Paleocene age of the Ojo Alamo Sandstone on the basis of palynological data obtained in the Barrel Spring area (palynologic sample D6901, Table 6), published in Fassett et al. (2002), was invalid because they could not replicate those data; they stated (p. 402) that their "processing of several samples yielded no identifiable palynomorphs." Sullivan et al., however, did not specify where exactly their sampling had been done, did not supply photographs of their sample sites, or state how many samples had been collected and analyzed. It is here suggested that this vague reference to sampling from an unknown locality at an unknown distance below the base of the Ojo Alamo Sandstone with the results being samples barren of palynomorphs does not obviate the data reported by Fassett et al. (2002). Those data contained the results of palynologic analysis of a rock sample from a specifically identified locality, less than 1 m below the base of the Ojo Alamo, that contained a diverse palynomorph assemblage of Paleocene age. As demonstrated in the discussion above, samples barren of palynomorphs have been frustratingly common throughout the San Juan Basin

(see Figure 63), however, rock samples barren of palynomorphs, from whatever locality, have no geochronologic value to prove or disprove anything.

In addition, Sullivan, Lucas, and Braman (2005, p. 402) stated that they found "no physical evidence of an unconformity . . . of at least 7.5 million years" in uppermost Kirtland Formation strata in the Barrel Spring area. Unconformities can be subtle, and it is here suggested that because these authors did not carefully trench the interval in the uppermost Kirtland up to the base of the Ojo Alamo Sandstone in the Barrel Spring area, they did not observe the subtle lithologic changes shown on Figure 63 and discussed in detail above. The rocks of the uppermost Kirtland Formation, immediately beneath the Ojo Alamo Sandstone in the Ojo Alamo Sandstone type area, are 73.04 Ma based on a $^{40}\text{Ar}/^{39}\text{Ar}$ single-crystal sanidine age. In addition, palynomorphs identified from multiple rock samples from within and immediately below the Ojo Alamo Sandstone in the Barrel Spring area have an early, but not earliest Paleocene age. (See Figure 58 for a depiction of these relations.) Therefore, an unconformity of about 7.8 m.y. must be present at or near the base of the Ojo Alamo in this area, even though this hiatus is not, at first glance, physically apparent.

Sample 110303-D was collected from a coaly, carbonaceous shale bed about 0.3 m below the base of the Ojo Alamo Sandstone at a locality 225 m east of the trench locality (Figure 51). According to Nichols, this sample also yielded a diverse and well-preserved assemblage (Table 13.2) of early Maastrichtian age. At this locality, the K-T interface is apparently at the base of the Ojo Alamo Sandstone. This finding supports the suggestion above that the Paleocene rocks in the uppermost Kirtland Formation in the Barrel Spring area (Figure 63) represent sedimentation in an isolated bog or pond present on the Paleocene erosion surface just before deposition of the overlying Ojo Alamo Sandstone conglomerates began. The squeeze-ups of this unconsolidated and somewhat fluid material (Figure 63) into the basal part of the Ojo Alamo are diagnostic of these Paleocene bog deposits that filled isolated low spots on the pre Ojo Alamo Sandstone erosion surface.

The palynomorphs listed in the column headed: "Locality D6901" ("archival split 24-5") on Table 14 (see Table Appendix, page 127), were identified by D.H. Nichols (personal commun., 2003) from a new analysis of a sample reported by Nichols to be a split of USGS archival sample 24-5

(from USGS Paleobotany Locality 6901, Figure 56). The label “24-5” is from Fassett et al. (2002). The palynomorph assemblage from the “archival split” appears to differ markedly from the assemblage identified from the original analysis of this sample (column headed “Locality D6901 (sample 24-5)” on Table 14). There are only 12 common palynomorphs (33%) out of the 36 palynomorphs identified from these two sample preparations, and 24 palynomorphs (67%) are not common. A composite list of palynomorphs from USGS localities D6877-A, -B, and -C from the San Juan River locality (Figure 1) has also been added to Table 14 for comparative purposes. This Paleocene assemblage has a greater degree of commonality of palynomorphs with the original D6901 list than does the “archival split”: 15 common palynomorphs out of 36 (42%) vs. 19 not-common (58%). This higher percentage of common palynomorphs is even more remarkable in consideration of the fact that these two sample localities are nearly 50 km apart. The low percentage of commonality of palynomorphs (33%) from sample D6901 and “archival split 24-5” (reported to be from the original D6901 sample) casts serious doubt as to whether these two palynomorph lists actually came from splits of the same sample. It is suggested that “archival split 24-5” may have come from a different USGS archival sample from Cretaceous strata and not from the original “24-5” sample.

Northeast San Juan Basin. The locations of the four palynologic samples from the northeast part of the San Juan Basin are shown on Figure 1. Palynomorphs identified by R.H. Tschudy from the D4119 locality were published in Fassett and Hinds (1971) and are listed on Table 7 (they are also shown on Table 15 (see Table Appendix, page 128) with the three other palynomorph lists from the northeastern San Juan Basin). The other three samples (D5393, D5394, and D5408) were collected by R.T. Ryder in 1975 and were reported on by Tschudy (personal commun., 1976). Two of these samples (D5393 and D5394) were collected from the lowermost part of the Fruitland Formation: D5393 was from a mine dump from a coal bed 6 m above the base of the Fruitland and D5394 was collected from a bed 3 m above the base of the Fruitland near an outlier (Klutter Mountain) of Pictured Cliffs Sandstone, Fruitland Formation, and Ojo Alamo Sandstone (Figure 1) about 19 km east of locality D5393. The D4119 locality, also from a coal bed a few meters above the base of the Fruitland, is located about 9 km southeast of the D5393

locality (Figure 1). Tschudy wrote of the palynomorph assemblage from locality D5393:

*This assemblage is clearly of Late Cretaceous age. The estimation of lower Fruitland is consistent with the palynomorphs found. *Kuylisporites* has not been found in rocks younger than middle Campanian and is present in the lower part of the Fruitland Formation in the Gasbuggy core.*

For the D5394 assemblage, Tschudy reported that:

*This assemblage is of Late Cretaceous Campanian age. All taxa have been found previously in the Fruitland Formation. The presence of *Phaseolidites stanleyi* suggests lower Fruitland, but I am unable to restrict the assemblage to the lower part of the Fruitland.*

Tschudy's comments in Fassett and Hinds (1971, p. 21) regarding sample D4119 are:

*Sample D4119 I believe to be Cretaceous. The coal yielded a poor corroded assemblage. I was able to find only two specimens of the marker genus *Proteacidites*. This assemblage appears to have a closer resemblance to the Trinidad and Vermejo of the Raton Basin than to the assemblage reported by Anderson from the southern San Juan Basin.*

As Table 15 indicates, the three palynomorph lists for samples from the lowermost Fruitland Formation in the northeastern San Juan Basin, all relatively close together, have remarkably few common taxa. This would seem to indicate that local environmental conditions had a profound affect on the plant assemblages even at closely spaced localities; at least in this part of the San Juan Basin.

The fourth palynomorph list on Table 15 is for sample D5408; this sample was collected from the Animas Formation about 150 m above its base (Figure 1). Tschudy (personal commun., 1975) wrote that this sample:

*. . . yielded a very sparse palynomorph flora . . . The presence of these two species of *Momipites* [Table 15] in an otherwise very poor assemblage, definitely indicates a Paleocene age for the sample.*

Composite Palynomorph Lists by Locality

Mesa Portales and Anderson's Localities Near Cuba, New Mexico. Table 16 (see Table Appendix, page 129) shows composite palynomorph lists for the southeastern part of the San Juan Basin, including all of the palynomorphs identified at and near Mesa Portales (Tables 7 and 9) and in Anderson (1960, table 1), Table 5. These lists consist of palynomorphs identified from the Fruitland and Kirtland Formations, the Ojo Alamo Sandstone, and the Nacimiento Formation. There are 144 taxa listed on Table 16; of these only 12 (9%) are common to the Cretaceous Fruitland-Kirtland Formations and the Paleocene Ojo Alamo Sandstone. At first glance this evidence would seem to indicate an enormous die-off of plants at the K-T interface in the southeastern part of the basin. However, because of the 7.8m.y. hiatus at the K-T boundary, representing all of Maastrichtian, part of Campanian, and also a small part of earliest Paleocene time, this apparent sudden die-off actually represents species that died off over a nearly 8 m.y. period and not suddenly at the end of the Cretaceous. There are 72 taxa in Paleocene strata listed on Table 16; 22 taxa (31%) are common to the Ojo Alamo Sandstone and Nacimiento Formation. There was apparently continuous deposition across the contact between these formations (Fassett 1966), consequently this relatively small percentage of common forms probably indicates a distinct change in depositional environments in this area from Ojo Alamo to Nacimiento time. There are 37 taxa listed on Table 16 from the Nacimiento vs. 57 for the Ojo Alamo, thus, this disparity in numbers of taxa preserved and identified from these two formations may be skewing this percentage.

Pot Mesa Locality. The composite list of palynomorphs identified from the Pot Mesa locality (Table 17, Figures 59, 60) (see Table Appendix, page 130) are all from the Cretaceous Kirtland Formation. No samples collected for palynologic analysis from the Paleocene Ojo Alamo Sandstone at Pot Mesa were productive. There are 58 taxa shown on the palynomorph list on Table 17.

Ojo Alamo Sandstone Type Area. Table 18 (see Table Appendix, page 131) shows composite palynomorph lists for the Ojo Alamo type area and nearby areas to the west (Figures 1, 3, and 4). Table 18 lists 112 taxa; of these, 11 of 81 taxa (14%) are common to the Fruitland and Kirtland Formations, 17 of 73 taxa (23%) are common to the Kirtland and the Paleocene uppermost Kirtland, 13 of 52 taxa (25%) are common to the uppermost

Kirtland and upper Ojo Alamo, and 5 of 37 taxa (14%) are common to the upper Ojo Alamo Sandstone and lower Nacimiento Formation. Cretaceous taxa total 81, and Paleocene taxa total 52.

San Juan River Locality. The palynomorphs listed on Table 19 (see Table Appendix, page 132) from the San Juan River locality were all originally reported to be from the Ojo Alamo Sandstone, however, as discussed above, the palynomorphs identified by Newman (1987) from that locality were probably not collected from the Ojo Alamo but were probably from the underlying Kirtland Formation. For this reason, Newman's palynomorph list is shown to be from the Cretaceous Kirtland Formation on Table 19. There are 48 taxa listed on this table; six are from the Kirtland Formation, and 43 are from the Ojo Alamo Sandstone. The only common palynomorph to the two lists is *Tschudypollis* and because palynomorph assemblages identified from the Ojo Alamo Sandstone are Paleocene in age, the specimens of *Tschudypollis* in the Ojo Alamo Sandstone are considered to be reworked. (See discussion of reworking of Cretaceous palynomorphs into Paleocene strata in Nichols and Fleming 2002.)

Northeast San Juan Basin. Table 20 (see Table Appendix, page 133) lists the palynomorphs identified from the northeastern part of the San Juan Basin from the lowermost Fruitland Formation and from the lower part of the Animas Formation. Of the 36 taxa listed, only two (6%) are common to the Fruitland and Animas Formations. This low percentage of commonality is clearly skewed by the small number (6) of palynomorphs identified from the Animas in this area.

Palynomorph Lists by Formation

Fruitland Formation. Table 21 (see Table Appendix, page 134) contains composite lists of palynomorphs from four areas in the San Juan Basin. Two areas—the Ojo Alamo type area and the Mesa Portales area—are in the southern part of the basin, and two areas—the Gasbuggy core and the northeastern San Juan Basin area are in the northern part of the basin. Of the 155 taxa listed on Table 21, there is a low percentage of common taxa between these areas; the Ojo Alamo type area and the Mesa Portales areas only have six palynomorphs in common (5%) out of 110 taxa from those two areas. This low percentage is probably skewed by the different numbers of taxa identified from these two areas: 29 from the Ojo Alamo type area and 87 from the Mesa Portales area. The Mesa Portales and Gasbuggy core lists have 18 of

121 taxa in common (15%). The Gasbuggy core and the northeast San Juan Basin lists have 12 of 106 taxa in common (11%). These relatively low percentages of commonality of palynomorphs for Fruitland Formation assemblages suggest that depositional environments were variable across the basin during Fruitland Formation time. Moreover, the time-transgressive nature of Fruitland Formation strata—becoming about 2 m.y. younger from southwest to northeast across the basin—probably contributed to the lack of commonality for assemblages in the southwest and northeast.

Kirtland Formation. Palynomorphs collected from the Kirtland Formation were identified from only the two localities shown on Table 22 (see Table Appendix, page 135). The Pot Mesa area is 62 km south-east of the Ojo Alamo type area (Figure 3). The Fruitland-Kirtland interval is about 145 m thinner at Pot Mesa than at the Ojo Alamo type area, thus palynomorphs collected from the upper part of the Kirtland Formation at Pot Mesa are about 145 m stratigraphically lower than the upper-Kirtland samples from the Ojo Alamo type area. The Pot Mesa samples from upper Kirtland strata are thus considerably older than those from the Ojo Alamo type area. That is probably the reason why there are only 11 common taxa (10%) out of a total of 108 palynomorphs identified from the two localities.

Comparison of Fruitland and Kirtland Formations Palynomorphs. Table 23 (see Table Appendix, page 136) lists 206 palynomorph taxa identified from the Fruitland and Kirtland Formations from all localities in the San Juan Basin. Of these, 46 taxa (22%) are common to the Fruitland and Kirtland Formations. Of the 206 total taxa, 106 are present only in the Fruitland, and 53 are present only in the Kirtland. The Cretaceous index palynomorph *Tschudypollis* spp. is ubiquitous and the most abundant form in all Fruitland and Kirtland samples. A preliminary zonation of the Fruitland-Kirtland is presented in the “Cretaceous-Palynomorph Zonation section” of this appendix, below.

Ojo Alamo Sandstone. The Paleocene Ojo Alamo Sandstone and the Paleocene (uppermost) parts of the Kirtland and Fruitland Formation have yielded 101 palynomorphs in the San Juan Basin (Table 24) (see Table Appendix, page 137). Table 25 (see Table Appendix, page 138) shows that the Ojo Alamo Sandstone and underlying Cretaceous rocks have yielded 243 taxa between them; of these taxa, 192 are restricted to Cretaceous strata, 51 are common to Cretaceous strata, and 51 were

found only in Paleocene strata. (The two occurrences of reworked *Tschudypollis* shown on Table 24 are not included in these numbers.) A comparison of Cretaceous and Paleocene palynomorphs within the San Juan Basin and with other Western Interior basins is presented in the section of this report labeled “Comparison of Palynomorphs,” below.

The guide palynomorphs, *Brevicolporites colpella* and (or) *Momipites tenuipolus* have been identified from Ojo Alamo Sandstone samples at numerous localities in the San Juan Basin.

These palynomorphs are known to be restricted to Paleocene-age strata throughout the Western Interior of North America (Nichols and Johnson 2002). Nichols (2002) discussed the significance of *M. tenuipolus* as a Paleocene index fossil throughout the Western Interior. Nichols (p. 124), and in his discussion of biozone P1 in the Raton Basin, stated that:

Momipites tenuipolus and *M. leffingwellii* occur only in the middle to upper part of the biozone [P1], thereby delimiting a basal Paleocene subzone in which *M. inaequalis* is present but the other species of *Momipites* are absent. This basal Paleocene subzone of Zone P1 is recognizable in the Denver Basin, as well.

This finding is in accord with statements by R.H. Tschudy in numerous reports to the author (written commun. cited above) that *M. tenuipolus* “is limited to the Paleocene but is not present in the lowermost Paleocene” in the San Juan Basin. In his conclusions, Nichols (2003, p. 130-131) emphasized that:

With attention to the influence of paleolatitude, local zonations can be integrated into a comprehensive nonmarine biostratigraphy for the lower Cenozoic of the Rocky Mountains and Great Plains region.

The Raton Basin of northeastern New Mexico and southeastern Colorado is only 230 km east of the San Juan Basin and is at the same latitude. It is thus reasonable to conclude that in the San Juan Basin, *M. tenuipolus* is also restricted to the upper part of biozone P1 and is absent from lowermost Paleocene rocks. *M. tenuipolus* has been identified from a sample less than a meter below the base of the Ojo Alamo Sandstone in the Ojo Alamo type area and 8 m above the K-T interface at Mesa Portales. Because *M. tenuipolus* is only present in the

upper part of zone P1, it can thus be concluded that the lowermost part of zone P1 (the lowermost Paleocene) is missing in the San Juan Basin. This finding agrees with paleomagnetic data indicating that the base of the Ojo Alamo Sandstone has an age of about 65.2 Ma (see Figures 34 and 35) suggesting a 0.3 m.y. gap in the lowermost Paleocene in the southern part of the San Juan Basin.

Nacimiento Formation. Palynomorphs identified from the Paleocene Nacimiento and Animas Formations are listed in Table 26 (see Table Appendix, page 139). Samples from these formations at nine localities in the San Juan Basin yielded 69 identified palynomorphs; sample collections ranged from near the base to 150 m above the base of these formations. The two localities labeled “WNW 2008—Kimbeto Arroyo” were discussed in Williamson et al. 2008. These authors determined that (p. 9): “Both palynomorph assemblages, which are reported here, contain palynomorphs that are characteristic of early Paleocene assemblages that are widespread in the Rocky Mountain region.” The taxa identified from the samples collected from strata 19 m above the base of the Nacimiento Formation (top of the Ojo Alamo Sandstone) were found to contain “palynomorphs characteristic of P1–P3 pollen zones” and the assemblage from samples 105 m above the base of the Nacimiento contained “palynomorphs characteristic of P3.” The P1 through P3 pollen zones mentioned here refer to the Paleocene pollen zonation established in the northern part of the Western Interior of North America by Nichols (2003). The paper by Williamson et al. (2008) is the first to correlate the Paleocene palynomorph zonation of the northern part of the Western Interior with palynomorph assemblages in the southern part in New Mexico.

Williamson et al. (2008, p. 3) identified the palynomorph *Momipites triorbicularis* in their sample 105 m above the base of the Nacimiento Formation and stated that this taxa “is indicative of palynostratigraphic Zone P3.” Nichols (2003, figure 2), however, shows this guide fossil’s first appearance as more specifically being at or near the boundary between the P3 and P4 zones with its range extending up into the middle of zone P5. This diagnostic fossil was also identified from a sample collected 150 m above the base of the Animas Formation at locality D5408 in the northern San Juan Basin in Colorado (Table 26). The presence of this palynomorph 45 m above its presence lower in the Nacimiento Formation would thus indicate that the strata at this higher level are in zone

P4, and that the P3–P4 boundary is just above the sample 105 m above the base of the Nacimiento.

Nichols (2003, figure 2) shows the boundary between biozones P2 and P3 to be between the last occurrence of *M. inaequalis* and the first occurrence of *M. triorbicularis*. *M. inaequalis* is present 20 m above the base of the Nacimiento at the D3803 locality (Table 26), and *M. triorbicularis* is present at the Kimbeto Arroyo locality 105 m above the base of the Nacimiento (Table 26). The boundary between zones P2 and P3 must, therefore, be between these two stratigraphic levels in the San Juan Basin—probably not far above the stratigraphic level of *M. inaequalis*.

Williamson et al. (2008) also pointed out that the Paleocene index fossil *M. tenuipolus* was found in their lower sample, 19 m above the base of the Nacimiento Formation, and Table 26 shows that this palynomorph was also found 150 m above the base of the Nacimiento at the D5408 locality. As this table shows, *M. tenuipolus* is by far the most common palynomorph identified from Nacimiento Formation samples and is present in seven of the nine palynomorph lists shown.

Palynomorph lists from the Nacimiento Formation and the Ojo Alamo Sandstone are compared in Table 27 (see Table Appendix, page 140). This table shows that 101 palynomorphs have been identified from the Ojo Alamo Sandstone, 69 from the Nacimiento Formation, and 49 palynomorphs are common to both formations. The total number of palynomorphs from both formations is 125. Fifty six palynomorphs are present only in the Ojo Alamo Sandstone, and 24 are found only in the Nacimiento Formation. The high percentage of commonality of palynomorphs for the Ojo Alamo and Nacimiento formations attests to uninterrupted deposition across the boundary between these two formations. These data thus further reinforce the findings presented elsewhere in this report that the Ojo Alamo Sandstone is Paleocene in age.

Cretaceous-Palynomorph Zonation

Table 28 (see Table Appendix, page 141) shows the zonation of palynomorphs from the lower and upper parts of the Fruitland Formation and the upper Kirtland Formation in the southern part of the San Juan Basin. As the time-stratigraphic cross sections of Figures 34 and 35 show, Fruitland and Kirtland strata are late Campanian in age in the southwest part of the basin; the uppermost part of the late Campanian and all of the Maastrichtian are missing. Figure 64 shows the stratigraphic positions of these three palynomorph

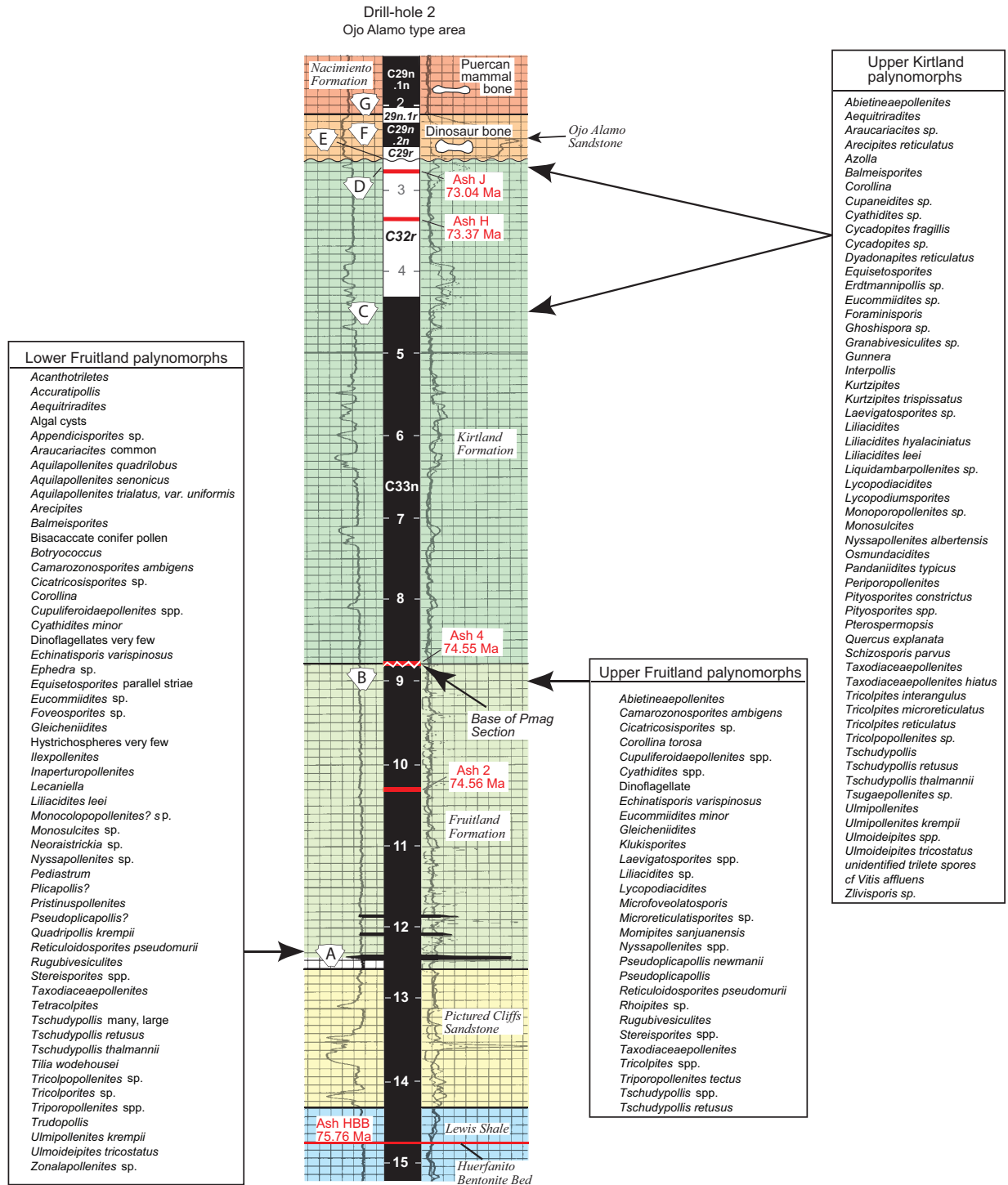


Figure 64. Stratigraphic levels of palynomorph assemblages from Fruitland and Kirtland Formations in Ojo Alamo Sandstone type area. Geophysical log from Figure 33, palynomorph lists from Table 28; log explanations on Figure 33. Lower Fruitland palynomorphs approximately 75.1 Ma, upper Fruitland palynomorphs about 74.6 Ma, and upper Kirtland palynomorphs; samples at D level about 73.0 Ma, and at C level about 73.8 Ma. Majority of upper Kirtland palynomorphs from D sample level, just above Ash J level. Palynomorph-assemblage ages interpolated from ash-bed ages shown.

assemblages projected into drill-hole 2 (see Figures 33-35) near the Ojo Alamo Sandstone type area. Table 28 shows that 34 palynomorphs from lower Fruitland samples are not present in stratigraphically higher Cretaceous samples, 12 palynomorphs are common to the lower and upper Kirtland samples, and eight palynomorphs are present in the lower Fruitland and upper Kirtland samples. Eight palynomorphs are unique to the upper Fruitland samples, and 21 palynomorphs identified from upper Fruitland samples are not present in upper Kirtland samples. Eight taxa are common to the upper Fruitland and upper Kirtland samples, and three are common to all three sample lists. As for upper Kirtland samples, 40 taxa are found only in these samples.

Table 28 clearly shows the progressive disappearance of palynomorphs and the appearance of new taxa going stratigraphically upward through the Campanian Fruitland and Kirtland Formations in the San Juan Basin. Of the taxa present in the lower Fruitland palynomorph list of this table, only two genera reappear in Paleocene strata: *Araucariacites* as *A. australis* and *Tripoporollenites* as *T. plektosus* and *T. rugatus* (Table 29) (see Table Appendix, page 142). Of the taxa present in the lower and (or) upper Fruitland but absent in the upper Kirtland of Table 28, five genera also appear in the Paleocene: *Gleicheniidites* as *G. senonicus*, *Momipites sanjuanensis*, *Nyssapollenites* spp as *N. explanatus*, *Tricolpites* spp., and *Tripoporollenites* as *T. tectus* and *T. plektosus* (Table 29).

Comparison of Cretaceous and Tertiary Palynomorphs

Table 29 compares Cretaceous (Campanian) and Paleocene palynomorph assemblages in the San Juan Basin; 244 palynomorphs are listed on this table. Of these, 50 taxa (20%) are present only in Paleocene strata, 143 taxa (59%) are present only in Cretaceous strata, and 51 taxa (21%) are common to Cretaceous and Paleocene strata. The 23 taxa shown in magenta are Cretaceous index palynomorphs in the Raton Basin (Fleming 1990) and (or) the Northern Great Plains (Nichols and Johnson 2002). The palynomorphs shown in blue are Paleocene index fossils in the Raton Basin or Northern Great Plains. All but one of the Cretaceous index palynomorphs of the Raton Basin and Northern Great Plains *Tricolpites* spp. are absent in Paleocene strata of the San Juan Basin. Taxa, reported to be Cretaceous index fossils in the Raton Basin are present in Paleocene strata at three different localities in the San Juan Basin.

As Table 29 shows, *Brevicolporites colpella* and *Momipites* spp. are Paleocene index palynomorphs in the Northern Great Plains (Nichols and Johnson 2002). Fleming (1990, p. 247) stated that: "in the Raton Formation [in the Raton Basin], *Momipites tenuipolus* first appears 16 m above the K-T boundary in the *Momipites inaequalis* zone and ranges to near the top of the formation." Fleming, however, indicated that *B. colpella* may have been identified in Cretaceous strata in the Raton Basin. It would appear that both *B. colpella* and *M. tenuipolus* are Paleocene index palynomorphs in the San Juan Basin. A more detailed comparison of palynomorph occurrences in the San Juan Basin and other Western Interior basins is made difficult by the fact that in those basins there was apparently continuous deposition across the Cretaceous-Tertiary boundary, whereas in the southern San Juan Basin, there is a nearly 8 m.y. hiatus at the K-T interface with all of the Maastrichtian, the uppermost part of the Campanian, and a small interval of lowermost Paleocene absent. A comparison of palynomorphs found in Campanian strata in the San Juan Basin (Table 28) with palynomorph assemblages of the same age from other Western Interior basins would be instructive, but is beyond the scope of this report.

Summary of Palynology

This appendix synthesizes all published palynologic data for rocks adjacent to the Cretaceous-Tertiary (K-T) interface in the San Juan Basin, and in addition, presents additional new palynomorph lists to add to the basin's published palynologic database. Palynomorphs identified from the Upper Cretaceous Fruitland and Kirtland Formations are twice as abundant as those from the Paleocene Ojo Alamo Sandstone and the Nacimiento and Animas Formations. This is because the collection sites for Cretaceous samples are much more numerous, the samples from the Ojo Alamo have generally yielded far fewer identifiable palynomorphs, and because palynomorph diversity is apparently less for the Ojo Alamo, Nacimiento, and Animas formations.

Composite-palynomorph lists are presented in Tables 16 through 25 synthesizing all available palynologic data for the San Juan Basin. Tables 16 through 20 present composite palynomorph lists for each locality where such data have been obtained; Tables 21 through 24 compare palynomorph lists for Cretaceous and Paleocene strata, and Table 25 lists all palynomorphs identified from Cretaceous and Paleocene strata for the entire

basin. Table 26 lists palynomorphs from the Nacimiento and Animas Formations, and Table 27 compares Ojo Alamo Sandstone with Nacimiento-Animas palynomorphs. Table 28 shows the palynologic zonation of uppermost Cretaceous strata, and Table 29 compares the total Cretaceous vs. Paleocene palynomorph lists.

The discussions above address the statistical variations in numbers of palynomorphs identified from the formations adjacent to the Cretaceous-Tertiary interface in the San Juan Basin, and represent the empirical observations of a non-palynologist. A much more nuanced interpretation of these data could, and should, be made by an experienced palynologist. These numbers are skewed by the variable numbers of sample-collection localities in each formation and by variations in the diversity of palynomorphs present in these samples. In addition, going upward in the stratigraphic section from the lower Fruitland Formation through the Kirtland Formation (upper Campanian) the depositional environments change progressively from near shore, swampy conditions, to coastal plain, and ultimately to well-drained, continental, fluvial environments well inland of the Western Interior Seaway's regressive shoreline far to the northeast. These different environments undoubtedly contributed to the stratigraphic variations in palynomorph assemblages in the Fruitland and Kirtland and, to a degree, may cloud the evolution, extinction, and first occurrences of palynomorphs going upward in

the section. The depositional environments for palynomorph-sample localities within the Ojo Alamo Sandstone and overlying Nacimiento Formation were probably less variable across the basin.

The last occurrences of 22 taxa in Cretaceous strata of the San Juan Basin are in agreement with last occurrences of these taxa in the Raton Basin (Fleming 1990) and the Northern Great Plains (Nichols and Johnson 2002). These last occurrences unequivocally mark the Cretaceous-Tertiary (K-T) interface in the San Juan Basin. The last occurrence of the principle Cretaceous index fossil: *Tschudypollis* (formerly *Proteacidites*); sharply defines the K-T interface in the southeastern San Juan Basin at Mesa Portales, in Anderson's (1960) collecting localities and in the Gasbuggy core. In addition, the Paleocene index palynomorphs *Brevicolporites colpella* and *Momipites tenuipolus* have been identified in the Paleocene Ojo Alamo Sandstone (and the Paleocene part of the uppermost Kirtland Formation) at two localities in the San Juan Basin. Because *M. tenuipolus* is restricted to the upper part of biozone P1 and is not present in lowermost Paleocene strata in the Western Interior of North America (Nichols 2003), the presence of this guide fossil in the lowermost part of the Ojo Alamo Sandstone supports paleomagnetic evidence suggesting that as much as 0.3 m.y. are not represented by Paleocene rocks in the San Juan Basin.

TABLE 1. AGES OF SOME LATE CRETACEOUS WESTERN INTERIOR AMMONITE-ZONE BOUNDARIES OF GRADSTEIN ET AL. (2004) AND THIS REPORT

W. Interior Ammonite Zone	Gradstein et al. (2004)		This report	
	Age (Ma)	Duration (m.y.)	Age (Ma)	Duration (m.y.)
<i>Baculites compressus</i>	73.50	0.72	73.90	?
<i>Didymoceras cheyennense</i>	74.28	0.78	74.50	0.60
<i>Exiteloceras jenneyi</i>	75.05	0.77	74.65	0.15
<i>Didymoceras stvensoni</i>	75.74	0.69	74.98	0.33
<i>Didymoceras nebrascense</i>	76.38	0.64	75.76	0.78

Note: Ages are for base of ammonite zones.

TABLE 2. VERTEBRATE BONE SAMPLES FROM OJO ALAMO SANDSTONE AND KIRTLAND FORMATION COLLECTED FOR CHEMICAL ANALYSIS; U AND RARE-EARTH ELEMENT (REE) VALUES SHOW												
OJO ALAMO SANDSTONE - PALEOCENE												
Figure designation	Sample No.	Sample of:	Meters Above Base of OA	Location	1/41/4 Sec., Tsp. R.	Longitude	Latitude	Notes	Quadrangle	U (ppm)	La/b(n)	Sum REE
1-SJR	FBHF	Hadrosaur femur	15.2	NWNE 36, 29N, 14W	108.25836	36.68774	Small core of hadrosaurid, indeterminate	Kirtland	33	3.2	1004	
4-B	022899-OA1	Limb bone	7.3	NENE 32, 25N, 12W	108.13746	36.36251	Fragment of limb bone	Alamo Mesa West	530	14.0	785	
4-F	051298-BB1	Sauropod femur	1.8	NWNE 3, 24N, 12W	108.09684	36.34984	Small core. <i>Alamosaurus sanjuanensis</i> (also SMP VP-1.138)	Alamo Mesa East	834	7.2	1989	
4-G	SMP VP-1494	Sauropod vertebra	3.5	SWSE 34, 25N, 12W	108.09524	36.35103	Small fragment, <i>Alamosaurus sanjuanensis</i> (from R.M. Sullivan)	Alamo Mesa East	657	6.2	38	
4-H	020103	Bone fragment	4.6	NWNW 7, 24N, 11W	108.05111	36.33376	Small bone fragment from lag deposit	Alamo Mesa East	190	11.6	5916	
4-I	P-19147	Hadrosaur scapula	6.1	NWNW 7, 24N, 11W	108.04946	36.33449	Sample from outer cortical surface (from S.G. Lucas)	Alamo Mesa East	681	12.0	1287	
4-J(1)	022799-B1	Limb bone	8.2	SWNW17, 24N, 11W	108.03267	36.31647	Fragment of large limb bone	Alamo Mesa East	720	5.0	1417	
4-J(2)	022799-B2	Limb bone	8.2	SWNW17, 24N, 11W	108.03267	36.31647	Fragment of different limb bone from same locality	Alamo Mesa East	822	10.6	2244	
4-K	022799-C	Limb bone	5.8	SWNW17, 24N, 11W	108.03267	36.31618	Fragment of limb bone	Alamo Mesa East	436	7.7	6174	
4-L	022799-A	Limb bone	5.8	SENE 17, 24N, 11W	108.02990	36.31638	Fragment of large limb bone	Alamo Mesa East	232	1.6	73	
4-O	051504	Ceratops frill	3.7	SESE 17, 24N, 11W	108.01707	36.30754	Ceratopsian frill fragment	Alamo Mesa East	312	4.9	1149	
4-N	SMP VP-1625	Sauropod femur	4.9	SESE 17, 24N, 11W	108.01645	36.30753	Fragment of <i>Alamosaurus sanjuanensis</i> (from R.M. Sullivan)	Alamo Mesa East	366	4.0	1445	
11-B	072598-4C	Tyrannosaurid femur	1.8	SWSW 4, 22N, 9W	107.80185	36.16244	Fragment of femur of Tyrannosauridae, indeterminate (also SMP VP-1.113)	Kimbeo	166	1.6	58	
11-C	072598-1C	Limb bone	2.4	SWSW 4, 22N, 9W	107.80032	36.16340	Fragment from fragmented limb bone	Kimbeo	247	4.7	541	
11-D	P-35957	Sauropod femur	4.6	SESW 4, 22N, 9W	107.79382	36.16375	Large femur of <i>Alamosaurus sanjuanensis</i> - (from S.G. Lucas)	Kimbeo	89	5.2	247	
									Mean	422	6.6	1624
									Std. Dev.	269	3.8	1920
									Median	386	5.2	1149
									MIN	33	1.6	38
									MAX	834	14	6174
KIRTLAND FORMATION - CRETACEOUS												
Figure designation	Sample No.	Sample of:	Meters Below Base of OA	Location	1/41/4 Sec., Tsp. R.	Longitude	Latitude	Notes	Quadrangle	U (ppm)	La/b(n)	Sum REE
1-FSS	040403	Bone fragment	213.4	NENE 24, 30N, 15W	108.36338	36.80334	Single bone fragment (collected by L. Kaitenback and C. Griffith)	Youngs Lake	9	13.9	2882	
4-A(1)	070498-B	Ceratops frill	9.1	SWNE 31, 25N, 12W	108.14788	36.35922	Bone fragment from lag deposit	Alamo Mesa West	22	17.1	5231	
4-A(2)	070498-8A	Vertebra	9.1	SWNE 31, 25N, 12W	108.14788	36.35922	Bone fragment from lag deposit	Alamo Mesa West	14	14.2	3934	
4-A(3)	070498-8B	Limb bone	9.1	SWNE 31, 25N, 12W	108.14788	36.35922	Bone fragment from lag deposit	Alamo Mesa West	2	20.9	955	
4-A(4)	070498-8C	Turtle limb bone	9.1	SWNE 31, 25N, 12W	108.14788	36.35922	Bone fragment from lag deposit	Alamo Mesa West	45	27.2	2865	
4-A(5)	090498-8X	Limb bone	9.1	SWNE 31, 25N, 12W	108.14788	36.35922	Bone fragment from lag deposit	Alamo Mesa West	45	14.6	2070	
4-A(6)	090498-8Y	Limb bone	9.1	SWNE 31, 25N, 12W	108.14788	36.35922	Bone fragment from lag deposit	Alamo Mesa West	25	18.2	5626	
4-E	022899-A	Limb bone	54.9	SWNE 31, 25N, 12W	108.13891	36.34727	Fragment of thin bone protruding from ss rib	Alamo Mesa West	2	22.4	2091	
4-D	020203-A	Large femur	10.7	NWNW 33, 25N, 12W	108.12511	36.36464	Fragment of large femur	Alamo Mesa West	14	11.2	2073	
4-O	SMP VP-1468	Large femur	6.1	SESE 17, 24N, 11W	108.07360	36.34083	Small black to reddish fragment (from R.M. Sullivan)	Alamo Mesa East	27	5.6	261	
4-M	022799-D	Limb bone	6.1	SENE 17, 24N, 11W	108.02802	36.31428	Bone fragment	Alamo Mesa East	27	6.2	378	
11-A	072598-6C	Turtle-bone	18.3	NENE 8, 22N, 9W	107.80543	36.16004	Small turtle-bone fragment	Kimbeo	38	3.9	5610	
59-A	110803-A	Hadrosaur metatarsal	39.6	SWSW 8, 20N, 6W	107.50146	35.97507	Hadrosaurid, indeterminate	Star Lake	2	9.7	3010	
59-B	040104	Limb bone	12.2	CNE16, 20N, 6W	107.47317	35.96781	Bone fragment from limb bone	Star Lake	4	13.1	66	
59-C	110803-B	Fragmented femur	0.1	NENE16, 20N, 6W	107.47122	35.97008	Fragment of specimen UNMTOA-2 (originally labeled from Ojo Alamo)	Star Lake	30	7.7	2705	
									Mean	20	13.7	2650
									Std. Dev.	15	6.9	1912
									Median	23	13.7	2398
									MIN	2	3.9	66
									MAX	45	27.2	5626
									Ratios of Means Ojo Alamo/Kirtland	21	0.5	0.6
Samples from collection site 020203 are not included in data set because they were from vertebrate fragments that may not be in place												
4-C(1)	020203-B	Bone fragment	10.6	NWNE32, 25N, 12W	108.13005	36.36271	Bone eroded from overlying Ojo Alamo	Alamo Mesa West	110	5.4	6428	
4-C(2)	020203-T	Turtle shell	10.6	NWNE32, 25N, 12W	108.13005	36.36271	Turtle-shell fragment eroded from overlying Ojo Alamo Sandstone	Alamo Mesa West	86	6.0	7410	

NOTES: Chemical analyses by J.R. Budahn, USGS, Denver; chemistry data for 18 samples in blue were published in Fassett et al. 2002; 14 samples in brown published here for first time. Samples with numbers that are dates collected by J.E. Fassett (except for sample 040403) on dates shown; other analyzed samples from R.M. Sullivan and S.G. Lucas, as shown; samples ordered from west to east.

TABLE 3. CHEMICAL COMPOSITION OF NEW VERTEBRATE-BONE SAMPLES FROM OJO ALAMO SANDSTONE AND KIRTLAND FORMATION, SAN JUAN BASIN, NM														
Sample number	Kirtland Formation						Ojo Alamo Sandstone						Provenance uncertain	
	040403	020203-A	VP-1468	110803-A	040104	110803-B	VP-1494	020103	P-19147	VP-1625	051504	P-35957	020203-B	020203-T
Distance in m from base of Ojo Alamo	213	10.7	6.1	39.6	12.2	0.1	3.5	4.6	6.1	4.9	3.7	4.6	10.6	10.6
	below	below	below	below	below	below	above	above	above	above	above	above	below	below
Major and minor elements (wt%)														
Ca	29.1	37.0	23.0	30.3	24.3	30.3	34.9	32.0	29.4	36.2	37.9	22.5	32.8	25.9
Fe	0.26	0.37	18.40	1.15	0.46	1.15	0.50	0.38	0.289	0.66	0.37	0.33	0.66	10.60
Na	0.55	0.24	0.43	0.50	0.02	0.504	0.24	0.38	0.738	0.32	0.30	0.29	0.35	0.33
Trace elements (ppm)														
Sc	2.5	1.9	0.4	8.6	0.8	8.6	0.6	3.2	3.2	5.3	0.7	1.2	4.3	19.7
Co	0.9	0.9	5.2	4.2	7.2	4.2	6.3	38.2	3.9	27.4	15.3	137.0	2.9	6.2
Zn	142.0	114.0	78.6	185.0	4.8	185.0	43.0	235.0	60.1	109.0	61.3	158.0	278.0	398.0
As	0.7	2.3	14.7	5.2	21.5	5.2	13.2	11.3	2.7	13.5	10.6	3.6	6.1	31.0
Sb	0.4	0.3	14.8	1.7	0.2	1.7	1.1	1.7	0.4	1.3	1.2	0.6	1.0	6.4
U	9.0	13.9	26.6	2.0	3.9	29.6	657.0	190.0	681.0	386.0	312.0	89.0	110.0	85.5
Th	0.38	0.35	0.10	3.8	0.04	3.8	0.20	0.94	1.5	0.43	0.21	0.16	0.66	0.88
Hf	0.15	0.04	0.16	2.2	0.01	2.2	0.14	1.04	1.5	0.22	1.05	0.24	0.37	0.84
Ta	0.02	0.03	0.05	0.27	0.02	0.27	0.01	0.06	0.12	0.02	0.02	0.03	0.05	0.07
La	1228	1672	302	2122	35.7	660	86.5	3633	341	749	916	229	3441	3666
Ce	1060	867	91.3	1080	29.4	1080	3.4	2410	549	525	409	88.6	2370	2710
Nd	839	409	33.3	513	17.6	513	1.7	1380	224	361	203	40.6	1670	1870
Sm	200	86.6	7.0	120	3.5	120	0	308	43.1	85.3	53.5	9.9	420	556
Eu	46.5	18.8	1.8	30.9	0.72	30.9	0.14	75.6	12.6	20.7	16.1	2.2	79.5	95.1
Gd	269	98.1	13.0	172	2.5	172	0.60	402	72	123	97.4	15.9	493	670
Tb	39.1	15.1	2.2	24.7	0.37	24.7	0.13	60.5	9.1	18.9	15.4	2.5	74.7	103.0
Ho	21.5	17.1	3.8	29.1	0.36	29.1	0.48	63.6	11.0	26.1	18.1	3.5	73.8	95.4
Tm	4.1	5.3	1.7	10.3	0.11	10.3	0.44	12.5	3.4	7.1	7.4	1.6	21.3	21.9
Yb	18.6	31.4	11.3	57.8	0.57	57.8	2.9	66.0	19.2	39.3	39.3	9.3	135	129
Lu	2.2	4.6	1.7	7.0	0.07	7.0	0.55	7.8	2.8	5.2	5.1	1.4	20.5	19.8
Sum REE	2882	2073	261	3010	66.0	2705	38.0	5916	1287	1445	1149	247	6428	7410
La/Yb(N)	13.9	11.2	5.6	9.7	13.1	7.7	6.2	11.6	12.0	4.0	4.9	5.2	5.4	6.0
Mean U	14.2						Mean U	386					Mean U	97.75
Mean Sum Ree	1833						Mean Sum Ree	1680					Mean Sum Ree	6919
Mean La/Yb(n)	10.2						Mean La/Yb(n)	7.3					Mean La/Yb(n)	5.7

Notes: Chemical analyses by J. R. Budahn, USGS, Denver, CO; additional elements (K, Rb, Ca, Cr, Zr, W, Se, Ni, Au, Br, Mo) not tabulated because reported analytical precision resulting from interelement interferences, fission yield corrections, and/or counting statistics typically exceeds 15% (relative standard deviation). (n)--chondrite-normalized abundance

TABLE 4. SUMMARY STATISTICS FOR CHEMICAL PARAMETERS DISTINGUISHING KIRTLAND FORMATION BONES FROM OJO ALAMO SANDSTONE BONES

Chemical parameter	Ojo Alamo Sandstone (15 samples)					Kirtland Formation (15 samples)				
	Minimum	Maximum	Median	Mean	Standard deviation	Minimum	Maximum	Median	Mean	Standard deviation
U	33	834	436	447	298	2	45	25	24	16
La _n /Yb _n	2	14	5	6	4	4	27	17	16	8
Sum REE	38	6174	1004	1587	1883	66	5626	2865	3196	2000

Note: n = chondrite-normalized abundance.

TABLE 6. PUBLISHED PALYNOFORM LISTS FROM OJO ALAMO SANDSTONE TYPE AREA

Locality SGL 00-046	Locality P4300 & BAA-3	Locality D6901	Locality D6880	Locality D6391 & BAA-1	Locality BAA-2
Upper Kirtland Fm.	Upper Kirtland Fm.	Uppermost Kirtland Fm.	Upper Ojo Alamo Ss.	Uppermost Ojo Alamo Ss.	Lowermost Nacimiento Fm.
<i>Arecipites reticulatus</i>	<i>Arecipites reticulatus</i>	<i>Araucariacites australis</i> <i>Arecipites reticulatus</i>	<i>Arecipites reticulatus</i> <i>Arecipites</i> sp.	<i>Arecipites</i> cf. <i>A. microreticulatus</i>	<i>Arecipites</i> cf. <i>A. reticulatus</i>
		<i>Azolla cretacea</i>	<i>Brevicolporites colpella</i>	<i>Azolla</i> cf. <i>A. schopfi</i>	
			<i>Cercidiphyllites</i> sp.		
			<i>Chenopodipollis</i> sp.		
			<i>Corollina torosa</i>		
			<i>Cupanioidites</i> sp.		<i>Cupanioidites</i> cf. <i>C. major</i>
		<i>Cupuliferoideaepollenites minutus</i>	<i>Cupuliferoideaepollenites minutus</i>		
		<i>Cyathidites minor</i>			
<i>Cycadopites fragilis</i>					
<i>Dyadonapites reticulatus</i>		<i>Dyadonapites reticulatus</i>	<i>Fraxinopollenites variabilis</i>		
		<i>Ghoshispora</i> sp.			
		<i>Laevigatosporites</i> sp.	<i>Laevigatosporites</i> spp.		
		<i>Liliacidites hyaliniatus?</i>			
		<i>Liliacidites leei</i>			
		<i>Liliacidites leei</i>			
		<i>Liliacidites</i> sp. of Anderson			
		<i>Momipites inaequalis</i>	<i>Momipites inaequalis</i>	<i>Momipites inaequalis</i>	
		<i>Momipites</i> sp.			
		<i>Momipites tenuipolus</i>	<i>Momipites tenuipolus</i>	<i>Momipites tenuipolus</i>	<i>Momipites</i>
		<i>Osmundacidites wellmannii</i>			
		" <i>Palaeoisoetes</i> " sp.	<i>Ovoidites</i> sp. " <i>Palaeoisoetes</i> " sp.		
			" <i>Palaeoisoetes</i> " sp.		
			" <i>Palaeoisoetes</i> " sp.		
		<i>Pandanidites typicus</i>	<i>Pandanidites radicus</i> <i>Pandanidites typicus</i>		<i>Paliurus triplicatus?</i>
				<i>Pinus</i> sp.	
		<i>Pityosporites</i> spp.	<i>Pityosporites</i> sp. <i>Podocarpus</i> sp.		<i>Podocarpus</i> sp.
			<i>Polypodiisporonites</i> sp.		
			<i>Psilastephanocolpites</i> sp.		
			" <i>Quercus</i> " <i>explanata</i>	<i>Quercus explanata</i>	<i>Quercus</i> sp.
<i>Proteacidites retusus</i>	<i>Proteacidites retusus</i>	<i>Proteacidites retusus</i>			
<i>Proteacidites thalmannii</i>	<i>Proteacidites thalmannii</i>	<i>Proteacidites thalmannii</i>			
		<i>Rhoipites</i> sp.		<i>Rectosulcites latus</i>	<i>Rectosulcites latus</i>
<i>Schizosporis parvus</i>			<i>Syncolporites minimus</i>		
		<i>Taxodiaceaeepollenites hiatus</i>	<i>Tetracolpites</i> 2 sp.		
		<i>Tetraporina</i> sp.			
			<i>Tricolpites anguloluminosus</i>		
			<i>Tricolpites foveolate</i>		
		<i>Tricolpites interangulus</i>	<i>Tricolporites rhomboides</i>		
			<i>Tricolpites scabrata</i>		
<i>Tricolpites microreticulatus</i>					
<i>Tricolpites reticulatus</i>					
		<i>Tricolpites?</i> sp. cf. <i>Gurneria</i>			
		<i>Tricolpites</i> spp.			
<i>Ulmipollenites kremplii</i>	<i>Ulmipollenites</i>	<i>Ulmipollenites kremplii</i>	<i>Ulmipollenites kremplii</i> <i>Ulmipollenites</i> 3 and 4 pores <i>Ulmoidelipites tricoastatus</i>	<i>Ulmipollenites tricoastatus</i>	<i>Ulmoidelipites tricoastatus</i>
		" <i>Ulmoidelipites?</i> " <i>tricoastatus</i>			

Notes: Palynomorphs identified by the following: SGL 00-046 by D. R. Braman in Sullivan et al. (2005, p. 401); P4300, D6901, and D6880 by D. J. Nichols in Fassett et al. (2002, table 2); By R. H. Tschudy in Fassett et al. (1987, p. 27); BAA-1, -2, -3 by R. Y. Anderson in Baltz et al. (1966, p. D17), complete lists of palynomorphs not available for the BAA localities and the few species identified at BAA-1 and -3 localities are combined with lists for D6391 and P4300, respectively; samples P4300 and SGL 00-046 from same carbonaceous shale bed at same locality; sample localities shown on Figures 4 and 51.

TABLE 7. LIST OF PALYNOMORPHS IDENTIFIED BY R. H. TSCHUDY IN FASSETT AND HINDS (1971, TABLE 1) AT MESA PORTALES AND TWO OTHER LOCALITIES IN SAN JUAN BASIN								
Age	Palynomorphs	U. S. Geological Survey paleobotany locality numbers						
		Paleocene			Cretaceous			
		D3738-A	D3738-B	D3803	D3738-C	D4017-A	D4017-B	D4017-C
P	<i>Momipites</i> sp. (<i>Momipites inaequalis</i> And.)	X		X				
P	<i>Monosulcites</i> sp. (<i>Rectosulcites latus</i> And.)	X		X				
P	<i>Triatriopollenites</i> sp. A	X						
P	<i>Triatriopollenites</i> sp. B	X						
P, K?	<i>Cupaneidites</i> sp. (<i>Cupaneidites</i> aff. <i>C. major</i> And.)	X	X			X		
	<i>Laevigatosporites</i> sp (<i>Polypodiidites</i> sp. And.)	X						
P	<i>Tricolporites</i> sp. (<i>Tricolporites anguloluminosus</i> And.)	X		X				
P, K	<i>Tricolpopollenites</i> sp. (<i>Quercus explanata</i> And.)	X		X		X		X
	<i>Abietinaepollenites</i> sp. (<i>Podocarpus sellowiformis</i> And.)	X	X		X			
	<i>Classopollis</i> sp.		X					
	<i>Abietinaepollenites</i> sp. (<i>Podocarpus northrupi</i> And.)		X					
P, K	<i>Zlivisporis</i> sp.		X		X			
P, K	<i>Ulmipollenites</i> sp. (<i>Ulmoideipites tricostatus</i> And.)		X		X	X		X
P, K	<i>Liliacidites</i> sp.		X		X			
P	<i>Pollyporopollenites</i> sp.		X					
P	<i>Tricolporites</i> sp. (<i>Tricolporites rhomboides</i> And.)			X				
P	<i>Tricolporites</i> sp.			X				
	<i>Tricolporites</i> sp. (? <i>Eleagnaceae</i>)			X				
	<i>Osmundacidites</i> sp.			X				
P	<i>Tricolporites</i> sp.			X				
K	<i>Proteacidites</i> (<i>Proteacidites thalmanii</i> And.)				X	X	X	X
K	<i>Proteacidites</i> (<i>Proteacidites retusus</i> And.)				X			
K	<i>Monoporopollenites</i> sp.				X			
K	<i>Araucariacites</i> sp.				X	X	X	
	<i>Erdtmannipollis</i> sp.				X			
K	<i>Granabivesiculites</i> sp.				X			
P, K	<i>Liliacidites</i> sp. (<i>Liliacidites leei</i> And.)				X	X		X
P, K	<i>Liliacidites</i> sp. (<i>Liliacidites hyalaciniatus</i> And.)				X			
	<i>Liquidambarpollenites</i> sp.				X			
K	<i>Tricolpites interangulus</i> Newman					X		
	<i>Tricolpopollenites</i> sp.					X	X	X
	<i>Eucommiidites</i> sp.					X	X	X
	<i>Foveosporites</i> sp. cf. <i>F. canalis</i> Balme						X	
	<i>Inaperturopollenites</i> cf. <i>I. hiatus</i> (R. Pot) Th. & Pf.						X	
K	<i>Ephedra</i> sp. cf. <i>E. voluta</i> Stanley						X	X
K	<i>Zonalapollenites</i> sp.						X	
K	<i>Neoraistrickia</i> sp.							X
K	<i>Tricolpopollenites</i> sp. A							X
K	<i>Monosulcites</i> sp.							X
K	<i>Tricolporites</i> sp.							X
K	<i>Tricolpopollenites</i> sp. B							X
K	<i>Tiliaepollenites</i> sp. (<i>Tilia wodehousei</i> And.)							X
P, K	<i>Tricolpopollenites</i> sp. C							X

Note: Palynomorphs listed by age; generally youngest to oldest going down and left to right; *Proteacidites* was renamed *Tschudyipollis* by Nichols (2002); D3738-A, -B from Ojo Alamo Sandstone, D3803 from Nacimiento Formation, all other samples from Kirtland and (or) Fruitland Formation; sample locality for sample D4119 shown on Figure 1, all other sample localities shown on figure 21. In left column P = Paleocene, K = Cretaceous

TABLE 8. LIST OF PALYNOMORPHS IDENTIFIED BY R. H. TSCHUDY (1973) FROM SAMPLES OF GASBUGGY CORE; MODIFIED FROM TSCHUDY (1973) APPENDIX TABLE

Palynomorphs	Nacimiento Formation		Ojo Alamo Sandstone						Fruitland Formation																	
	3436.6	3453.5-3455.8	3515.6	3574.4	3584	3619.6	3638.1	3655.8	3714.7	3716.5	3725.8	3752.5	3757.5	3775	3790.3	3805	3807.5	3811.9	3824.6	3844	3851-3853	3869-6-3870	3879.5-3881.4	3906-3907.8	3912-3913	
<i>Nyssa puercoensis</i>	X			X		1			1																	
<i>Biretisporites</i> sp.		1			2		1	X			1	X	1								1	1				X
Unclassified triletes	2	2	x						13	11	3	12	5	19	10	5	5	9	1	1	10	7	3	3	3	X
<i>Laevigatosporites</i> sp.		7	X			1	1	X	10	10	19	7	9	14	13	13	11	7	28	25	10	3	3	3	3	
Unclassified bisaccates		32			10	1	3		1	1	1	1	2	X	8	X		X				2	1			
<i>Classopollis</i> sp.		28	1	X	60	3	21				1	5	X			X					23	2				
<i>Taxodiaceapollenites</i> sp.		1			2		4			1		X	X	1						1	3	1				
<i>Equisetosporites</i> spp.		5							1	3	1	X	X	X			1	2					3			
cf. <i>Ephedra voluta</i>		4			5		1																			
<i>Liliacidites complexus</i>		1			1		2		2	1				1	2	8	3	1	1	6	7				24	
<i>Salixipollenites</i> sp.		1																								
<i>Pandaniidites radicus</i>		1													1			X								
<i>Engelhardtia</i> type		1	X		3	46	X	X	1												X					
<i>Momipites sanjuanensis</i>		4			2	1	2		7	4	8		2	7	1	3	8	X	2	1	2	3	20		X	
<i>Periporopollenites</i> sp.		2			2	X	4																			
<i>Ulmipollenites</i> spp.		9			2		7										1									
Hystriospheraeids & dinoflagellates		X				X																				
<i>Cyathidites</i> spp.			X		1	X	X	X	3	1	4	9	3	8	2	2	1	1			1	2	1			
<i>Stereisporites</i> spp.			X						1	X	X		1		X		X					1	4			
<i>Cyrilla minima</i>		98						X				1		2	1						1			1	4	
<i>Maceopolipollenites tenuipolus</i>		1																								
<i>Echinatisporis</i> sp.					1				1		1	X	X								1	6			18	
<i>Arecipites</i> spp.					3	4	22		4	2	4	1	2	3	5	1	3	2	1	18	1		2			
<i>Aquilapollenites</i> spp.					1																	1				
cf. <i>Tripoporipollenites rugatus</i>											1		1	X	X	3	X	1	2	X				56	1	
<i>Deltoidospora</i> spp.						X													X							
<i>Tricolpites anguloluminosus</i>						X	X																			
<i>Tricolpites vulgaris</i>						X																			1	
cf. <i>Cupanioidites</i>						X																				
<i>Vitis? affluens</i>					X	35	X						1								X	X	X		2	
<i>Quercus explanata</i>						2						1				X		X							1	
Unclassified triporates					1	3	1	X	2	3		3	1	4	1	2	6	1	4			7	6	4	2	
<i>Tricolpites</i> sp.							1						X		X		X	X	X	2					1	
<i>Cupanioidites major</i>							X																			
<i>Quadrupollenites</i> sp.							X																		1	
<i>Tricolporites rhomboides</i>							X											X	4							
<i>Ericaceipollenites</i> sp.	PALEOCENE						1		3	1				1	X	X	1	X	X							
<i>Proteacidites</i> spp.	CAMPANIAN					2	X		14	14	25	28	12	12	19	17	9	24	15	2	6	17	11	X	4	
<i>Foraminisporis</i> sp.							X				1	3	X	X	X	X								X		
cf. <i>Concavisporites verrucosus</i>									X		1				2											
<i>Ghoshispora</i> spp.									2	1			2	X	1	2	2	2				5				
<i>Cicatricosisporites</i> spp.									1		X	X		X								X	2			
<i>Liliacidites</i> spp.									2		1		2								2					
<i>Tricolpites reticulatus</i>									18			1	X	X	9	8	7		X	X	1	X	1			
<i>Accuratipollis</i> spp.									2	1		X		8		1	6	6	3		X		1		1	
<i>Illexpollenites</i> sp.									2		4	23	29	3	5	4	3	11	4			1	8			
cf. <i>Tilia wodehousei</i>									1		1						X					1				
cf. <i>Taurocusporites</i>											1	X	X		2				X							
<i>Lycopodiacidites</i> spp.											1	X	X		2											
<i>Camarozonosporites</i> spp.											X														1	
<i>Lycopodiumsporites</i> spp.											2				X		X									
<i>Microfoveolatosporis canaliculatus</i>											1			1	2	2	1	2	X	4	1		1	X	X	
<i>Araucariacites</i>											1															
<i>Zonalapollenites</i>											1						1			5	X					
cf. <i>Radialetes costatus</i>											1															
<i>Aquilapollenites quadrilobus</i>											1			X	X					X						
<i>Triplanosporites</i> sp.												1														
cf. <i>Zlivisporis</i>												1	X			1						1				
<i>Tricolpites</i> sp.												3														
cf. <i>Minorpollis</i>												X										1				
<i>Aequitriradites spinulosus</i>													1												1	
<i>Aquila 36 C</i>													1													
<i>Alsophilidites</i> sp.													1													
<i>Gleicheniidites</i> spp.													1				X	X	2					X		
<i>Polypodiidites</i> sp.													1				X							1		
<i>Vitis? affluens</i> (C ₃ -r 43)													1					X	1						1	
<i>Aquilapollenites turbidus</i>													1			X	X	X	1							
<i>Aquilapollenites attenuatus</i>													X	X				X								
<i>Leptolepidites major</i>													1												X	
<i>Aquilapollenites 18</i>														X												
<i>Kuylisporites</i> sp.																1									X	
<i>Klukisporites</i> spp.																X			1						X	
<i>Phaseolidites stanleyi</i>															2				X	3					1	
<i>Aquilapollenites 4E</i>																										

TABLE 10. COMPARISON OF PALYNOMORPH LISTS FROM FOUR PALYNOLOGISTS FOR SAN JUAN RIVER SITE SAMPLES, SAN JUAN BASIN, NM			
Locality R3508 - Frederiksen	Localities 6877-A, -B, -C - Nichols	Locality SGL 00-047 - Braman	Locality "Near Farmington" - Newman
		<i>Alisporites bilateralis</i>	
	<i>Arecipites reticulatus</i>	<i>Arecipites reticulatus</i>	
	<i>Arecipites</i> sp.		
	<i>Azolla cretacea</i>		
			<i>Balmeisporites</i>
	<i>Brevicolporites colpella</i>		
	<i>Chenopodipollis</i> sp.		
	<i>Cicatricosisporites</i> spp.		
		<i>Circulina parva</i>	
		<i>Classopollis classoides</i>	
	<i>Corollina torosa</i> (incl. monads and tetrads)		
	<i>Cupanieidites</i> sp.		
		<i>Cupanieidites</i> cf. <i>C. reticularis</i>	
	<i>Cupuliferoideaepollenites minutus</i>		
	<i>Cyathidites minor</i>	<i>Cyathidites minor</i>	
		<i>Cycadopites fragilis</i>	
		<i>Equisetosporites lajwantis</i>	
	<i>Fraxinopollenites variabilis</i>		
			<i>Gunnera</i>
			<i>Interpollis</i>
			<i>Kurtzipites</i>
	<i>Laevigatosporites</i> sp.		
		<i>Laevigatosporites haardtii</i>	
<i>Lycopodium novomexicanum</i>			
<i>Momipites inaequalis</i>	<i>Momipites inaequalis</i>		
<i>Momipites tenuipolus</i>	<i>Momipites tenuipolus</i>	<i>Momipites tenuipolus</i>	
	<i>Nyssapollenites</i> sp.		
		<i>Nyssapollenites explanatus</i>	
		<i>Ovoidites ligneolus</i>	
	" <i>Palaeoisoetes</i> " sp.		
" <i>Paliurus</i> " <i>triplicatus</i>	" <i>Paliurus</i> " <i>triplicatus</i>		
<i>Pandaniidites</i>	<i>Pandaniidites typicus</i>	<i>Pandaniidites typicus</i>	
	<i>Pityosporites</i> sp.		
<i>Proteacidites</i>		<i>Proteacidites thalmanii</i>	<i>Proteacidites</i>
<i>Rectosulcites latus</i>			
		<i>Schizosporis parvus</i>	
	<i>Taxodiaceaeepollenites hiatus</i>	<i>Taxodiaceaeepollenites hiatus</i>	
		<i>Taxodiaceaeepollenites vacuipites</i>	
	<i>Tricolpites</i> sp.		
	<i>Triporetetes novomexicanum</i>		
		<i>Triporetetes simplex</i>	
<i>Ulmipollenites krempii</i>	<i>Ulmipollenites krempii</i>		
<i>U. tricostatus</i>	<i>U. tricostatus</i>		
		<i>Ulmoideipites krempii</i>	
			<i>Ulmoideipites</i> spp. 3 and 4 pored smooth to verrucate forms

Note: Samples analyzed by Frederiksen and Nichols (USGS) and by Braman (Royal Tyrell Museum of Paleontology) from same bed of coaly-carbonaceous shale 15 m above base of Ojo Alamo Sandstone; sample analyzed by Newman (Colorado School of Mines, retired) from a stratigraphically lower mudstone bed of uncertain stratigraphic provenance; palynomorph identifications in written commun. from: Frederiksen (1985), Nichols (1994), and Braman (2000) and in Newman (1987, p. 159); palynomorph list headed "Localities 6877-A, -B, -C" was labeled "25Ga, b, c, composite list" in Fassett and others (2002, table 2); *Lycopodium novomexicanum* (Nacimiento 2 florule) is now *Zlivisporis novomexicanum* (Nichols 2005, written commun.).

TABLE 11. LIST OF PALYNOMORPHS IDENTIFIED FROM USGS DRILL HOLE SL 10-1, POT MESA LOCALITY (FIGURE 59) SOUTHERN SAN JUAN BASIN, NEW MEXICO					
Depths in meters (feet)	28.6 m (93.8 ft)	28.8 m (94.5 ft)	29.4 m (96.6 ft)	65.5 m (215 ft)	66.6 m (218.5 ft)
U. S. Geological Survey locality number	D5783-A	D5783-B	D5783-C	D5783-D	D5783-E
<i>Equisetosporites</i> 5	X	X			
<i>Corollina</i>	X	X			
<i>Abietineaepollenites</i>	X	X			X
<i>Periporopollenites</i>	X	X			X
<i>Foraminisporis</i>	X	X			
<i>Lycopodiumsporites</i>	X	X			
<i>Zlivisporis</i>	X	X			
<i>Aequitriradites</i>	X	X			
<i>Balmeisporites</i>	X	X			
<i>Lycopodiacidites</i>	X	X	X	X	
<i>Azolla</i>	X				
<i>Liliacidites</i>	X				
<i>Pterospermopsis</i>	X				
<i>Proteacidites</i>	X	X	X	X	X
<i>cf Vitis affluens</i>		X			
<i>Ulmipollenites</i>		X	X		X
<i>Monosulcites</i>		X			
<i>Osmundacidites</i>		X			
<i>Taxodiaceaeapollenites</i>		X	X		X
<i>Kurtzipites trispissatus</i>		X			
<i>Quercus explanata</i>		X			
<i>Nyssapollenites albertensis</i>		X			
<i>Momipites sanjuanensis</i>				X	X
<i>Microfoveolatosporis</i>				X	
<i>Dinoflagellate</i>					X
<i>Alnipollenites</i>					X
<i>Tricolpites vulgaris</i>					X
<i>Rugubivesiculites</i>					X
<i>Echinatisporis</i>					X
<i>Aquilapollenites</i>					X
<i>Tricolporites rhomboides</i>					X
<i>Gleicheniidites</i>					X
<i>Pseudoplicapollis</i>					X
<i>Cicatricosisporites</i>					X
<i>Camarozonosporites</i>					X
<i>Klukisporites</i>					X

Note: Palynomorphs listed by age; generally youngest to oldest going down; identifications by R. H Tschudy (1977, written commun.); *Proteacidites* renamed *Tschudypollis* by Nichols (2002)

TABLE 12. COMPARISON OF PALYNOMORPH LISTS IDENTIFIED FROM POT MESA AREA SAMPLES (FIGURE 60) ALL SAMPLES FROM CRETACEOUS KIRTLAND FORMATION		
Localities D5783-A, -B, -C, -D, -E	Locality D6879	Newman locality
Identification by R. H. Tschudy (1977)	Identification by D. J. Nichols (1994)	Identification by K. Newman (1987)
<i>Abietinaepollenites</i>		
<i>Aequitriradites</i>		
<i>Alnipollenites</i>		
<i>Aquilapollenites</i>		
<i>Azolla</i>	<i>Azolla cretacea</i>	
<i>Balmeisporites</i>		<i>Balmeisporites</i>
<i>Camarozonosporites</i>		
	<i>Chenopodipollis</i> sp.	
<i>Cicatricosisporites</i>		
<i>Corollina</i>	<i>Corollina torosa</i>	
	<i>Cupanieidites</i> sp.	
	<i>Cupuliferoidaepollenites minor</i>	
	<i>Cyathidites minor</i>	
<i>Dinoflagellate</i>		
<i>Echinatisporis</i>		
	<i>Ephedra multicosata</i>	
<i>Equisetosporites</i> 5		
	<i>Erdtmanipollis cretacea</i>	
<i>Foraminisporis</i>		
	<i>Fraxinopollenites variabilis</i>	
<i>Gleicheniidites</i>		
	<i>Gunnera microreticulata</i>	<i>Gunnera</i>
		<i>Interpollis</i>
<i>Klukisporites</i>		
<i>Kurtzipites trispissatus</i>	<i>Kurtzipites trispissatus</i>	<i>Kurtzipites</i>
	<i>Laevigatosporites</i> sp.	
<i>Liliacidites</i>	<i>Liliacidites complexus</i>	
	<i>Liliacidites leei</i>	
<i>Lycopodiacidites</i>		
<i>Lycopodiumsporites</i>		
<i>Microfoveolatosporis</i>		
<i>Momipites sanjuanensis</i>		
<i>Monosulcites</i>		
<i>Nyssapollenites albertensis</i>		
	<i>Nyssapollenites</i> sp.	
<i>Osmundacidites</i>		
	" <i>Palaeoisoetes</i> " sp.	
	<i>Pandaniidites typicus</i>	
<i>Periporopollenites</i>		
<i>Proteacidites</i>	<i>Proteacidites retusus</i>	<i>Proteacidites</i>
	<i>Proteacidites thalmannii</i>	
<i>Pseudoplicapollis</i>		
	<i>Pseudoschizaea</i>	
<i>Pterospermopsis</i>		
<i>Quercus explanata</i>		
<i>Rugubivesiculites</i>		
<i>Taxodiaceapollenites</i>		
	" <i>Tilia</i> " <i>wodehousei</i>	
<i>Tricolpites vulgaris</i>		
<i>Tricolporites rhomboides</i>		
	<i>Triporoletes novomexicanum</i>	
<i>Ulmipollenites</i>		
	<i>Ulmipollenites tricostatus</i>	
		<i>Ulmoideipites</i> spp.3 and 4 pored smooth to verrucate forms
cf <i>Vitis affluens</i>		
<i>Zlivisporis</i>		

Note: *Proteacidites* renamed *Tschudyipollis* by Nichols (2002); list of palynomorphs identified by Tschudy is composite from five drill-hole samples from drill hole USGS SL 10-1 (Figure 59); palynomorph lists for each sample on Table 11

TABLE 11. LIST OF PALYNOMORPHS IDENTIFIED FROM USGS DRILL HOLE SL 10-1, POT MESA LOCALITY (FIGURE 59) SOUTHERN SAN JUAN BASIN, NEW MEXICO					
Depths in meters (feet)	28.6 m (93.8 ft)	28.8 m (94.5 ft)	29.4 m (96.6 ft)	65.5 m (215 ft)	66.6 m (218.5 ft)
U. S. Geological Survey locality number	D5783-A	D5783-B	D5783-C	D5783-D	D5783-E
<i>Equisetosporites</i> 5	X	X			
<i>Corollina</i>	X	X			
<i>Abietineaepollenites</i>	X	X			X
<i>Periporopollenites</i>	X	X			X
<i>Foraminisporis</i>	X	X			
<i>Lycopodiumsporites</i>	X	X			
<i>Zlivisporis</i>	X	X			
<i>Aequitriradites</i>	X	X			
<i>Balmeisporites</i>	X	X			
<i>Lycopodiacidites</i>	X	X	X	X	
<i>Azolla</i>	X				
<i>Liliacidites</i>	X				
<i>Pterospermopsis</i>	X				
<i>Proteacidites</i>	X	X	X	X	X
<i>cf Vitis affluens</i>		X			
<i>Ulmipollenites</i>		X	X		X
<i>Monosulcites</i>		X			
<i>Osmundacidites</i>		X			
<i>Taxodiaceaeapollenites</i>		X	X		X
<i>Kurtzipites trispissatus</i>		X			
<i>Quercus explanata</i>		X			
<i>Nyssapollenites albertensis</i>		X			
<i>Momipites sanjuanensis</i>				X	X
<i>Microfoveolatosporis</i>				X	
<i>Dinoflagellate</i>					X
<i>Alnipollenites</i>					X
<i>Tricolpites vulgaris</i>					X
<i>Rugubivesiculites</i>					X
<i>Echinatisporis</i>					X
<i>Aquilapollenites</i>					X
<i>Tricolporites rhomboides</i>					X
<i>Gleicheniidites</i>					X
<i>Pseudoplicapollis</i>					X
<i>Cicatricosisporites</i>					X
<i>Camazonosporites</i>					X
<i>Klukisporites</i>					X

Note: Palynomorphs listed by age; generally youngest to oldest going down; identifications by R. H Tschudy (1977, written commun.); *Proteacidites* renamed *Tschudypollis* by Nichols (2002)

TABLE 12. COMPARISON OF PALYNOMORPH LISTS IDENTIFIED FROM POT MESA AREA SAMPLES (FIGURE 60) ALL SAMPLES FROM CRETACEOUS KIRTLAND FORMATION		
Localities D5783-A, -B, -C, -D, -E	Locality D6879	Newman locality
Identification by R. H. Tschudy (1977)	Identification by D. J. Nichols (1994)	Identification by K. Newman (1987)
<i>Abietinaepollenites</i>		
<i>Aequitriradites</i>		
<i>Alnipollenites</i>		
<i>Aquilapollenites</i>		
<i>Azolla</i>	<i>Azolla cretacea</i>	
<i>Balmeisporites</i>		<i>Balmeisporites</i>
<i>Camarozonosporites</i>		
	<i>Chenopodipollis</i> sp.	
<i>Cicatricosisporites</i>		
<i>Corollina</i>	<i>Corollina torosa</i>	
	<i>Cupanieidites</i> sp.	
	<i>Cupuliferoidaepollenites minor</i>	
	<i>Cyathidites minor</i>	
<i>Dinoflagellate</i>		
<i>Echinatisporis</i>		
	<i>Ephedra multicosata</i>	
<i>Equisetosporites</i> 5		
	<i>Erdtmanipollis cretacea</i>	
<i>Foraminisporis</i>		
	<i>Fraxinopollenites variabilis</i>	
<i>Gleicheniidites</i>		
	<i>Gunnera microreticulata</i>	<i>Gunnera</i>
		<i>Interpollis</i>
<i>Klukisporites</i>		
<i>Kurtzipites trispissatus</i>	<i>Kurtzipites trispissatus</i>	<i>Kurtzipites</i>
	<i>Laevigatosporites</i> sp.	
<i>Liliacidites</i>	<i>Liliacidites complexus</i>	
	<i>Liliacidites leei</i>	
<i>Lycopodiacidites</i>		
<i>Lycopodiumsporites</i>		
<i>Microfoveolatosporis</i>		
<i>Momipites sanjuanensis</i>		
<i>Monosulcites</i>		
<i>Nyssapollenites albertensis</i>		
	<i>Nyssapollenites</i> sp.	
<i>Osmundacidites</i>		
	" <i>Palaeoisoetes</i> " sp.	
	<i>Pandaniidites typicus</i>	
<i>Periporopollenites</i>		
<i>Proteacidites</i>	<i>Proteacidites retusus</i>	<i>Proteacidites</i>
	<i>Proteacidites thalmannii</i>	
<i>Pseudoplicapollis</i>		
	<i>Pseudoschizaea</i>	
<i>Pterospermopsis</i>		
<i>Quercus explanata</i>		
<i>Rugubivesiculites</i>		
<i>Taxodiaceapollenites</i>		
	" <i>Tilia</i> " <i>wodehousei</i>	
<i>Tricolpites vulgaris</i>		
<i>Tricolporites rhomboides</i>		
	<i>Triporoletes novomexicanum</i>	
<i>Ulmipollenites</i>		
	<i>Ulmipollenites tricostatus</i>	
		<i>Ulmoideipites</i> spp.3 and 4 pored smooth to verrucate forms
cf <i>Vitis affluens</i>		
<i>Zlivisporis</i>		

Note: *Proteacidites* renamed *Tschudyipollis* by Nichols (2002); list of palynomorphs identified by Tschudy is composite from five drill-hole samples from drill hole USGS SL 10-1 (Figure 59); palynomorph lists for each sample on Table 11

TABLE 13.1. UNPUBLISHED PALYNOMORPH LISTS FROM CRETACEOUS USGS PALEOBOTANY LOCALITIES IN AND NEAR OJO ALAMO SANDSTONE				
TYPE AREA; PALEOBOTANY LOCALITIES SHOWN ON FIGURES 1, 3, and 4				
Locality D6902	Locality D6900	Locality D9157	Moncisco Mesa	Localities D8179, D8180 (composite)
Lowermost Fruitland Fm.	Uppermost Fruitland Fm.	Upper Kirtland Fm.	Uppermost Kirtland Fm.	Uppermost Kirtland Fm.
<i>Appendicisporites</i> sp.				<i>Aquilapollenites quadrilobus</i>
			<i>Aquilapollenites</i> 3 sp.	<i>Aquilapollenites</i> sp.
	<i>Arecipites</i> sp.		Bisaccate conifer	
<i>Camarozonosporites ambigens</i>	<i>Camarozonosporites ambigens</i>			
<i>Cicatricosisporites</i> sp.	<i>Cicatricosisporites</i> sp.			
	<i>Corollina torosa</i>	<i>Corollina</i> sp.		<i>Corollina</i> sp.
<i>Cupuliferoideaepollenites minutus</i>				
<i>Cupuliferoideaepollenites</i> spp.	<i>Cupuliferoideaepollenites</i> spp.			
<i>Cyathidites minor</i>	<i>Cyathidites</i> spp.			
		<i>Cycadopites</i> sp.		
<i>Echinatisporis varispinosus</i>	<i>Echinatisporis varispinosus</i>			
<i>Ephedripites</i> sp. D				<i>Erdtmanipollis cretaceus</i>
	<i>Eucommiidites minor</i>			
		<i>Ghoshispora</i> sp.		
	<i>Laevigatosporites</i> spp.	<i>Laevigatosporites</i> sp.	<i>Gunnera</i>	<i>Gunnera microreticulata</i>
			Larger fern tetrad	
<i>Liliacidites leei</i>		<i>Liliacidites leei</i>		
	<i>Liliacidites</i> sp.		<i>Liliacidites reticulata</i>	<i>Liliacidites</i> sp.
			<i>Loranthacites</i>	
	<i>Microreticulatisporites</i> sp.			
<i>Monocolopollenites?</i> sp.				? <i>Monosulcites perspinosus</i> of Anderson (1966)
<i>Nyssapollenites</i> sp.	<i>Nyssapollenites</i> spp.			
			<i>Pandaniidites</i>	
		<i>Pityosporites</i> spp.		<i>Pandaniidites typicus</i>
<i>Proteacidites retusus</i>	<i>Proteacidites retusus</i>	<i>Proteacidites retusus</i>		<i>Pityosporites</i> spp.
	<i>Proteacidites</i> spp.		<i>Proteacidites</i> spp. (many)	<i>Proteacidites</i> sp.
	<i>Pseudoplicapollis newmanii</i>	<i>Proteacidites thalmanii</i>		
<i>Pseudoplicapollis</i> sp.				
<i>Reticuloideosporites pseudomurii</i>	<i>Reticuloideosporites pseudomurii</i>			
	<i>Rhoipites</i> sp.			
<i>Stereisporites</i> spp.	<i>Stereisporites</i> spp.			
	<i>Taxodiaceaeepollenites hiatus</i>	<i>Taxodiaceaeepollenites hiatus</i>		
<i>Tricolpites</i> spp.	<i>Tricolpites</i> spp.			<i>Tricolpites</i> sp.
<i>Triporopollenites</i> spp.				
	<i>Triporopollenites tectus</i>			
		<i>Tsugaepollenites</i> sp.		
			<i>Ulmipollenites</i>	
<i>Ulmipollenites krempii</i>				<i>Ulmoideipites krempii</i>
				<i>Ulmoideipites tricostatus</i>
		unidentified trilete spores		

Note: Palynomorphs from USGS paleobotany localities D6902, D6900, and Moncisco Mesa identified by R. H. Tschudy (1976, 1983, written commun.); palynomorph identifications from other localities by D. J. Nichols (1995, 2000 written commun.); *Proteacidites* renamed *Tschudypollis* by Nichols (2002).

TABLE 13.2. UNPUBLISHED PALYNOMORPH LISTS FROM CRETACEOUS USGS PALEOBOTANY LOCALITIES IN AND NEAR THE OJO ALAMO SANDSTONE TYPE AREA (Cont.):					
PALEOBOTANY LOCALITIES SHOWN ON FIGURES 1, 3, 4, AND 51					
Locality D9156-A	Locality D9156-B	Locality 82303-E	Locality 82403-A	Locality 110303-D	Archival Split 24-5
Uppermost Kirtland Fm.	Uppermost Kirtland Fm.	Uppermost Kirtland Fm.	Uppermost Kirtland Fm.	Uppermost Kirtland Fm.	Uppermost Kirtland Fm.
<i>Arecipites microreticulatus</i>	<i>Arecipites microreticulatus</i>	<i>Arecipites columellus</i>	<i>Arecipites columellus</i>	<i>Arecipites microreticulatus</i>	<i>Arecipites microreticulatus</i>
<i>Arecipites reticulatus</i>	<i>Azolla circinata</i>	<i>Arecipites reticulatus</i>	<i>Arecipites reticulatus</i>	<i>Arecipites reticulatus</i>	
<i>Azolla circinata</i>	<i>Azolla cretacea</i> (relatively abundant)	<i>Azolla cretacea</i>	<i>Azolla cretacea</i>		<i>Azolla cretacea</i>
	<i>Azolla</i> microspores				
	<i>Cingulatisporites lancei</i>		<i>Cicatricosisporites</i> sp.		
		<i>Corollina torosa</i>	<i>Corollina torosa</i>		<i>Corollina torosa</i>
<i>Cyathidites</i> spp.	<i>Cyathidites</i> spp.	<i>Cyathidites</i> sp.			<i>Cyathidites</i> sp.
	<i>Dyadonapites reticulatus</i>	<i>Dyadonapites reticulatus</i>	<i>Dyadonapites reticulatus</i>		<i>Dyadonapites reticulatus</i>
		<i>Foraminisporis undulatus</i>	<i>Foraminisporis undulatus</i>		
<i>Ghoshispora</i> spp. (relatively abundant)		<i>Ghoshispora</i> sp.	<i>Ghoshispora</i> sp.	<i>Ghoshispora</i> sp.	<i>Ghoshispora</i> sp.
<i>Illexpollenites compactus</i>	<i>Inaperturopollenites</i> sp.			<i>Inaperturopollenites</i> sp.	
		<i>Inaperturotetradites scabratus</i>		<i>Inaperturotetradites scabratus</i>	
	<i>Laevigatosporites</i> spp.	<i>Laevigatosporites</i> sp.	<i>Laevigatosporites</i> sp.	<i>Laevigatosporites</i> sp.	<i>Laevigatosporites</i> sp.
	<i>Liliacidites leei</i>			<i>Liliacidites leei</i>	
		<i>Liliacidites</i> sp. cf. <i>L. complexus</i>	<i>Liliacidites</i> sp. cf. <i>L. complexus</i>		
<i>? Monosulcites perspinosus</i> of Anderson (1966)		<i>Momipites inaequalis</i>	<i>Momipites inaequalis</i>	<i>Momipites inaequalis</i>	<i>Momipites inaequalis</i>
		<i>Osmundacidites stanleyi</i>	<i>Osmundacidites stanleyi</i>		<i>Osmundacidites stanleyi</i>
		<i>Palaeoisoetes subengelmannii</i>	<i>Palaeoisoetes subengelmannii</i>		<i>Palaeoisoetes subengelmannii</i>
		<i>Pandaniidites typicus</i>	<i>Pandaniidites typicus</i>	<i>Pandaniidites typicus</i>	<i>Pandaniidites typicus</i>
<i>Pityosporites</i> spp. (relatively abundant)	<i>Pityosporites</i> spp. (common)	<i>Pityosporites typicus</i>	<i>Pityosporites</i> sp.	<i>Pityosporites</i> spp. (common)	<i>Pityosporites</i> sp.
<i>Proteacidites thalmanii</i>	<i>Proteacidites</i> sp. cf. <i>P. retusus</i>				
	<i>Proteacidites thalmanii</i>				
	<i>Retitriletes</i> sp. ("Lycopodiumsporites")				
		<i>Rhoipites</i> sp.	<i>Rhoipites</i> sp.		<i>Rhoipites</i> sp.
	<i>Taxodiaceapollenites hiatus</i>		<i>Taxodiaceapollenites hiatus</i>		<i>Taxodiaceapollenites hiatus</i>
<i>Tricolpites interangulus</i>	<i>Tricolpites interangulus</i>	<i>Tricolpites interangulus</i>	<i>Tricolpites interangulus</i>	<i>Tricolpites interangulus</i>	<i>Tricolpites interangulus</i>
<i>Tricolpites</i> sp.	<i>Tricolpites</i> sp.			<i>Tricolpites</i> sp.	<i>Tricolpites</i> sp.
		<i>Tschudypollis retusus</i>	<i>Tschudypollis retusus</i>	<i>Tschudypollis retusus</i>	<i>Tschudypollis retusus</i>
		<i>Tschudypollis thalmanii</i>	<i>Tschudypollis thalmanii</i>	<i>Tschudypollis thalmanii</i>	<i>Tschudypollis</i> sp.
		<i>Tschudypollis</i> sp.	<i>Tschudypollis</i> sp.	<i>Tschudypollis</i> sp.	<i>Tschudypollis</i> sp.
				<i>Tsugaepollenites</i> sp.	<i>Tsugaepollenites</i> sp.
<i>Ulmoideipites tricostatus</i>	<i>Ulmoideipites tricostatus</i>			<i>Ulmipollenites</i> sp.	<i>Ulmipollenites</i> sp.
unidentified dinoflagellate cysts	unidentified acritarchs				
unidentified pollen tetrad				unidentified pollen tetrad	unidentified pollen tetrad
unidentified trilete spores	unidentified trilete spores				
<i>Ulmipollenites</i>					

Note: Palynomorphs identified by D. J. Nichols (2000, 2003 written commun.)

TABLE 14. COMPARISON OF PALYNOMORPH LISTS AT USGS PALEOBOTANY LOCALITY D6901 NEAR BARREL SPRING, A PURPORTED SPLIT OF THAT SAMPLE, AND THE D6877 SAN JUAN RIVER LOCALITY (FIGURES 1 AND 51)		
Localities D6877-A, -B, -C	Locality D6901 (sample 24-5)	Locality 6901 ("archival split 24-5")
	<i>Araucariacites australis</i>	
		<i>Arecipites microreticulatus</i>
<i>Arecipites reticulatus</i>	<i>Arecipites reticulatus</i>	
<i>Arecipites</i> sp.		
<i>Azolla cretacea</i>	<i>Azolla cretacea</i>	<i>Azolla cretacea</i>
<i>Brevicolporites colpella</i>		
<i>Corollina torosa</i> (incl. monads and tetrads)	<i>Corollina torosa</i>	<i>Corollina torosa</i>
<i>Cupanieidites</i> sp.	<i>Cupanieidites</i> sp.	
<i>Cupuliferoidaepollenites minutus</i>	<i>Cupuliferoidaepollenites minutus</i>	
<i>Chenopodipollis</i> sp.		
<i>Cicatricosisporites</i> spp.		
<i>Cyathidites minor</i>	<i>Cyathidites minor</i>	
		<i>Cyathidites</i> sp.
	<i>Dyadonapites reticulatus</i>	<i>Dyadonapites reticulatus</i>
<i>Fraxinoipollenites variabilis</i>		
	<i>Ghoshispora</i> sp.	<i>Ghoshispora</i> sp.
<i>Laevigatosporites</i> sp.	<i>Laevigatosporites</i> sp.	<i>Laevigatosporites</i> sp.
	<i>Liliacidites leei</i>	
	<i>Liliacidites</i> sp.	
<i>Momipites inaequalis</i>	<i>Momipites inaequalis</i> <i>Momipites</i> sp.	<i>Momipites inaequalis</i>
<i>Momipites tenuipolus</i>	<i>Momipites tenuipolus</i>	
<i>Nyssapollenites</i> sp.		<i>Osmundacidites stanleyi</i>
	<i>Osmundacidites wellmannii</i>	
" <i>Palaeoisoetes</i> " sp.	" <i>Palaeoisoetes</i> " sp.	
" <i>Paliurus</i> " <i>triplicatus</i>		<i>Palaeoisoetes subengelmannii</i>
<i>Pandaniidites typicus</i>	<i>Pandaniidites typicus</i>	<i>Pandaniidites typicus</i>
<i>Pityosporites</i> sp.	<i>Pityosporites</i> sp. <i>Rhoipites</i> sp.	<i>Pityosporites</i> sp. <i>Rhoipites</i> sp.
<i>Taxodiaceapollenites hiatus</i>	<i>Taxodiaceapollenites hiatus</i> <i>Tetraporina</i> sp.	<i>Taxodiaceapollenites hiatus</i>
	<i>Tricolpites?</i> sp. cf. <i>Gunnera</i>	<i>Tricolpites interangulus</i>
		<i>Tricolpites</i> sp.
	<i>Proteacidites retusus</i>	<i>Tschudypollis retusus</i> <i>Tschudypollis</i> sp.
	<i>Proteacidites thalmanii</i>	
<i>Tricolpites</i> sp.	<i>Tricolpites</i> spp.	
<i>Triporoletes novomexicanum</i>		<i>Tsugaepollenites</i> sp.
<i>Ulmipollenites krempii</i>	<i>Ulmipollenites krempii</i>	
		<i>Ulmipollenites</i> sp.
<i>Ulmipollenites tricostatus</i>		
		unidentified pollen tetrad

Note: Localities D6877-A, -B, -C (Figure 1, San Juan River site) are the same localities labeled 25Ga, b, c by Fassett and others (2002), composite palynomorph list from Table 10; locality 6901 is same as locality 24-5 in Fassett and others (2002), palynomorph list from Table 10; palynomorphs in list headed Locality 6901 ("archival split 24-5") were identified from a sample reported by Nichols to be a split of original 24-5 sample (all palynomorphs identified by D. J. Nichols, 1994, 2003, written commun.); *Proteacidites* was renamed *Tschudypollis* by Nichols (2002).

TABLE 15. PALYNOMORPH LISTS FROM NORTHEAST PART OF SAN JUAN BASIN			
Locality D5393	Locality D5394	Locality D4119	Locality D5408
Lowermost Fruitland Fm.	Lowermost Fruitland Fm.	Lowermost Fruitland Fm.	Lower Animas Fm.
	<i>Accuratipollis</i>		
	<i>Alnus</i> 3 pored		<i>Alnus</i> 3 pored
			<i>Anguloluminosus</i>
	<i>Aquilapollenites senonicus</i>		
<i>Appendicisporites</i>			
<i>Clavatipollenites</i>	<i>Clavatipollenites</i>		
	<i>Cyrilla mimima</i>		
<i>Echinatisporis</i>	<i>Echinatisporis</i>		
<i>Engelhardtia</i> type			
<i>Gleicheniidites</i>	<i>Gleicheniidites</i>		
	<i>Illexpollenites</i>		
<i>Interporopollenites</i>			
<i>Kuylisporites</i>			
	<i>Liliacidites complexus</i>		
<i>Microfoveolatosporis</i>	<i>Microfoveolatosporis</i>		
	<i>Minorpollis</i>		
<i>Momipites sanjuanensis</i>	<i>Momipites sanjuanensis</i>		<i>Momipites tenuipolis</i>
			<i>Momipites triorbicularis</i>
		<i>Monosulcites</i> sp.	
	<i>Phaseolidites stanleyi</i>		
	<i>Polypodiisporites amplus</i>		
<i>Proteacidites</i>	<i>Proteacidites</i>		
<i>Stereisporites</i>			
		<i>Tilaeopollenites</i> sp. (<i>Tilia wodehousei</i> And.)	
<i>Tricolpites anguloluminosus</i>	<i>Tricolpites anguloluminosus</i>		
	<i>Tricolpites reticulatus</i>		
			<i>Tricolpites</i>
		<i>Tricolpopollenites</i> sp. A	
		<i>Tricolpopollenites</i> sp. B	
		<i>Tricolpopollenites</i> sp. C	
		<i>Tricolporites</i> sp.	
<i>Triporopollenites rugatus</i>			
<i>Triporopollenites tectus</i>			
<i>Ulmipollenites</i>			<i>Ulmipollenites</i>
	<i>Vitis affluens</i>		

Notes: Samples D5393, 5394, and D5408 (Figure 1) collected by R. T. Ryder, USGS in 1975; palynomorphs identified by R. H. Tschudy (1975 written commun.); palynomorph list by Tschudy for sample D4119 (Figure 1) from Fassett and Hinds (1971) reproduced on Table 7; *Proteacidites* renamed *Tschudypollis* by Nichols (2002).

TABLE 16. COMPOSITE PALYNOFORM LISTS FOR SOUTHEAST PART OF SAN JUAN BASIN		
CRETACEOUS (CAMPANIAN)	TERTIARY (PALEOCENE)	
Fruiliand-Kirtland Formation	Ojo Alamo Sandstone	Nacimiento Formation
	<i>Abietinaepollenites</i> sp. (<i>Podocarpus northrupi</i>)	
	<i>Abietinaepollenites</i> sp. (<i>Podocarpus sellowiformis</i>)	
<i>Acanthotriletes</i>		
<i>Accuratipollis</i>		<i>Acer striata</i>
<i>Aequilifradites</i>		
Algal cysts	<i>Alnipollenites</i>	
<i>Alnipollenites</i> 4 pored	<i>Alnus?</i> sp.	
<i>Aquilapollenites quadricolobus</i>		
<i>Aquilapollenites senonicus</i>		
<i>Aquilapollenites triatatus, var. uniformis</i>		
<i>Araucariacites</i> sp.		
<i>Arecipites microreticulatus</i> n. sp.		
<i>Arecipites</i>	<i>Arecipites</i>	<i>Arecipites</i> sp.
<i>Arecipites reticulatus</i>		<i>Arecipites reticulatus</i>
<i>Balmesporites</i>		
Bisaccate conifer pollen	<i>Bombacacipites nacimientoensis</i>	<i>Bombacacipites nacimientoensis</i>
<i>Botryococcus</i>	<i>Brevicoprites colpella</i>	
<i>Cicatricosporites</i>		
<i>Conferitsulcites knowltoni</i>	<i>Classopollis</i> sp.	
	<i>Conferitsulcites knowltoni</i>	
	<i>Conferitsulcites</i> sp.	
<i>Corollina</i>	<i>Cupaneidites</i> aff. <i>C. major</i>	<i>Cupaneidites</i> aff. <i>C. major</i>
<i>Cupaneidites</i> aff. <i>C. reticularis</i>	<i>Cupuliferoidaeipollenites minutus</i>	<i>Cupuliferoidaeipollenites minutus</i>
Dinoflagellates very few	<i>Fraxinopollenites variabilis</i>	<i>Fraxinopollenites variabilis</i>
<i>Ephedra</i> sp. cf. <i>E. voluta</i>		
<i>Equisetosporites parallel striae</i>		
<i>Equisetosporites spiral</i>		
<i>Erdimannipollis</i> sp.		
<i>Eucommidites</i> sp.		
<i>Extratropipollenites</i> sp.		
Fern spores not abundant		
<i>Foveotriletes scrobicularis</i>		
<i>Foveosporites</i> sp. cf. <i>F. canalis</i>		
<i>Gleichenidites</i>		<i>Gleichenidites senonicus</i>
<i>Granabivesiculites</i> sp.		
<i>Hystrichospheres</i> very few		
<i>Ilexpollenites</i>		
<i>Inaperturopollenites</i> cf. <i>I. hiatus</i>	<i>Intertriletes reticulatus</i>	
<i>Klukisporites</i>		
<i>Kurtzipites</i>		
<i>Kurtzipites trispissatus</i>	<i>Laevigatosporites</i> sp. (<i>Polypodidites</i> sp.)	
<i>Lecaniella</i>		
<i>Liliacidites complexus</i>		
<i>Liliacidites hyalaciniatus</i>	<i>Liliacidites hyalaciniatus</i>	
<i>Liliacidites leei</i>	<i>Liliacidites leei</i>	<i>Liliacidites leei</i>
<i>Liliacidites</i> sp.	<i>Liliacidites</i> sp.	
<i>Liquidambarpollenites</i> sp.	<i>Lycopodiadites</i>	
		<i>Lygodiosporites?</i> sp.
<i>Monoporopollenites</i> sp.		
<i>Monosulcites persiphosus</i>		
<i>Monosulcites</i> sp.		
<i>Navisulcites marginatus</i>		
<i>Neoraistrickia</i> sp.		
	<i>Momipites inaequalis</i>	<i>Nyssa puercoensis</i>
<i>Momipites sanjuanensis</i>		<i>Momipites inaequalis</i>
<i>Momipites</i> sp.	<i>Momipites tenuipolus</i>	<i>Momipites tenuipolus</i>
	<i>Monolete</i> fern spores	
	<i>Monosulcites</i> sp. (<i>Rectosulcites latus</i>)	
	<i>Nyssapollenites</i> sp.	<i>Nyssapollenites</i> sp.
		<i>Osmundacidites</i> sp.
<i>Pailurus triplicatus</i>	<i>Pailurus triplicatus</i>	
<i>Pediastrum</i>		
<i>Periporopollenites</i> sp.	<i>Periporopollenites</i>	
<i>Perotriletes cubensis</i>		" <i>Pinus haploxylo</i> type"
		" <i>Pinus sylvestris</i> type"
	<i>Pityosporites</i> sp.	<i>Pityosporites</i> sp.
<i>Plicapollis?</i>		
	<i>Podocarpidites</i> cf. <i>P. sellowiformis</i>	
	<i>Podocarpus northrupi</i>	
	<i>Podocarpus sellowiformis</i>	<i>Podocarpus sellowiformis</i>
	<i>Podocarpus zuniensis</i>	
<i>Pollenites?</i> sp.		
<i>Polypodidites</i> spp.	<i>Polypodidites</i> spp.	<i>Polypodidites</i> spp.
	<i>Polyporopollenites</i> sp.	
<i>Pristinuspollenites</i>		
<i>Pseudoplicapollis?</i>	<i>Psilastephanocolpites</i> sp.	<i>Psilastephanocolpites</i> sp.
<i>Quadrupollis krempii</i>		
	<i>Quercus explanata</i>	" <i>Quercus</i> " <i>explanata</i>
	<i>Quercus?</i> sp.	
	<i>Rectosulcites latus</i>	
<i>Rugubivesiculites</i>		<i>Rugulatisporites</i> sp.
	<i>Salix</i> sp.	<i>Salix</i> sp.
	<i>Siltaria</i> cf. <i>S. scabriestima</i>	
<i>Sphagnum</i> sp.		
	<i>Sporites neglectus</i>	
<i>Sporites?</i> sp. A		
<i>Taxodiaceapollenites</i>		
<i>Tetracopites</i>		<i>Tetradites</i> sp.
		<i>Tilia danei</i>
<i>Tilia wodehousei</i>		
<i>Trichopeltinites</i>		
	<i>Triatropollenites</i> sp. A	
	<i>Triatropollenites</i> sp. B	
	<i>Trichotomosulcites contractus</i>	
	<i>Tricolpites anguloluminosus</i>	<i>Tricolpites anguloluminosus</i>
<i>Tricolpites interangulus</i>		
	<i>Tricolpites</i>	<i>Tricolpites</i> spp.
<i>Tricolpites</i> sp. A	<i>Tricolpites</i> sp. B	
<i>Tricolpopollenites</i> sp.		
<i>Tricolpopollenites</i> sp. A		
<i>Tricolpopollenites</i> sp. B		
<i>Tricolpopollenites</i> sp. C		
<i>Tricolpopollenites</i> sp. (<i>Quercus explanata</i>)	<i>Tricolpopollenites</i> sp. (<i>Quercus explanata</i>)	
<i>Tricolporites</i> sp.		<i>Tricolporites rhomboides</i>
		<i>Tricolporites</i> sp.
		<i>Tricolporites</i> sp. (? <i>Eleagnaceae</i>)
<i>Tricolporites traversei</i>		
	Trilete fern spores	
<i>Triletes?</i> sp. A		
	<i>Triporopollenites plektosus</i>	<i>Triporopollenites plektosus</i>
	<i>Triporopollenites</i> sp. (cf. <i>Casiaromodotes</i>)	<i>Triporopollenites</i> sp. (cf. <i>Casiaromodotes</i>)
	<i>Triporopollenites tectus</i>	<i>Triporopollenites tectus</i>
<i>Trudopollis</i>		
<i>Tschudyipollis</i> many, large		
<i>Tschudyipollis retusus</i>		
<i>Tschudyipollis thalmanii</i>		
<i>Tschudyipollis</i> sp.	<i>Ulmipollenites</i>	
<i>Ulmipollenites</i> 3, 4 pored		
	<i>Ulmipollenites</i> sp. (<i>Ulmoidipites tricostatus</i>)	
	<i>Ulmoidipites krempii</i>	<i>Ulmoidipites krempii</i>
	<i>Ulmoidipites planeraeformis</i>	
<i>Ulmoidipites tricostatus</i>	<i>Ulmoidipites tricostatus</i>	<i>Ulmoidipites tricostatus</i>
<i>Zonalapollenites</i> sp.		
<i>Zivisporis novomexicanum</i>		<i>Zivisporis novomexicanum</i>
<i>Zivisporis</i> sp.	<i>Zivisporis</i> sp.	

Note: Fruiliand-Kirtland palynomorph list is composite of Kirtland-C and D4017.A, -B, and -C from Table 7, and localities D5628-A, -B, -C and D5652 from Table 9. Ojo Alamo list is composite from Ojo Alamo forules 1 and 2 from Table 5, localities D3738-A, -B from Table 7, and localities D6583-A, -B from Table 9. Nacimiento list is a composite of Nacimiento forules 1 and 2 from Table 5, locality D3803 from Table 7, and locality D6878 from Table 9. palynomorph authorships not shown on this and succeeding tables.

TABLE 17. COMPOSITE LIST OF PALYNOMORPHS FROM KIRTLAND FORMATION, POT MESA AREA
<i>Abietinaepollenites</i>
<i>Aequitriradites</i>
<i>Alnipollenites</i>
<i>Aquilapollenites</i>
<i>Azolla</i>
<i>Azolla cretacea</i>
<i>Balmeisporites</i>
<i>Camarozonosporites</i>
<i>Chenopodipollis</i> sp.
<i>Cicatricosisporites</i>
<i>Corollina</i>
<i>Corollina torosa</i>
<i>Cupanieidites</i> sp.
<i>Cupuliferoideaepollenites minor</i>
<i>Cyathidites minor</i>
<i>Dinoflagellate</i>
<i>Echinatisporis</i>
<i>Ephedra multicosata</i>
<i>Equisetosporites</i> 5
<i>Erdtmanipollis cretacea</i>
<i>Foraminisporis</i>
<i>Fraxinopollenites variabilis</i>
<i>Gleicheniidites</i>
<i>Gunnera microreticulata</i>
<i>Klukisporites</i>
<i>Kurtzipites trispissatus</i>
<i>Liliacidites</i>
<i>Liliacidites complexus</i>
<i>Liliacidites leei</i>
<i>Lycopodiacidites</i>
<i>Lycopodiumsporites</i>
<i>Microfoveolatosporis</i>
<i>Momipites sanjuanensis</i>
<i>Monosulcites</i>
<i>Nyssapollenites albertensis</i>
<i>Nyssapollenites</i> sp.
<i>Osmundacidites</i>
" <i>Palaeoisoetes</i> " sp.
<i>Pandaniidites typicus</i>
<i>Periporopollenites</i>
<i>Proteacidites</i>
<i>Proteacidites retusus</i>
<i>Proteacidites thalmannii</i>
<i>Pseudoplicapollis</i>
<i>Pseudoschizaea</i>
<i>Pterospermopsis</i>
<i>Quercus explanata</i>
<i>Rugubivesiculites</i>
<i>Taxodiaceapollenites</i>
" <i>Tilia</i> " <i>wodehousei</i>
<i>Tricolpites vulgaris</i>
<i>Tricolporites rhomboides</i>
<i>Triporoletes novomexicanum</i>
<i>Ulmipollenites</i>
<i>Ulmipollenites tricostatus</i>
<i>Ulmoideipites</i> spp., 3 and 4 pored, smooth to verrucate forms cf <i>Vitis affluens</i>
<i>Zlavisporis</i>
Note: Palynomorphs represent a composite list of taxa from Cretaceous Kirtland Formation shown on Table 12.
<i>Proteacidites</i> is now named <i>Tschudypollis</i> .

TABLE 18. COMPOSITE PALYNOMORPH LISTS FROM OJO ALAMO SANDSTONE TYPE AREA				
CRETACEOUS			PALEOCENE	
Fruitland Formation	Kirtland Formation	Uppermost Kirtland Formation	Upper Ojo Alamo	Lowermost Nacimiento Fm.
<i>Appendicisporites</i> sp.	<i>Appendicisporites</i> sp. <i>Aquilapollenites quadrilobus</i> <i>Aquilapollenites</i> 3 sp.		Algal cysts	
	<i>Arecipites columellas</i> <i>Arecipites microreticulatus</i> <i>Arecipites reticulatus</i>	<i>Arauciacites australis</i>		
<i>Arecipites</i> sp.		<i>Arecipites reticulatus</i>	<i>Arecipites reticulatus</i> <i>Arecipites</i> sp.	<i>Arecipites</i> cf. <i>A. reticulatus</i>
	<i>Azolla circinata</i> <i>Azolla cretacea</i> [relatively abundant] <i>Azolla microspores</i>	<i>Azolla cretacea</i>		
			<i>Azolla</i> cf. <i>A. schopfi</i>	
	Bissacate conifer		<i>Brevicolporites colpella</i>	
<i>Camarozonosporites ambigens</i>			<i>Cercidiphyllites</i> sp. <i>Chenopodiopsis</i> sp.	
	<i>Cingulatisporites lancei</i> <i>Cicatricosisporites</i> sp. <i>Corollina</i> sp.			
<i>Corollina torosa</i>	<i>Corollina torosa</i>	<i>Corollina torosa</i>	<i>Corollina torosa</i> <i>Cupaneidites</i> aff. <i>C. major</i>	<i>Cupaneidites</i> cf. <i>C. major</i>
		<i>Cupaneidites</i> sp. <i>Cupuliferoidaepollenites minutus</i>	<i>Cupaneidites</i> sp. <i>Cupuliferoidaepollenites minutus</i>	
<i>Cupuliferoidaepollenites minutus</i> <i>Cupuliferoidaepollenites</i> spp. <i>Cyathidites minor</i>		<i>Cyathidites minor</i>		
	<i>Cyathidites</i> spp. <i>Cycadopites fragillii</i> <i>Cycadopites</i> sp. <i>Dyadonapites reticulatus</i>	<i>Dyadonapites reticulatus</i>		
<i>Echinatisporis varispinosus</i> <i>Ephedripites</i> sp. D				
	<i>Erdtmanipollis cretaceus</i>			
<i>Eucommiidites minor</i>	<i>Foraminisporis undulatus</i>		<i>Fraxinopollenites variabilis</i>	
	<i>Ghoshispora</i> sp. <i>Gunnera</i> <i>Gunnera microreticulata</i> <i>Ilexpollenites compactus</i> <i>Inaperturopollenites</i> sp. <i>Inaperturotetradites scabratus</i>	<i>Ghoshispora</i> sp.		
<i>Laevigatosporites</i> spp.	<i>Laevigatosporites</i> sp. Larger fern tetrad <i>Liliacidites hyalacinatus?</i>	<i>Laevigatosporites</i> sp.	<i>Laevigatosporites</i> spp.	
<i>Liliacidites leei</i>	<i>Liliacidites leei</i> <i>Liliacidites reticulata</i>	<i>Liliacidites leei</i>		
<i>Liliacidites</i> sp.	<i>Liliacidites</i> sp. <i>Liliacidites</i> sp. cf. <i>L. complexus</i> <i>Loranthacites</i>	<i>Liliacidites</i> sp.		
<i>Microreticulatisporites</i> sp.	<i>Momipites inaequalis</i>	<i>Momipites inaequalis</i> <i>Momipites</i> sp. <i>Momipites tenuipolus</i>	<i>Momipites inaequalis</i> <i>Momipites</i> sp. <i>Momipites tenuipolus</i>	<i>Momipites</i>
<i>Monocolopollenites?</i> sp.	? <i>Monosulcites perspinosus</i>			
<i>Nyssapollenites</i> sp.	<i>Osmundacidites stanleyi</i>			
		<i>Osmundacidites wellmannii</i>		
		" <i>Palaeoisoetes</i> " sp.	Ovoidites sp. "Palaeoisoetes" sp.	
	<i>Palaeoisoetes subengelmannii</i>		" <i>Paliurus</i> " <i>triplicatus</i>	<i>Paliurus triplicatus?</i>
	<i>Pandaniidites</i>		<i>Pandaniidites radicus</i> <i>Pandaniidites typicus</i>	
	<i>Pandaniidites typicus</i> <i>Pityosporites constrictus</i> <i>Pityosporites</i> spp. <i>Pityosporites typicus</i>	<i>Pandaniidites typicus</i> <i>Pityosporites</i> sp.	<i>Pityosporites</i> sp.	
			<i>Podocarpus</i> sp. <i>Polypodiisporonites</i> sp.	<i>Podocarpus</i> sp.
<i>Pseudoplicapollis newmanii</i> <i>Pseudoplicapollis</i> sp.			<i>Psilastephanocolpites</i> sp. "Quercus" <i>explanata</i> <i>Quercus</i> sp.	
<i>Reticuloidosporites pseudomurii</i>			<i>Rectosulcites latus</i>	
	<i>Retriletes</i> sp. ("Lycopodiumsporites")			
<i>Rhoipites</i> sp.	<i>Schizosporis parvus</i>	<i>Rhoipites</i> sp.		
<i>Stereisporites</i> spp.			<i>Syncolporites minimus</i>	
<i>Taxodiaceapollenites hiatus</i>	<i>Taxodiaceapollenites hiatus</i>	<i>Taxodiaceapollenites hiatus</i>	<i>Tetracolpites</i> 2 sp. <i>Tetraporina</i> sp. <i>Tricolpites anguloluminosus</i> <i>Tricolpites foveolate</i>	
		<i>Tricolpites?</i> sp. cf. <i>Gunnera</i>		
	<i>Tricolpites interangulus</i> <i>Tricolpites microreticulatus</i> <i>Tricolpites reticulatus</i>			
			<i>Tricolpites scabrata</i>	
<i>Tricolpites</i> spp.	<i>Tricolpites</i> sp.	<i>Tricolpites</i> spp.	<i>Tricolporites rhomboides</i>	
<i>Triporopollenites</i> spp. <i>Triporopollenites tectus</i> <i>Tschudypollis retusus</i> <i>Tschudypollis</i> sp.	<i>Tschudypollis retusus</i> <i>Tschudypollis</i> spp. (many) <i>Tschudypollis thalmannii</i> <i>Tsugaepollenites</i> sp. <i>Ulmipollenites</i>	<i>Tschudypollis retusus</i> (reworked) <i>Tschudypollis thalmannii</i> (reworked)		
<i>Ulmipollenites krempii</i>	<i>Ulmipollenites krempii</i> <i>Ulmipollenites</i> sp.	<i>Ulmipollenites krempii</i>	<i>Ulmipollenites krempii</i> <i>Ulmipollenites</i> 3 and 4 pored.	
	<i>Ulmoideipites krempii</i> ("Ulmoideipites") <i>tricostatus</i> unidentified acritarchs unidentified dinoflagellate cysts unidentified pollen tetrad unidentified triete spores	<i>Ulmoideipites tricostatus</i>	<i>Ulmoideipites tricostatus</i>	

Notes: Composite palynomorph lists are based on palynomorph lists on Tables 6, 13.1, and 13.2; the Paleocene Uppermost Kirtland Formation list is from locality D6901.

TABLE 19. COMPOSITE LIST OF PALYNOMORPHS IDENTIFIED FROM SAN JUAN RIVER LOCALITY	
Kirtland Formation - Cretaceous	Ojo Alamo Sandstone - Paleocene
	<i>Alisporites bilateralis</i>
	<i>Arecipites reticulatus</i>
	<i>Arecipites</i> sp.
	<i>Azolla cretacea</i>
<i>Balmeisporites</i>	
	<i>Brevicolporites colpella</i>
	<i>Chenopodipollis</i> sp.
	<i>Cicatricosporites</i> spp.
	<i>Lycopodium novomexicanum</i>
	<i>Momipites inaequalis</i>
	<i>Momipites tenuipolus</i>
	<i>Corollina torosa</i> (incl. monads and tetrads)
	<i>Cupanieidites</i> cf. <i>C. reticularis</i>
	<i>Cupuliferoidaepollenites minutus</i>
	<i>Cyathidites minor</i>
	<i>Cycadopites fragilis</i>
	<i>Equisetosporites lajwantis</i>
	<i>Fraxinoipollenites variabilis</i>
<i>Gunnera</i>	
<i>Interpollis</i>	
<i>Kurtzpites</i>	
	<i>Laevigatosporites</i> sp.
	<i>Laevigatosporites haardti</i>
	<i>Momipites inaequalis</i>
	<i>Momipites inaequalis</i>
	<i>Momipites tenuipolus</i>
	<i>Nyssapollenites</i> sp.
	<i>Nyssapollenites explanatus</i>
	<i>Ovoidites ligneolus</i>
	" <i>Palaeoisoetes</i> " sp.
	" <i>Paliurus</i> " <i>triplicatus</i>
	<i>Pandaniidites</i>
	<i>Pandaniidites typicus</i>
	<i>Pityosporites</i> sp.
	<i>Rectosulcites latus</i>
	<i>Schizosporis parvus</i>
	<i>Taxodiaceapollenites hiatus</i>
	<i>Taxodiaceapollenites vacupites</i>
	<i>Tricolpites</i> sp.
	<i>Triporoletes novomexicanum</i>
	<i>Triporoletes simplex</i>
<i>Tschudypollis</i>	<i>Tschudypollis</i> (reworked)
	<i>Tschudypollis thalmanni</i> (reworked)
	<i>Ulmipollenites krempii</i>
	<i>U. tricostatus</i>
	<i>Ulmoideipites krempi</i>
<i>Ulmoideipites</i> spp. 3 and 4 pored smooth to verrucate forms	
	<i>Zlivisporis novomexicanum</i>
Note: Palynomorph lists are from Table 10	

TABLE 20. COMPOSITE PALYNOMORPH LISTS FROM	
NORTHEAST SAN JUAN BASIN	
Lowermost Fruitland Fm. (Cretaceous)	Lower Animas Fm. (Paleocene)
<i>Accuratipollis</i>	
<i>Alnus</i> 3 pored	<i>Alnus</i> 3 pored
<i>Aquilapollenites senonicus</i>	
<i>Appendicisporites</i>	
<i>Clavatipollenites</i>	
<i>Cyrilla mimima</i>	
<i>Echinatisporis</i>	
<i>Engelhardtia</i> type	
<i>Gleicheniidites</i>	
<i>Ilexpollenites</i>	
<i>Interporopollenites</i>	
<i>Kuylisporites</i>	
<i>Liliacidites complexus</i>	
<i>Microfoveolatosporis</i>	
<i>Minorpollis</i>	
<i>Momipites sanjuanensis</i>	
	<i>Momipites tenuipolis</i>
	<i>Momipites triorbicularis</i>
<i>Monosulcites</i> sp.	
<i>Phaseolidites stanleyi</i>	
<i>Polypodiisporites amplus</i>	
<i>Stereisporites</i>	
<i>Tilaepopollenites</i> sp. (<i>Tilia wodehousei</i> And.)	
	<i>Tricolpites</i>
<i>Tricolpites anguloluminosus</i>	<i>Tricolpites anguloluminosus</i>
<i>Tricolpites reticulatus</i>	
<i>Tricolopopollenites</i> sp. A	
<i>Tricolopopollenites</i> sp. B	
<i>Tricolopopollenites</i> sp. C	
<i>Tricolporites</i> sp.	
<i>Tripoporopollenites rugatus</i>	
<i>Tripoporopollenites tectus</i>	
<i>Tschudypollis</i>	
<i>Ulmipollenites</i>	<i>Ulmipollenites</i>
<i>Vitis affluens</i>	
Note: Palynomorphs listed are from Table 15	

TABLE 21. COMPOSITE PALYNOMORPH LISTS FROM FRUITLAND FORMATION, SAN JUAN BASIN, NEW MEXICO

Ojo Alamo Ss Type Area	Mesa Portales Area	Gasbuggy Core	Northeast SJ Basin
	<i>Acanthotriletes</i>		
	<i>Accuratipollis</i>	<i>Accuratipollis</i> spp.	<i>Accuratipollis</i>
	<i>Aequitriradites</i>	<i>Aequitriradites</i> sp.	
		<i>Aequitriradites spinulosus</i>	
	Algal cysts		
	<i>Alnipollenites</i> 4 pored		<i>Alnus</i> 3 pored
<i>Appendicisporites</i> sp.		<i>Alsophilidites</i> sp.	
		<i>Appendicisporites</i> spp.	<i>Appendicisporites</i>
		<i>Aquila</i> 4 E	
		<i>Aquila</i> 17	
		<i>Aquila</i> 18	
		<i>Aquila</i> 36 C	
		<i>Aquila</i> 42	
		<i>Aquilapollenites attenuatus</i>	
		<i>Aquilapollenites delicatus</i>	
	<i>Aquilapollenites quadriobus</i>	<i>Aquilapollenites quadriobus</i>	
	<i>Aquilapollenites senonicus</i>	<i>Aquilapollenites senonicus</i>	<i>Aquilapollenites senonicus</i>
	<i>Aquilapollenites triolatus</i> , var. <i>uniformis</i>		
		<i>Aquilapollenites turbidus</i>	
	<i>Araucariacites</i> sp.	<i>Araucariacites</i>	
	<i>Arecipites microreticulatus</i>		
	<i>Arecipites reticulatus</i>		
<i>Arecipites</i> sp.	<i>Arecipites</i>		
	<i>Balmesporites</i>		
	<i>Bisaccate</i> conifer pollen		
<i>Camazonosporites ambigenis</i>	<i>Botryococcus</i>		
		<i>Camazonosporites</i> spp.	
<i>Cicatricosisporites</i> sp.	<i>Cicatricosisporites</i>	<i>Cicatricosisporites</i> spp.	
		<i>Cicatricosisporites</i> spp.	<i>Clavatipollenites</i>
		cf. <i>Concavisporites verrucosus</i>	
	<i>Conferisulcites knowltoni</i>		
<i>Corollina tarosa</i>	<i>Corollina</i>		
	<i>Cupanioidites</i> aff. <i>C. reticularis</i>		
<i>Cupuliferoidaeipollenites minutus</i>			
<i>Cupuliferoidaeipollenites</i> spp.			
<i>Cyathidites minor</i>			<i>Cyrtia minima</i>
	<i>Dinoflagellates</i> very few		
<i>Echinatisporis varispinosus</i>			<i>Echinatisporis</i>
			<i>Engelhardtia</i> type
	<i>Ephedra</i> sp. cf. <i>E. voluta</i>		
<i>Ephedripites</i> sp. D	<i>Equisetosporites parallel striae</i>		
	<i>Equisetosporites spiral</i>		
	<i>Erdmannipollis</i> sp.		
<i>Eucommiidites minor</i>	<i>Eucommiidites</i> sp.	<i>Eucommiidites</i> sp.	
	<i>Extratropipollenites</i> sp.		
	Fern spores not abundant		
		<i>Foraminisporis</i> sp.	
	<i>Foveolites scrobicularis</i>		
	<i>Foveosporites</i> sp. cf. <i>F. canalis</i>		
	<i>Gleichenidites</i>	<i>Gleichenidites</i> spp.	<i>Gleichenidites</i>
		<i>Ghoshispora</i> spp.	
	<i>Granabivesiculites</i> sp.		
	<i>Hystriospheres</i> very few		
	<i>Ilexpollenites</i>	<i>Ilexpollenites</i> sp.	<i>Ilexpollenites</i>
	<i>Inaperturopollenites</i> cf. <i>I. hiatus</i>		
	<i>Klukisporites</i>	<i>Klukisporites</i> spp.	<i>Interporipollenites</i>
		<i>Kuylisporites</i> sp.	<i>Kuylisporites</i>
	<i>Kurtzipites</i>		
<i>Laevigatosporites</i> spp.	<i>Kurtzipites trispissatus</i>	<i>Kurtzipites trispissatus</i>	
	<i>Lecaniella</i>		
		<i>Leptolepidites major</i>	
	<i>Liliacidites complexus</i>		<i>Liliacidites complexus</i>
	<i>Liliacidites hyalaciniatus</i>		
<i>Liliacidites leei</i>	<i>Liliacidites leei</i>		
<i>Liliacidites</i> sp.	<i>Liliacidites</i> sp.	<i>Liliacidites</i> spp.	
	<i>Liquidambarpollenites</i> sp.		
		<i>Lycopodiacidites kuepperi</i>	
		<i>Lycopodiacidites</i> sp.	
		<i>Lycopodiumsporites</i> spp.	
		<i>Microfoveolatosporis canaliculatus</i>	
<i>Microreticulatisporites</i> sp.		<i>Microreticulatisporites</i> sp.	<i>Microfoveolatosporis</i>
		cf. <i>Minoripollis</i>	
<i>Monocolopollenites?</i> sp.			<i>Minoripollis</i>
	<i>Monoporipollenites</i> sp.		<i>Momipites sanjuanensis</i>
	<i>Monosulcites perspinosus</i>		
	<i>Monosulcites</i> sp.		<i>Monosulcites</i> sp.
	<i>Navisulcites marginatus</i>		
	<i>Neoraistrickia</i> sp.		
<i>Nyssapollenites</i> sp.	<i>Momipites sanjuanensis</i>		
	<i>Momipites</i> sp.		
	<i>Paliurus triplicatus</i>		
	<i>Pediastrum</i>		
	<i>Periporipollenites</i> sp.		
	<i>Perotriletes cubensis</i>		
		<i>Phaseolidites stanleyi</i>	<i>Phaseolidites stanleyi</i>
	<i>Plicapollis?</i>		
	<i>Pollenites?</i> sp.		
	<i>Polypodidites</i> spp.	<i>Polypodidites</i> sp.	
		<i>Polypodisporites amplus</i>	<i>Polypodisporites amplus</i>
		<i>Polypodisporites</i> sp.	
	<i>Pristinuspollenites</i>		
<i>Pseudoplicapollis newmanii</i>	<i>Pseudoplicapollis?</i>		
<i>Pseudoplicapollis</i> sp.			
	<i>Quadripollis krempii</i>		
<i>Reticuloidosporites pseudomurii</i>		cf. <i>Radialetes costatus</i>	
<i>Rhoipites</i> sp.			
	<i>Rugubivesiculites</i>		
	<i>Sphagnum</i> sp.		
<i>Stereisporites</i> spp.	<i>Sporites?</i> sp. A		<i>Stereisporites</i>
		<i>Subtriporipollenites</i> sp.	
		cf. <i>Taucosporites</i>	
<i>Taxodiaceapollenites hiatus</i>	<i>Taxodiaceapollenites</i>		
	<i>Tetracolpites</i>		
	<i>Tilia wodehousei</i>	cf. <i>Tilia wodehousei</i>	<i>Tiliaepollenites</i> sp. (<i>Tilia wodehousei</i>)
		<i>Toroisporis</i> sp.	
	<i>Trichopeltinites</i>		<i>Tricolpites anguluminosus</i>
		<i>Tricolpites hiars</i>	
	<i>Tricolpites interangulus</i> Newman		
	<i>Tricolpites</i> sp. A	<i>Tricolpites reticulatus</i>	<i>Tricolpites reticulatus</i>
<i>Tricolpites</i> spp.		<i>Tricolpites</i> sp.	
	<i>Tricolpopollenites</i> sp.		
	<i>Tricolpopollenites</i> sp. A		<i>Tricolpopollenites</i> sp. A
	<i>Tricolpopollenites</i> sp. B		<i>Tricolpopollenites</i> sp. B
	<i>Tricolpopollenites</i> sp. C		<i>Tricolpopollenites</i> sp. C
	<i>Tricolpopollenites</i> sp. (<i>Quercus explanata</i>)		
	<i>Tricolparites</i> sp.		<i>Tricolporites</i> sp.
	<i>Tricolparites traversei</i>		
	<i>Triletes?</i> sp. A		
		<i>Triplanosporites</i> sp.	
<i>Triporipollenites</i> spp.			<i>Triporipollenites rugatus</i>
<i>Triporipollenites tectus</i>			<i>Triporipollenites tectus</i>
	<i>Trudopollis</i>	<i>Trudopollis meekeri</i>	
	<i>Tschudyipollis</i> many large	<i>Trudopollis</i> sp.	
<i>Tschudyipollis retusus</i>	<i>Tschudyipollis retusus</i>		
	<i>Tschudyipollis thalmani</i>		
<i>Tschudyipollis</i> sp.	<i>Tschudyipollis</i> sp.	<i>Tschudyipollis</i> sp.	<i>Tschudyipollis</i>
			<i>Ulmipollenites</i>
<i>Ulmipollenites krempii</i>	<i>Ulmipollenites</i> 3, 4 pored		
	<i>Ulmoidipites tricostatus</i>		
		<i>Vitis?</i> <i>Affluens</i>	
	<i>Zonalapollenites</i> sp.	<i>Zonalapollenites</i>	
	<i>Zivisporis novomexicanum</i>		
	<i>Zivisporis</i> sp.	cf. <i>Zivisporis</i>	

Note: Palynomorphs listed are from Tables 8, 16, 18, and 20

TABLE 22. COMPOSITE LISTS OF PALYNOMORPHS FROM KIRTLAND FORMATION	
Ojo Alamo Type Area	Pot Mesa Locality
	<i>Abietinaepollenites</i>
<i>Appendicisporites</i> sp.	
	<i>Aequitriradites</i>
	<i>Alnipollinites</i>
<i>Aquilapollenites</i> 3 sp.	<i>Aquilapollenites</i>
<i>Aquilapollenites quadrilobus</i>	
<i>Arecipites columellas</i>	
<i>Arecipites microreticulatus</i>	
<i>Arecipites reticulatus</i>	
	<i>Azolla</i>
<i>Azolla circinata</i>	
<i>Azolla cretacea</i> (relatively abundant)	<i>Azolla cretacea</i>
<i>Azolla</i> microspores	
	<i>Balmeisporites</i>
Bissacate conifer	
	<i>Camazonosporites</i>
	<i>Chenopodipollis</i> sp.
<i>Cicatricosisporites</i> sp.	<i>Cicatricosisporites</i>
<i>Cingulatisporites lancei</i>	
<i>Corollina</i> sp.	<i>Corollina</i>
<i>Corollina torosa</i>	<i>Corollina torosa</i>
	<i>Cupanieidites</i> sp.
	<i>Cupuliferoidaepollenites minor</i>
	<i>Cyathidites minor</i>
<i>Cyathidites</i> spp.	
<i>Cycadopites fragillis</i>	
<i>Cycadopites</i> sp.	
	<i>Dinoflagellate</i>
<i>Dyadonapites reticulatus</i>	
	<i>Echinatisporis</i>
	<i>Ephedra multicostata</i>
	<i>Equisetosporites</i> 5
<i>Erdtmanipollis cretaceus</i>	<i>Erdtmanipollis cretacea</i>
	<i>Foraminisporis</i>
<i>Foraminisporis undulatus</i>	
	<i>Fraxinoipollenites variabilis</i>
<i>Ghoshispora</i> sp.	
	<i>Gleicheniidites</i>
<i>Gunnera</i>	
<i>Gunnera microreticulata</i>	<i>Gunnera microreticulata</i>
<i>Ilexpollenites compactus</i>	
<i>Inaperturopollenites</i> sp.	
<i>Inaperturotetradites scabratus</i>	
	<i>Klukisporites</i>
	<i>Kurtzipites trispissatus</i>
<i>Laevigatosporites</i> sp.	
Larger fern tetrad	
	<i>Liliacidites</i>
	<i>Liliacidites complexus</i>
<i>Liliacidites hyalacinatus?</i>	
<i>Liliacidites leei</i>	<i>L. leei</i>
<i>Liliacidites reticulata</i>	
<i>Liliacidites</i> sp.	
<i>Liliacidites</i> sp. cf <i>L. complexus</i>	
<i>Loranthacites</i>	
	<i>Lycopodiacidites</i>

	<i>Lycopodiumsporites</i>
	<i>Microfaveolatisporis</i>
<i>Momipites inaequalis</i>	
	<i>Momipites sanjuanensis</i>
	<i>Monosulcites</i>
? <i>Monosulcites perspinosus</i>	
	<i>Nyssapollenites albertensis</i>
	<i>Nyssapollenites</i> sp.
	<i>Osmundacidites</i>
<i>Osmundacidites stanleyi</i>	
	" <i>Palaeoisoetes</i> " sp.
<i>Palaeoisoetes subengelmannii</i>	
<i>Pandaniidites</i>	
<i>Pandaniidites typicus</i>	<i>Pandaniidites typicus</i>
	<i>Periporopollenites</i>
<i>Pityosporites constrictus</i>	
<i>Pityosporites</i> spp.	
<i>Pityosporites typicus</i>	
	<i>Pseudoplicapollis</i>
	<i>Pseudoschizaea</i>
	<i>Pterospermopsis</i>
	<i>Quercus explanata</i>
<i>Retitriletes</i> sp. (" <i>Lycopodiumsporites</i> ")	
	<i>Rugubivesiculites</i>
<i>Schizosporis parvus</i>	
	<i>Taxodiaceapollenites</i>
<i>Taxodiaceapollenites hiatus</i>	
	<i>Tilia wodehousei</i>
<i>Tricolpites interangulus</i>	
<i>Tricolpites microreticulatus</i>	
<i>Tricolpites reticulatus</i>	
<i>Tricolpites</i> sp.	
	<i>Tricolpites vulgaris</i>
	<i>Tricolporites rhomboides</i>
	<i>Triporoletes novomexicanum</i>
<i>Tschudypollis retusus</i>	<i>Tschudypollis retusus</i>
<i>Tschudypollis</i> spp. (many)	<i>Tschudypollis</i> spp.
<i>Tschudypollis</i> spp.	<i>Tschudypollis</i> spp.
<i>Tsugaepollenites</i> sp.	
<i>Ulmipollenites</i>	<i>Ulmipollenites</i>
<i>Ulmipollenites krempii</i>	
<i>Ulmipollenites</i> sp.	
	<i>Ulmipollenites tricostatus</i>
("Ulmoidipites") <i>tricostatus</i>	
	<i>Ulmoidipites</i> spp. 3 and 4 pored smooth to verrucate forms
unidentified acritarchs	
unidentified dinoflagellate cysts	
unidentified pollen tetrad	
unidentified trilete spores	
	cf <i>Vitis affluens</i>
	<i>Zlivisporis</i>
Note: Palynomorphs listed are from Tables 17 and 18.	

TABLE 23. COMPARISON OF PALYNOMORPHS FROM KIRTLAND AND FRUITLAND FORMATIONS FROM ALL S.J. BASIN LOCALITIES!			
Fruitland Formation	Kirtland Formation	Fruitland Formation (continued)	Kirtland Formation (continued)
	<i>Abietinaepollenites</i>	<i>Liquidambarpollenites</i> sp.	
<i>Acanthotriletes</i>			<i>Loranthacites</i>
<i>Accuratipollis</i>		<i>Lycopodiacidites kuepperi</i>	
<i>Aequitriradites</i>	<i>Aequitriradites</i>	<i>Lycopodiacidites</i> spp.	<i>Lycopodiacidites</i>
<i>Aequitriradites spinulosus</i>		<i>Lycopodiumsporites</i> spp.	<i>Lycopodiumsporites</i>
Algal cysts		<i>Microfoveolatosporis</i>	<i>Microfoveolatosporis</i>
	<i>Alnipollinites</i>	<i>Microfoveolatosporis canaliculatus</i>	
<i>Alnipollenites</i> 4 pored		<i>Microreticulatisporites</i> sp.	
<i>Alnus</i> 3 pored		cf. <i>Minorpollis</i>	
<i>Alsophilidites</i> sp.			<i>Momipites inaequalis</i>
<i>Appendicisporites</i> spp.	<i>Appendicisporites</i> sp.	<i>Momipites sanjuanensis</i>	<i>Momipites sanjuanensis</i>
<i>Aquila</i> 4 E		<i>Momipites</i> sp.	
<i>Aquila</i> 4 E		<i>Monocolopollenites?</i> sp.	
<i>Aquila</i> 18		<i>Monoporopollenites</i> sp.	
<i>Aquila</i> 36 C		<i>Monosulcites perspinosus</i>	
<i>Aquila</i> 42	<i>Aquilapollenites</i> 3 sp.	<i>Monosulcites</i> sp.	<i>Monosulcites</i>
			? <i>Monosulcites perspinosus</i>
<i>Aquilapollenites attenuatus</i>		<i>Navisulcites marginatus</i>	
<i>Aquilapollenites delicatus</i>		<i>Neoraistrickia</i> sp.	
<i>Aquilapollenites quadrilobus</i>	<i>Aquilapollenites quadrilobus</i>		<i>Nyssapollenites albertensis</i>
<i>Aquilapollenites senonicus</i>		<i>Nyssapollenites</i> sp.	<i>Nyssapollenites</i> sp.
<i>Aquilapollenites trialatus, var uniformis</i>			<i>Osmundacidites</i>
<i>Aquilapollenites turbidus</i>			<i>Osmundacidites stanleyi</i>
<i>Araucariacites</i> sp.			" <i>Palaeisoetes</i> " sp.
<i>Arecipites</i>			<i>Palaeisoetes subengelmannii</i>
	<i>Arecipites columellas</i>	<i>Paliurus triplicatus</i>	
<i>Arecipites microreticulatus</i>	<i>Arecipites microreticulatus</i>		<i>Pandaniidites</i>
<i>Arecipites reticulatus</i>	<i>Arecipites reticulatus</i>		<i>Pandaniidites typicus</i>
	<i>Azolla</i>	<i>Pediastrum</i>	
	<i>Azolla circinata</i>	<i>Periporopollenites</i> sp.	<i>Periporopollenites</i>
	<i>Azolla cretacea</i> (relatively abundant)	<i>Peroirletes cubensis</i>	
	<i>Azolla</i> microspores	<i>Phaseolidites stanleyi</i>	
<i>Balmesporites</i>			<i>Pityosporites constrictus</i>
<i>Bisaccate conifer pollen</i>	<i>Bisaccate conifer</i>		<i>Pityosporites</i> spp.
<i>Botryococcus</i>			<i>Pityosporites typicus</i>
<i>Camarozonosporites ambigens</i>		<i>Plicapollis?</i>	
<i>Camarozonosporites</i> spp.	<i>Camarozonosporites</i>	<i>Pollenites?</i> sp.	
	<i>Chenopodiipollis</i> sp.	<i>Polypodiidites</i> spp.	
<i>Cicatricosisporites</i>	<i>Cicatricosisporites</i> sp.	<i>Polypodiisporites amplius</i>	
	<i>Cingulatisporites lancei</i>	<i>Polypodiisporites</i> sp.	
<i>Clavatipollenites</i>		<i>Pristinuspollenites</i>	
cf. <i>Concavisporites verrucosus</i>		<i>Pseudoplicapollis?</i>	<i>Pseudoplicapollis</i>
<i>Conferisulcites knowltoni</i>		<i>Pseudoplicapollis newmanii</i>	
<i>Corollina</i>	<i>Corollina</i> sp.	<i>Pseudoplicapollis</i> sp.	
<i>Corollina torosa</i>	<i>Corollina torosa</i>		<i>Pseudoschizaea</i>
	<i>Cupanieidites</i> sp.		<i>Pterospermopsis</i>
<i>Cupanedites</i> aff. <i>C. reticularis</i>		<i>Quadripollis krempii</i>	
	<i>Cupuliferoidaepollenites minor</i>		<i>Quercus explanata</i>
<i>Cupuliferoidaepollenites minutus</i>		cf. <i>Radialetes costatus</i>	
<i>Cupuliferoidaepollenites</i> spp.		<i>Reticuloidosporites pseudomurii</i>	
<i>Cyathidites minor</i>	<i>Cyathidites minor</i>		<i>Retitriletes</i> sp. ("Lycopodiumsporites")
	<i>Cyathidites</i> spp.	<i>Rhoipites</i> sp.	
	<i>Cycadopites fragillius</i>	<i>Rugbivesiculites</i>	<i>Rugbivesiculites</i>
	<i>Cycadopites</i> sp.		<i>Schizosporis parvus</i>
<i>Cyrella mimima</i>		<i>Sphagnum</i> sp.	
<i>Dinoflagellates</i> very few	<i>Dinoflagellate</i>	<i>Sporites?</i> sp. A	
	<i>Dyadonapites reticulatus</i>	<i>Stereisporites</i> spp.	
<i>Echinatisporis</i>	<i>Echinatisporis</i>	<i>Subtriporopollenites</i> sp.	
<i>Echinatisporis varispinosus</i>		cf. <i>Taurocusporites</i>	
<i>Engelhardtia</i> type		<i>Taxodiaceaeapollenites</i>	<i>Taxodiaceaeapollenites</i>
	<i>Ephedra multicostata</i>	<i>Taxodiaceaeapollenites hiatus</i>	<i>Taxodiaceaeapollenites hiatus</i>
<i>Ephedra</i> sp. cf. <i>E. voluta</i>		<i>Tetracopites</i>	
<i>Ephedripites</i> sp. D		<i>Tilia wodehousei</i>	<i>Tilia wodehousei</i>
	<i>Equisetosporites</i> 5	<i>Toroisporis</i> sp.	
<i>Equisetosporites parallel striae</i>		<i>Trichopeltinites</i>	
<i>Equisetosporites spiral</i>		<i>Tricolpites anguloluminosus</i>	
	<i>Erdmanipollis cretaceus</i>	<i>Tricolpites hians</i>	
<i>Erdmannipollis</i> sp.		<i>Tricolpites interangulus</i> Newman	<i>Tricolpites interangulus</i>
<i>Eucommiidites minor</i>			<i>Tricolpites microreticulatus</i>
<i>Eucommiidites</i> sp.		<i>Tricolpites reticulatus</i>	<i>Tricolpites reticulatus</i>
<i>Extratropopollenites</i> sp.		<i>Tricolpites</i> spp.	<i>Tricolpites</i> sp.
Fern spores not abundant		<i>Tricolpites</i> sp. A	
<i>Foraminisporis</i> sp.	<i>Foraminisporis</i>		<i>Tricolpites vulgaris</i>
	<i>Foraminisporis undulatus</i>	<i>Tricolpopollenites</i> sp.	
<i>Foveotriletes scrobicularis</i>		<i>Tricolpopollenites</i> sp. A	
<i>Foveosporites</i> sp. cf. <i>F. canalis</i>		<i>Tricolpopollenites</i> sp. B	
	<i>Fraxinopollenites variabilis</i>	<i>Tricolpopollenites</i> sp. C	
<i>Ghoshispora</i> spp.	<i>Ghoshispora</i> sp.	<i>Tricolpopollenites</i> sp. (Quercus explanata)	
<i>Gleicheniidites</i>	<i>Gleicheniidites</i>		<i>Tricolporites rhomboides</i>
<i>Granabivesiculites</i> sp.		<i>Tricolporites</i> sp.	
	<i>Gunnera</i>	<i>Tricolporites traversei</i>	
	<i>Gunnera microreticulata</i>	<i>Triletes?</i> sp. A	
<i>Hystrichospheres</i> very few		<i>Triplanosporites</i> sp.	
<i>Ilexpollenites</i>			<i>Triporetetes novomexicanum</i>
	<i>Ilexpollenites compactus</i>	<i>Triporopollenites rugatus</i>	
	<i>Inaperturopollenites</i> sp.	<i>Triporopollenites</i> spp.	
<i>Inaperturopollenites</i> cf. <i>I. hiatus</i>		<i>Triporopollenites tectus</i>	
	<i>Inaperturotetradites scabratus</i>	<i>Tnudopollis</i>	
<i>Interporopollenites</i>		<i>Tnudopollis meekeri</i>	
<i>Klukisporites</i>	<i>Klukisporites</i>	<i>Tschudypollis retusus</i>	<i>Tschudypollis retusus</i>
<i>Klukisporites</i> spp.		<i>Tschudypollis</i> many, large	<i>Tschudypollis</i> spp. (many)
<i>Kurtzipites</i>		<i>Tschudypollis thalmanni</i>	<i>Tschudypollis thalmanni</i>
<i>Kurtzipites trispissatus</i>	<i>Kurtzipites trispissatus</i>		<i>Tsugaepollenites</i> sp.
<i>Laevigatosporites</i> spp.	<i>Laevigatosporites</i> spp.	<i>Ulmipollenites</i>	<i>Ulmipollenites</i>
	Larger fern tetrad	<i>Ulmipollenites</i> 3, 4 pored	
<i>Lecaniella</i>		<i>Ulmipollenites krempii</i>	<i>Ulmipollenites krempii</i>
<i>Leptolepidites major</i>			<i>Ulmipollenites</i> sp.
<i>Liliacidites complexus</i>	<i>Liliacidites complexus</i>	<i>Ulmoidipites tricostatus</i>	("Ulmoidipites") <i>tricostatus</i>
<i>Liliacidites hyalaciniatus</i>	<i>Liliacidites hyalaciniatus?</i>		<i>Ulmoidipites</i> spp. 3 and 4 pored smooth to verrucate forms
<i>Liliacidites leei</i>	<i>Liliacidites leei</i>	<i>Vitis?</i> affluens (C3-r 43)	cf. <i>Vitis affluens</i>
	<i>Liliacidites reticulata</i>	<i>Zivisporis novomexicanum</i>	
<i>Liliacidites</i> sp.	<i>Liliacidites</i> sp.	<i>Zivisporis</i> sp.	<i>Zivisporis</i>
	<i>Liliacidites</i> sp. cf. <i>L. complexus</i>	<i>Zonalapollenites</i> sp.	

Note: Palynomorphs listed are from Tables 21 and 22; Fruitland-Kirtland palynomorph zonation shown on Figure 64.

TABLE 24. COMPOSITE PALYNOMORPH LISTS FROM PALEOCENE OJO ALAMO SANDSTONE, SAN JUAN BASIN, NEW MEXICO			
San Juan River Locality	Ojo Alamo Ss Type Area	Southeast SJ Basin	Gasbuggy Core
		<i>Abietinaepollenites</i> sp. (<i>Podocarpus northrupi</i>)	
		<i>Abietinaepollenites</i> sp. (<i>Podocarpus sellowiformis</i>)	
		<i>Acer striata</i>	
	Algal cysts		
<i>Allisporites bilateralis</i>			<i>Aquilapollenites</i> spp.
	<i>Araucariacites australis</i>		
<i>Arecipites reticulatus</i>	<i>Arecipites reticulatus</i>	<i>Arecipites reticulatus</i>	
<i>Arecipites</i> sp.	<i>Arecipites</i> sp.	<i>Arecipites</i> sp.	<i>Arecipites</i> spp.
<i>Azolla cretacea</i>	<i>Azolla cretacea</i>		
	<i>Azolla</i> cf. <i>A. schopfi</i>		
		<i>Bombacipites nacimientoensis</i>	<i>Biretisporites</i> sp.
<i>Brevicolporites colpella</i>	<i>Brevicolporites colpella</i>		
	<i>Cercidiphyllites</i> sp.		
<i>Chenopodipollis</i> sp.	<i>Chenopodipollis</i> sp.		
<i>Cicatricosisporites</i> spp.			<i>Classopollis</i> sp.
<i>Corollina torosa</i> (incl. monads and tetrads)	<i>Corollina torosa</i>		
	<i>Cupaneidites</i> aff. <i>C. major</i>	<i>Cupaneidites</i> aff. <i>C. major</i>	<i>Cupaneidites major</i>
<i>Cupaneidites</i> cf. <i>C. reticularis</i>			cf. <i>Cupaneidites</i>
	<i>Cupaneidites</i> sp.		
<i>Cupuliferoideaepollenites minutus</i>	<i>Cupuliferoideaepollenites minutus</i>	<i>Cupuliferoideaepollenites minutus</i>	
<i>Cyathidites minor</i>	<i>Cyathidites minor</i>		
<i>Cycadopites fragilis</i>			<i>Cyathidites</i> spp.
			<i>Cynilla minima</i>
			<i>Deltoidospora</i> spp.
	<i>Dyadonapites reticulatus</i>		
			<i>Echinatisporis</i> sp.
			<i>Engelhardtia</i> type
<i>Equisetosporites lajwantis</i>			cf. <i>Ephedra voluta</i>
			<i>Equisetosporites</i> spp.
			<i>Ericaceoipollenites</i> sp.
			<i>Formaminisporis</i> spp.
<i>Fraxinoipollenites variabilis</i>	<i>Fraxinoipollenites variabilis</i>	<i>Fraxinoipollenites variabilis</i>	
	<i>Ghoshispora</i> sp.		
		<i>Gleicheniidites senonicus</i>	<i>Hystriochosphaerids & dinoflagellates</i>
<i>Laevigatosporites haardti</i>			
<i>Laevigatosporites</i> sp.	<i>Laevigatosporites</i> spp.		<i>Laevigatosporites</i> sp.
	<i>Liliacidites leei</i>	<i>Liliacidites leei</i>	
	<i>Liliacidites</i> sp.		
<i>Momipites inaequalis</i>	<i>Momipites inaequalis</i>	<i>Momipites inaequalis</i>	<i>Momipites sanjuanensis</i>
	<i>Momipites</i> sp.		
<i>Momipites tenuipolus</i>	<i>Momipites tenuipolus</i>	<i>Momipites tenuipolus</i>	<i>Momipites tenuipolus</i>
<i>Nyssapollenites explanatus</i>		<i>Nyssapollenites</i> sp.	
<i>Nyssapollenites</i> sp.		<i>Nyssa puercoensis</i>	<i>Nyssa puercoensis</i>
	<i>Osmundacidites wellmannii</i>		
<i>Ovoidites ligneolus</i>			
	<i>Ovoidites</i> sp.		
" <i>Palaeoisoetes</i> " sp.	" <i>Palaeoisoetes</i> " sp.		
" <i>Paliurus</i> " <i>triplicatus</i>	" <i>Paliurus</i> " <i>triplicatus</i>		
<i>Pandaniidites</i>			<i>Pandaniidites radicus</i>
	<i>Pandaniidites radicus</i>		
<i>Pandaniidites typicus</i>	<i>Pandaniidites typicus</i>		
			<i>Periporopollenites</i> sp.
<i>Pityosporites</i> sp.	<i>Pityosporites</i> sp.	<i>Pityosporites</i> sp.	
		<i>Podocarpus sellowiformis</i>	
	<i>Podocarpus</i> sp.		
		<i>Polypodiidites</i> spp.	
	<i>Polypodiisporonites</i> sp.		
	<i>Psilastephanocolpites</i> sp.	<i>Psilastephanocolpites</i> sp.	
			<i>Quadrupollenites</i> sp.
	" <i>Quercus</i> " <i>explanata</i>	<i>Quercus explanata</i>	<i>Quercus explanata</i>
	<i>Quercus</i> sp.		
<i>Rectosulcites latus</i>	<i>Rectosulcites latus</i>		
		<i>Salix</i> sp.	
<i>Schizosporis parvus</i>			<i>Stereisporites</i> spp.
	<i>Syncolporites minimus</i>		
<i>Taxodiaceapollenites hiatus</i>			<i>Taxodiaceapollenites</i> sp.
<i>Taxodiaceapollenites vacupites</i>			
	<i>Tetracolpites</i> 2 sp.		
	<i>Tricolpites anguloluminosus</i>	<i>Tricolpites anguloluminosus</i>	<i>Tricolpites anguloluminosus</i>
	<i>Tricolpites foveolate</i>		
	<i>Tricolpites scabrata</i>		
			<i>Tricolpites vulgaris</i>
<i>Tricolpites</i> sp.		<i>Tricolpites</i> spp.	<i>Tricolpites</i> sp.
	<i>Tricolporites rhomboides</i>	<i>Tricolporites rhomboides</i>	<i>Tricolporites rhomboides</i>
		<i>Tricolporites</i> sp.	
	<i>Triporetetes novomexicanum</i>		
	<i>Triporetetes simplex</i>		
		<i>Triporopollenites plektosus</i>	
			cf. <i>Triporopollenites rugatus</i>
		<i>Triporopollenites</i> sp. (cf. <i>Casiaromodotes</i>)	
		<i>Triporopollenites tectus</i>	
<i>Tschudypollis</i> (reworked)			<i>Tschudypollis</i> spp. (reworked)
<i>Tschudypollis thalmanni</i> (reworked)			
<i>Ulmipollenites krempii</i>	<i>Ulmipollenites krempii</i>		
	<i>Ulmipollenites</i> 3 and 4 pored.		<i>Ulmipollenites</i> spp.
		<i>Ulmoideipites krempii</i>	
<i>Ulmoideipites tricostatus</i>	<i>Ulmoideipites tricostatus</i>	<i>Ulmoideipites tricostatus</i>	
			Unclassified bisaccates
			Unclassified triletes
			Unclassified triporates
			<i>Vitis? affluens</i>
<i>Zlivisporis novomexicanum</i>		<i>Zlivisporis novomexicanum</i>	
		<i>Zlivisporis</i> sp.	

Note: Palynomorphs from San Juan River site from Table 19; from O.A. type area, Table 18; from S.E. San Juan Basin, Table 16, and from Gasbuggy core, Table 8

TABLE 25. COMPOSITE PALYNOMORPH LISTS FOR CRETACEOUS AND PALEOCENE STRATA, SAN JUAN BASIN			
Cretaceous - Campanian	Lowermost Paleocene	Cretaceous - Campanian (Cont.)	Lowermost Paleocene (Cont.)
<i>Abietinaepollenites</i>		<i>Momipites sanjuanensis</i>	<i>Momipites sanjuanensis</i>
	<i>Abietinaepollenites</i> sp. (<i>Podocarpus northrupi</i>)	<i>Momipites</i> sp.	<i>Momipites</i> sp.
	<i>Abietinaepollenites</i> sp. (<i>Podocarpus sellowiformis</i>)		<i>Momipites tenuipolus</i>
<i>Acanthotriletes</i>		<i>Monocolopollenites?</i> sp.	
<i>Accuratipollis</i>		<i>Monoporopollenites</i> sp.	
	<i>Acer striata</i>	<i>Monosulcites perspinosus</i>	
<i>Aequitriradites</i>		<i>Monosulcites</i> sp.	
<i>Aequitriradites spinulosus</i>		<i>Naviculites marginatus</i>	
Algal cysts	Algal cysts	<i>Neoraistrickia</i> sp.	
	<i>Alisporites bilateralis</i>	<i>Nyssapollenites albertensis</i>	
<i>Alnipollenites</i> 4 pored			<i>Nyssapollenites explanatus</i>
<i>Alnus</i> 3 pored		<i>Nyssapollenites</i> sp.	<i>Nyssapollenites</i> sp.
<i>Alsophilidites</i> sp.			<i>Nyssa puercoensis</i>
<i>Appendicisporites</i> spp.		<i>Osmundacidites</i>	
<i>Aquilapollenites attenuatus</i>		<i>Osmundacidites stanleyi</i>	
<i>Aquilapollenites delicatus</i>			<i>Osmundacidites wellmannii</i>
<i>Aquilapollenites quadriobus</i>			<i>Ovoidites ligneolus</i>
<i>Aquilapollenites senonicus</i>			<i>Ovoidites</i> sp.
<i>Aquilapollenites</i> sp.	<i>Aquilapollenites</i> spp.		" <i>Palaeoisoetes</i> " sp.
<i>Aquilapollenites trialatus</i> , var. <i>uniformis</i>		<i>Palaeoisoetes subengelmannii</i>	
<i>Aquilapollenites turbidus</i>		<i>Paliurus triplicatus</i>	" <i>Paliurus</i> " <i>triplicatus</i>
	<i>Araucariacites australis</i>		<i>Pandanidites</i>
<i>Araucariacites</i> sp.			<i>Pandanidites radicus</i>
<i>Arecipites columellus</i>		<i>Pandanidites typicus</i>	<i>Pandanidites typicus</i>
<i>Arecipites microreticulatus</i>		<i>Pediastrum</i>	
<i>Arecipites reticulatus</i>	<i>Arecipites reticulatus</i>	<i>Periporopollenites</i> sp.	<i>Periporopollenites</i> sp.
<i>Arecipites</i>	<i>Arecipites</i> sp.	<i>Perotriletes cubensis</i>	
<i>Azolla circinata</i>		<i>Phaseolidites stanleyi</i>	
<i>Azolla cretacea</i>	<i>Azolla cretacea</i>	<i>Pityosporites constrictus</i>	
<i>Azolla</i> microspores		<i>Pityosporites</i> spp.	<i>Pityosporites</i> sp.
	<i>Azolla</i> cf. <i>A. schopfi</i>	<i>Pityosporites typicus</i>	
<i>Balmesporites</i>		<i>Plicapollis?</i>	
	<i>Biretisporites</i> sp.		<i>Podocarpus sellowiformis</i>
Bisaccate conifer pollen			<i>Podocarpus</i> sp.
	<i>Bombacacipites nacimientoensis</i>	<i>Pollenites?</i> sp.	
<i>Botryococcus</i>		<i>Polypodiidites</i> spp.	<i>Polypodiidites</i> spp.
	<i>Brevicolporites colpella</i>	<i>Polypodiisporites amplius</i>	
<i>Camazonosporites ambigens</i>		<i>Polypodiisporites</i> sp.	
<i>Camazonosporites</i> spp.			<i>Polypodiisporonites</i> sp.
	<i>Cercidiphyllites</i> sp.	<i>Pristinuspollenites</i>	
<i>Chenopodiipollis</i> sp.	<i>Chenopodiipollis</i> sp.	<i>Pseudoplicapollis?</i>	
<i>Cicatricosisporites</i> sp.	<i>Cicatricosisporites</i> spp.	<i>Pseudoplicapollis newmanii</i>	
<i>Cingulatisporites lancei</i>		<i>Pseudoschizaea</i>	
	<i>Classopollis</i> sp.	<i>Pseudoplicapollis</i> sp.	
<i>Clavatipollenites</i>			<i>Psilastephanocolpites</i> sp.
cf. <i>Concavisporites verrucosus</i>		<i>Pterospermopsis</i>	
<i>Conferisulcites knowltoni</i>			<i>Quadrupollenites</i> sp.
<i>Corollina</i>		<i>Quadrupollis krempii</i>	
<i>Corollina torosa</i>	<i>Corollina torosa</i> (incl. monads and tetrads)	<i>Quercus explanata</i>	" <i>Quercus</i> " <i>explanata</i>
	<i>Cupanieidites</i> aff. <i>C. major</i>		<i>Quercus</i> sp.
<i>Cupanieidites</i> aff. <i>C. reticularis</i>	<i>Cupanieidites</i> cf. <i>C. reticularis</i>	cf. <i>Radialetes costatus</i>	
	<i>Cupanieidites</i> sp.		<i>Rectosulcites latus</i>
<i>Cupuliferoidaeipollenites minor</i>		<i>Reticuloidosporites pseudomurii</i>	
<i>Cupuliferoidaeipollenites minutus</i>	<i>Cupuliferoidaeipollenites minutus</i>	<i>Retitriletes</i> sp. (" <i>Lycopodiumsporites</i> ")	
<i>Cupuliferoidaeipollenites</i> spp.		<i>Rhoipites</i> sp.	
<i>Cyathidites minor</i>	<i>Cyathidites minor</i>	<i>Rugubivesiculites</i>	
<i>Cyathidites</i> spp.			<i>Salix</i> sp.
<i>Cycadopites fragilis</i>	<i>Cycadopites fragilis</i>	<i>Schizosporis parvus</i>	<i>Schizosporis parvus</i>
<i>Cycadopites</i> sp.		<i>Sphagnum</i> sp.	
	<i>Cyrilla minima</i>	<i>Sporites?</i> sp.	
	<i>Deltoidospora</i> spp.	<i>Stereisporites</i> spp.	<i>Stereisporites</i> spp.
Dinoflagellates		<i>Subtriporopollenites</i> sp.	
<i>Dyadonapites reticulatus</i>	<i>Dyadonapites reticulatus</i>		<i>Syncolporites minimus</i>
<i>Echinatisporis</i>	<i>Echinatisporis</i> sp.	cf. <i>Taurosporites</i>	
<i>Echinatisporis varispinosus</i>		<i>Taxodiaceaeipollenites hiatus</i>	<i>Taxodiaceaeipollenites hiatus</i>
<i>Engelhardia</i> type	<i>Engelhardia</i> type	<i>Taxodiaceaeipollenites</i>	<i>Taxodiaceaeipollenites</i> sp.
<i>Ephedra multicostata</i>			<i>Taxodiaceaeipollenites vacuipites</i>
<i>Ephedra</i> sp. cf. <i>E. voluta</i>	cf. <i>Ephedra voluta</i>	<i>Tetracolpites</i>	<i>Tetracolpites</i> 2 sp.
<i>Ephedripites</i> sp.		<i>Triaepollenites</i> sp. (<i>Tilia wodehousei</i>)	
	<i>Equisetosporites lajwantis</i>	cf. <i>Tilia wodehousei</i>	
<i>Equisetosporites</i> parallel striae		<i>Torisporis</i> sp.	
<i>Equisetosporites</i> spiral		<i>Trichopeltites</i>	
<i>Equisetosporites</i> sp.	<i>Equisetosporites</i> spp.	<i>Tricolpites anguloluminosus</i>	<i>Tricolpites anguloluminosus</i>
<i>Erdtmannipollis</i> cretaceous			<i>Tricolpites foveolate</i>
<i>Erdtmannipollis</i> sp.	<i>Ericaceoipollenites</i> sp.	<i>Tricolpites hians</i>	
		<i>Tricolpites interangulus</i> Newman	
<i>Eucommiidites minor</i>		<i>Tricolpites microreticulatus</i>	
<i>Eucommiidites</i> sp.		<i>Tricolpites reticulatus</i>	
<i>Extratropopollenites</i> sp.		<i>Tricolpites</i> sp. A	
Fern spores not abundant			<i>Tricolpites scabrata</i>
<i>Foraminisporis</i> sp.	<i>Foraminisporis</i> spp.	<i>Tricolpites</i> spp.	<i>Tricolpites</i> spp.
<i>Foraminisporis undulatus</i>			<i>Tricolpites vulgaris</i>
<i>Foveotriletes scrobicularis</i>			
<i>Foveosporites</i> sp. Cf. <i>F. canalis</i>		<i>Tricolpopollenites</i> sp.	
<i>Fraxinoipollenites variabilis</i>	<i>Fraxinoipollenites variabilis</i>	<i>Tricolpopollenites</i> sp. (<i>Quercus explanata</i>)	
<i>Ghoshispora</i> spp.	<i>Ghoshispora</i> sp.	<i>Tricolporites</i> sp.	
	<i>Gleicheniidites senonicus</i>	<i>Tricolporites traversei</i>	
<i>Gleicheniidites</i> spp.			<i>Tricolporites rhomboides</i>
<i>Granabivesiculites</i> sp.			<i>Tricolpites</i> sp.
<i>Gunnera microreticulata</i>		<i>Triletes?</i> sp.	
<i>Hystrichosphaeres</i>	<i>Hystrichosphaeres</i> & dinoflagellates	<i>Triplanosporites</i> sp.	
<i>Ilexpollenites compactus</i>		<i>Triporetetes novomexicanum</i>	<i>Triporetetes novomexicanum</i>
<i>Interporopollenites</i>			<i>Triporetetes simplex</i>
<i>Inaperturopollenites</i> cf. <i>I. hiatus</i>		<i>Triporopollenites rugatus</i>	
<i>Inaperturotetradites scabratus</i>			<i>Triporopollenites plektosus</i>
<i>Klukisporites</i>			cf. <i>Triporopollenites rugatus</i>
<i>Kurtzpollis</i>		<i>Triporopollenites</i> spp.	<i>Triporopollenites</i> sp.
<i>Kurtzpollis trispissatus</i>			<i>Triporopollenites</i> sp. (cf. <i>Casiaromodotes</i>)
<i>Kuyllisporites</i> sp.		<i>Triporopollenites tectus</i>	<i>Triporopollenites tectus</i>
	<i>Laevigatosporites haardtii</i>	<i>Trudopollis meekeri</i>	
<i>Laevigatosporites</i> spp.	<i>Laevigatosporites</i> sp.	<i>Trudopollis</i> sp.	
Large fern tetrad		<i>Tschudypollis</i> many, large	<i>Tschudypollis</i> (reworked)
<i>Lecaniella</i>		<i>Tschudypollis retusus</i>	
<i>Leptolepidites major</i>		<i>Tschudypollis</i> sp.	
<i>Liliacidites</i>		<i>Tschudypollis thalmanii</i>	<i>Tschudypollis thalmanii</i> (reworked)
<i>Liliacidites complexus</i>		<i>Tsugaepollenites</i> sp.	
<i>Liliacidites hyalaciniatus</i>		<i>Ulmipollenites</i>	
<i>Liliacidites leei</i>	<i>Liliacidites leei</i>	<i>Ulmipollenites krempii</i>	<i>Ulmipollenites</i> spp.
<i>Liliacidites reticulata</i>		<i>Ulmipollenites</i> 3, 4 pored	<i>Ulmipollenites</i> 3 and 4 pored.
<i>Liliacidites</i> sp.	<i>Liliacidites</i> sp.	<i>Ulmoidipites</i> spp. 3 and 4 pored smooth to verrucate forms	
<i>Liliacidites</i> sp. cf. <i>L. complexus</i>		<i>Ulmoidipites</i> <i>tricastatus</i>	<i>Ulmoidipites</i> <i>tricastatus</i>
<i>Liquidambarpollenites</i> sp.			Unclassified bisaccates
<i>Loranthacites</i>			Unclassified triletes
<i>Lycopodiacidites kuepperi</i>			Unclassified triporates
<i>Lycopodiacidites</i> spp.		unidentified acritarchs	
<i>Lycopodiumsporites</i> spp.		unidentified dinoflagellate cysts	
<i>Microfoveolatosporis</i>		unidentified pollen tetrad	
<i>Microfoveolatosporis canaliculatus</i>		unidentified trilete spores	
<i>Microreticulatisporites</i> sp.		cf. <i>Vitis affluens</i>	<i>Vitis?</i> <i>affluens</i>
cf. <i>Minorpollis</i>		<i>Zonalapollenites</i>	
<i>Momipites inaequalis</i>	<i>Momipites inaequalis</i>	<i>Zivisporis novomexicanum</i>	<i>Zivisporis novomexicanum</i>
		<i>Zivisporis</i>	<i>Zivisporis</i> sp.

Notes: Cretaceous strata include Kirtland, Fruitland, and Kirtland-Fruitland Formations undivided; Paleocene strata include the Ojo Alamo Sandstone and in places the Paleocene uppermost part of the Kirtland and (or) Fruitland Formation. Palynomorphs listed are from Tables 23 and 24.

TABLE 27. PALYNOMORPHS IDENTIFIED FROM THE OJO ALAMO SANDSTONE AND NACIMIENTO FORMATION

Ojo Alamo Sandstone P. Palynomorphs	Nacimiento Formation P. Palynomorphs	Ojo Alamo Sandstone P. Palynomorphs (Cont.)	Nacimiento Formation P. Palynomorphs (Cont.)
<i>Abietinaepollenites</i> sp. (<i>Podocarpus northrupi</i>)		<i>Pallidus</i> sp.	
<i>Aberinaepollenites</i> sp. (<i>Podocarpus sellowiformis</i>)		<i>Pandanidites</i>	
<i>Acer striata</i>		<i>Pandanidites radicus</i>	<i>Pandanidites radicus</i>
Algal Cysts		<i>Pandanidites typicus</i>	
<i>Allisporites bilateralis</i>		<i>Periporopollenites</i> sp.	<i>Periporopollenites</i> sp. "Pinus haploxyton type" Rudolph, 1935 "Pinus sylvestris type" Rudolph, 1935
<i>Aquilapollenites</i> spp.		<i>Pityosporites</i> sp.	
<i>Araucariacites australis</i>		<i>Podocarpus sellowiformis</i>	
<i>Arecipites reticulatus</i>		<i>Podocarpus</i> sp.	
<i>Arecipites</i> sp.		<i>Polypodioidites</i> spp.	
<i>Asolla cretacea</i>		<i>Polypodisporonites</i> sp.	
<i>Azolla</i> cf. <i>A. schopfii</i>			
<i>Biretisporites</i> sp.		<i>Polytricolpites</i> spp.	
<i>Bombacacipites naciementoensis</i>		<i>Polytricolpites</i> spp.	
<i>Brevicopipites colpella</i>		<i>Psilastephanocolpites</i> sp.	
<i>Cercidiphyllites</i> sp.		<i>Quadracolpites</i> sp.	
<i>Chenopodioidites</i> sp.		" <i>Quercus</i> " <i>explanata</i>	
<i>Cicatricosisporites</i> spp.		<i>Quercus</i> sp.	
<i>Claosporites</i> sp.		<i>Rectosulcites latus</i>	
<i>Corollina torosa</i> (incl. monads and tetrads)		<i>Rectosulcites</i> sp.	
<i>Cupanioidites</i> aff. <i>C. major</i>		<i>Salix</i> sp.	
<i>Cupanioidites</i> cf. <i>C. reticularis</i>		<i>Schizosporis parvus</i>	
<i>Cupanioidites</i> sp.		<i>Stereisporites</i> spp.	
<i>Cupuliferoidaeipollenites minutus</i>		<i>Syncoelotes minimus</i>	
<i>Cyathidites minor</i>		<i>Syncoelotes</i> sp.	
<i>Cycadoidites fragilis</i>		<i>Taxodiaceapollenites hiatus</i>	
<i>Denticospora</i> spp.		<i>Taxodiaceapollenites</i> sp.	
<i>Dyabonapites reticulatus</i>		<i>Taxodiaceapollenites vacuipites</i>	
<i>Echinatisporis</i> sp.		<i>Tetracolpites</i> 2 sp.	
<i>Engelhardtia</i> type			
cf. <i>Ephedra voluta</i>		<i>Tetradites</i> sp.	
<i>Equisetosporites laiwantis</i>		<i>Tilia daniel n. sp.</i>	
<i>Equisetosporites</i> spp.		<i>Triatropopollenites</i> sp.	
<i>Ericaceopollenites</i> sp.		<i>Triatropopollenites trina</i>	
<i>Foraminisporis</i> spp.		<i>Tricolpites anguloluminosus</i>	
<i>Fraxinopollenites variabilis</i>		<i>Tricolpites scabrata</i>	
<i>Groshospora</i> sp.		<i>Tricolpites</i> spp.	
<i>Gleicheniidites senonicus</i>		<i>Tricolpites</i> sp. (<i>Quercus explanata</i> And.)	
<i>Hystriochsphaerids & dinoflagellates</i>		<i>Tricolpites</i> sp. (<i>Tricolpites anguloluminosus</i> And.)	
<i>Laevigatosporites haardtii</i>		<i>Tricolpites</i> sp. (? <i>Elaeagnaceae</i>)	
<i>Laevigatosporites</i> sp.		<i>Tricolpites</i> sp. (<i>Tricolpites rhomboides</i> And.)	
<i>Lilacidites leei</i>		<i>Tricolpites</i> sp.	
<i>Lilacidites</i> sp.		<i>Triporolites rhomboides</i>	
<i>Lygodiosporites?</i> sp.		<i>Triporolites novomexicanum</i>	
<i>Momipites coryboides</i>		<i>Triporolites simplex</i>	
<i>Momipites inaequalis</i>		<i>Triporopollenites plektosus</i>	
<i>Momipites sanjuanensis</i>		cf. <i>Triporopollenites rugatus</i>	
<i>Momipites tenuipolus</i>		<i>Triporopollenites rugatus</i>	
<i>Myssapollenites explanatus</i>		<i>Triporopollenites</i> sp. (cf. <i>Casuarinidites</i>)	
<i>Myssapollenites</i> sp.		<i>Triporopollenites tectus</i>	
<i>Nyssa puercoensis</i>		<i>Ulmipollenites</i> spp.	
<i>Osmundacidites wellmannii</i>		<i>Ulmipollenites kreppli</i>	
<i>Ovoidites lignicola</i>		<i>Ulmipollenites tricoelatus</i>	
<i>Ovoidites</i> sp.		<i>Ulmipollenites</i> 3 and 4 porid.	
" <i>Palaeoisocetes</i> " sp.		<i>Ulmoidipites tricoelatus</i>	
		<i>Ulmoidipites</i> sp.	
		Unclassified bisaccates	
		Unclassified liliates	
		Unclassified triporates	
		<i>Vitis ? affluens</i>	
		<i>Zlivisporis novomexicanum</i>	
		<i>Zlivisporis</i> sp.	

Notes: "Ojo Alamo P" = "Ojo Alamo Sandstone Plus" - includes samples from the Ojo Alamo plus samples from underlying strata of Paleocene age.

TABLE 28. PALYNOLOGIC ZONATION OF UPPER CAMPANIAN STRATA, SOUTHERN S. J. BASIN		
Lower Fruitland	Upper Fruitland	Upper Kirtland
<i>Corollina</i>		<i>Corollina</i>
<i>Equisetosporites parallel striae</i>		<i>Equisetosporites</i>
<i>Eucommiidites</i> sp.		<i>Eucommiidites</i> sp.
<i>Liliacidites leei</i>		<i>Liliacidites leei</i>
<i>Taxodiaceapollenites</i>	<i>Taxodiaceapollenites</i>	<i>Taxodiaceapollenites</i>
<i>Tschudypollis</i> many, large	<i>Tschudypollis</i> spp.	<i>Tschudypollis</i>
<i>Tschudypollis retusus</i>	<i>Tschudypollis retusus</i>	<i>Tschudypollis retusus</i>
<i>Tschudypollis thalmanii</i>		<i>Tschudypollis thalmanii</i>
	<i>Abietineaepollenites</i>	<i>Abietineaepollenites</i>
		<i>Aequitriradites</i>
		<i>Araucariacites</i> sp.
		<i>Arecipites reticulatus</i>
		<i>Azolla</i>
		<i>Balmeisporites</i>
		<i>Cupaneidites</i> sp.
	<i>Cyathidites</i> spp.	<i>Cyathidites</i> sp.
		<i>Cycadopites fragillis</i>
		<i>Cycadopites</i> sp.
		<i>Dyadonapites reticulatus</i>
		<i>Erdtmannipollis</i> sp.
		<i>Foraminisporis</i>
		<i>Ghoshispora</i> sp.
		<i>Granabivesiculites</i> sp.
		<i>Gunnera</i>
		<i>Interpollis</i>
		<i>Kurtzipites</i>
		<i>Kurtzipites trispissatus</i>
	<i>Laevigatosporites</i> spp.	<i>Laevigatosporites</i> sp.
		<i>Liliacidites hyalaciniatus</i>
	<i>Liliacidites</i> sp.	<i>Liliacidites</i>
		<i>Liquidambarpollenites</i> sp.
	<i>Lycopodiacidites</i>	<i>Lycopodiacidites</i>
		<i>Lycopodiumsporites</i>
		<i>Monoporopollenites</i> sp.
		<i>Monosulcites</i>
		<i>Nyssapollenites albertensis</i>
		<i>Osmundacidites</i>
		<i>Pandaniidites typicus</i>
	<i>Periporopollenites</i>	<i>Periporopollenites</i>
		<i>Pityosporites constrictus</i>
		<i>Pityosporites</i> spp.
		<i>Pterospermopsis</i>
		<i>Quercus explanata</i>
		<i>Schizosporis parvus</i>
	<i>Taxodiaceapollenites hiatus</i>	<i>Taxodiaceapollenites hiatus</i>
		<i>Tricolpites interangulus</i>
		<i>Tricolpites microreticulatus</i>
		<i>Tricolpites reticulatus</i>
		<i>Tricolpopollenites</i> sp.
		<i>Tsugaepollenites</i> sp.
	<i>Ulmipollenites</i>	<i>Ulmipollenites</i>
		<i>Ulmipollenites krempii</i>
		<i>Ulmoideipites</i> spp.
		<i>Ulmoideipites tricostatus</i>
		unidentified trilete spores
		cf <i>Vitis affluens</i>
		<i>Zlivisporis</i> sp.

<i>Camarozonosporites ambigens</i>	<i>Camarozonosporites ambigens</i>	
<i>Cicatricosisporites</i> sp.	<i>Cicatricosisporites</i> sp.	
	<i>Corollina torosa</i>	
<i>Cupuliferoidaepollenites</i> spp.	<i>Cupuliferoidaepollenites</i> spp.	
Dinoflagellates very few	Dinoflagellate	
<i>Echinatisporis varispinosus</i>	<i>Echinatisporis varispinosus</i>	
	<i>Eucommiidites minor</i>	
<i>Gleicheniidites</i>	<i>Gleicheniidites</i>	
	<i>Klukisporites</i>	
	<i>Microfoveolatosporis</i>	
	<i>Microreticulatisporites</i> sp.	
	<i>Momipites sanjuanensis</i>	
<i>Nyssapollenites</i> sp.	<i>Nyssapollenites</i> spp.	
	<i>Pseudoplicapollis newmanii</i>	
<i>Pseudoplicapollis?</i>	<i>Pseudoplicapollis</i>	
<i>Reticuloidosporites pseudomurii</i>	<i>Reticuloidosporites pseudomurii</i>	
	<i>Rhoipites</i> sp.	
<i>Rugubivesiculites</i>	<i>Rugubivesiculites</i>	
<i>Stereisporites</i> spp.	<i>Stereisporites</i> spp.	
<i>Tricolpites</i> spp.	<i>Tricolpites</i> spp.	
	<i>Triporopollenites tectus</i>	
<i>Acanthotriletes</i>		
<i>Accuratipollis</i>		
<i>Aequitriradites</i>		
Algal cysts		
<i>Appendicisporites</i> sp.		
<i>Araucariacites</i> common		
<i>Aquilapollenites quadrilobus</i>		
<i>Aquilapollenites senonicus</i>		
<i>Aquilapollenites trialatus</i> , var. <i>uniformis</i>		
<i>Arecipites</i>		
<i>Balmeisporites</i>		
Bisaccate conifer pollen		
<i>Botryococcus</i>		
<i>Cyathidites minor</i>		
<i>Ephedra</i> sp.		
<i>Foveosporites</i> sp.		
Hystrichospheres very few		
<i>Ilxpollenites</i>		
<i>Inaperturopollenites</i>		
<i>Lecaniella</i>		
<i>Monocolopopollenites?</i> s p.		
<i>Monosulcites</i> sp.		
<i>Neoraistrickia</i> sp.		
<i>Pediastrum</i>		
<i>Plicapollis?</i>		
<i>Pristinuspollenites</i>		
<i>Quadripollis krempii</i>		
<i>Tetracolpites</i>		
<i>Tilia wodehousei</i>		
<i>Tricolpopollenites</i> sp.		
<i>Tricolporites</i> sp.		
<i>Triporopollenites</i> spp.		
<i>Trudopollis</i>		
<i>Ulmipollenites krempii</i>		
<i>Ulmoideipites tricostatus</i>		
<i>Zonalapollenites</i> sp.		
Note. Palynomorph lists from Tables 21, 22, 23.		

TABLE 29. COMPARISON OF PALYNOMORPHS FROM CRETACEOUS (CAMPANIAN) AND PALEOCENE STRATA IN SAN JUAN BASIN, NEW MEXICO AND COLORADO

Paleocene - Ojo Alamo Sandstone Plus	Cretaceous - Fruitland and Kirtland Formations	Cretaceous - Fruitland and Kirtland Formations (Cont.)
<i>Abietinaepollenites</i> sp. (<i>Podocarpus northrupi</i>)		<i>Botryococcus</i>
<i>Abietinaepollenites</i> sp. (<i>Podocarpus sellowiformis</i>)		<i>Camarozonosporites ambigens</i> ^{NSP}
<i>Acer striata</i>		<i>Camarozonosporites</i> spp. ^{NSP}
<i>Alisporites bilateralis</i>		<i>Cingulatisporites lancei</i>
<i>Araucariacites australis</i>		<i>Clavatisporites</i>
<i>Azolla</i> cf. <i>A. schopfi</i>		cf. <i>Concavisporites verrucosus</i>
<i>Biretisporites</i> sp.		<i>Confetisulcites knowltoni</i>
<i>Bombacacipites nacimientensis</i>		<i>Corollina</i>
<i>Brevipollenites colpeila</i> ^{NSP}		<i>Cupuliferoidaepollenites minor</i>
<i>Cercidiphyllites</i> sp.		<i>Cupuliferoidaepollenites</i> spp.
<i>Classopollis</i> sp.		<i>Cyathidites</i> sp.
<i>Cupanieidites</i> aff. <i>C. major</i>		<i>Cycadipites</i> sp.
<i>Cupanieidites</i> sp.		<i>Dinoflagellates</i>
<i>Cynilla minima</i>		<i>Echinatisporis varispinosus</i>
<i>Deltoidospora</i> spp.		<i>Ephedra multicosata</i>
<i>Equisetosporites lajvantis</i>		<i>Ephedripites</i> sp.
<i>Ericaceipollenites</i> sp.		<i>Equisetosporites parallel striae</i>
<i>Gleicheniidites senonicus</i>		<i>Equisetosporites spiral</i>
<i>Laevigatosporites haardtii</i>		<i>Erdmannipollis cretaceus</i>
<i>Momipites tenuipollis</i> ^{NSP}		<i>Erdmannipollis</i> sp.
<i>Nyssapollenites explanatus</i>		<i>Eucommiidites minor</i>
<i>Nyssa puercoensis</i>		<i>Eucommiidites</i> sp.
<i>Osmundacidites wellmannii</i>		<i>Extratropopollenites</i> sp.
<i>Ovoidites ligneolus</i>		Fern spores not abundant
<i>Ovoidites</i> sp.		<i>Foraminisporis undulatus</i>
<i>Palaeoisocetes</i> sp.		<i>Foveotriletes scrobicularis</i>
<i>Pandaniidites</i>		<i>Foveosporites</i> sp. Cf. <i>F. canalis</i>
<i>Pandaniidites radicus</i>		<i>Gleicheniidites</i> sp.
<i>Podocarpus sellowiformis</i>		<i>Granbivesiculites</i> sp.
<i>Podocarpus</i> sp.		<i>Gunthera microreticulata</i> ^{NSP}
<i>Polypodiisporites</i> sp.		<i>Hesperipollenites compactus</i> ^{NSP}
<i>Psilastephanocolpites</i> sp.		<i>Interporopollenites</i>
<i>Quadrupollenites</i> sp.		<i>Inaperturopollenites</i> cf. <i>I. hiatus</i>
<i>Quercus</i> sp.		<i>Inaperturotetradites scabratus</i>
<i>Rectosulcites latus</i>		<i>Klukisporites</i>
<i>Salix</i> sp.		<i>Kurtzipites</i> ^{NSP}
<i>Syncolpites minimus</i>		<i>Kurtzipites trispissatus</i> ^{NSP}
<i>Taxodiaceaeapollenites vacuipites</i>		<i>Kuylisporites</i> sp.
<i>Tricolpites foveolate</i>		Larger fern tetrad
<i>Tricolpites scabrata</i>		<i>Lecaniella</i>
<i>Tricolpites vulgaris</i>		<i>Leptospidites major</i>
<i>Tricolpites rhomboides</i>		<i>Liliacidites</i>
<i>Tricolpites</i> sp.		<i>Liliacidites complexus</i> ^{NSP}
<i>Triporetetes simplex</i>		<i>Liliacidites hyalaciniatus</i>
<i>Triporetetes plektosus</i>		<i>Liliacidites reticulata</i>
cf. <i>Triporetetes rugatus</i>		<i>Liliacidites</i> sp. cf. <i>L. complexus</i>
Unclassified bisaccates		<i>Liquidambarpollenites</i> sp.
Unclassified triletes		<i>Loranthacites</i>
Unclassified triporates		<i>Lycopodiacidites kuepperi</i>
Algal cysts	Algal cysts	<i>Lycopodiacidites</i> spp.
<i>Aquilapollenites</i> spp.	<i>Aquilapollenites</i> sp. ^{NSP}	<i>Lycopodiumsporites</i> spp.
<i>Arecipites reticulatus</i>	<i>Arecipites reticulatus</i>	<i>Microfoveolatosporis</i>
<i>Arecipites</i> sp.	<i>Arecipites</i>	<i>Microfoveolatosporis canaliculatus</i>
<i>Azolla cretacea</i>	<i>Azolla cretacea</i>	<i>Microreticulatisporites</i> sp.
<i>Chenopodiipollis</i> sp.	<i>Chenopodiipollis</i> sp.	cf. <i>Minorpollis</i>
<i>Cicatricosisporites</i> spp.	<i>Cicatricosisporites</i> sp.	<i>Monocolopopollenites?</i> sp.
<i>Corollina torosa</i> (incl. monads and tetrads)	<i>Corollina torosa</i>	<i>Monoporopollenites</i> sp.
<i>Cupanieidites</i> cf. <i>C. reticularis</i>	<i>Cupanieidites</i> aff. <i>C. reticularis</i>	<i>Monosulcites perspinosus</i>
<i>Cupuliferoidaepollenites minutus</i>	<i>Cupuliferoidaepollenites minutus</i>	<i>Monosulcites</i> sp.
<i>Cyathidites minor</i>	<i>Cyathidites minor</i>	<i>Navisulcites marginatus</i>
<i>Cycadipites fragilis</i>	<i>Cycadipites fragilis</i>	<i>Neoraistrickia</i> sp.
<i>Dyadonapites reticulatus</i>	<i>Dyadonapites reticulatus</i>	<i>Nyssapollenites albertensis</i>
<i>Echinatisporis</i> sp.	<i>Echinatisporis</i>	<i>Osmundacidites</i>
<i>Engelhardtia</i> type	<i>Engelhardtia</i> type	<i>Osmundacidites stanleyi</i>
cf. <i>Ephedra voluta</i>	<i>Ephedra</i> sp. cf. <i>E. voluta</i>	<i>Palaeoisocetes subengelmannii</i>
<i>Equisetosporites</i> spp.	<i>Equisetosporites</i> sp.	<i>Pediastrum</i>
<i>Foraminisporis</i> spp.	<i>Foraminisporis</i> sp.	<i>Periporopollenites</i> sp.
<i>Fraxinopollenites variabilis</i>	<i>Fraxinopollenites variabilis</i>	<i>Perotriletes cubensis</i>
<i>Ghoshispora</i> sp.	<i>Ghoshispora</i> spp.	<i>Phaseolidites stanleyi</i>
<i>Hystichosphaerids & dinoflagellates</i>	<i>Hystichosphaeres</i>	<i>Pityosporites constrictus</i>
<i>Laevigatosporites</i> sp.	<i>Laevigatosporites</i> spp.	<i>Pityosporites typicus</i>
<i>Liliacidites leei</i>	<i>Liliacidites leei</i>	<i>Plicapollis?</i>
<i>Liliacidites</i> sp.	<i>Liliacidites</i> sp.	<i>Pollenites?</i> sp.
<i>Momipites inaequalis</i>	<i>Momipites inaequalis</i>	<i>Polypodiisporites amplius</i>
<i>Momipites sanjuanensis</i>	<i>Momipites sanjuanensis</i>	<i>Polypodiisporites</i> sp.
<i>Momipites</i> sp.	<i>Momipites</i> sp.	<i>Pristinuspollenites</i>
<i>Nyssapollenites</i> sp.	<i>Nyssapollenites</i> sp.	<i>Pseudoplicapollis?</i>
<i>"Paliurus" triplicatus</i>	<i>Paliurus triplicatus</i>	<i>Pseudoplicapollis newmanii</i>
<i>Pandaniidites typicus</i>	<i>Pandaniidites typicus</i>	<i>Pseudoschizaea</i>
<i>Periporopollenites</i> sp.	<i>Periporopollenites</i> sp.	<i>Pseudoplicapollis</i> sp.
<i>Pityosporites</i> sp.	<i>Pityosporites</i> spp.	<i>PterospERMopsis</i>
<i>Polypodiidites</i> spp.	<i>Polypodiidites</i> spp.	<i>Quadrupollis krempii</i>
<i>"Quercus" explanata</i>	<i>Quercus explanata</i>	cf. <i>Radialetes costatus</i>
<i>Schizosporis parvus</i>	<i>Schizosporis parvus</i>	<i>Reticuloidosporites pseudomunri</i>
<i>Stereisporites</i> spp.	<i>Stereisporites</i> spp.	<i>Retitriletes</i> sp. (" <i>Lycopodiumsporites</i> ")
<i>Taxodiaceaeapollenites hiatus</i>	<i>Taxodiaceaeapollenites hiatus</i>	<i>Rhoipites</i> sp.
<i>Taxodiaceaeapollenites</i> sp.	<i>Taxodiaceaeapollenites</i>	<i>Rugbivesiculites</i>
<i>Tetracolpites</i> 2 sp.	<i>Tetracolpites</i>	<i>Sphaerium</i> sp.
<i>Tricolpites anguloluminosus</i>	<i>Tricolpites anguloluminosus</i>	<i>Sporites?</i> sp.
<i>Tricolpites</i> spp.	<i>Tricolpites</i> spp. ^{NSP}	<i>Subtriporopollenites</i> sp.
<i>Triporetetes novomexicanum</i>	<i>Triporetetes novomexicanum</i>	cf. <i>Tauropusporites</i>
<i>Triporetetes</i> sp.	<i>Triporetetes</i> spp.	<i>Tiliaepollenites</i> sp. (<i>Tilia wodehousei</i>)
<i>Triporetetes tectus</i>	<i>Triporetetes tectus</i>	cf. <i>Tilia wodehousei</i> ^{NSP}
<i>Ulmipollenites</i>	<i>Ulmipollenites</i>	<i>Toroisporis</i> sp.
<i>Ulmipollenites krempii</i>	<i>Ulmipollenites krempii</i>	<i>Trichopollenites</i> ^{NSP}
<i>Ulmipollenites</i> 3 and 4 pored	<i>Ulmipollenites</i> 3, 4 pored	<i>Tricolpites hians</i>
<i>Ulmoidipites tricosatus</i>	<i>Ulmoidipites tricosatus</i>	<i>Tricolpites interangulus Newman</i>
<i>Vitis? affluens</i>	cf. <i>Vitis affluens</i>	<i>Tricolpites microreticulatus</i> ^{NSP}
<i>Zlivisporis novomexicanum</i>	<i>Zlivisporis novomexicanum</i>	<i>Tricolpites reticulatus</i> ^{NSP}
<i>Zlivisporis</i> sp.	<i>Zlivisporis</i>	<i>Tricolpites</i> sp. A
	<i>Abietinaepollenites</i>	<i>Tricolpites</i> sp. B
	<i>Acanthotriletes</i>	<i>Tricolpites</i> sp. C
	<i>Accusipollis</i> ^{NSP}	<i>Tricolpites</i> sp. D
	<i>Aequitriadites</i>	<i>Tricolpites traversei</i>
	<i>Aequitriadites spinulosus</i>	<i>Triletes?</i> sp.
	<i>Ainipollenites</i> 4 pored	<i>Tripinosporites</i> sp.
	<i>Ainus</i> 3 pored	<i>Triporetetes rugatus</i> ^{NSP}
	<i>Alsophilidites</i> sp.	<i>Trudopollis meekeri</i>
	<i>Appendicisporites</i> spp.	<i>Trudopollis</i> sp.
	<i>Aquilapollenites attenuatus</i> ^{NSP}	<i>Tschudyipollis many, large</i> ^{NSP}
	<i>Aquilapollenites delicatus</i> ^{NSP}	<i>Tschudyipollis retusus</i> ^{NSP}
	<i>Aquilapollenites quadrilobus</i> ^{NSP}	<i>Tschudyipollis</i> sp. ^{NSP}
	<i>Aquilapollenites senonicus</i> ^{NSP}	<i>Tschudyipollis thalmanii</i> ^{NSP}
	<i>Aquilapollenites triangularis, var. uniformis</i>	<i>Tsugaepollenites</i> sp.
	<i>Aquilapollenites turbidus</i> ^{NSP}	<i>Ulmipollenites</i> ^{NSP}
	<i>Araucariacites</i> sp.	<i>Ulmoidipites</i> spp. 3 and 4 pored smooth to verrucate forms
	<i>Arecipites columellus</i>	unidentified acritarchs
	<i>Arecipites microreticulatus</i>	unidentified dinoflagellate cysts
	<i>Azolla circinata</i>	unidentified pollen tetrad
	<i>Azolla microspores</i>	unidentified trilete spores
	<i>Balmeisporites</i>	<i>Zonalapollenites</i>
	<i>Bisaccate conifer pollen</i>	

Note: Blue = palynomorphs that occur only in the Paleocene throughout Western Interior, magenta = palynomorphs extinct at end of Cretaceous: in Raton Basin (superscript ^{NSP}) per Fleming (1990); in Northern Great Plains (superscript ^{NSP}) per Nichols and Johnson (2002); Paleocene Ojo Alamo Sandstone Plus includes Ojo Alamo Sandstone plus uppermost Paleocene part of underlying strata at some localities.